Codage et traitement de signal avancé pour les systèmes MIMO

Abdelkader Medles

Télécom Paris (ENST)
Institut Eurécom

THÈSE

Présentée pour obtenir le grade de docteur
de l'Ecole Nationale Supérieure
des Télécommunications

Spécialité: Communication et Electronique

Abdelkader Medles

Codage et traitement de signal avancé pour les systèmes MIMO

Soutenue le 15 Avril 2004 devant le jury composé de

Jean-Claude Belfiore	Président
Phillipe Loubaton	Rapporteurs
Emre Telatar	
Karim Abed-Meraim	Examinateurs
Giuseppe Caire	
Meriem Jaidane	
Dirk Slock	Directeur de thèse

Télécom Paris (ENST)
Institut Eurécom

PhD THESIS

Presented in order to obtain the degree of
docteur de l'Ecole Nationale Supérieure des Télécommunications

Speciality: Communication and Electronic

Abdelkader Medles

Coding and advanced signal processing for MIMO Systems

Defended on April 15, 2004 before the committee composed of

Jean-Claude Belfiore	Président
Phillipe Loubaton	Rapporteurs
Emre Telatar	
Karim Abed-Meraim	Examinateurs
Giuseppe Caire	
Meriem Jaidane	
Dirk Slock	Directeur de thèse

Acknowledgments

First, I would like to thank Prof. Dirk Slock, my thesis supervisor, for his guidance, encouragements, continuous help and availability.

I grateful to Prof. Belfiore, for doing me the honour of presiding the jury of my thesis, as well as Prof. Loubaton, Prof. Telatar, Prof. Abed-Meraim, Prof. Caire and Prof. Jaidane for accepting to be members of the jury.

I also thank Institut Eurécom for giving me the opportunity of performing my research in very good conditions. I specially thank the Mobile Communications Department staff, with whom I had a lot of interactions and discussions.

My gratitude goes to my parents and my family. To them I dedicate this thesis.

Abstract

The use of multiple transmit and multiple receive antennas in mobile communications offers a high potential to improve the bit rate and the link quality. This can be achieved by using a higher multiplexing rate and by exploiting the diversity contained in the channel, under the constraint of acceptable complexity. The channel knowledge availability has an important impact on the system design. In fact, the Channel State Information (CSI) at the transmitter (Tx) has an impact on the coding, whereas the quality of the channel knowledge at the receiver (Rx) side has an impact mainly on the detection and the channel estimation.

The first part of this thesis considers the case of absence of CSI at the Tx and perfect at the Rx. We propose the Space-Time Spreading (STS), which is a space-time coding scheme based on linear precoding that use a MIMO convolutive prefilter. STS achieves full multiplexing rate and is optimized to exploit maximum diversity and coding gains and to save the ergodic capacity. STS allows to use various receiver structures of low complexity. The Stripping MIMO Decision Feedback Equalizer (DFE), is a non-iterative receiver that detects the streams successively. The performances of the Stripping are evaluated in term of diversity versus multiplexing tradeoff. Another non-iterative receiver is the Conventional DFE applied to the MIMO case. It detects jointly symbols for different streams but proceed successively in time. The third proposed receiver is an iterative one. It takes advantage of the presence of the binary channel code, and iterates between the linear equalizer and the binary channel decoder. Simulations are provided to evaluate its performance.

In the second part we consider channels with partial CSI at the Tx and perfect CSI at RX. The partial knowledge in these cases can come from the decomposition of the channel in slow varying and fast varying parameters. It can also be the result of the reciprocity of the downlink and uplink physical channels. For those cases we provide suitable channel models and study the

ergodic capacity.

In the last part, the case of absence of CSI at both Tx and Rx is considered. The capacities of two channel models, block fading and time selective, are studied. Due to the absence of CSI at Rx in this case the channel needs to be estimated in practical systems. We propose semi-blind estimators that combine training and blind information. Identifiability conditions are derived and simulations are presented to evaluate performances.

Résumé

L'utilisation d'antennes multiple à la transmission et réception dans les communications mobiles, offre d'importantes perspectives pour accroître le débit et améliorer la qualité du lien. Cela peut être effectué en utilisant un plus important multiplexage spatial et en exploitant la diversité contenue dans le canal, tout en gardant une complexité acceptable. L'état de connaissance sur le canal a un impact important sur la conception de la chaine de transmission. En effet, l'information sur l'état du canal (CSI) au transmetteur (Tx) a un impact sur le codage alors que la qualité du CSI au récepteur (Rx) a principalement un impact sur la détection et l'estimation du canal.

Dans la première partie de cette thèse nous avons considéré le cas d'absence de CSI au Tx et un parfait CSI au Rx. On propose la dispersion spatio-temporelle (STS), qui est un schéma de codage spatio-temporel basé sur le précodage linéaire en utilisant un filtre multi-entrée multi-sortie (MIMO). Le STS effectue un multiplexage de flux maximal, qui est optimisé pour exploiter une diversité maximale, atteindre un bon gain codage et conserver la capacité ergodique. Un autre avantage du STS est qu'il permet d'utiliser une variété de récepteurs de complexité réduite. Le Stripping MIMO avec égalisation a retour de décision, est un récepteur non-itératif qui détecte les flux d'une manière successive. Les performances du Stripping sont données en terme du compromis entre diversité et multiplexage. Un autre récepteur non-itératif est l'égaliseur à retour de décision appliqué au cas MIMO. Il permet la détection des symboles des différents flux d'une manière conjointe mais successivement dans le temps. Le troisième récepteur proposé est itératif. Il profite de la présence d'un codage canal binaire et itère entre l'égaliseur linéaire et le décodeur canal binaire. Des simulations sont présentées pour évaluer les performances.

Dans la seconde partie on considère des canaux avec un CSI partiel au Tx et parfait au Rx. La connaissance partiale dans ces cas peut être le résultat de

la décomposition du canal en paramètres lents et rapides. Elle peut aussi être le résultat d'une réciprocité du canal physique entre la liaison montante et descendante. A ces différents cas on présente des modèles de canaux adaptés et on étudie la capacité ergodique.

Dans la dernière partie on traite du cas d'absence de CSI aux Tx et Rx. La capacité de deux modèles de canaux, évanescent par bloc et sélectif en temps, est étudiées. A cause de l'absence de CSI au Rx le canal doit être estimé dans les systèmes utilisés en pratique. On propose des estimateurs semi-aveugle qui combinent l'information de la séquence d'apprentissage et celle de la partie aveugle. Les conditions d'identifiabilité sont obtenues et des simulations sont proposées pour évaluer les performances.

Contents

List of Figures

List of Tables

Acronyms

Here are the main acronyms used in this document. The meaning of an acronym is usually indicated once, when it first occurs in the text.

AWGN	Additive White Gaussian Noise
BCJR	Bahl, Cocke, Jelinek and Raviv (algorithm)
BER	Bit Error Rate
BPSK	Binary Phase Shift Keying
CDMA	Code-Division Multiple Access
CRB	Cramer-Rao Bound
CSI	Channel State Information
DA	Data-Aided
DFE	Decision Feedback Equalizer
DFT	Discrete Fourier Transform
DSB	Deterministic Semiblind
DSBA	Deterministic Semiblind Augmented
FIR	Finite Impulse Response
IC	Interference Canceler or Interference Cancellation
IDFT	Inverse Discrete Fourier Transform
ISI	Inter-Symbol Interference
iff	if and only if
i.i.d.	independent & identically distributed
GSB	Gaussian Semiblind
GSBA	Gaussian Semiblind Augmented
QPSK	Quarternary Phase Shift Keying
LB	Lower Bound
LL	Log Likelihood
LLR	Log Likelihood Ratio

MAP	Maximum *A Posteriori*
MFB	Matched Filter Bound
MI	Mutual Information
MIMO	Multiple Input Multiple Output
MISO	Multiple Input Single Output
ML	Maximum Likelihood
MMSE	Minimum Mean Square Error
MRC	Maximum Ratio Combining
MSE	Mean Square Error
PIC	Parallel Interference Cancellation
PSP	Per-Survivor-Processing
pdf	probability density function
psdf	power spectral density function
Rx	Receiver
SB	Singleton Bound
SIC	Successive Interference Cancellation
SIMO	Single Input Multiple Output
SINR	Signal to Noise Plus Interference Ratio
SNR	Signal-to-Noise Ratio
ST	Space-Time
STC	Space-Time Code/Coding
STOD	Space Time Orthogonal Design
STS	Space Time Spreading
SVD	Singular Value Decomposition
S/P	Serial to Parallel conversion
sIsO	soft-Input soft-Output
TS	Training Sequence
Tx	Transmitter
UB	Upper Bound
UDL	Upper Diagonal Lower
UMTS	Universal Mobile Telecommunication System
vs.	versus
w.p.	with probability
w.r.t.	with respect to
ZF	Zero-Forcing

Notations

Here is a list of the main notations and symbols used in this document. We have tried to keep consistent notations throughout the document, but some symbols have different definitions depending on when they occur in the text.

a	Scalar variable
$\mathbf{a}$	Vector variable
$\mathbf{A}$	Matrix variable
$a(t)$, $a(\tau)$	Continous-time function of the temporal variable t or τ
$a(n)$	Discrete-time function $a(n) = a(nT)$ for a given T
a_n	Discrete-time function $a_n = a(nT)$ for a given T
$j = \sqrt{-1}$	The unity imaginary number
$\Re(x)$	Real part of x
$\Im(x)$	Imaginary part of x
$\mathbf{D}$	Diagonal matrix
$a(z)$	z-transform of $a(n)$
$(\cdot)^*$	Complex conjugate
$(\cdot)^T$	Transpose
$(\cdot)^t$	Block transpose
$(\cdot)^H$	Hermitian transpose
$\mathbf{A}^\dagger(z) = \mathbf{A}^H(1/z^*)$	
$\mathbf{I}_m$	$m \times m$ Dimensional Identity matrix
$\otimes$	Kronecker product
$\mathrm{E}\{\cdot\}$	Expectation operator
$\det\{\mathbf{A}\}$	Determinant of the matrix $\mathbf{A}$
$\mathrm{tr}\{\cdot\}$	Trace operator
$\mathrm{diag}\{\mathbf{A}\}$	Diagonal matrix of the diagonal elements of the matrix $\mathbf{A}$
$\doteq$	Exponential equality
$\mathrm{vec}(\mathbf{M})$	$\mathbf{M}$ written in a vector form
N_{tx}	Number of transmit antennas

N_{rx}	Number of receive antennas
N_s	Number of streams
P_X	$\mathbf{X}(\mathbf{X}^H\mathbf{X})^{-1}\mathbf{X}^H$: Projection on the column space of $\mathbf{X}$
E_b	Energy per information bit
E_b/N_0	Signal to noise ratio per information bit
N_0	One sided noise power spectral density of the AWGN channel
$I(X;Y)$	Mutual information between random variables X and Y
$P(A)$	Probability of event A.
$\mathcal{O}(.)$	Of the order of x.
δ_{ij}	Kronecker delta
$\ln(.)$	Natural logarithm
$h(X)$	Entropy mesure of the stochastic variable X
$\bigoplus_{i=1}^{N_{tx}} \mathbf{X}_i$	block-diag$\{\mathbf{X}_1, \ldots, \mathbf{X}_{N_{tx}}\}$

Chapter 1

Introduction

In this chapter we introduce the principle of multiple transmit antennas and multiple receive antennas used in wireless communication, which can be seen more generally as Multiple Input Multiple Output (MIMO) system. We first define the general channel model, and specify the capacity for the different cases of channel knowledge. We present some basics on the design of space-time codes in the case of absence of channel knowledge at the transmitter (Tx). We introduce then some notions on the diversity vs. multiplexing of Zheng & Tse and conclude this chapter by an overview of the different parts of this report.

Since the introduction, independently, of spatial multiplexing by A. Paulraj in a Stanford University patent and by Foschini [1] at Bell Labs in 1994, the use of multiple transmit and multiple receive antennas has become the focus of a lot of works. The reason behind this big interest of the scientific community is related to the ability of MIMO systems to offer a new spatial dimension, other than the time and frequency dimensions, that increases the ergodic (average) capacity of the channel by a multiplying factor equal to the minimum between the number of transmit vs. receive antennas (N_{tx} vs. N_{rx}) [2], and allows to lower the outage probability by the contribution of $N_{tx}.N_{rx}$ diversity components corresponding to all the channel coefficients. Unlike SISO flat channel, MIMO flat channel (with absence of channel state information at the transmitter) suffers from interference between different transmit antennas. The recent attempts to exploit this high potential for wireless communication have to make a compromise in order to handle an increase in rate and take advantage of the available diversity to combat fading and destructive interference whithin acceptable complexity limits.

This chapter is an introduction to the general framework. We present the general MIMO linear model in wireless communication, and detail the underlying models for specific situations. The capacities of such as channels are also introduced. We present the classical multi-antenna receive diversity and the space-time coding for MIMO systems. The diversity and multiplexing as defined by Zheng & Tse are also introduced. Finally we provide an overview of this thesis.

1.1 General MIMO Channel Model

Consider linear digital modulation over a linear channel with additive Gaussian noise. The number of antennas is N_{tx} at the transmitter side and N_{rx} at the receiver as represented in fig. 1.1. We assume a linear time invariant model for the effect of the channel on the transmitted signals. The received signal at Rx antenna i can be written in baseband as

$$y_i(t) \;=\; \sum_{n=1}^{N_{tx}} \sum_{l=-\infty}^{+\infty} x_n(l) h_{in}(t - lT_p) \;+\; v_i(t)\,, \tag{1.1}$$

where the $x_n(l)$ are the transmitted symbols from the antenna source n, T_p is the common symbol period, $h_{in}(t)$ is the (overall) channel impulse response

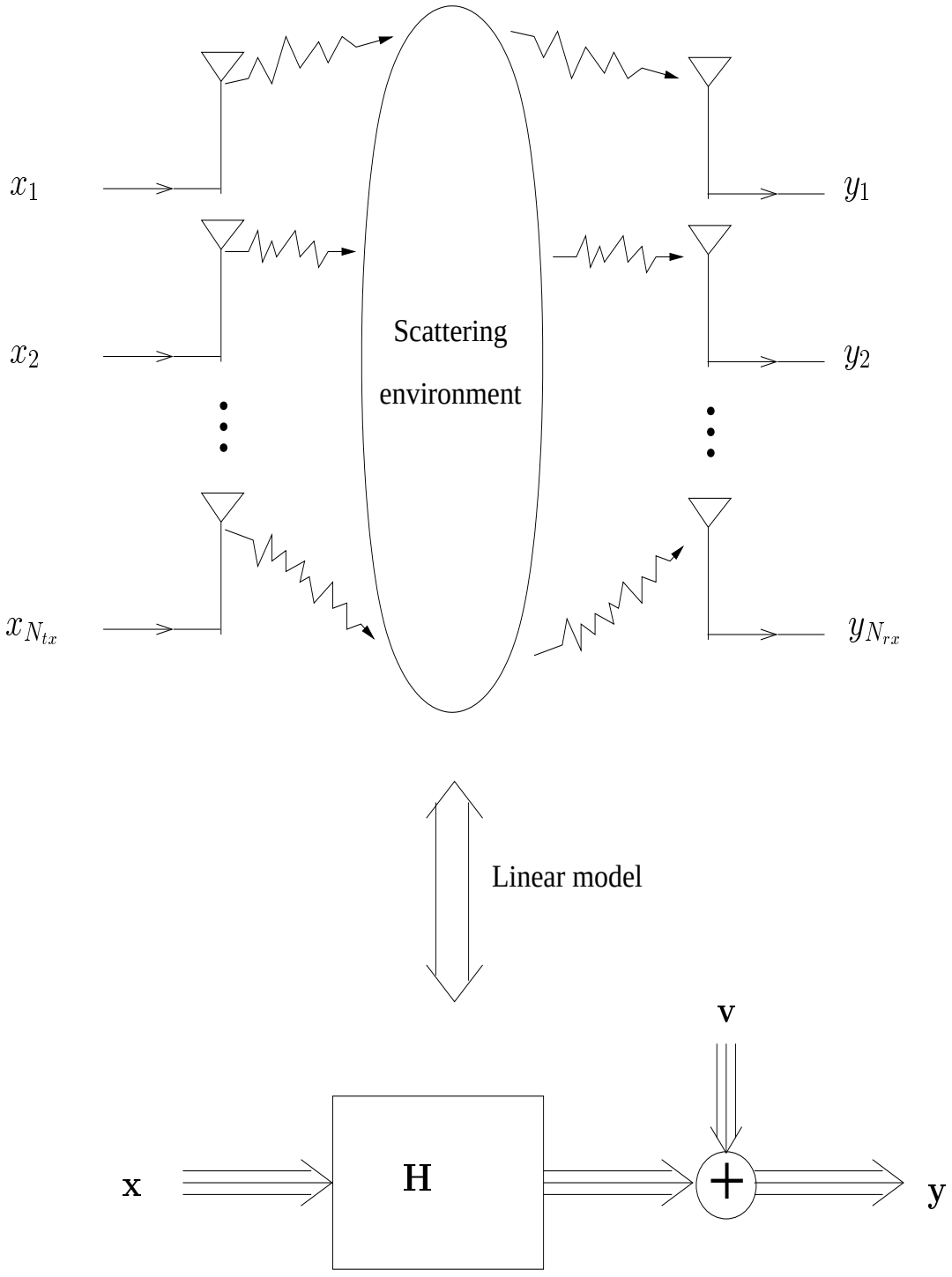

Figure 1.1: MIMO channel model.

from transmitter n to receiver antenna i. Assuming the $\{x_n(l)\}$ and $\{v_i(t)\}$ to be jointly (wide-sense) stationary, the processes $\{y_i(t)\}$ are jointly (wide-sense) cyclostationary with period T_p. If $\{y_i(t)\}$ is sampled with period T_p, the sampled process is (wide-sense) stationary. Sampling in this way leads to an equivalent discrete-time representation. We assume the MIMO channel to be causal and finite impulse response (FIR). In particular, after sampling we assume the impulse response to be of length L. The discrete-time Rx signal can be represented in vector form as

$$\begin{aligned} \mathbf{y}_k &= \sum_{n=1}^{N_{tx}} \sum_{l=0}^{L-1} \mathbf{h}_n(l) x_n(k-l) + \mathbf{v}_k \\ &= \sum_{l=0}^{L-1} \mathbf{H}_l \mathbf{x}_{k-l} + \mathbf{v}_k \,, \end{aligned} \tag{1.2}$$

where $\mathbf{H}_l$ is $N_{rx} \times N_{tx}$ with $(\mathbf{H}_l)_{in} = h_{in}(l)$ for $i = 1, 2, \ldots, N_{rx}$, $n = 1, 2, \ldots, N_{tx}$ and

$$\mathbf{y}_k = \begin{bmatrix} y_1(k) \\ y_2(k) \\ \vdots \\ y_{N_{rx}}(k) \end{bmatrix}, \mathbf{v}_k = \begin{bmatrix} v_1(k) \\ v_2(k) \\ \vdots \\ v_{N_{rx}}(k) \end{bmatrix}, \mathbf{h}_n(l) = \begin{bmatrix} h_{1n}(l) \\ h_{2n}(l) \\ \vdots \\ h_{N_{rx}n}(l) \end{bmatrix}. \tag{1.3}$$

The noise is assumed to follow a white Gaussian distribution, $\mathbf{v}_k \sim \mathcal{CN}(0, \sigma_v^2 \mathbf{I}_{N_{rx}})$, the transmitted signal is characterized by its power spectral density function (psdf) $S_{\mathbf{xx}}(z)$ with $\frac{1}{2\pi j} \oint \frac{dz}{z} \mathrm{tr}\, S_{\mathbf{xx}}(z) = N_{tx}\sigma_x^2$, $j = \sqrt{-1}$, and the signal-to-noise ratio is $SNR = N_{tx}\dfrac{\sigma_x^2}{\sigma_v^2} = N_{tx}\rho$. The notation tr(.) denotes the trace function.

Let q denote the time shift operator: $(q^{-1}\,\mathbf{x})_k = \mathbf{x}_{k-1}$, and $\mathbf{H}(q) = \sum_{l=0}^{L-1} \mathbf{H}_l q^{-l}$.

The received signal is then

$$\mathbf{y}_k = \mathbf{H}(q)\mathbf{x}_k + \mathbf{v}_k \,, \tag{1.4}$$

and the psdf of the received signal is

$$\mathbf{S}_{\mathbf{yy}}(z) = \mathbf{H}(z) S_{\mathbf{xx}}(z) \mathbf{H}^{\dagger}(z) + \sigma_v^2 \mathbf{I} \,, \tag{1.5}$$

where $\mathbf{H}(z)$ is z-transform of the channel impulse response.
We could also obtain multiple channels in the discrete time domain by oversampling the continuous-time received signals w.r.t. the symbol rate (in the case of the presence of excess bandwidth), the antennas could also be generalized sensors (polarization, 4 EM components [3, 4, 5]), and in the case of passband transmission of real symbol constellations we can also double the number of channels by taking the in-phase and in-quadrature components of the received signal.
We assume here the channel to be constant for the duration of one frame (or block), however the channel can vary from block to block, this is the reason why this model is called block fading channel model, which is the most common channel model used in papers dealing with wireless MIMO systems.
Two classes of channels are to be distinguished, flat channels ($L = 1$) and frequency selective channels ($L > 1$). The case $L > 1$ is also called Inter-Symbol Interference (ISI) channel. In most of the papers on MIMO the channel is assumed to be flat, the impulse response being simply then $\mathbf{H} = \mathbf{H}_0$.
In the different parts of this thesis report we will deal with different configuration of the Channel State Information (CSI): presence at Rx vs. Tx and absence vs. perfect or partial.
In the absence of CSI at Tx we still assume the knowledge of the average power of the channel $\mathrm{Etr}\{\mathbf{H}^H\mathbf{H}\}$ (by normalization $= N_{rx}.N_{tx}$) [2], in order to be able to construct a statistical model. This model is chosen to be a maximum entropy model to reflect the absence of CSI, it leads to Gaussian i.i.d. components and corresponds hence to the Rayleigh flat fading MIMO channel model.

1.1.1 Rayleigh Flat Fading MIMO Channel Model

This model has i.i.d. centered Gaussian components $(\mathbf{H})_{mk} \sim \mathcal{CN}(0, 1)$ for $1 \leq m \leq N_{rx}$ and $1 \leq k \leq N_{tx}$.
We denote $p = \min(N_{rx}, N_{tx})$ and $q = \max(N_{rx}, N_{tx})$. Let $\mathbf{USU}^H = \mathbf{H}^H\mathbf{H}$ be the eigenvector decomposition of $\mathbf{H}^H\mathbf{H}$, where $\mathbf{S} = \mathrm{diag}\{s_1, \ldots, s_p\}$ where the eigenvalues are organized in increasing order ($s_1 \leq s_2 \leq \ldots \leq s_p$), and $\mathbf{U} = [\mathbf{u}_1, \ldots, \mathbf{u}_p] : N_{tx} \times p$ contains the eigenvectors.
In [2], Telatar has shown that $\mathbf{U}$ is uniformly distributed over the Grassmann manifold and that the eigenvalues follow a Wishart distribution with a joint

pdf

$$p(s_1, \ldots, s_p) = K_{q,p}^{-1} \prod_{i=1}^{p} s_i^{q-p} \prod_{i<j} (s_i - s_j)^2 e^{-\sum_i s_i}, \tag{1.6}$$

where $K_{q,p}$ is a normalizing constant.

1.1.2 Separable Spatial Channel Model (Partial CSI at Tx)

In the case of partial CSI at the Tx, the MIMO channel is often modeled as a spatially separable channel model. In this model the channel is given by

$$\mathbf{H} = \mathbf{\Sigma}_1^{1/2} \mathbf{W} \mathbf{\Sigma}_2^{1/2}, \tag{1.7}$$

where $\mathbf{W}$ is a $N_{rx} \times N_{tx}$ random matrix of i.i.d. complex circular Gaussian elements with mean 0 and variance 1.
The matrix $\mathbf{\Sigma}_1$ is the receive array covariance matrix and $\mathbf{\Sigma}_2$ is the transmit array covariance matrix: $\mathrm{E}\{\mathbf{H}^H\mathbf{H}\} = \mathrm{tr}\{\mathbf{\Sigma}_1\}\mathbf{\Sigma}_2, \quad \mathrm{E}\{\mathbf{H}\mathbf{H}^H\} = \mathrm{tr}\{\mathbf{\Sigma}_2\}\mathbf{\Sigma}_1$. For $\mathbf{\Sigma}_1 = \mathbf{I}_{N_{rx}}, \mathbf{\Sigma}_2 = \mathbf{I}_{N_{tx}}$ we recover the Rayleigh flat fading MIMO channel model. In fact, the separable channel model is constructed as a generalization of the Rayleigh MIMO channel model used in case of no CSI at the Tx to the case when the second order statistics of the channel are present at the Tx.

1.1.3 Frequency Selective Rayleigh Fading MIMO Channel Model

We construct this model as a generalization of the Rayleigh MIMO channel model to the case of frequency selectivity, it incorporates the power delay profile knowledge for finite delay spread L. For this model $\mathbf{H}_l$, $l = 0, \ldots, L-1$ are independent, and each $\mathbf{H}_l$ has i.i.d Gaussian component $(\mathbf{H}_l)_{mk} \sim \mathcal{CN}(0, \sigma_l^2)$ for $1 \leq m \leq N_{rx}$ and $1 \leq k \leq N_{tx}$. σ_l^2, $0 \leq l \leq L-1$, reflect the power delay profile of the channel and are assumed to be non-zero.

1.2 Capacity of MIMO Channel

1.2.1 Flat Channel with Perfect CSI

For a flat channel with perfect CSI at the Tx and the Rx, the capacity is the maximum achievable rate under the power constraint, and is achieved by a frequency flat and zero-mean input

$$C(\mathbf{H}) = \max_{\mathrm{tr}\{\mathbf{S_{XX}}\}\leq P} \ln\det(\mathbf{I}_{N_{rx}} + \frac{1}{\sigma_v^2}\,\mathbf{H}\,\mathbf{S_{XX}}\,\mathbf{H}^H)\,, \tag{1.8}$$

where P is the power constraint limit, $\mathbf{S_{XX}}(z) = \mathbf{S_{XX}}$ is now simply the covariance and the solution is obtained by waterfilling on the eigenvalues of $\mathbf{H}^H\mathbf{H}$ (spatial waterfilling) [2]. The capacity is given in nats/second/Hz.
In the case of a MIMO frequency selective channel the solution is a waterfilling over the two dimensions space and frequency, the solution in this case is not trivial.

1.2.2 Ergodic Capacity (Imperfect CSI at Tx)

In the case of imperfect CSI (no or partial CSI) at the Tx and perfect CSI at Rx the channel has apriori distribution. The instantaneous capacity is now a stochastic quantity, a common measure is the average or *ergodic capacity*

$$C = \max_{\frac{1}{2\pi j}\oint \frac{dz}{z}\mathrm{tr}\{\mathbf{S_{XX}}\}\leq P} \mathrm{E}_{\mathbf{H}}\frac{1}{2\pi j}\oint \frac{dz}{z}\ln\det(\mathbf{I}_{N_{rx}} + \frac{1}{\sigma_v^2}\,\mathbf{H}(z)\,\mathbf{S_{XX}}(z)\,\mathbf{H}^\dagger(z))\,, \tag{1.9}$$

where the expectation $\mathrm{E}_{\mathbf{H}}$ is here w.r.t. the channel, and
$\frac{1}{2\pi j}\oint \frac{dz}{z}g(z) = \int_{-\frac{1}{2}}^{\frac{1}{2}} g(e^{j2\pi f})df$ is the integral over the unit circle for a function $g(.)$.
The ergodic capacity is hence the average of the instantaneous capacity, it takes its full sense if we are able to encode the information to transmit over several channel realizations (independent blocks). Finally it becomes achievable if the transmitted codewords experience an infinite number of channel realizations.
In the case of Rayleigh flat fading MIMO channel model, Telatar has shown in [2] that the ergodic capacity is achieved by a white input ($\mathbf{S_{XX}}(z) = \sigma_x^2\mathbf{I}_{N_{tx}}$, $\sigma_x^2 = \frac{P}{N_{tx}}$)

$$C = \mathrm{E}_{\mathbf{H}}\ln\det(\mathbf{I}_{N_{rx}} + \rho\mathbf{H}\mathbf{H}^H)\,. \tag{1.10}$$

In fact in this case the channel distribution is invariant by any permutation of the Tx antennas, they play symmetrical roles and hence there is no preferable direction of transmission, yielding to a spatially white input.
High SNR : Asymptotically for high SNR it is shown in [2] that
$C = \mathcal{O}\left(\min(N_{tx}, N_{rx}) \ln \rho\right)$, or equivalently that the MIMO channel performs asymptotically as well as an equivalent number of parallel AWGN channels equal to the rank of $\mathbf{H}$. These asymptotic performances of the ergodic capacity are the same as the one of the capacity for a MIMO channel with perfect CSI at Tx.
The ergodic capacity formula can be generalized to the frequency selective case, the following theorem gives the desired result.

Theorem 1: For a channel with a frequency selective Rayleigh fading model (section 1.1.3) the ergodic capacity is

$$C = \mathrm{E}_{\mathbf{H}} \frac{1}{2\pi j} \oint \frac{dz}{z} \ln \det(\mathbf{I}_{N_{rx}} + \rho\, \mathbf{H}(z)\mathbf{H}^{\dagger}(z)), \tag{1.11}$$

where $\rho = \frac{P}{N_{tx}\sigma_v^2}$
Proof : By applying the result of the flat channel case to each frequency, we conclude that for each frequency the psdf is spatially white, hence $\mathbf{S_{XX}}(z) = s_{\mathbf{XX}}(z)\mathbf{I}_{N_{tx}}$, with $\frac{1}{2\pi j}\oint \frac{dz}{z} s_{\mathbf{XX}}(z) \leq \frac{P}{N_{tx}}$. On the other hand, for every z_1 on the unit circle $\mathbf{H}_l z_1^{-l}$, $l = 0, \ldots, L-1$ have the same joint distribution as $\mathbf{H}_l$, $l = 0, \ldots, L-1$, and by consequence $\mathbf{H}(zz_1)$ as $\mathbf{H}(z)$, then

$$\begin{aligned}
&\mathrm{E}_{\mathbf{H}} \ln \det(\mathbf{I}_{N_{rx}} + \tfrac{s_{\mathbf{XX}}(z)}{\sigma_v^2}\mathbf{H}(z)\mathbf{H}^{\dagger}(z)) \\
&= \mathrm{E}_{\mathbf{H}} \ln \det(\mathbf{I}_{N_{rx}} + \tfrac{s_{\mathbf{XX}}(z)}{\sigma_v^2}\mathbf{H}(zz_1)\mathbf{H}^{\dagger}(zz_1)) \quad \forall z_1 \text{ with} |z_1| = 1 \\
&= \tfrac{1}{2\pi j}\oint \tfrac{dz_1}{z_1} \mathrm{E}_{\mathbf{H}} \ln \det(\mathbf{I}_{N_{rx}} + \tfrac{s_{\mathbf{XX}}(z)}{\sigma_v^2}\mathbf{H}(zz_1)\mathbf{H}^{\dagger}(zz_1)),
\end{aligned} \tag{1.12}$$

and the ergodic capacity

$$\begin{aligned}
&\tfrac{1}{2\pi j}\oint \tfrac{dz}{z} \mathrm{E}_{\mathbf{H}} \ln \det(\mathbf{I}_{N_{rx}} + \tfrac{s_{\mathbf{XX}}(z)}{\sigma_v^2}\mathbf{H}(z)\mathbf{H}^{\dagger}(z)) \\
&= \tfrac{1}{2\pi j}\oint \tfrac{dz}{z} \tfrac{1}{2\pi j}\oint \tfrac{dz_1}{z_1} \mathrm{E}_{\mathbf{H}} \ln \det(\mathbf{I}_{N_{rx}} + \tfrac{s_{\mathbf{XX}}(z)}{\sigma_v^2}\mathbf{H}(zz_1)\mathbf{H}^{\dagger}(zz_1)) \\
&= \tfrac{1}{2\pi j}\oint \tfrac{dz_2}{z_2} \tfrac{1}{2\pi j}\oint \tfrac{dz}{z} \mathrm{E}_{\mathbf{H}} \ln \det(\mathbf{I}_{N_{rx}} + \tfrac{s_{\mathbf{XX}}(z)}{\sigma_v^2}\mathbf{H}(z_2)\mathbf{H}^{\dagger}(z_2)) \\
&\leq \tfrac{1}{2\pi j}\oint \tfrac{dz_2}{z_2} \mathrm{E}_{\mathbf{H}} \ln \det(\mathbf{I}_{N_{rx}} + \tfrac{1}{2\pi j}\oint \tfrac{dz}{z} \tfrac{s_{\mathbf{XX}}(z)}{\sigma_v^2}\mathbf{H}(z_2)\mathbf{H}^{\dagger}(z_2)) \\
&\leq \tfrac{1}{2\pi j}\oint \tfrac{dz_2}{z_2} \mathrm{E}_{\mathbf{H}} \ln \det(\mathbf{I}_{N_{rx}} + \rho\, \mathbf{H}(z_2)\mathbf{H}^{\dagger}(z_2)),
\end{aligned} \tag{1.13}$$

in the second equality we operate a variable change $zz_1 \rightarrow z_2$, whereas in the third inequality we exploit the concavity of the $\ln\det$ function over the set of positive definite matrices. The final inequality shows that
$\mathrm{E}_H \frac{1}{2\pi j} \oint \frac{dz}{z} \ln\det(\mathbf{I}_{N_{rx}} + \rho\,\mathbf{H}(z)\mathbf{H}^\dagger(z))$ is an upper bound on the capacity, however this bound is achieved for $S_{\mathbf{XX}}(z) = \sigma_x^2 \mathbf{I}_{N_{tx}}$. □

1.2.3 Outage Capacity (Imperfect CSI at Tx)

For a channel with imperfect CSI at the Tx, and in the case where the encoder sees a limited number of channel realizations (for instance we consider the case of one channel realization) the ergodic capacity makes no sense, the outage capacity is then more appropriate. In fact, for a given SNR and rate R, it expresses the probability that the transmitted rate is larger then the instantaneous capacity (transmission failure)

$$\begin{aligned} P_{out}(R) &= P(C(\mathbf{H}) < R) \\ &= P(\tfrac{1}{2\pi j} \oint \tfrac{dz}{z} \ln\det(\mathbf{I}_{N_{rx}} + \rho\mathbf{H}(z)\, S_{\mathbf{XX}}(z)\, \mathbf{H}^\dagger(z)) < R)\,, \end{aligned} \tag{1.14}$$

where $S_{\mathbf{XX}}(z)$ is normalized here to have $(\frac{1}{2\pi j} \oint \frac{dz}{z} \mathrm{tr} S_{\mathbf{XX}}(z) = N_{tx})$.
For a given level α $(0 \leq \alpha \leq 1)$ of the outage, the outage capacity is defined as

$$C_{out}(\alpha) = (P_{out})^{-1}(\alpha)\,, \tag{1.15}$$

the choice of $S_{\mathbf{XX}}(z)$ is the one that maximizes C_{out}, papers like [6, 7, 8] studied this problem. They show that for separable spatial flat channel model with well conditionned $\mathbf{\Sigma}_2$, and for low outage (small α) the transmitter optimal input color tends to be white $S_{\mathbf{XX}}(z) = \sigma_x^2 \mathbf{I}_{N_{tx}}$.
An other important result for flat channel is shown in [9], where for asymptotically high SNR, Rayleigh flat fading channel and for any constant and finite rate R we have

$$P_{out}(R) = \mathcal{O}\left(\rho^{-N_{tx}.N_{rx}}\right). \tag{1.16}$$

The exponent of the SNR $N_{tx}.N_{rx}$ is called the diversity gain and is related to the diversity gain that arise in the space-time code design (section 1.4). The diversity gain corresponds to the asymptotic slope of the error probability (or outage probability), and is equal to the total number of independent diversity sources.

1.2.4 Asymptotic Behavior in Block Transmission

Let us assume that we transmit over a block of length T, the received signal can then be written as

$$\mathbf{Y} = \mathcal{A}_T(\mathbf{H})\mathbf{X} + \mathbf{V}\,, \tag{1.17}$$

where $\mathbf{Y} = [\mathbf{y}_1^T, \mathbf{y}_2^T, \ldots, \mathbf{y}_{T+L-1}^T]^T$, $\mathbf{X} = [\mathbf{x}_1^T, \mathbf{x}_2^T, \ldots, \mathbf{x}_T^T]^T$ and $\mathbf{V} = [\mathbf{v}_1^T, \mathbf{v}_2^T, \ldots, \mathbf{v}_{T+L-1}^T]^T$. $\mathcal{A}_T(\mathbf{H})$ is a $N_{rx}(T+L-1) \times N_{tx}T$ block toeplitz matrix with first block column $[\mathbf{H}_0^T, \mathbf{H}_1^T, \ldots, \mathbf{H}_{L-1}^T]^T$.

$$\mathcal{A}_T(\mathbf{H}) = \begin{bmatrix} \mathbf{H}_0 & 0 & \ldots & 0 \\ \mathbf{H}_1 & \mathbf{H}_0 & \ddots & \vdots \\ \vdots & \mathbf{H}_1 & \ddots & 0 \\ \mathbf{H}_{L-1} & \vdots & \ddots & \mathbf{H}_0 \\ 0 & \mathbf{H}_{L-1} & \vdots & \mathbf{H}_1 \\ \vdots & \ddots & \ddots & \vdots \\ 0 & \ldots & 0 & \mathbf{H}_{L-1} \end{bmatrix}. \tag{1.18}$$

The instantaneous capacity (per input symbol) of the block transmission for white input is

$$C_T(\mathbf{H}) = \frac{1}{T} \ln \det(\mathbf{I}_{N_{rx}T} + \rho \mathcal{A}_T(\mathbf{H})(\mathcal{A}_T(\mathbf{H}))^H)\,. \tag{1.19}$$

The following lemma gives an important result on the limit of $C_T(\mathbf{H})$ for large T.

Lemma 1: The limit of the capacity $C_T(\mathbf{H})$ is

$$\lim_{T\to+\infty} C_T(\mathbf{H}) = C(\mathbf{H}) = \frac{1}{2\pi j} \oint \frac{dz}{z} \ln \det(\mathbf{I} + \rho\, \mathbf{H}(z)\mathbf{H}^\dagger(z)). \tag{1.20}$$

Proof: This is a generalization of the SISO case shown in [10, 11], the proof is similar.

Corollary 1: $C_T(\mathbf{H})$ converges in distribution to $C(\mathbf{H})$.

Proof: The limit in eq.(1.20) implies that $C_T(\mathbf{H})$ converges *almost surely* to $C(\mathbf{H})$, and hence $C_T(\mathbf{H})$ converges *in distribution* to $C(\mathbf{H})$.

The principal consequence of Corollary 1 is that asymptotically for large block length $T >> L$, $C_T(\mathbf{H})$ have the same distribution as the one of $C(\mathbf{H})$, then all the stated results for the continuous capacity $C(\mathbf{H})$ apply asymptotically to $C_T(\mathbf{H})$.

1.3 Conventional Multi-Antenna Receive Diversity

The classical Multi-antenna diversity technique is well-known to improve the quality of the wireless link [12, 13, 14, 15]. The channel in these cases is SIMO ($N_{tx} = 1$), for flat channel the received signal is written

$$\mathbf{y}_k = \mathbf{h}x_k + \mathbf{v}_k \,, \tag{1.21}$$

where

$$\mathbf{h} = \begin{bmatrix} h_1 \\ h_2 \\ \vdots \\ h_{N_{rx}} \end{bmatrix} \,, \tag{1.22}$$

and the transmitted signal x_k is a scalar now.
By applying a Maximum Ratio Combining (MRC) receiver

$$\begin{aligned} y_k &= \frac{\mathbf{h}^H}{||\mathbf{h}||}\mathbf{y}_k \\ &= ||\mathbf{h}||x_k + v_k \,, \end{aligned} \tag{1.23}$$

where $||\mathbf{h}|| = \sqrt{\sum_{i=1}^{N_{rx}} |h_i|^2}$ and $v_k = \frac{\mathbf{h}^H}{||\mathbf{h}||}\mathbf{v}_k$ follows a zero-mean Gaussian distribution with variance σ_v^2.
The result is a SISO fading channel with instantaneous capacity $C(\rho||\mathbf{h}||^2) = \ln(1 + \rho||\mathbf{h}||^2)$, achieved for Gaussian white input.
The instantaneous capacity $C(\rho||\mathbf{h}||^2)$ is an increasing and not bounded function of the effective SNR: $\rho||\mathbf{h}||^2$. Then for a given $R > 0$ there exists $\alpha > 0$ that verifies $\alpha = C^{-1}(R)$ and such that

$$P_{out}(R) = P(C(\rho||\mathbf{h}||^2) < R) = P(||\mathbf{h}||^2 < \frac{\alpha}{\rho}) \,. \tag{1.24}$$

The quality of the wireless link is related to the effective SNR ($\rho||\mathbf{h}||^2$) distribution, $P(||\mathbf{h}||^2 < \frac{\alpha}{\rho})$ is a measure of this quality, and the above equalities show the tight relation between the outage capacity and this measure.
$||\mathbf{h}||^2$ has a Chi-square pdf with $2N_{rx}$ degrees of freedom, we can then evaluate $P_{out}(R,\rho)$ analytically. However, we can also apply the Chernoff bound to derive an upper bound, this method is simpler and applies for the case where the components of $\mathbf{h}$ are still Gaussian but not i.i.d.

$$P(||\mathbf{h}||^2 < \frac{\alpha}{\rho}) = \mathrm{E}\,\mathbf{1}_{\{\rho||\mathbf{h}||^2-\alpha\}<0}\,, \tag{1.25}$$

and $\mathbf{1}_{\{||\mathbf{h}||^2<\frac{\alpha}{\rho}\}}$ is upper bounded by $e^{-\lambda(\rho||\mathbf{h}||^2-\alpha)}$, for any $\lambda > 0$, then

$$\begin{aligned} P(||\mathbf{h}||^2 < \tfrac{\alpha}{\rho}) &\leq \min_{\lambda>0} \mathrm{E}\, e^{-\lambda(\rho||\mathbf{h}||^2-\alpha)} \\ &= \min_{\lambda>0} \Phi_\Delta(\lambda) \\ &= \min_{\lambda>0} e^{\lambda\alpha} \int e^{-\lambda\rho||\mathbf{h}||^2} f(\mathbf{h}) d\mathbf{h}\,, \end{aligned} \tag{1.26}$$

where $f(\mathbf{H})$ is the pdf of $\mathbf{h}$, $\Delta = \rho||\mathbf{h}||^2 - \alpha$ and $\Phi_\Delta(\lambda) = \mathrm{E}\, e^{-\lambda\Delta}$ is the characteristic function of Δ. The second inequality corresponds to the Chernoff upper bound.
The channel components are assumed to be Gaussian with covariance $\mathbf{C_{hh}} = \mathbf{UDU}^H$ and rank r(= number of diversity sources). $\mathbf{D}$ is an $r \times r$ positive definite diagonal matrix containing the eigenvalues and $\mathbf{U}$ is $N_{rx} \times r$ unitary matrix of the eigenvectors ($\mathbf{U}^H\mathbf{U} = \mathbf{I}_r$). The integral is

$$\frac{1}{\det(\pi\mathbf{D})} \int e^{-\lambda\rho\mathbf{h}^H\mathbf{U}\mathbf{U}^H\mathbf{h}} e^{-\mathbf{h}^H\mathbf{U}\mathbf{D}^{-1}\mathbf{U}^H\mathbf{h}} d\mathbf{h} = \frac{\det(\lambda\rho\mathbf{I}_r + \mathbf{D}^{-1})^{-1}}{\det(\mathbf{D})}\,, \tag{1.27}$$

where we use equality $||\mathbf{h}||^2 = \mathbf{h}^H\mathbf{U}\mathbf{U}^H\mathbf{h}$. By taking $\lambda = 1$ the upper bound is finally

$$\begin{aligned} P(||\mathbf{h}||^2 < \tfrac{\alpha}{\rho}) &\leq \frac{e^\alpha}{\det(\,\rho\mathbf{D}+\mathbf{I}_r)} \\ &= \mathcal{O}\left(\rho^{-r}\right)\,. \end{aligned} \tag{1.28}$$

This shows that the MRC exploits all the available sources of diversity in a SIMO channel.

1.4 Space-Time Coding for MIMO System

The MIMO channel capacity as we have seen in section 1.2, shows a high bandwidth potential and offers big diversity advantage to improve the wire-

less link. The main problem is how to deal with the inter-antennas interference, the first response was given in [1]. The proposed scheme, called V-BLAST, transmits independent streams on the different antennas and use Successive Interference Cancellation (SIC) at the receiver side. Even if this scheme allows to achieve a high data rate, it is far from exploiting all the diversity advantage of the MIMO channel. In [16] Tarokh *et al* proposed to use new codes, called later Space-Time Codes (STC), that combine the channel code with the multiple transmit antenna aspect, and they also introduced a new design criteria for there construction.

Space-Time Code Design Criteria

The STC design applies for non-adaptive scheme, non-adaptive in the SNR, the rate is then constant and the number of codewords is finite.
We consider the transmission of the coded symbols for a duration of T symbol periods over a flat MIMO channel. The space-time code can be then represented in $N_{tx} \times T$ matrix form: $\mathbf{C} = \frac{1}{\sigma_x}[\mathbf{x}_1, \mathbf{x}_2, \ldots, \mathbf{x}_T]$. The accumulated received signal is

$$\mathbf{Y} = \sigma_x \mathbf{H}\, \mathbf{C} + \mathbf{V}\,, \tag{1.29}$$

where $\mathbf{Y} = [\mathbf{y}_1, \mathbf{y}_2, \ldots, \mathbf{y}_T]$ and $\mathbf{V} = [\mathbf{v}_1, \mathbf{v}_2, \ldots, \mathbf{v}_T]$ are $N_{rx} \times T$ matrices.
We consider a Rayleigh flat fading i.i.d. MIMO channel, and a Maximum Likelihood (ML) receiver. The channel is unknown at the Tx (no CSI at Tx) and perfectly known at the Rx (perfect CSI at Rx). For a transmitted $\mathbf{C}$, the union bound gives us an upper bound on the error probability

$$P(error/\mathbf{C}) \leq \sum_{\mathbf{C}' \in \{\mathcal{C} - \{\mathbf{C}\}\}} P(\mathbf{C} \to \mathbf{C}')\,, \tag{1.30}$$

where $P(\mathbf{C} \to \mathbf{C}')$ is the Pairwise Error Probability (PEP) or the probability of deciding erroneously $\mathbf{C}'$ for transmitted $\mathbf{C}$. $\mathcal{C}$ is the code book.
The STC design tries to minimize the error probability by minimizing the PEP.
The ML decision rule is given by

$$\hat{\mathbf{C}} = \arg\min_{\mathbf{C} \in \mathcal{C}} ||\mathbf{Y} - \sigma_x \mathbf{H}\mathbf{C}||_F\,, \tag{1.31}$$

where $||\mathbf{M}||_F^2 = \mathrm{tr}\,\{\mathbf{M}^H\mathbf{M}\}$ is the Frobenius norm of $\mathbf{M}$. Then the conditional PEP of $\mathbf{C}$ and $\mathbf{C}'$ is given by

$$P(\mathbf{C} \to \mathbf{C}'/\mathbf{H}) = P(\delta \leq 0)\,, \tag{1.32}$$

where δ is the decision metric difference

$$\begin{aligned} \delta &= ||\mathbf{Y} - \sigma_x \mathbf{H}\mathbf{C}'||_F^2 - ||\mathbf{Y} - \sigma_x \mathbf{H}\mathbf{C}||_F^2 \\ &= ||\sigma_x \mathbf{H}(\mathbf{C} - \mathbf{C}') + \mathbf{V}||_F^2 - ||\mathbf{V}||_F^2 \\ &= \sigma_x^2 ||\mathbf{H}(\mathbf{C} - \mathbf{C}')||_F^2 - 2\sigma_x \Re\mathrm{tr}\{\mathbf{V}^H \mathbf{H}(\mathbf{C} - \mathbf{C}')\}\,. \end{aligned} \tag{1.33}$$

Let $d = ||\mathbf{H}(\mathbf{C} - \mathbf{C}')||_F^2$ and $a = 2\sigma_x \Re\mathrm{tr}\{\mathbf{V}^H \mathbf{H}(\mathbf{C} - \mathbf{C}')\} \sim \mathcal{N}(0, 2\sigma_x^2 \sigma_v^2 d)$. $\Re$ denotes the real part and $\Im$ will denote the imaginary part. By applying the Chernoff bound we get

$$P(\mathbf{C} \to \mathbf{C}'/\mathbf{H}) \leq \min_{s>0} \mathrm{E}(e^{-s\delta}/\mathbf{H})\,. \tag{1.34}$$

$\mathrm{E}(e^{-s\delta}/\mathbf{H})$ is the characteristic function of δ and equals $e^{-(s-s^2\sigma_v^2)\sigma_x^2 d}$, the minimum of which is achieved for $s = \frac{1}{2\sigma_v^2}$. The Chernoff upper bound is then

$$P(\mathbf{C} \to \mathbf{C}'/\mathbf{H}) \leq e^{-\rho\frac{d}{4}}\,. \tag{1.35}$$

The PEP is the average of $P(\mathbf{C} \to \mathbf{C}'/\mathbf{H})$ over the channel distribution. Let $\mathbf{U}\mathbf{\Lambda}\mathbf{U}$ be the eigenvector decomposition of the hermitian of $\mathbf{C} - \mathbf{C}'$, then

$$\begin{aligned} d &= \mathrm{tr}\{\mathbf{H}(\mathbf{C} - \mathbf{C}')(\mathbf{C} - \mathbf{C}')^H \mathbf{H}^H\} \\ &= \mathrm{tr}\{\mathbf{H}\mathbf{U}\mathbf{\Lambda}\mathbf{U}\mathbf{H}^H\} \\ &= \mathrm{tr}\{\mathbf{H}'\mathbf{\Lambda}\mathbf{H}'^H\}\,, \end{aligned} \tag{1.36}$$

where $\mathbf{H}' = \mathbf{H}\mathbf{U}$ has the same distribution as $\mathbf{H}$. We can write then

$$\begin{aligned} P(\mathbf{C} \to \mathbf{C}') &= \mathrm{E}\ P(\mathbf{C} \to \mathbf{C}'/\mathbf{H}) \\ &\leq \mathrm{E}\ \exp\left(-\tfrac{\rho}{4}\textstyle\sum_{l=1}^{N_{tx}} \sum_{k=1}^{N_{rx}} \lambda_l |h'_{kl}|^2\right) \\ &= \textstyle\prod_{l=1}^{N_{tx}} \prod_{k=1}^{N_{rx}} \mathrm{E}\ \exp\left(-\tfrac{\rho}{4}\lambda_l |h'_{kl}|^2\right) \\ &= \textstyle\prod_{l=1}^{N_{tx}} \left(1 + \tfrac{\rho}{4}\lambda_l\right)^{-N_{rx}}\,. \end{aligned} \tag{1.37}$$

Which constitutes the desired Chernoff bound on the PEP.
The eigenvalues λ_l, $l = 1, \ldots, N_{tx}$ are sorted in decreasing order. Let r be the number of the non-zero values (= rank of $\mathbf{C} - \mathbf{C}'$). Less-tight upper bound is then given by

$$P(\mathbf{C} \to \mathbf{C}') \leq \left(\frac{\rho}{4}\right)^{-r.N_{rx}} \left(\prod_{l=1}^{r} \lambda_l\right)^{-N_{rx}}\,. \tag{1.38}$$

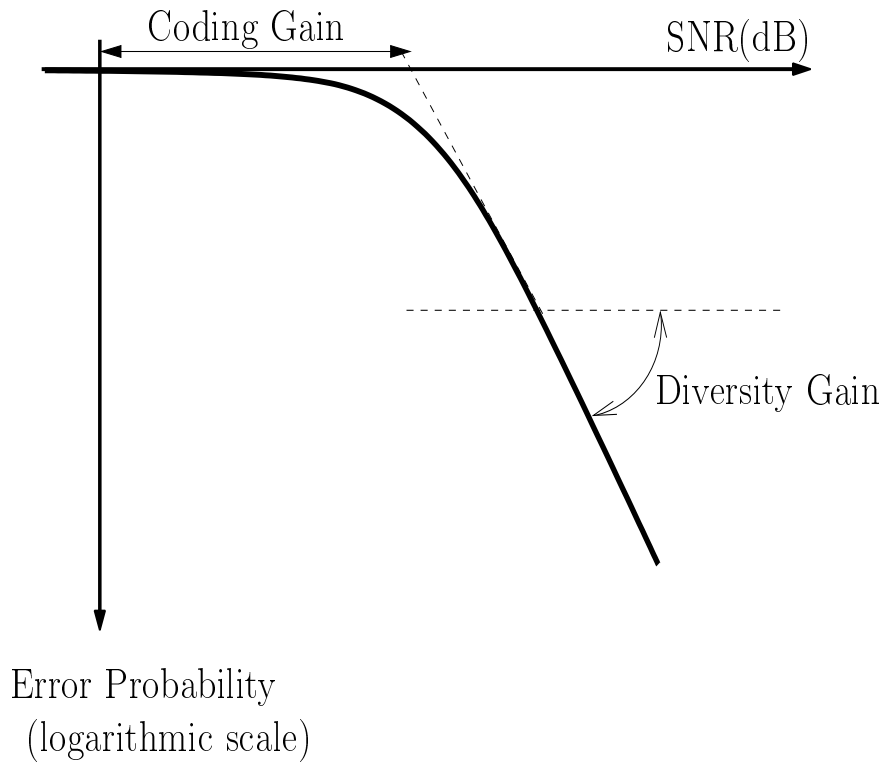

Figure 1.2: PEP vs. SNR

For high SNR this bound becomes tight

$$P(\mathbf{C} \to \mathbf{C}') \approx \left(\frac{\rho}{4}\right)^{-r.N_{rx}} \left(\prod_{l=1}^{r} \lambda_l\right)^{-N_{rx}} . \tag{1.39}$$

Diversity Gain : The total diversity order is the exponent of the SNR and is given by $r.N_{rx}$. Over the all codebook the diversity is given by $r_{min}.N_{rx}$, where r_{min} is the minimum rank of $\mathbf{\Lambda}$ over all the possible code words differences in $\mathcal{C}$. $r_{min}.N_{rx}$ is called the diversity gain.
Coding Gain : Moreover the PEP is a decreasing function of the product $\prod_{l=1}^{r} \lambda_l$, this last one should be made as large as possible for the error events with rank r_{min}. $\min \prod_{l=1}^{r_{min}} \lambda_l$ is called the coding gain. For $r_{min} = N_{tx}$, $\mathbf{\Lambda}$ is full rank and $\prod_{l=1}^{N_{tx}} \lambda_l = \det\left[(\mathbf{C}-\mathbf{C}')(\mathbf{C}-\mathbf{C}')^H\right]$.
In a plot that represents the PEP as function of the SNR in a logarithmic scale, the curve becomes asymptotically a line with a negative slope that

corresponds to the diversity gain, where the coding gain corresponds to the position of the line (see fig. 1.2).

1.5 Diversity and Multiplexing as Defined by Zheng & Tse

In [9] Zheng and Tse give a new definition of the diversity and spatial multiplexing that considers adaptive SNR schemes. In fact, a scheme $\mathcal{C}(\rho)$ is a family of codes of block length T(one for each SNR level), that supports a bit rate $R(\rho)$.
This scheme is to achieve *spatial multiplexing* r and diversity gain d if the data rate verifies

$$\lim_{\rho\to\infty} \frac{R(\rho)}{\ln(\rho)} = r\,, \tag{1.40}$$

and the average error probability verifies

$$\lim_{\rho\to\infty} \frac{\ln P_e(\rho)}{\ln(\rho)} = -d\,. \tag{1.41}$$

For block length $T \to +\infty$ the error probability becomes the outage capacity. For each r, $d^*(r)$ is defined to be the supremum of the diversity advantage achieved over schemes. The maximal diversity gain is defined by $d^*_{max} = d^*(0)$ and the maximal spatial multiplexing gain is $r^*_{max} = sup\{r : d^*(r) > 0\}$.
We will use the special symbol $\doteq$ to denote the exponential equality, *i.e.*, we write $f(\rho) \doteq \rho^b$ to denote

$$\lim_{\rho\to\infty} \frac{\ln f(\rho)}{\ln(\rho)} = b\,. \tag{1.42}$$

Zheng & Tse considered a Rayleigh flat MIMO channel model, and using results on the distribution of the eigenvalues (section 1.1.1) they showed the following results.

Optimal Tradeoff Curve : Assume $T \geq N_{rx} + N_{tx} - 1$. The optimal tradeoff curve $d^*(r)$ is given by the piecewise-linear function connecting the points $(k, d^*(k))$, $k = 0, 1, \ldots, p$, where

$$d^*(k) = (p-k)(q-k)\,. \tag{1.43}$$

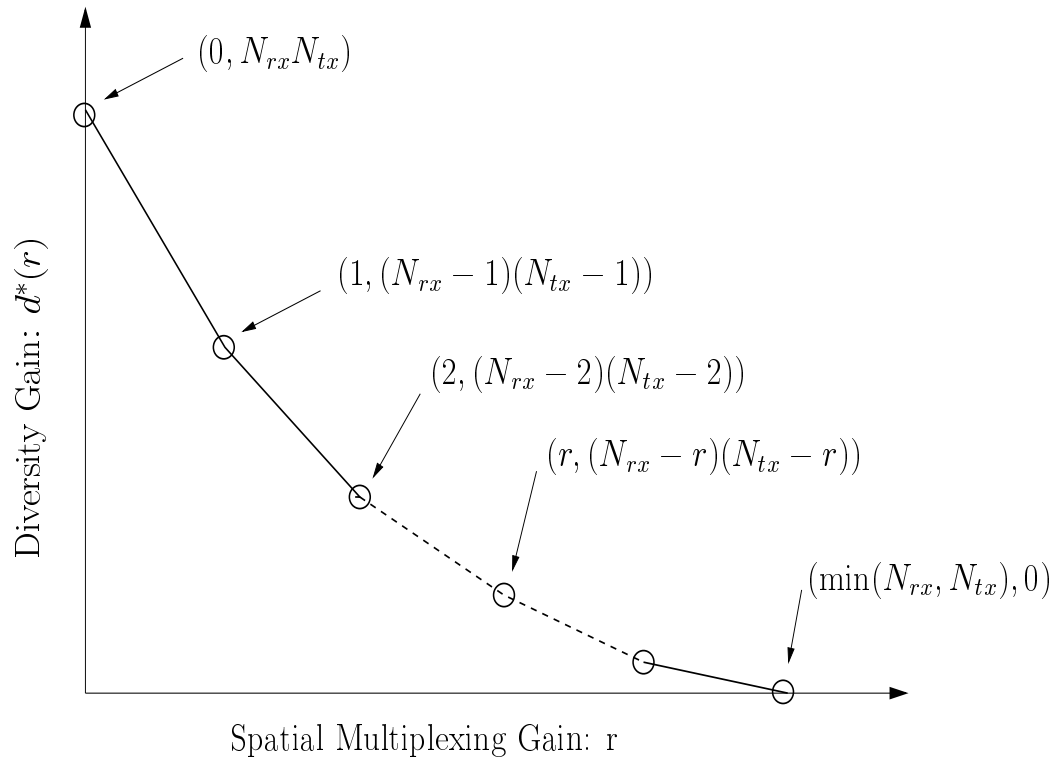

Figure 1.3: Diversity vs. multiplexing optimal tradeoff

Recall that $p = \min\{N_{rx}, N_{tx}\}$, $q = \max\{N_{rx}, N_{tx}\}$. In particular $d^*_{max} = N_{tx}.N_{rx}$ and $r^*_{max} = \min(N_{rx}, N_{tx})$.

1.6 Thesis Overview and Outline

This thesis is composed of three parts. The first one deals with absence of channel state information at the transmitter (and perfect CSI at the receiver), the second with partial CSI at the Tx (perfect CSI at the Rx) and the last one considers the absence of CSI at both Tx and Rx. A brief overview of the general framework of this thesis and of each part is given in this section. An abstract and an introduction is provided at the beginning of each chapter.

The CSI availability is a fundamental link between the several chapters of this thesis. For each CSI configuration however, specific problems are treated. In

some cases, practical solutions are proposed and analyzed; in other cases, theoretical performances and fundamental limits are investigated. Our work deals with different "hot" topics in MIMO: Space-Time Coding (STC) and decoding, MIMO channel modeling, capacity studies and MIMO channel estimation. Other works that were done during the thesis period include the use of multiple antennas in the UMTS standard [17, 18, 19, 20], the channel in these cases is either SIMO or MISO (with $N_{tx} = 2$). Being out of the focus of this thesis, these works are not reported here.

1.6.1 Part One: Absence of CSI at Tx (and Perfect CSI at Rx)

This case is the most popular in the literature and has been the first one to be considered *e.g.* [1, 16, 21, 2]. The Tx has no knowledge of the channel, which is modeled as Rayleigh fading MIMO channel, either flat (subsection 1.1.1) or frequency selective (subsection 1.1.3). At the Rx side, the channel is assumed to be perfectly known; in practice this means that there is enough training to provide a good channel estimate.

In chapter 2, we propose a new STC scheme that is based on linear precoding using a MIMO prefilter to exploit diversity. The inputs of the prefilter are called streams, and each symbol from any stream gets spread over space (antennas) and time by the action of the prefilter. This scheme is consequently named Space-Time Spreading (STS). STS is shown to preserve the ergodic capacity and to achieve full rate and full diversity. The optimization of the MIMO prefilter is done in order to maximize the Matched Filter Bound (MFB) and the coding gain. This scheme was the first to show such good properties[1]. In addition we show that this scheme can easily be generalized to the case of a frequency selective channel, preserving the above properties, and being therefore is highly attractive. The optimal decoder of the STS scheme is the ML decoder. However, this detector has a high numerical complexity and offers no possibility for combination with binary channel decoding. This problem is handled in chapter 3 and 4.

In chapter 3, we propose two low complexity non-iterative receiver strategies. Non-ML receivers have in general an impact on the diversity and coding

[1] later other schemes were proposed in [22, 23]

gains, and even on the channel coding setup. The Stripping MIMO Decision Feedback Equalizer (DFE) is a Successive Interference Cancellation (SIC) receiver for the different streams. In fact, the streams are processed successively, each stream is equalized, decoded, and then its contribution gets subtracted from the received signal before processing the next stream. The Stripping DFE receiver is shown to be a very performant receiver for SNR adaptive schemes, especially for the diversity vs. multiplexing tradeoff. In fact, we generalize in this chapter the diversity vs. multiplexing tradeoff of Zheng & Tse to the frequency selective channel with finite delay spread. We show also that the Stripping DFE allows to reach an important portion of this tradeoff. To achieve the optimal diversity vs. multiplexing tradeoff of the Stripping DFE, the study suggests to use stream-dependent rates and hence different constellation sizes. However, for the non-adaptive SNR case, the streams experience different diversity and coding gains, and the binary channel coding is stream dependent and should compensate this non-symmetry. Another receiver strategy is the Conventional MIMO DFE. In this case the streams are decoded jointly and in a causal manner. The past detected symbols contribution are subtracted using feedback. To avoid performance loss due to error propagation, Per Survivor Processing (PSP) can be used. The conventional MIMO DFE receiver achieves the same diversity and coding gain for all streams.

In chapter 4, we propose an iterative turbo receiver strategy. This receiver is a turbo detector as it iterates between a Parallel Interference Cancellation (PIC) linear estimator of the streams (prefilter-channel cascade, seen as an inner code), and a binary channel decoder (binary channel coder, seen as an outer code). This technique has the same complexity as the turbo receiver for the bit interleaved technique applied to MIMO systems or its variant (Threading), and shows an important gain in performance over this last technique. This receiver is also very adapted to exploit multi-block diversity if present and is very flexible, in particular for the case of less receive antennas than transmit antennas ($N_{rx} < N_{tx}$).

1.6.2 Part Two: Partial CSI at Tx (and Perfect CSI at Rx)

In this part the channel knowledge at the Tx side is based on feedback from the Rx, or is due to reciprocity of the uplink and the downlink if both share the same carrier frequency. However, this knowledge is often partial because of the delay in the feedback and the limited (or absence of) calibration of antennas. To study these cases, an adapted channel model will be formulated in chapter 5. In the first case, we will use the pathwise channel model accounting for the decomposition of the channel into a long term part (path array responses, known from the feedback) and the unknown short term part (complex path gains). In the second case, the limited reciprocity will be reflected in the channel model by introducing a random scalar per antenna. For each of these partial CSI channel models, we will analyze the MIMO ergodic capacity, and show that our results present important consequences for the Tx design.

1.6.3 Part Three: Absence of CSI at Rx (and none at Tx)

In this case both Tx and Rx have no CSI. We will take the approach in which the channel will be estimated at the Rx. To this end, we will assume that some training/pilot symbols are present, but not necessarily enough to have a high quality estimate.

In chapter 6, will be considered two popular fading channel models. The first one is the block-fading model and the second is the time selective model. We will show that the average Mutual Information (MI) over a transmission burst can be decomposed into symbol position dependent contributions. The MI component at a certain symbol position optimally combines semi-blind information at that symbol position (exploiting perfect causal input recovery up to that position combined with blind information from the rest (future) of the burst). We will also analyze the asymptotic regime for which we will be able to formulate optimal channel estimates, and to evaluate the capacity loss with respect to the case of perfect CSI at the Rx. Asymptotically, the decrease in MI involves Fisher information matrices corresponding to certain channel estimation problems.

The mutual information decomposition suggests to combine the training and blind parts to estimate the channel. Chapter 7 proposes semi-blind approaches which exploit the information from the two parts. These techniques have a complexity not (immensely) much higher than that of training based techniques. For the flat channel case, the presented technique achieves the Cramèr-Rao Bound. In the frequency selective channel case, we will use a quadratic semi-blind criterion that combines a training based least-squares criterion with a blind criterion based on linear prediction.

Part I

Absence of CSI at TX

Chapter 2

Linear Convolutive Space-Time Precoding

The use of multiple transmit and receive antennas allows to transmit multiple signal streams in parallel and hence to increase capacity. In this chapter we introduce a simple convolutive linear precoding scheme that we call Space-Time Spreading (STS). This scheme spreads the transmitted symbols in time and space, involving spatial spreading and delay diversity. Such linear precoding allows to attain full diversity without loss in ergodic capacity. We show that the generalization of STS to the frequency selective MIMO channel achieve full diversity, and investigate the complexity of the ML detector.

2.1 Introduction

The use of MIMO systems offers a new spatial dimension, and increases the ergodic capacity of the channel by a multiplicative factor equals to the rank of the channel (subsection 1.2.2). It lowers the outage probability by the contribution of $N_{tx}.N_{rx}$ diversity components corresponding to all the channel coefficients in flat channel case. However, the MIMO channel (with imperfect CSI at Tx) suffers from interference between different transmit antennas. The recent attempts that try to exploit this high potential for wireless communication have to make a compromise in order to handle an increase in rate. They need to take advantage of the available diversity to combat fading and destructive interference while keeping an acceptable complexity. Trellis code introduced by Tarokh *et al* [16] takes a SISO-like solution using a binary channel coding designed to map directly on transmit antennas and adapted to the use of the ML decoder (Viterbi decoder). The binary channel code in this technique has to be very powerful to be able to exploit multi antenna diversity, time diversity and to handle high bit rate leading to a fundamental limit on performance under the constraint of complexity. New approaches then appeared aiming to exploit diversity of the channel by linear transformation of symbols. In this category space-time block codes from Orthogonal Design [21] transform the MIMO channel in one SISO coefficient that captures all the diversity and by then use the binary channel codes designed for Gaussian channel. This technique, even if it succeeds to exploit all the available diversity, is far from achieving the potential multiplexing rate.
More recent schemes [22, 23, 24] based on constellation rotating, succeeds to exploit all the diversity without a loss of rate but need to perform a ML decoding leading to an exponential (in N_{tx} and the constellation size) complexity that limits its use. The present chapter presents the STS technique that we have introduced first in [25], this scheme is based on Linear Precoding with a MIMO paraunitary filter, and allows to exploit all the available diversity. As we will see in chapter 3 this scheme can be combined with conventional and non-conventional low complexity receivers. In chapter 4 we show how STS can be combined with the binary Channel Code (CC) to use a turbo detector and to exploit the multi-block diversity if present. These properties allow to avoid the ML detector complexity and make the scheme very attractive.
Approaches proposed so far deal with flat channel, however this is far to be the case in existing mobile systems. In fact, multipaths that arise in mobile

environments leads to frequency selective channel with finite delay spread. The STS approach applies as well for frequency selective channel as for flat channel. It leads to full diversity [26], and is then the first technique that it is shown to exploit full diversity in the frequency selective case (within Time Division Multiple Access context).
In most of this chapter we assume the channel to be flat, however the stated results are valid for selective channels as well unless denoted.

We begin this chapter by presenting the linear prefiltering approach. We then introduce the design criteria: capacity, matched filter bound and pairwise error probability, in order to specify our STS scheme. We study the influence of the circular convolution and the frequency selectivity of the channel. We end the chapter by a discussion on the ML detector for the STS scheme.

Results presented in this chapter were published in [25, 26, 27, 28].

2.2 Linear Prefiltering Approach

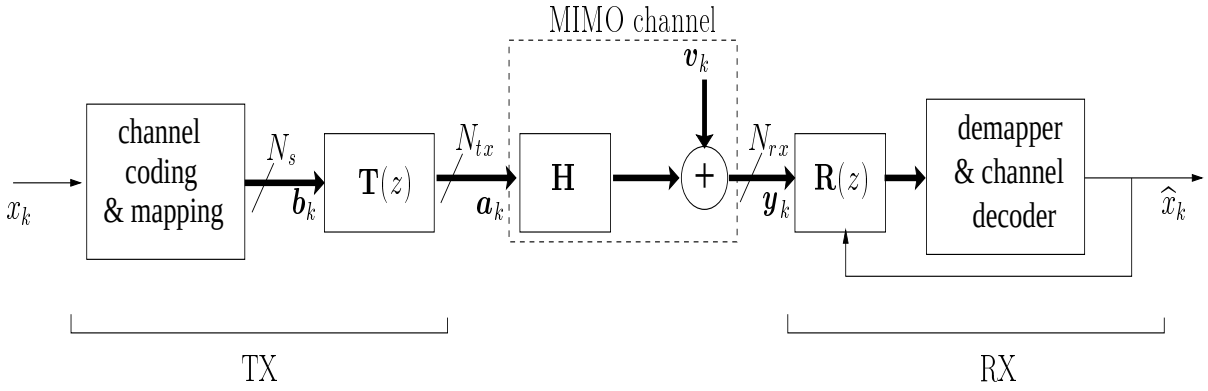

Figure 2.1: General ST coding setup.

A general Space-Time (ST) coding setup is sketched in fig. 2.1. The incoming stream of bits gets transformed to N_s symbol streams through a combination of binary channel coding, interleaving, symbol mapping and demultiplexing. The result is a vector stream of symbols $\boldsymbol{b}_k$ containing N_s symbols per symbol period. The N_s streams then get mapped linearly to the N_{tx} transmit antennas and this part of the transmission is called linear ST precoding. The output is a vector stream of symbols $\boldsymbol{a}_k$ containing N_{tx}

symbols per symbol period. The linear precoding is spatiotemporal since a linear function of $\boldsymbol{b}_k$ may appear in multiple components (space) and multiple time instances (time) of $\boldsymbol{a}_k$. The vector sequence $\boldsymbol{a}_k$ gets transmitted over a MIMO channel $\mathbf{H}$ with N_{rx} receive antennas, leading to the symbol rate vector received signal $\boldsymbol{y}_k$ after sampling. The linear precoding can be considered to be an inner code, while the binary channel coding etc. can be considered to be an outer code. As the number of streams is a factor in the overall code-rate, we shall call the case $N_s = N_{tx}$ the full rate case, while $N_s = 1$ corresponds to the single rate case. Instead of multiple antennas, more general multiple channels can be considered by oversampling, by using polarization diversity or other EM component variations, by working in beam-space, or by considering in-phase and in-quadrature (or equivalently real and complex) components. In the case of oversampling, some excess bandwidth should be introduced at the transmitter, possibly involving spreading which would then be part of the linear precoding.

As we shall see below, channel capacity can be attained by a full rate system without precoding ($\mathbf{T}(z) = I$). In that case, the binary channel coding has to be fairly intense since it has to spread the information contained in each transmitted bit over space (across Tx antennas) and time, as pictured on the left part in fig. 2.2 and [29]. The goal of introducing the linear precoding is to simplify (possibly going as far as eliminating) the binary channel coding part [16]. In the case of linear dispersion codes [30],[31], transmission is not continuous but packet-wise (block-wise). In that case, a packet of T vector symbols $\boldsymbol{a}_k$ (hence a $N_{tx} \times T$ matrix) gets constructed as a linear combination of fixed matrices in which the combination coefficients are symbols b_k. A particular case is the Alamouti code [32] which is a full diversity single rate code corresponding to block length $T = N_{tx} = 2$, $N_s = 1$.

The STS scheme focuses on continuous transmission, large blocks ($T >> 1$), in which linear precoding corresponds to MIMO prefiltering. This linear convolutive precoding can be considered as a special case of linear dispersion codes (making abstraction of the packet boundaries) in which the fixed matrices are time-shifted versions of the impulse responses of the columns of $\mathbf{T}(z)$ (see fig. 2.1). Whereas in the absence of linear precoding, the last operation of the encoding part is spatial demultiplexing (Serial-to-Parallel (S/P) conversion) (see left part of fig. 2.2), this S/P conversion is the first operation in the case of linear precoding (see the right part of fig. 2.2). After the S/P conversion, we have a mixture of binary channel coding, interleaving and symbol mapping, separately per stream. The existing V-BLAST

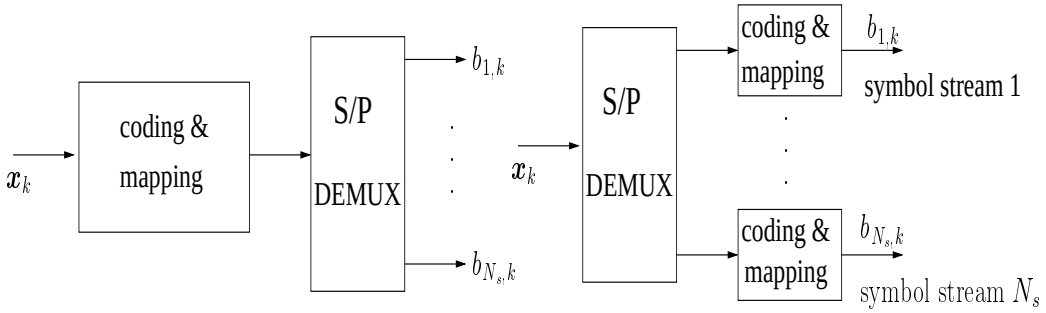

Figure 2.2: Two channel coding, interleaving, symbol mapping and demultiplexing alternatives.

systems are special cases of this approach. V-BLAST is a full rate system with $\mathbf{T}(z) = \mathbf{I}_{N_{tx}}$ which leads to quite limited diversity. The delay transmit diversity used in the UMTS standard is a single rate system with $\mathbf{T}(z) = [1 \; z^{-1}, \ldots, z^{-(N_{tx}-1)}]^T$ which leads to full diversity. We would like to introduce a prefiltering matrix $\mathbf{T}(z)$ without taking a hit in terms of capacity, while achieving full diversity. The MIMO prefiltering will allow us to capture all diversity (spatial, and frequential for channels with delay spread) and will provide some coding gain. The optional binary channel coding per stream then serves to provide additional coding gain and possibly (with interleaving) to capture the temporal diversity (Doppler spread) if there is any. Finally, though time-invariant filtering may evoke continuous transmission, the prefiltering approach is also immediately applicable to block transmission by replacing convolution by circulant convolution.

2.3 Capacity

Consider the MIMO flat AWGN channel

$$\boldsymbol{y}_k = \mathbf{H}\,\boldsymbol{a}_k + \boldsymbol{v}_k = \mathbf{H}\,\mathbf{T}(q)\,\boldsymbol{b}_k + \boldsymbol{v}_k\,, \tag{2.1}$$

where the noise power spectral density matrix is $S_{\boldsymbol{vv}}(z) = \sigma_v^2\,\mathbf{I}_{N_{rx}}$, $q^{-1}\,\boldsymbol{b}_k = \boldsymbol{b}_{k-1}$. The **ergodic capacity** with absence of CSI at the Tx and perfect CSI at the Rx is given by

$$\begin{aligned} C(S_{\boldsymbol{aa}}) &= \mathrm{E}_H \tfrac{1}{2\pi j} \oint \tfrac{dz}{z} \ln\det(I + \tfrac{1}{\sigma_v^2}\,\mathbf{H}\,S_{\boldsymbol{aa}}(z)\,\mathbf{H}^H) \\ &= \mathrm{E}_H \tfrac{1}{2\pi j} \oint \tfrac{dz}{z} \ln\det(I + \tfrac{1}{\sigma_v^2}\,\mathbf{H}\,\mathbf{T}(z)\,S_{\boldsymbol{bb}}(z)\,\mathbf{T}^\dagger(z)\,\mathbf{H}^H) \\ &= \mathrm{E}_H \tfrac{1}{2\pi j} \oint \tfrac{dz}{z} \ln\det(I + \rho\,\mathbf{H}\,\mathbf{T}(z)\,\mathbf{T}^\dagger(z)\,\mathbf{H}^H)\,, \end{aligned} \tag{2.2}$$

where we assume that the channel coding and interleaving per stream leads to spatially and temporally white symbols: $S_{\boldsymbol{bb}}(z) = \sigma_b^2 \, \mathbf{I}_{N_{tx}}$, and $\rho = \frac{\sigma_b^2}{\sigma_v^2} = \frac{SNR}{N_{tx}}$. The channel is modeled as Rayleigh flat fading, see subsection 1.1.1. As we have shown in section 1.2 for such a channel model, the optimization of the capacity subject to the Tx power constraint $\frac{1}{2\pi j} \oint \frac{dz}{z} \mathrm{tr}(S_{\boldsymbol{aa}}(z)) \leq N_{tx}\sigma_b^2$ leads to the requirement of a white (and Gaussian) vector transmission signal $S_{\boldsymbol{aa}}(z) = \sigma_b^2 \, I$. Combined with the whiteness of the vector stream $\boldsymbol{b}_k$ resulting from the channel encoding, this leads to the requirement for the prefilter to be paraunitary: $\mathbf{T}(z)\mathbf{T}^\dagger(z) = \mathbf{I}$ in order to avoid capacity loss.

Motivated by the consideration of diversity also (see below), we propose to use the following paraunitary prefilter

$$\begin{array}{rcl} \mathbf{T}(z) & = & \mathbf{D}(z) \, \mathbf{Q} \\ \mathbf{D}(z) & = & \mathrm{diag}\left\{1, \, z^{-1}, \ldots, z^{-(N_{tx}-1)}\right\}, \quad \mathbf{Q}^H\mathbf{Q} = I \, , \quad |\mathbf{Q}_{ik}| = \frac{1}{\sqrt{N_{tx}}} \, , \end{array} \tag{2.3}$$

where $\mathbf{Q}$ is a (constant) unitary matrix with equal magnitude elements (example of those include: Walsh Hadamard and the Discrete Fourier Transform matrices). Note that for a channel with delay spread, the prefilter can be immediately adapted by replacing the elementary delay z^{-1} by z^{-L} for a channel of length (delay spread) L. For the flat propagation channel $\mathbf{H}$ combined with the prefilter $\mathbf{T}(z)$ in (2.3), symbol stream n ($b_{n,k}$) passes through the equivalent SIMO channel

$$\sum_{i=1}^{N_{tx}} z^{-(i-1)} \mathbf{H}_{:,i} \mathbf{Q}_{i,n} \, , \tag{2.4}$$

which now has memory due to the delay diversity introduced by $\mathbf{D}(z)$. It is important that the different columns $\mathbf{H}_{:,i}$ of the channel matrix get spread out in time to get full diversity; otherwise the streams just pass through a linear combination of the columns, as in V-BLAST, which offers limited diversity. The delay diversity only becomes effective by the introduction of the mixing/rotation matrix $\mathbf{Q}$, which has equal magnitude elements for uniform diversity spreading. The prefilter introduced in [33] is essentially the same as the one in eq.(2.3). However, the symbol stream $\boldsymbol{b}_k$ in [33] is a sub-sampled stream, sub-sampled by a factor N_{tx}. As a result, the system is single rate. The advantage in that case though is that no interference between the rotated streams occurs, which simplifies detection.

2.4 Matched Filter Bound and Diversity

The Matched Filter Bound (MFB) is the maximum attainable SNR for symbol-wise detection, when the interference from all other symbols has been removed. Hence the multi-stream MFB equals the MFB for a given stream. For V-BLAST ($\mathbf{T}(z) = \mathbf{I}$), the MFB for stream n is

$$\mathrm{MFB}_n = \rho ||\mathbf{H}_{:,n}||_2^2 \,, \tag{2.5}$$

hence, diversity is limited to N_{rx}. For the proposed $\mathbf{T}(z) = \mathbf{D}(z)\,\mathbf{Q}$ on the other hand, stream n has MFB

$$\mathrm{MFB}_n = \rho \frac{1}{N_{tx}} \, ||\mathbf{H}||_F^2 \,, \tag{2.6}$$

hence this $\mathbf{T}(z)$ provides the same full diversity $N_{tx}N_{rx}$ for all streams. Larger diversity order leads to larger outage capacity.

2.5 Pairwise Error Probability $\mathbf{P}_e$

This section studies the pairwise error probability of the STS scheme. The study will allow us to complete the specification of the precoding matrix $\mathbf{T}(z)$ and derive some interesting optimality results. We will also study the influence of the introduction of the circular convolution and the effect of frequency selective channels on the error probability.

The received signal is

$$\boldsymbol{y}_k = \mathbf{H}\ \mathbf{T}(q)\ \boldsymbol{b}_k + \boldsymbol{v}_k = \mathbf{H}\ \mathbf{D}(q)\ \mathbf{Q}\ \boldsymbol{b}_k + \boldsymbol{v}_k = \mathbf{H}\ \mathbf{D}(q)\ \boldsymbol{c}_k + \boldsymbol{v}_k \,, \tag{2.7}$$

where $\boldsymbol{c}_k = \mathbf{Q}\,\boldsymbol{b}_k = [c_1(k),\, c_2(k),\, \ldots,\, c_{N_{tx}}(k)]^T$. We consider now the transmission of the coded symbols over a duration of T symbol periods. The accumulated received signal is then

$$\mathbf{Y} = \sigma_b \mathbf{H}\ \mathbf{C} + \mathbf{V} \,, \tag{2.8}$$

where $\mathbf{Y}$ and $\mathbf{V}$ are $N_{rx} \times T$ matrices and $\mathbf{C}$ is $N_{tx} \times T$. The structure of $\mathbf{C}$ is detailed below

$$\mathbf{C} = \frac{1}{\sigma_b} \begin{bmatrix} c_1(1) & \ldots & \ldots & \ldots & \ldots & c_1(T-N_{tx}+1) & 0 & \ldots & 0 \\ 0 & \ddots & \ldots & \ldots & \ldots & \ldots & \ddots & \ddots & \vdots \\ \vdots & \ddots & \ddots & \ldots & \ldots & \ldots & \ldots & \ddots & 0 \\ 0 & \ldots & 0 & c_{N_{tx}}(1) & \ldots & \ldots & \ldots & \ldots & c_{N_{tx}}(T-N_{tx}+1) \end{bmatrix} \tag{2.9}$$

During the duration of the packet only $T - N_{tx} + 1$ symbols vector are transmitted. This results into the loss of a fraction $\frac{N_{tx}-1}{T}$ of the continuous transmission capacity (section 2.3). However we assume the packet length large enough for this loss to be negligible.

Over a Rayleigh flat fading i.i.d. MIMO channel, the probability of deciding erroneously $\mathbf{C}'$ for transmitted $\mathbf{C}$ is upper bounded by (see section 1.4)

$$\mathbf{P}(\mathbf{C} \to \mathbf{C}') \leq \prod_{i=1}^{r}(1 + \frac{\rho}{4}\lambda_i)^{-N_{rx}} \leq (\prod_{i=1}^{r}\lambda_i)^{-N_{rx}}(\frac{\rho}{4})^{-N_{rx}\,r}, \tag{2.10}$$

where r and λ_i are rank and eigenvalues of $(\mathbf{C} - \mathbf{C}')(\mathbf{C} - \mathbf{C}')^H$.
Let i be the time index of the first error, and introduce
$\boldsymbol{e}_k = [e_1(k), e_2(k), \ldots, e_{N_{tx}}(k)]^T = \frac{1}{\sigma_b}(\boldsymbol{c}_k - \boldsymbol{c}'_k)$, then

$$\mathbf{C} - \mathbf{C}' = \begin{bmatrix} 0 & \ldots & 0 & e_1(i) & \ldots & \ldots & \ldots & \ldots \\ \vdots & \ddots & \ddots & \ddots & \ddots & \ldots & \ldots & \ldots \\ 0 & \ldots & \ldots & \ldots & 0 & e_{N_{tx}}(i) & \ldots & \ldots \end{bmatrix}. \tag{2.11}$$

We denote $\mathbf{C} - \mathbf{C}' = [\mathbf{E}_1, \mathbf{E}_2, \mathbf{E}_3]$, where $\mathbf{E}_1$ is the $N_{tx} \times (i-1)$ zeros matrix that contains the first $(i-1)$ columns of $\mathbf{C} - \mathbf{C}'$. $\mathbf{E}_2$ is a $N_{tx} \times N_{tx}$ matrix

$$\mathbf{C} - \mathbf{C}' = \begin{bmatrix} e_1(i) & \ldots & \ldots & . \\ 0 & e_2(i) & \ddots & \vdots \\ \vdots & \ddots & \ddots & \vdots \\ 0 & \ldots & 0 & e_{N_{tx}}(i) \end{bmatrix}, \tag{2.12}$$

and $\mathbf{E}_3$ contains the remaining columns.
Under the condition

$$\prod_{n=1}^{N_{tx}} e_n(i) \neq 0 \tag{2.13}$$

the rank $r = N_{tx}$, and

$$\begin{array}{rcl} \prod_{i=1}^{N_{tx}} \lambda_i & = & \det[(\mathbf{C} - \mathbf{C}')(\mathbf{C} - \mathbf{C}')^H] \\ & = & \det(\mathbf{E}_2\mathbf{E}_2^H + \mathbf{E}_3\mathbf{E}_3^H) \\ & \geq & \det(\mathbf{E}_2\mathbf{E}_2^H) \\ & = & \prod_{n=1}^{N_{tx}} |e_n(i)|^2. \end{array} \tag{2.14}$$

We can then find a new and less tight upper bound on the pairwise error probability

$$\mathbf{P}(\mathbf{C} \to \mathbf{C}') \leq (\prod_{n=1}^{N_{tx}} |e_n(i)|^2)^{-N_{rx}} \,.\, (\frac{\rho}{4})^{-N_{rx}\, N_{tx}} \quad . \tag{2.15}$$

This upper bound is the same as the one in eq.(2.10) iff the i^{th} error is the only error in the block.
Under the condition in eq.(2.13) the full diversity $N_{rx}\, N_{tx}$ is guaranteed, and the coding gain is: $\min\limits_{\boldsymbol{e}_i \neq 0} \prod\limits_{n=1}^{N_{tx}} |e_n(i)|^2$.
The condition of eq.(2.13) is well known in the design of lattice constellations (see [34, 35]), a field based on the theory of numbers.

2.5.1 Choice of Q

Case $N_{tx} = 2^k$
For $N_{tx} = 2^k$, $k \in \mathbb{Z}^+$, a solution that satisfies our criteria of unitary matrix and equal magnitude components of $\mathbf{Q}$, is the Vandermonde matrix

$$\mathbf{Q}^s = \frac{1}{\sqrt{N_{tx}}} \begin{bmatrix} 1 & \theta_1 & \dots & {\theta_1}^{N_{tx}-1} \\ 1 & \theta_2 & \dots & {\theta_2}^{N_{tx}-1} \\ \vdots & \vdots & & \vdots \\ 1 & \theta_{N_{tx}} & \dots & {\theta_{N_{tx}}}^{N_{tx}-1} \end{bmatrix} , \tag{2.16}$$

where the θ_i are the roots of $\theta^{N_{tx}} - j = 0$, $j = \sqrt{-1}$. $\mathbf{Q}^s$ can be also factorized to a product of the N_{tx}-point Inverse Discrete Fourier Transform matrix by a diagonal matrix

$$\mathbf{Q}^s = IDFT_{N_{tx}} \, \mathrm{diag}\,\{1, \theta_1, \theta_1^2, \dots, \theta_1^{N_{tx}-1}\}. \tag{2.17}$$

This choice of the $\mathbf{Q}$ matrix for $N_{tx} = 2^k$ verifies the condition of eq.(2.13), and as we will show in the next subsection allows to achieve the maximum possible coding gain under the constraint of the SPS scheme.
Fig. 2.5.1 shows the STS of one stream, where fig. 2.5.1 shows the STS of all the streams.

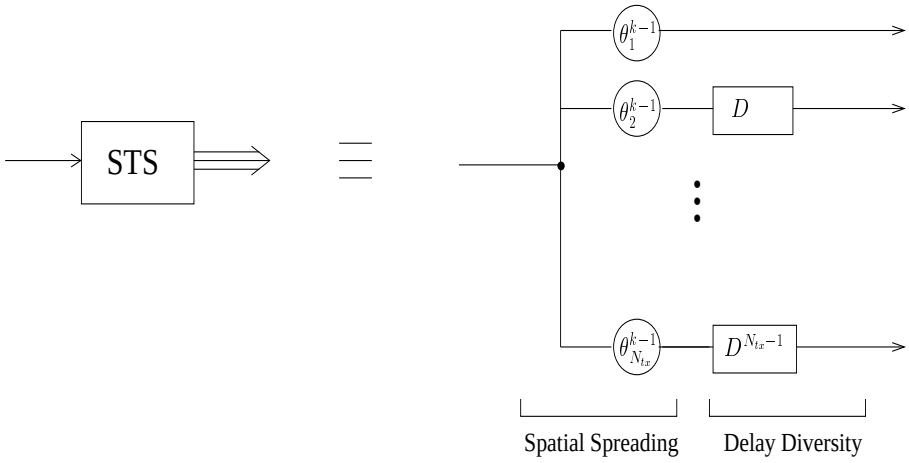

Figure 2.3: STS of one stream

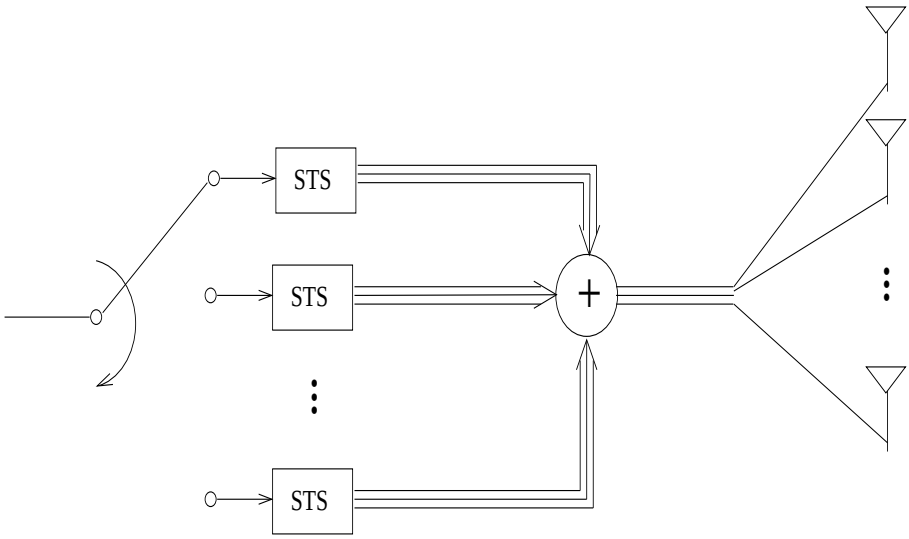

Figure 2.4: STS of all streams

Case $N_{tx} \neq 2^k$
In [22] a solution of the same form of eq.(2.17) has been proposed, with $\theta_1 = e^{j2\pi\frac{p}{P}}$. P is an integer chosen to verifies $\phi(P) = 2mN_{tx}$, where $\phi(P)$ is the Euler number and m is a positive integer. p is selected from $[1, P/N_{tx})$ such that $gcd(P/N_{tx}(n-1)+p, P) = 1$, $\forall n$.
This solution verifies the condition in eq.(2.13). In order to maximize the coding gain, P need to be selected so that m is as small as possible.

2.5.2 Optimality for QAM Constellations in the Case $N_{tx} = 2^k$

For $N_{tx} = 2^k (k \in \mathbb{Z}^+)$, $\mathbf{Q}^s$ leads to the satisfaction of (2.13) (see [34]). It guarantees for any $N_{tx} \times 1$ vector $\mathbf{x}$ from a constellation $\mathcal{X}$ with $\mathbf{x} \in (\mathbb{Z}[j])^{N_{tx}}/0)$ $(\mathbb{Z}[j] = \{a + jb \,|\, a, b \in \mathbb{Z}\})$ and $\mathbf{z} = \mathbf{Q}^s\mathbf{x}$, that $({N_{tx}}^{N_{tx}/2} \prod_{n=1}^{N_{tx}} z_n) \in \mathbb{Z}[j]/0$, and hence

$$\prod_{n=1}^{N_{tx}} |z_n|^2 \geq \left(\frac{1}{N_{tx}}\right)^{N_{tx}} . \tag{2.18}$$

For finite QAM constellations with $(2M)^2$ points, any symbol can be written as: $b_n(i) = d\{(2l-1) + j(2p-1)\}$ where $d \in \mathbb{R}^{+*}$, $l, p \in \{-M+1, -M+2, \ldots, M\}$ and $\sigma_b^2 = \frac{2(4M^2-1)d^2}{3}$.
For $n = 1, \ldots, N_{tx}$, $\frac{1}{\sigma_b}(b_n(i) - b'_n(i)) = \frac{2d}{\sigma_b}(l' + jp')$, $l', p' \in \{-2M+1, -2M+2, \ldots, 2M-1\}$. The first error $\boldsymbol{e}_i = \frac{1}{\sigma_b}\mathbf{Q}^s(\boldsymbol{b}_i - \boldsymbol{b}'_i)$ verifies $\frac{\sigma_b}{2d}\boldsymbol{e}_i \in (\mathbb{Z}[j])^{N_{tx}}/0)$. The lower bound of (2.18), which is valid in fact for any Vandermonde matrix $\mathbf{Q}$ of the form in (2.16) built with roots of a polynomial of order N_{tx} with coefficients in $\mathbb{Z}[j]$ and satisfying a certain number of conditions [34] (hence $\mathbf{Q}^s$ is a special case of this family), becomes

$$\min_{\boldsymbol{e}_i \neq 0} \prod_{n=1}^{N_{tx}} |e_n(i)|^2 \geq \left(\frac{4d^2}{\sigma_b^2}\right)^{N_{tx}} \left(\frac{1}{N_{tx}}\right)^{N_{tx}} = \left(\frac{4d^2}{N_{tx}\sigma_b^2}\right)^{N_{tx}} . \tag{2.19}$$

In what follows, we derive an upper bound for the coding gain for any matrix $\mathbf{Q}$ with normalized columns. The minimal product of errors $\prod_n |e_n(i)|^2$ is upper bounded by a particular error instance corresponding to a single error in the $\boldsymbol{b}$'s, when $\frac{1}{\sigma_b}(\boldsymbol{b}_i - \boldsymbol{b}'_i) = \frac{2d}{\sigma_b}\boldsymbol{w}_{n_0}$, where $\boldsymbol{w}_{n_0}$ is the vector with one in the

n_0^{th} coefficient and zeros elsewhere, hence

$$\min_{\boldsymbol{e}_i \neq 0} \prod_{n=1}^{N_{tx}} |e_n(i)|^2 \leq \left(\frac{4d^2}{\sigma_b^2}\right)^{N_{tx}} \prod_{n=1}^{N_{tx}} |\mathbf{Q}_{n,n_0}|^2 \quad . \tag{2.20}$$

Now, given that $\sum_{n=1}^{N_{tx}} |\mathbf{Q}_{n,n_0}|^2 = 1$, then by applying Jensen's inequality, we get

$$\prod_{n=1}^{N_{tx}} |\mathbf{Q}_{n,n_0}|^2 \leq \left(\frac{1}{N_{tx}}\right)^{N_{tx}} \quad . \tag{2.21}$$

Hence,

$$\min_{\boldsymbol{e}_i \neq 0} \prod_{n=1}^{N_{tx}} |e_n(i)|^2 \leq \left(\frac{4d^2}{\sigma_b^2}\right)^{N_{tx}} \left(\frac{1}{N_{tx}}\right)^{N_{tx}} = \left(\frac{4d^2}{N_{tx}\sigma_b^2}\right)^{N_{tx}} \tag{2.22}$$

is an upper bound for the coding gain for any matrix $\mathbf{Q}$ with normalized columns. Now, the intersection of the sets of matrices that lead to the lower bound (2.19) and the upper bound (2.22) includes the unitary matrix $\mathbf{Q}^s$ given in (2.16), which hence achieves the upper bound on the coding gain: $\min_{\boldsymbol{e}_i \neq 0} \prod_{n=1}^{N_{tx}} |e_n(i)|^2 = \left(\frac{4d^2}{N_{tx}\sigma_b^2}\right)^{N_{tx}} = \left(\frac{6}{(4M^2-1)N_{tx}}\right)^{N_{tx}}$.

Remark 1: Jensen's inequality (2.21) becomes an equality iff all the coefficients $\mathbf{Q}_{n,n_0}$, $n = 1, \ldots, N_{tx}$ have the same module $1/\sqrt{N_{tx}}$. This holds for any $n_0 = 1, \ldots, N_{tx}$. Hence we conclude that a necessary condition on any unitary matrix $\mathbf{Q}$ to maximize the coding gain is to have equal magnitude coefficients. This is equivalent to our condition to achieve the same maximum MFB for all streams (full diversity).

Remark 2: In the case when $N_{tx} \neq 2^k$, the coding gain is closely related to the size of the used QAM constellation, and is in general lower then the upper bound given above.

Remark 3: For QPSK constellation ($M = 1$): $\sigma_b^2 = 2d^2$ and the coding is $\min_{\boldsymbol{e}_i \neq 0} \prod_{n=1}^{N_{tx}} |e_n(i)|^2 = \left(\frac{2}{N_{tx}}\right)^{N_{tx}}$.

Remark 4: To achieve the diversity regime, which corresponds to the SNR region where the error probability decays exponentially with an exponent equals to the full diversity, the following condition needs to be satisfied: $\rho >> 4\frac{1}{\min_i \lambda_i} = \frac{2(4M^2-1)N_{tx}}{3} = 4\left(\frac{1}{codinggain}\right)^{\frac{1}{N_{tx}}}$, this follows from the error

$$\mathbf{C}-\mathbf{C}'=\begin{bmatrix} e_1(1) & e_1(2) & \cdots & \cdots & \cdots & e_1(T-1) & e_1(T) \\ e_2(T) & & & & & & e_2(T-1) \\ \vdots & \ddots & \ddots & \ddots & \ddots & \ddots & \vdots \\ \vdots & \ddots & \ddots & \ddots & \ddots & \ddots & \vdots \\ e_{N_{tx}}(T-N_{tx}+2)\ldots & e_{N_{tx}}(T) & e_{N_{tx}}(1) & \ldots & \ldots & e_{N_{tx}}(T-N_{tx}+1) \end{bmatrix}$$

probability upper bound in (2.10).

In what follow we assume $\mathbf{Q}=\mathbf{Q}^s$.

2.5.3 Circular Convolution

The size of the block is T symbol periods. Even if $T \gg N_{tx}$ the insertion of a guard interval leads to a non-zero $\frac{N_{tx}-1}{T}$ fraction loss in the original rate. A way to avoid this is to use circular convolution (or wrapping). The inconvenience of this though is that the codeword difference matrix $\mathbf{C}-\mathbf{C}'$ is no longer triangular matrice; the study of the coding gain hence gets more involved. For $m > i$, $\boldsymbol{e}(i) \neq 0$ and $\boldsymbol{e}(m) \neq 0$ are two successive errors if they verify one of the following two conditions

- $\forall k \in 1,\ldots,m-i-1,\ \boldsymbol{e}(i+k)=0$
- or $\forall k \in 1,\ldots,T-m+i-1,\ \boldsymbol{e}((m+k)\,mod\,T)=0$

The codeword difference matrix is

Let $F_e = \{(i,m)\,|m > i\,,\ \boldsymbol{e}(i)\,\text{and}\,\boldsymbol{e}(m)\ \text{are 2 successive errors}\}$ be the field of successive errors.
If there exists $(i_0,m_0) \in F_e$ with $m_0 - i_0 \geq N_{tx}$, then in the same way as has been argued in the previous section we can bound the error probability by the single error probability of $e(i_0)$ (equivalently of $e(m_0)$); this yields the same result for diversity and coding gain as stated before. Now, for the event when there are no successive errors separated by more than $N_{tx}-1$, there

are at least $\frac{T}{N_{tx}-1}$ nonzero errors $\boldsymbol{e}(i)$. From (2.10) a bound for the error probability of this event is given by

$$\begin{aligned}
&\mathbf{P}(\mathbf{C} \to \mathbf{C}') \leq \textstyle\prod_{i=1}^{r}(1+\frac{\rho}{4}\lambda_i)^{-N_{rx}} \leq (1+\frac{\rho}{4}\textstyle\sum_{i=1}^{r}\lambda_i)^{-N_{rx}} \\
&= (1+\tfrac{\rho}{4}\tfrac{1}{\sigma_b^2}||\mathbf{C}-\mathbf{C}'||_F^2)^{-N_{rx}} = (1+\tfrac{\rho}{4}\textstyle\sum_{i=0}^{T-1}||\boldsymbol{e}(i)||_2^2)^{-N_{rx}} \\
&\leq (1+\tfrac{\rho}{4}\tfrac{T}{N_{tx}-1}\min_{\boldsymbol{e}(i)\neq 0}||\boldsymbol{e}(i)||_2^2)^{-N_{rx}} \\
&= (1+\tfrac{\rho}{4}\tfrac{T}{N_{tx}-1}\tfrac{6}{4M^2-1})^{-N_{rx}}\,.
\end{aligned} \tag{2.23}$$

The probability of such an error event is less than the upper bound given in (2.15), and hence this bound remains valid when
$SNR \leq \frac{1}{3}N_{tx}^2(4M^2-1)\,T^{\frac{1}{N_{tx}-1}}$. This interval contains the SNR range of interest for most applications.

2.5.4 Frequency Selective Channel Case

The multipaths channel now has a finite delay spread of L symbol periods: $\mathbf{H}(z) = \sum_{i=0}^{L-1}\mathbf{H}_i z^{-i}$. We assume the channel to follow the frequency selective Rayleigh fading MIMO model of subsection 1.1.3. We propose as precoding filter $\mathbf{T}(z) = \mathbf{D}(z^L)\,\mathbf{Q}$. The received signal is then

$$\mathbf{Y} = \sigma_b\,\bar{\mathbf{H}}\,\tau(\mathbf{C}) + \mathbf{V}\,, \tag{2.24}$$

where $\bar{\mathbf{H}} = [\mathbf{H}_0, \mathbf{H}_1, \ldots, \mathbf{H}_{L-1}]$ and $\tau(\mathbf{C})$ is a block Toeplitz matrix with $\mathbf{C}$ as the first block row, where $\mathbf{C}$ is

$$\mathbf{C} = \frac{1}{\sigma_b}\begin{bmatrix}
c_1(1) & \ldots & \ldots & \ldots & c_1(T-N_{tx}L+1) & 0_{1\times(N_{tx}-1)L} \\
0_{1\times L} & c_2(1) & \ldots & \ldots & \ldots & \vdots \\
\vdots & \ddots & \ddots & \ldots & c_{N_{tx}-1}(T-N_{tx}L+1) & 0_{1\times L} \\
 & 0_{1\times(N_{tx}-1)L} & & c_{N_{tx}}(1) & \ldots & c_{N_{tx}}(T-N_{tx}L+1)
\end{bmatrix} \tag{2.25}$$

and

$$\tau(\mathbf{C}) = \begin{bmatrix}
\mathbf{C} & & & 0_{N_{tx}\times(L-1)} & \\
0_{N_{tx}\times 1} & \mathbf{C} & & 0_{N_{tx}\times(L-2)} & \\
\vdots & \ddots & \ddots & \ddots & \vdots \\
 & 0_{N_{tx}\times(L-2)} & & \mathbf{C} & 0_{N_{tx}\times 1} \\
 & 0_{N_{tx}\times(L-1)} & & & \mathbf{C}
\end{bmatrix}. \tag{2.26}$$

Let $\mathbf{S} = \text{diag}\{\sigma_0 I_{N_{tx}}, \ldots, \sigma_{L-1} I_{N_{tx}}\}$, then $\bar{\mathbf{H}}\,\mathbf{S}^{-1}$ has i.i.d. normalized Gaussian elements. The upper bound for the pairwise error probability given in (2.15) is still valid, where r and λ_i are now the rank and eigenvalues of $\mathbf{S}[\tau(\mathbf{C}) - \tau(\mathbf{C}')][\tau(\mathbf{C}) - \tau(\mathbf{C}')]^H \mathbf{S}^H$.
Let us define the permutation matrix $\mathcal{P}$ of size $N_{tx}L \times N_{tx}L$ such that: $\mathcal{P}\boldsymbol{u}_k = \boldsymbol{u}_{p(k)}$ where $\boldsymbol{u}_k$ is the $N_{tx}L \times 1$ vector with 1 in the k^{th} position and zeros elsewhere, $p(k) = ((k-1)\, mod\, N_{tx})\, L + (k\, div\, N_{tx}) + 1$. Permuting the rows of $\tau(\mathbf{C}) - \tau(\mathbf{C}')$ gives

$$\mathcal{P}\left(\tau(\mathbf{C}) - \tau(\mathbf{C}')\right) = \begin{bmatrix} \mathbf{E}_1 & \\ 0_{L\times L} & \mathbf{E}_2 \\ 0_{L\times 2L} & \mathbf{E}_3 \\ \vdots & \vdots \\ 0_{L\times(N_{tx}-1)L} & \mathbf{E}_{N_{tx}} \end{bmatrix}, \tag{2.27}$$

where

$$\mathbf{E}_k = \begin{bmatrix} e_k(1) & e_k(2) & \ldots & \ldots & \ldots & \ldots \\ 0 & \ddots & \ddots & \ldots & \ldots & \ldots \\ \vdots & \ddots & \ddots & \ddots & \ldots & \ldots \\ & 0_{1\times(L-1)} & & e_k(1) & e_k(2) & \ldots \end{bmatrix}. \tag{2.28}$$

As stated for the flat channel case, the pairwise error probability $\mathbf{P}(\mathbf{C} \to \mathbf{C}')$ is upper bounded by

$$\left(\prod_{k=0}^{L-1} \sigma_k^2\right)^{-N_{rx}\, N_{tx}} \left(\prod_{n=1}^{N_{tx}} |e_n(i)|^2\right)^{-N_{rx}\, L} \left(\frac{\rho}{4}\right)^{-N_{rx}\, N_{tx}\, L}, \tag{2.29}$$

where i is the time index of the first error. From the exponent of ρ we can conclude that the proposed scheme exploits the full diversity (degree $N_{rx}\, N_{tx}\, L$).
The $\mathbf{Q}$ matrix proposed in the previous section is still optimal for $N_{tx} = 2^k$, as it maximizes the coding gain $\min\limits_{\boldsymbol{e}(i)\neq 0} \prod\limits_{n=1}^{N_{tx}} |e_n(i)|^2 \sim N^{-N}$ ($N = N_{tx}$: size of $\mathbf{Q}$). An alternative approach to handle the frequency selective channel case uses OFDM and involves a $\mathbf{Q}$ of size $N = N_{tx}\,.\,L$. The increase in size of $\mathbf{Q}$ leads to a substantial decrease in coding gain though.

For the case when we use circular convolution with a block of size T, the same analysis holds as for the case of a flat channel. The upper bound of the

error probability is now valid for $SNR \leq \frac{1}{3} L N_{tx}^2 (4M^2 - 1) T^{\frac{1}{N_{tx} L - 1}}$, where we have assumed a flat power delay profile for the channel:
$\sigma_i^2 = \frac{1}{L}, i = 0, \ldots, L-1$.

2.6 ML Reception

In principle, we can perform Maximum Likelihood reception since the delay diversity transforms the flat channel into a channel with finite memory and increases this memory for frequency selective channel. One can then assume a Viterbi decoder to achieve the ML performances, its number of states being then the product of the constellation sizes of the N_{tx} streams to the power $N_{tx}L - 1$. Hence, if all the streams have the same constellation size $|\mathcal{A}|$, the number of states would be $|\mathcal{A}|^{N_{tx}(N_{tx}L-1)}$, which will be much too large in typical applications. Suboptimal ML reception can be performed in the form of sphere decoding [36]. The complexity of this can still be too large though and therefore suboptimal receiver structures will be considered in the next sections.
Moreover, the use of the ML decoder doesn't allow to take advantage of the presence of the binary channel code in typical application.
For these reasons, less complex receivers are to be considered in the next sections. These receivers are of two types, iterative and non-iterative, they takes advantage of the presence of the binary CC and have some incidence on the transmitter coding setup.

In [37] it is shown that there exist good lattice codes that achieve the optimal diversity vs. multiplexing tradeoff (section 1.5), under the assumption of the use of a sphere decoder. Our STS cheme can be seen as a structured lattice code. Hence a way to show that the STS with ML decoder achieves the optimal diversity vs. multiplexing tradeoff is then to show that STS verifies the conditions of a good lattice code [37].

2.7 Conclusion

In this chapter we have presented our STS scheme based on linear convolutive precoding. We motivated our choice and we have presented the nice properties exhibited by this scheme such as the preservation of the ergodic

capacity, the full diversity and the maximum coding gain. The STS is also easily generalized to the case of frequency selective channels and saves these nice properties.
On the other hand we haven't been able to study the diversity vs. multiplexing tradeoff achieved by STS, when using a ML decoder. A way to do it, is to see this scheme as a structured lattice code and to use elements introduced in [37].

Chapter 3

Non-Iterative Rx: Design Alternatives

In this chapter we propose two types of receiver structure for the Space-Time Spreading (STS) scheme proposed in chapter 2. The first receiver is the Stripping MIMO DFE also called Successive Interference Cancellation. It is a generalization of the V-BLAST Receiver to the STS scheme. For this Rx structure we propose a suitable binary channel coding and investigate the diversity vs. multiplexing tradeoff achieved by the STS scheme. We compare these performances with the optimal tradeoff obtained in the case of frequency selective MIMO channel. Another choice for the receiver is the Conventional MIMO DFE, generalization of the SISO DFE Rx to the MIMO case. In this case we study the impact on the coding and diversity gains and investigate the consequences on the binary channel code.

3.1 Introduction

In the previous chapter we have seen that the optimal ML detector for the STS scheme leads to high numerical complexity. In order to reduce the Rx complexity, this chapter proposes two new non-iterative receivers for STS.
The first one is the Stripping MIMO DFE Rx. It uses a successive detection and cancellation of streams, hence it is a SIC Rx. In each stream the decoder proceeds in a causal manner, detecting and canceling the symbols sequentially. The combination of the Tx and Rx, coding and decoding, decomposes virtually the MIMO channel into N_s parallel SISO frequency selective channels (N_s is the number of used streams). These virtual channels are not equivalent in the sense that they experience different diversity and coding gains. The decomposition of the MIMO channel in several SISO channels allows to use binary channel coding and decoding techniques developed for the SISO case. Another advantage of Stripping is the possibility to achieve high multiplexing rates when adapting each stream encoding to the SNR. Conventional coding and diversity gain criteria are not adapted to the Stripping Rx evaluation. In fact, the performance in the case of a non-adaptive constant rate is dominated by the SISO virtual channel that experiences the lowest diversity. However, Stripping is very suitable for SNR adaptive rates. Performances in this case can be studied using the diversity vs. multiplexing tradeoff criterion introduced by Zheng & Tse in [9]. The generalization of this criterion to the frequency selective case is provided in this chapter, and a comparison of the diversity vs. multiplexing tradeoff achieved by the Stripping MIMO DFE and other popular schemes is given.
The second proposed Rx is the Conventional MIMO DFE. The encoded symbol vectors $\boldsymbol{b}_k$ are now detected sequentially and the streams are hence processed jointly. For the detection of $\boldsymbol{b}_k$ different choices are possible, one of them is the weighted minimum distance detector. For this choice, the different streams experience the same diversity and coding gains. However, in the case of large block length the error propagation can deteriorate the performance. To combat error propagation, the Rx can take advantage of the presence of a binary channel code. Per-Survivor-Processing (PSP) is a convenient way to combine the Conventional MIMO DFE Processing and the decoder of a convolutive binary channel code if present.

This chapter begins by presenting the Stripping MIMO DFE applied to the STS scheme. We then investigate the influence of this Rx processing on the streams capacities. These results allow us to generalize the diversity

vs. multiplexing tradeoff of Zheng & Tse to the frequency selective channel case. We also investigate the tradeoff curve achieved by the Stripping MIMO DFE Rx. In the second part of this chapter we introduce the Conventional MIMO DFE for our scheme, and study the diversity gain achieved by this Rx technique. We finally provide a comparison between the Conventional and the Stripping and present some open problems.

Part of the results presented in this chapter were published in [25, 38, 39]. However, the results on diversity vs. multiplexing tradeoff are recent and not yet published.

3.2 Stripping MIMO DFE (Successive Interference Cancellation) Receiver

This section introduces the Stripping MIMO DFE Rx for our STS scheme. We detail the MMSE ZF and the MMSE design for this Rx. The matrix spectral factorization, the comparison with the V-BLAST and the practical implementation are also discussed.

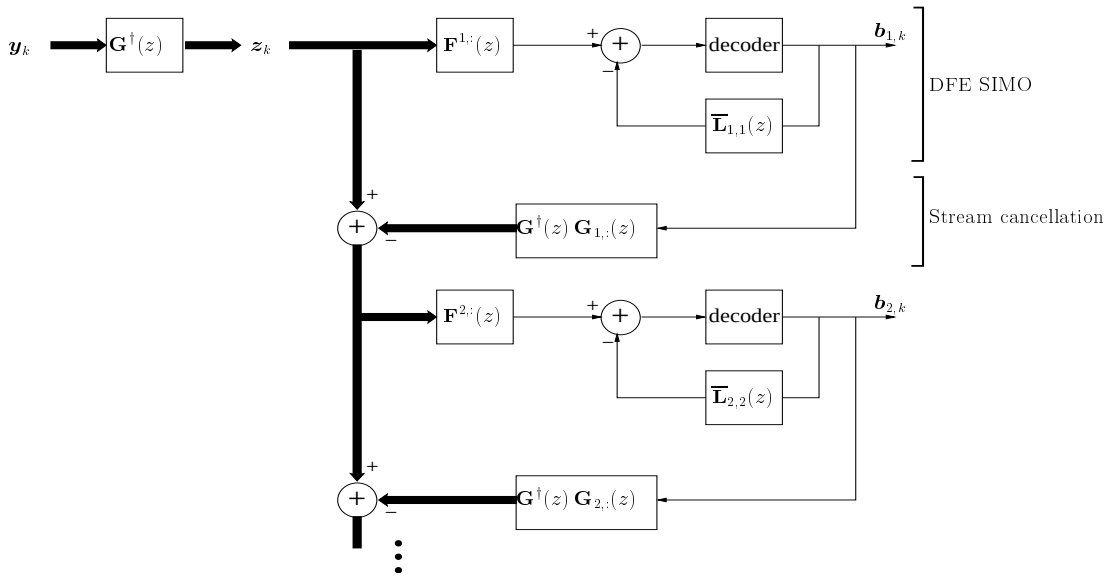

Figure 3.1: Stripping MIMO DFE receiver.

This approach is the extension of the V-BLAST receiver to the spatiotemporal case. In fact, we use a SIC that nulls the interference from the remain-

ing interfering streams, detects and decodes the present stream, cancels its contribution in the received signal and proceeds to the next stream. This allows to incorporate binary channel decoding before cancellation, which leads to the stripping approach of Verdu & Müller or Varanasi & Guess [40, 41, 42]. In fact, the streams need to be encoded independently, to be able to decode them successively.

Let $\mathbf{G}(z) = \mathbf{H}(z)\,\mathbf{T}(z) = \mathbf{H}(z)\,\mathbf{D}(z)\,\mathbf{Q}$ be the cascade transfer function of channel and linear precoding. $\mathbf{Q}$ is a $N_{tx} \times N_s$ matrix containing N_s ($N_s \leq N_{tx}$) first columns of the matrix defined in eq. (2.16). The matched filter Rx is

$$\mathbf{z}_k = \mathbf{G}^\dagger(q)\,\boldsymbol{y}_k = \mathbf{G}^\dagger(q)\,\mathbf{G}(q)\,\boldsymbol{b}_k + \mathbf{G}^\dagger(q)\,\boldsymbol{v}_k = \mathbf{R}^{ZF}(q)\,\boldsymbol{b}_k + \mathbf{G}^\dagger(q)\,\boldsymbol{v}_k\,, \quad (3.1)$$

where $\mathbf{R}^{ZF}(z) = \mathbf{G}^\dagger(z)\,\mathbf{G}(z)$, and the psdf of $\mathbf{G}^\dagger(q)\,\boldsymbol{v}_k$ is $\sigma_v^2\,\mathbf{R}^{ZF}(z)$. The Stripping DFE Rx is then of the form

$$\widehat{\mathbf{b}}_k \;=\; -\;\underbrace{\overline{\mathbf{L}}(q)}_{\text{feedback}}\;\mathbf{b}_k + \;\underbrace{\mathbf{F}(q)}_{\text{feedforward}}\;\mathbf{z}_k\,, \quad (3.2)$$

where

$$\mathbf{I} + \overline{\mathbf{L}}(z) = \mathbf{L}(z) = \begin{bmatrix} L_{11}(z) & 0 & \dots & 0 & 0 \\ L_{21}(z) & L_{22}(z) & 0 & \ddots & 0 \\ \vdots & L_{32}(z) & \ddots & \ddots & \vdots \\ \vdots & \ddots & \ddots & L_{N_s-1,N_s-1}(z) & 0 \\ L_{N_s1}(z) & L_{N_s2}(z) & \dots & L_{N_s,N_s-1}(z) & L_{N_sN_s}(z) \end{bmatrix} \quad (3.3)$$

The feedback $\overline{\mathbf{L}}(z) = \mathbf{L}(z) - \mathbf{I}$ is strictly "causal" [43]. This means that $\mathbf{L}(z)$ is lower triangular, with diagonal elements, $\mathbf{L}_{ii}(z), i = 1, \dots, N_{tx}$, causal, monic[1] and minimum phase[2] [44]. The lower triangular elements $\mathbf{L}_{ij}(z)$, $i > j$, are arbitrary (non causal) transfer functions. W.r.t. a classical causal MIMO spectral factor, the degrees of freedom of the strictly causal upper triangular elements have been transferred to the anticausal part of the lower triangular elements.

By $\mathbf{L}$ we refer in general to a lower diagonal matrix.

[1] A monic SISO filter has first coefficient equal to 1

[2] A rational $f(z)$ is said to be minimum phase if all of its poles and zeros are inside the unit circle

The main difference between the Stripping MIMO DFE and the classical MIMO DFE is the priority between the streams causality and the time causality. In fact, in the Stripping we use first the causality between streams in the processing order then the time causality for the processing inside the stream. In the classical MIMO DFE, the processing order is first done on the basis of the time causality, then on the basis of the streams causality.

Two design critera for feedforward and feedback filters are possible: MMSE ZF and MMSE.

3.2.1 Stripping MMSE ZF DFE Rx Design

In the Zero-Forcing (ZF) design we cancel all the interference. To handle the ZF design the overall channel has to be invertible or equivalently $\mathbf{G}(z)$ must be full column rank. This constrains the number of streams to $N_s \leq \min\{N_{tx}, N_{rx}\}$. In order to satisfy this condition we choose $N_s = \min\{N_{tx}, N_{rx}\}$. Consider the Upper Diagonal Lower (UDL) triangular matrix spectral factorization of $\mathbf{R}^{ZF}(z)$

$$\mathbf{R}^{ZF}(z) \;=\; \mathbf{G}^{\dagger}(z)\mathbf{G}(z) \;=\; \mathbf{L}^{\dagger}(z)\,\Sigma\,\mathbf{L}(z)\,, \tag{3.4}$$

where $\mathbf{L}(z) = \sum_k \mathbf{L}_k\, z^{-k}$ with $\mathrm{diag}\,(\mathbf{L}_0) = I$ (monic), $\Sigma > 0$ is diagonal and constant, and $\mathbf{L}(z)$ is structured as in (3.3).
This factorization is the analog of the UDL factorization applied to $\mathbf{H}^H\mathbf{H}$ in the case of V-BLAST [45]. Then $\mathbf{F}(z) = \Sigma^{-1}\,\mathbf{L}^{-\dagger}(z)$, $\overline{\mathbf{L}}(z) = \mathbf{L}(z) - I$.
The total feedforward filter is a scaled Whitened Matched Filter (WMF)

$$\mathbf{F}(z)\mathbf{G}^{\dagger}(z) = \Sigma^{-\frac{1}{2}}\,\Sigma^{-\frac{1}{2}}\mathbf{L}^{-\dagger}(z)\mathbf{G}^{\dagger}(z) = \Sigma^{-\frac{1}{2}}\,\mathbf{U}(z)\,, \tag{3.5}$$

where $\mathbf{U}(z)$ is a paraunitary, lossless WMF.
The forward filter output

$$\mathbf{F}(q)\,\mathbf{z}_k = \mathbf{L}(q)\,\mathbf{b}_k + \mathbf{F}(q)\mathbf{G}^{\dagger}(q)\,\mathbf{v}_k = \mathbf{L}(q)\,\mathbf{b}_k + \mathbf{e}_k\,, \tag{3.6}$$

where $\mathbf{S_{ee}}(z) = \sigma_v^2\,\Sigma^{-1}$. Assuming perfect feedback to be correct, the actual symbol estimate is

$$\widehat{\mathbf{b}}_k = -\overline{\mathbf{L}}(q)\mathbf{b}_k + \mathbf{F}(q)\mathbf{z}_k = (\mathbf{L}(q) - \overline{\mathbf{L}}(q))\,\mathbf{b}_k + \mathbf{e}_k = \mathbf{b}_k + \mathbf{e}_k\,. \tag{3.7}$$

At the equalizer output n: $\mathrm{SNR}_n = \rho\,\Sigma_{nn}$.
We can detect the $\mathbf{b}_k$ elementwise by backsubstitution (feedback) and symbol-by-symbol detection.
Using coding arguments similar to the one used for the SISO case in [46, 47], the capacity of the n^{th} processed stream is then

$$C_n^{MMSEZF\,DFE} = \ln(1 + \mathrm{SNR}_n^{MMSEZF})\,. \tag{3.8}$$

3.2.2 Stripping MMSE DFE Rx Design

The MMSE design makes a compromise between interference cancellation and noise enhancement. For this design the number of stream is fixed to $N_s = N_{tx}$.
Consider now the backward channel model based on LMMSE [45]

$$\begin{array}{rcl} \widehat{\mathbf{b}}_k = \mathbf{b}_k + \widetilde{\mathbf{b}}_k \Rightarrow \quad \mathbf{b}_k &=& \widehat{\mathbf{b}}_k \;-\; \widetilde{\mathbf{b}}_k \\ &=& \mathbf{S}_{\mathbf{bz}}(q)\,\mathbf{S}_{\mathbf{zz}}^{-1}(q)\,\mathbf{z}_k \;-\; \widetilde{\mathbf{b}}_k\,. \end{array} \tag{3.9}$$

$\widehat{\mathbf{b}}_k$ is the LMMSE estimate of $\mathbf{b}_k$ based on $\mathbf{z}_k$, where

$$\begin{array}{rcl} \mathbf{S}_{\mathbf{bz}}(z) &=& \mathbf{S}_{\mathbf{bb}}(z)\,\mathbf{G}^\dagger(z)\mathbf{G}(z) \\ \mathbf{S}_{\mathbf{zz}}(z) &=& \mathbf{G}^\dagger(z)\mathbf{G}(z)\,\mathbf{S}_{\mathbf{bb}}(z)\,\mathbf{G}^\dagger(z)\mathbf{G}(z) + \sigma_v^2\,\mathbf{G}^\dagger(z)\mathbf{G}(z) \end{array} \tag{3.10}$$

Hence the LMMSE MIMO estimator filter is

$$\mathbf{S}_{\mathbf{bz}}(z)\,\mathbf{S}_{\mathbf{zz}}^{-1}(z) \;=\; \mathbf{R}^{-1}(z)\,, \tag{3.11}$$

with $\mathbf{R}(z) \;=\; \mathbf{G}^\dagger(z)\mathbf{G}(z) + \sigma_v^2\,\mathbf{S}_{\mathbf{bb}}^{-1}(z) \;=\; \mathbf{G}^\dagger(z)\mathbf{G}(z) + \frac{1}{\rho}\,\mathbf{I}$.
Now $\mathbf{b}_k \;=\; \mathbf{R}^{-1}(q)\mathbf{z}_k - \widetilde{\mathbf{b}}_k$. The MMSE estimate satisfies the orthogonality principle

$$\begin{array}{rcl} \mathbf{S}_{\mathbf{bb}}(z) = \mathbf{S}_{\widetilde{\mathbf{b}}\widetilde{\mathbf{b}}}(z) + \mathbf{S}_{\widehat{\mathbf{b}}\widehat{\mathbf{b}}}(z) \Rightarrow \mathbf{S}_{\widetilde{\mathbf{b}}\widetilde{\mathbf{b}}}(z) &=& \mathbf{S}_{\mathbf{bb}}(z) - \mathbf{S}_{\mathbf{bz}}(z)\mathbf{S}_{\mathbf{zz}}^{-1}(z)\mathbf{S}_{\mathbf{zb}}(z) \\ &=& \sigma_v^2\,\mathbf{R}^{-1}(z)\,. \end{array} \tag{3.12}$$

Apply again matrix spectral factorization

$$\mathbf{R}(z) \;=\; \mathbf{L}^\dagger(z)\,\Sigma\,\mathbf{L}(z)\,, \tag{3.13}$$

then $\mathbf{b}_k \;=\; \mathbf{L}^{-1}(q)\,\Sigma^{-1}\,\mathbf{L}^{-\dagger}(q)\,\mathbf{z}_k - \widetilde{\mathbf{b}}_k$. The forward filter output is now

$$\mathbf{F}(q)\,\mathbf{z}_k = \Sigma^{-1}\,\mathbf{L}^{-\dagger}(q)\,\mathbf{z}_k \;=\; \mathbf{L}(q)\,\mathbf{b}_k + \mathbf{L}(q)\,\widetilde{\mathbf{b}}_k = \mathbf{L}(q)\,\mathbf{b}_k + \mathbf{e}_k\,, \tag{3.14}$$

where $\mathbf{S_{ee}}(z) = \sigma_v^2 \mathbf{L}(z)\mathbf{R}^{-1}(z)\mathbf{L}^{\dagger}(z) = \sigma_v^2 \Sigma^{-1}$.
Assuming the feedback to be correct, the actual symbol estimate is then

$$\widehat{\mathbf{b}}_k = -\overline{\mathbf{L}}(q)\mathbf{b}_k + \mathbf{F}(q)\mathbf{z}_k = (\mathbf{L}(q) - \overline{\mathbf{L}}(q))\,\mathbf{b}_k + \mathbf{e}_k = \mathbf{b}_k + \mathbf{e}_k\,. \tag{3.15}$$

At the equalizer output n again: $\mathrm{SNR}_n = \rho\,\Sigma_{nn}$.
In general the following property is verified [46]

$$\Sigma^{MMSE} > \Sigma^{MMSEZF} \;\Rightarrow\; \mathrm{SNR}_n^{MMSE} > \mathrm{SNR}_n^{MMSEZF}\,, \tag{3.16}$$

and even $\mathrm{SNR}_n^{UMMSE} = \mathrm{SNR}_n^{MMSE} - 1 > \mathrm{SNR}_n^{MMSEZF}$ where UMMSE refers to Unbiased MMSE.
The capacity of the n^{th} processed stream under the MMSE design is

$$C_n^{MMSE\,DFE} = \ln \mathrm{SNR}_n^{MMSE} = \ln(1 + \mathrm{SNR}_n^{UMMSE})\,. \tag{3.17}$$

3.2.3 Matrix Spectral Factorization Considerations

Conventionally: $\mathbf{L}(z) = \sum_{k=0}^{+\infty} \mathbf{L}_k\, z^{-k}$, where $\mathbf{L}_0$ is unit diagonal and lower triangular. Consider a generalization with relative delays via linear prediction $\mathbf{P}(z) = \mathbf{L}^{-1}(z)$ applied to $\widetilde{\mathbf{b}}_k$: the conventional linear predictor $\mathbf{P}_c(z)$ applied to

$$\mathbf{Z}(q)\,\widetilde{\mathbf{b}}_k = \begin{bmatrix} \widetilde{b}_{1,k} \\ \widetilde{b}_{2,k-d_1} \\ \vdots \\ \widetilde{b}_{N_{tx},k-d_{N_{tx}-1}} \end{bmatrix} \tag{3.18}$$

leads to the generalized predictor: $\mathbf{P}(z) = \mathbf{Z}^{-1}(z)\,\mathbf{P}_c(z)\,\mathbf{Z}(z)$. We can obtain the triangular spectral factor or predictor as the limiting case as delays $(0 < d_1 < d_2 < \ldots < d_{N_{tx}-1}$, and $d_2 - d_1, d_3 - d_2, \ldots, d_{N_{tx}-1} - d_{N_{tx}-2})$ $\to +\infty$. Strictly lower triangular elements of $\mathbf{P}(z)$ are non-causal Wiener filters to estimate a signal component in terms of the previous signal components, the diagonal elements are SISO prediction error filters of the resulting residual signals [43].
With triangular spectral factors and feedback filters: we detect one symbol stream over all time and then pass to the next symbol stream. With a conventional feedback filter: we process all symbols one after another at a given

time instant, and then pass to the next time instant. The advantage of triangular factors/feedback: the Rx can incorporate binary channel decoding in detection before the use of symbols in feedback. It allows much more reliable feedback and corresponds to the stripping approach of Verdu & Müller or Varanasi & Guess [40, 41, 42]. In practice, a finite relative delays between streams (3.18) suffice.

3.2.4 Stripping DFE and V-BLAST

The Stripping DFE works as follows (see fig. 3.1):
1. A SIMO DFE applied to detect a stream, the design of the SIMO DFE considers the remaining streams as colored noise, this can take advantage of a binary channel code independent for each stream. Binary CCs suitable for frequency selective channels and DFE Rx exist [48, 49].
2. The detected and decoded stream is substracted from the Rx signal and passed on to the next stream.
For the first stream, all remaining streams are interference, whereas the last stream gets detected in the single stream scenario. Hence, triangular MIMO DFE is an extension of V-BLAST to the dynamic case. Here, the dynamics (temporal dispersion) have been introduced by linear convolutive precoding (introducing delay diversity) plus the channel dynamic if present (nonzero delay spread). The advantages are:

- no ordering issue: the streams can be processed in any order,
- higher diversity order.

The ordering issue of the Stripping Rx has been treated in [38]. The second point that considers diversity will be studied in section 3.4.2 dealing with the diversity vs. multiplexing tradeoff.

3.2.5 Practical Implementation of SIC Receiver

Although the complexity of a suboptimal receiver like the Stripping DFE can still be considered quite high, a practical approximation is possible as follows. One should consider the Noise Predictive DFE form [50, 51]. In this case, the forward filter is in fact the Linear MMSE (LMMSE) receiver. The backward filter is then a MIMO noise prediction filter. We suggest to use the triangular MIMO predictor structure for reasons already mentioned.

The complexity of the MIMO predictor can be adjusted by adjusting the prediction order. This gives performance in between that of the LMMSE receiver and that of the DFE. The LMMSE receiver/forward filter can be approximated by polynomial expansion.

3.3 SIC Receiver Processing and Capacity Issues

In this section we study the influence of the proposed Stripping approach. We derive the capacity and investigate the influence of SIC processing on streams capacities for both designs: MMSE and MMSE ZF.

3.3.1 Stripping MMSE DFE Rx

We consider the Stripping receiver with MMSE DFE design of section 3.2.2. This receiver performs a successive detection of the steams. We choose $\{1, 2, \ldots, N_{tx}\}$ to be the order of detection of the streams.
At step n, the receiver has already detected and canceled steams $\{1, 2, \ldots, n-1\}$. We denote $\mathbf{V}_n = [\mathbf{e}_n, \mathbf{e}_{n+1}, \ldots, \mathbf{e}_{N_{tx}}]$, where $\mathbf{e}_n$ is the $N_{tx} \times 1$ vector with 1 at the n^{th} position and all other entries are zeros.
In section 3.2.2 we have shown that the capacity of the n^{th} processed stream denoted $C_n^{MMSE\,DFE}$ satisfies

$$C_n^{MMSE\,DFE} = \ln \mathrm{SNR}_n^{MMSE} = \ln \rho \Sigma_{nn} \,, \tag{3.19}$$

where Σ is the diagonal part of the UDL spectral factorization of $\mathbf{R}(z)$ *i.e.* $\mathbf{L}(z)^\dagger \Sigma \mathbf{L}(z) = \mathbf{R}(z)$. By identification we can show that $([\mathbf{V}_n^H \mathbf{R}(z) \mathbf{V}_n]^{-1})_{11} = \frac{1}{\Sigma_{nn} \mathbf{L}_{nn}(z) \mathbf{L}_{nn}(z)^\dagger}$, where the diagonal coefficient $\mathbf{L}(z)_{nn}$ is causal, monic and minimum phase, hence it satisfies $\frac{1}{2\pi j} \oint \frac{dz}{z} \ln(\mathbf{L}(z)_{nn} \mathbf{L}(z)_{nn}^\dagger) = 0$ (see arguments developed in appendix 3.A, and [44])[3]. The capacity of the n^{th} processed stream is finally

$$C_n^{MMSE\,DFE} = \ln(\rho \Sigma_{nn}) = -\frac{1}{2\pi j} \oint \frac{dz}{z} \ln([\mathbf{V}_n^H \rho \mathbf{R}(z) \mathbf{V}_n]^{-1})_{11} \,. \tag{3.20}$$

[3] $\frac{1}{2\pi j} \oint \frac{dz}{z} \ln(f(z) f(z)^\dagger) = 0$ for $f(z)$ causal, monic and minimum phase

Capacity decomposition :
For a given channel realization

$$\begin{aligned} C(\mathbf{H}) &= \frac{1}{2\pi j}\oint \frac{dz}{z}\ln\det(\mathbf{I}_{N_{tx}}+\rho\,\mathbf{G}^{\dagger}(z)\mathbf{G}(z)) \\ &= \frac{1}{2\pi j}\oint \frac{dz}{z}\ln\det(\rho\ \mathbf{R}(z)) \\ &= \frac{1}{2\pi j}\oint \frac{dz}{z}\ln\det(\rho\,\mathbf{L}(z)^{\dagger}\Sigma\mathbf{L}(z)) \\ &= \ln\det(\rho\,\Sigma^{MMSE}) \\ &= \sum_{n=1}^{N_{tx}} C_n^{MMSE\,DFE}, \end{aligned} \tag{3.21}$$

where in the third equality we replaced $\mathbf{R}(z)$ by its UDL matrix spectral factorization, and in the fourth we exploit the fact that $\det(\mathbf{L}(z)) = \prod_{n=1}^{N_{tx}} \mathbf{L}_{nn}(z)$ is causal, monic and minimum phase.
This shows that the total capacity is the sum of the capacities of N_{tx} streams output, and hence Stripping with a MMSE DFE design preserves the capacity.

Bounds on the stream-wise capacities for the MMSE design:
The following lemma provides useful bounds on the capacities.
Lemma 1: The n^{th} processed stream capacity in the MMSE design is bounded by

$$c_n^1 \le C_n^{MMSE\,DFE} - \ln(\frac{1}{L}+\rho s_{N_{tx}(L-1)+n}) \le c_n^2\,, \tag{3.22}$$

where

$$c_n^1 = \begin{cases} \ln(\frac{1}{N_{tx}\gamma_{N_{tx}L}}) + (N_{tx}-n)\ln\left(\frac{N_{tx}-n}{(N_{tx}-n+1)\gamma_{N_{tx}L}}\right) & ,\ 1\le n\le N_{tx}-1 \\ \ln(\frac{1}{N_{tx}\gamma_{N_{tx}L}}) & ,\ n=N_{tx} \end{cases} \tag{3.23}$$

$$c_n^2 = \begin{cases} (N_{tx}-n)\ln\left(\frac{\gamma_{N_{tx}L}(N_{tx}-n+1)}{N_{tx}-n}\right)+\ln L & ,\ 1\le n\le N_{tx}-1 \\ \ln L & ,\ n=N_{tx} \end{cases} \tag{3.24}$$

$(s_n,\ n=1,\ldots,N_{tx}L)$ are the eigenvalues of $\bar{\mathbf{H}}^H\bar{\mathbf{H}}$ sorted in the increasing order where $\bar{\mathbf{H}}=[\mathbf{H}_0,\mathbf{H}_1,\ldots,\mathbf{H}_{L-1}]$. $\gamma_{N_{tx}L} = \sum_{l=0}^{N_{tx}L-1}\left(\begin{array}{c} l \\ N_{tx}L-1 \end{array}\right)^2$.

Proof : see appendix 3.B.

3.3.2 Stripping MMSE ZF DFE Rx

As denoted in subsection 3.2.1 the number of streams for this case is $N_s = \min\{N_{tx}, N_{rx}\}$. Again the processing order of the streams is $\{1, 2, \ldots, N_s\}$, and denote $\mathbf{V}_n = [\mathbf{e}_n, \mathbf{e}_{n+1}, \ldots, \mathbf{e}_{N_s}]$ where $\mathbf{e}_n$ is the $N_s \times 1$ vector with 1 at the n^{th} position and all other entries are zeros.
Using the same arguments as for the case of MMSE DFE design we can show that

$$\ln(\mathrm{SNR}_n^{MMSEZF}) = -\frac{1}{2\pi j} \oint \frac{dz}{z} \ln([\mathbf{V}_n^H \rho \mathbf{R}^{ZF}(z) \mathbf{V}_n]^{-1})_{11} \,. \tag{3.25}$$

Recall that $C_n^{MMSEZFDFE} = \ln(1 + \mathrm{SNR}_n^{MMSEZF})$, then by proceeding as in the MMSE case we can bound the capacity of each steam.

Bounds on the stream-wise capacities for the MMSE ZF design:
The following lemma gives the desired results.
Lemma 2: The n^{th} processed stream SNR in the MMSE ZF design is bounded by

$$c_n^1 \leq \ln(\mathrm{SNR}_n^{MMSEZF}) - \ln(\rho s_{N_{tx}L - N_s + n}) \leq c_n^2 \,, \tag{3.26}$$

and the capacity is bounded by

$$\ln(1 + e^{c_n^1} \rho s_{N_{tx}L - N_s + n}) \leq C_n^{MMSEZFDFE} \leq \ln(1 + e^{c_n^2} \rho s_{N_{tx}L - N_s + n}) \,, \tag{3.27}$$

where now

$$c_n^1 = \begin{cases} \ln(\frac{1}{N_{tx}\gamma_{N_{tx}L}}) + (N_s - n) \ln\left(\frac{N_s - n}{(N_s - n + 1)\gamma_{N_{tx}L}}\right) & , \; 1 \leq n \leq N_s - 1 \\ \ln(\frac{1}{N_{tx}\gamma_{N_{tx}L}}) & , \; n = N_s \end{cases} \tag{3.28}$$

$$c_n^2 = \begin{cases} (N_s - n) \ln\left(\frac{c_{N_{tx}L}(N_s - n + 1)}{N_s - n}\right) + \ln L & , \; 1 \leq n \leq N_s - 1 \\ \ln L & , \; n = N_s \end{cases} \tag{3.29}$$

Again, $(s_n,\ n = 1, \ldots, N_{tx}L)$ are the eigenvalues of $\bar{\mathbf{H}}^H\bar{\mathbf{H}}$ sorted in increasing order where $\bar{\mathbf{H}} = [\mathbf{H}_0, \mathbf{H}_1, \ldots, \mathbf{H}_{L-1}]$.

Proof : To bound the SNR we proceed similarly as for the MMSE case (see appendix 3.B) but we apply the all reasoning to $\ln(\mathrm{SNR}_n^{MMSEZF})$ (3.25) rather then $C_n^{MMSE\,DFE}$(3.20). We then use the obtained bounds to express the capacity (3.8). □

3.4 Diversity vs. Multiplexing Tradeoff

In this section we seek to study the diversity vs. multiplexing tradeoff (as defined by Zheng & Tse). Their work was applied to the MIMO flat case, we will generalize this notion to the frequency selective case and then we study the tradeoff achieved by the Stripping DFE.

3.4.1 Optimal Tradeoff Curve for the Frequency Selective Channel

For the flat channel, it was shown in Theorem 2 of [9] that for $T \geq N_{rx} + N_{tx} - 1$ the optimal tradeoff curve of the error probability $d^*(r)$ (section 1.5) corresponds to $d_{out}(r)$, where the outage probability satisfies $P_{out}(r \ln \rho) \doteq \rho^{-d_{out}(r)}$.
The equality

$$d^*(r) = d_{out}(r) \tag{3.30}$$

can be generalized to the frequency selective case by using the result derived in subsection 1.2.4. In fact, we have shown that the instantaneous capacity of a finite block length transmission, $C_T(\mathbf{H})$, has asymptotically for large block length T the same distribution as $C(\mathbf{H})$, which is the instantaneous capacity in the continuous transmission. This can be used in the proof of Theorem 2 in [9] to generalize eq. (3.30) to the case of frequency selective channel with $T >> L$.
In the sequel we study the outage capacity which will allow us to find the optimal tradeoff curve $d^*(r) = d_{out}(r)$.

For simplicity we assume that $\bar{\mathbf{H}} = [\mathbf{H}_0, \mathbf{H}_1, \ldots, \mathbf{H}_{L-1}]$ follows a Rayleigh flat fading MIMO distribution (subsection 1.1.1). This constrains the power

delay profile to be flat $\sigma_0 = \sigma_1 = \ldots = \sigma_{L-1} = 1$. The results derived below apply also for general power delay profile as long as $\sigma_l \neq 0$, $l = 0, \ldots, L-1$ (bounded away from zero). $\bar{\mathbf{H}}\bar{\mathbf{H}}^H$ has $m = \min\{N_{rx}, N_{tx}L\}$ nonzero eigenvalues $\mu_1 \leq \mu_2 \leq \ldots \leq \mu_m$. These eigenvalues follow the Wishart distribution given in subsection 1.1.1, in which $\min\{N_{rx}, N_{tx}\}$ is replaced by $\min\{N_{rx}, N_{tx}L\}$ and $\max\{N_{rx}, N_{tx}\}$ by $\max\{N_{rx}, N_{tx}L\}$. We observe that $\mu_n = s_{N_{tx}L-m+n}$, for $n = 1, \ldots, m$ where $(s_n,\ n = 1, \ldots, N_{tx}L)$ are all the eigenvalues of $\bar{\mathbf{H}}\bar{\mathbf{H}}^H$ (including zeros) that were introduced before.

We continue in the foot steps of [9] and use the following variable change $\mu_n \triangleq \rho^{-\alpha_n}$. At high SNR we have $(1 + \rho\mu_n) \doteq \rho^{(1-\alpha_n)^+}$, where $(x)^+$ denotes $\max\{0, x\}$ and the symbol $\doteq$ was introduced in section 1.5.
We denote $p = \min\{N_{rx}, N_{tx}\}$, $q = \max\{N_{rx}, N_{tx}\}$.
From the bounds given in eq. (3.22) and (3.27), we can show that

$$e^{C^{MMSE\,ZF\,DFE}_{p-N_{tx}+n}} \doteq e^{C^{MMSE\,DFE}_{n}} \doteq \rho^{(1-\alpha_{(m-N_{tx}+n)})^+} \quad \text{for } (N_{tx}-p+1) \leq n \leq N_{tx}\,. \tag{3.31}$$

If $N_{rx} \leq N_{tx}$: $p = N_{rx}$ and $s_{N_{tx}(L-1)+n} = 0$ for $1 \leq n \leq N_{tx} - N_{rx}$. Then for $1 \leq n \leq N_{tx} - p$ $C^{MMSE\,DFE}_n$ is bounded by a constant (3.22)

$$e^{C^{MMSE\,DFE}_{n}} \doteq 1 \quad \text{for } 1 \leq n \leq N_{tx} - p\,. \tag{3.32}$$

Theorem 1: For a channel with a frequency selective Rayleigh fading model (subsection 1.1.3), let the data rate be $R = r \ln \rho$ $(0 \leq r \leq p = \min\{N_{rx}, N_{tx}\})$. Then the outage probability satisfies

$$P_{out}(r \ln \rho) \doteq \rho^{-d_{out}(r)}\,, \tag{3.33}$$

where $d_{out}(r)$ is given by the piecewise-linear function connecting the points $(k, d_{out}(k))$, $k = 0, 1, \ldots, p$, where

$$d_{out}(k) = (Lq - k)(p - k)\,. \tag{3.34}$$

Recall that $p = \min(N_{rx}, N_{tx})$, $q = \max(N_{rx}, N_{tx})$. In particular $d^*_{max} = L.N_{tx}.N_{rx}$ and $r^*_{max} = \min(N_{rx}, N_{tx})$.

Proof : see appendix 3.C.

As stated above, for $T >> L$ this theorem gives the optimal tradeoff of the frequency selective MIMO fading channel: $d^*(r) = d_{out}(r)$ (see fig. 3.2 for $N_{tx} \leq N_{rx}$).

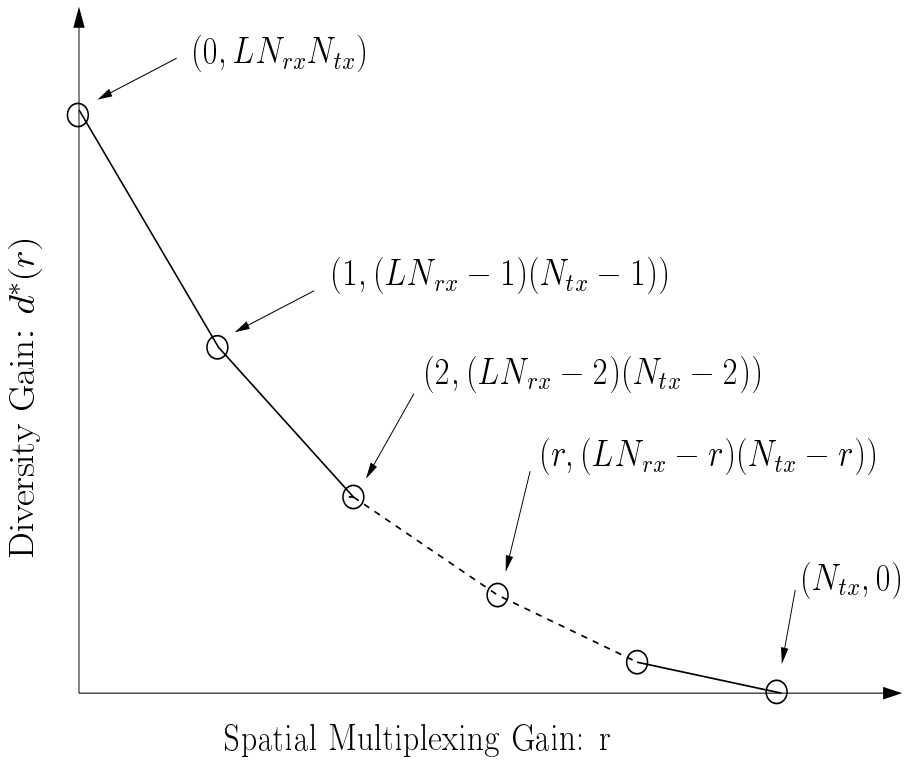

Figure 3.2: Diversity vs. multiplexing optimal tradeoff for frequency selective channel with $N_{tx} \leq N_{rx}$.

3.4.2 Tradeoff Curve for the SIC Rx

We will first study the outage probability behavior of the SIC Rx applied to our STS scheme. Then we show that the Stripping DFE Rx coupled with a QAM constellation achieves this upper bound tradeoff curve for any block length as long as $T >> N_{tx}L$.

An outage event occurs if the capacity of one of the streams is less then the allocated rate, when the previous streams were correctly decoded. The outage probability of a SIC receiver that uses N_s streams and for a data rate R is then

$$P_{out}^{SIC}(R) = \min_{R=\sum_{k=1}^{N_s} R_k} \sum_{i=1}^{N_s} P\left(C_i < R_i, C_1 \geq R_1, C_2 \geq R_2, \ldots, C_{i-1} \geq R_{i-1}\right) , \tag{3.35}$$

where C_i is the capacity of the i^{th} stream.
As we have seen before, the capacity is achieved by the MMSE DFE receiver, *i.e.* $C_i = C_i^{MMSE\,DFE}$. The outage probability as formulated is the minimum over all the different allocations R_i, $i = 1, \ldots, N_s$.
In the multiplexing case the total rate is $R = r \ln \rho$ and the different streams rates are $R_i = r_i \ln \rho$, $r_i \geq 0$, $i = 1, \ldots, N_s$. We then write $P_{out}^{SIC}(r \ln \rho) \doteq \rho^{-d_{out}^{SIC}(r)}$.
The following lemma is a preliminary result for the study of the outage:

Lemma 3: The outage probability characteristic for SIC: $d_{out}^{SIC}(r)$ is achieved by transmitting only on $N_s = p = \min\{N_{rx}, N_{tx}\}$ streams. And is equally achieved by the MMSE DFE and the MMSE ZF DFE receivers.

Proof : We have shown in eq. (3.22) that for $1 \leq i \leq N_{tx} - p$, $C_i^{MMSE\,DFE}$ is upper bounded by a constant. Hence $\lim_{\rho \to \infty} P(C_i^{MMSE\,DFE} < r_i \ln \rho) = 1$ for $r_i > 0$, and the outage probability is then achieved iff $r_i = 0$ for $1 \leq i \leq N_{tx} - p$. This last condition is equivalent to the use of $N_s = p = \min\{N_{rx}, N_{tx}\}$. On the other hand and as we have seen in eq. (3.31) for $1 \leq i \leq p$:

$$e^{C_i^{MMSEZF\,DFE}} \doteq e^{C_{N_{tx}-p+i}^{MMSE\,DFE}} \doteq \rho^{(1-\alpha_{(m-p+i)})^+}, \tag{3.36}$$

where $m = \min\{N_{rx}, N_{tx}L\}$. The behavior of the MMSE DFE and the MMSEZF DFE streams capacities is then the same for large SNR. As a consequence, it is sufficient to study the outage probability of the MMSEZF DFE Rx to find $d_{out}^{SIC}(r)$. □

Theorem 2: For a channel with a frequency selective Rayleigh fading model (subsection 1.1.3), the outage probability of the SIC Rx for the STS scheme satisfies

$$P_{out}^{SIC}(r \ln \rho) \doteq \rho^{-d_{out}^{SIC}(r)}, \tag{3.37}$$

where $d_{out}^{SIC}(r)$ is given by the piecewise-linear function connecting the points $(r_k^t, d_{out}^{SIC}(r_k^t))$, $k = 0, \ldots, p$,

$$\begin{aligned} r_k^t &= k - (m-k)(n-k) \sum_{i=1}^{k} \frac{1}{(m-k+i)(n-k+i)} \quad , \; k = 0, \ldots, p-1 \\ r_k^t &= p \quad , \; k = p \end{aligned} \tag{3.38}$$

and

$$\begin{array}{rcll} d_{out}^{SIC}(r_k^t) & = & (m-k)(n-k) & , \ k=0,\ldots,p-1 \\ d_{out}^{SIC}(r_k^t) & = & 0 & , \ k=p \end{array} \tag{3.39}$$

where $m = \min\{N_{rx}, N_{tx}L\}$, $n = \max\{N_{rx}, N_{tx}L\}$ and $p = \min\{N_{rx}, N_{tx}\}$. For the corresponding optimal rate allocation, and for $r \in [r_k^t, r_{k+1}^t]$, $k = 0,\ldots,p-1$, only $k+1$ streams are used.
The nonzero multiplexing rates are r_i, $p-k \leq i \leq p$, and satisfy

$$\begin{cases} (m-k)(n-k)(1-r_{p-k}) = (m-k+1)(n-k+1)(1-r_{p-k+1}) = \ldots = mn(1-r_p) \\ \sum_{i=p-k}^{p} r_i = r \end{cases} \tag{3.40}$$

Proof : see appendix 3.D.
The following theorem shows that the Stripping MMSE ZF DFE Rx, with adapted encoding constellations achieves the outage tradeoff $d_{out}^{SIC}(r)$.

Theorem 3: For block length T, $T >> N_{tx}L$, the use of QAM constellations with adapted rates by stream, allows the Stripping MMSE ZF DFE Rx applied for the STS scheme to achieve a diversity vs. multiplexing tradeoff equal to the outage tradeoff $d_{out}^{*,SIC}(r)$.

$$d^{*,SIC}(r) = d_{out}^{SIC}(r)\,. \tag{3.41}$$

Proof : see appendix 3.E.

Consequence of Theorem 3

- Theorem 3 gives a simple coding/decoding scheme (STS, QAM/ Stripping MIMO DFE), and shows that it achieves a high performance in term of the diversity vs. multiplexing tradeoff. In particular this scheme achieves the maximum rate and the maximum diversity $d_{max}^{*,SIC} = d_{max}^{*} = L.N_{tx}.N_{rx}$ and $r_{max}^{*,SIC} = r_{max}^{*} = \min(N_{rx}, N_{tx})$.
- Eq. (3.31) shows that the optimal diversity vs. multiplexing tradeoffs achieved by the Stripping MMSE ZF DFE and MMSE DFE design are the same.

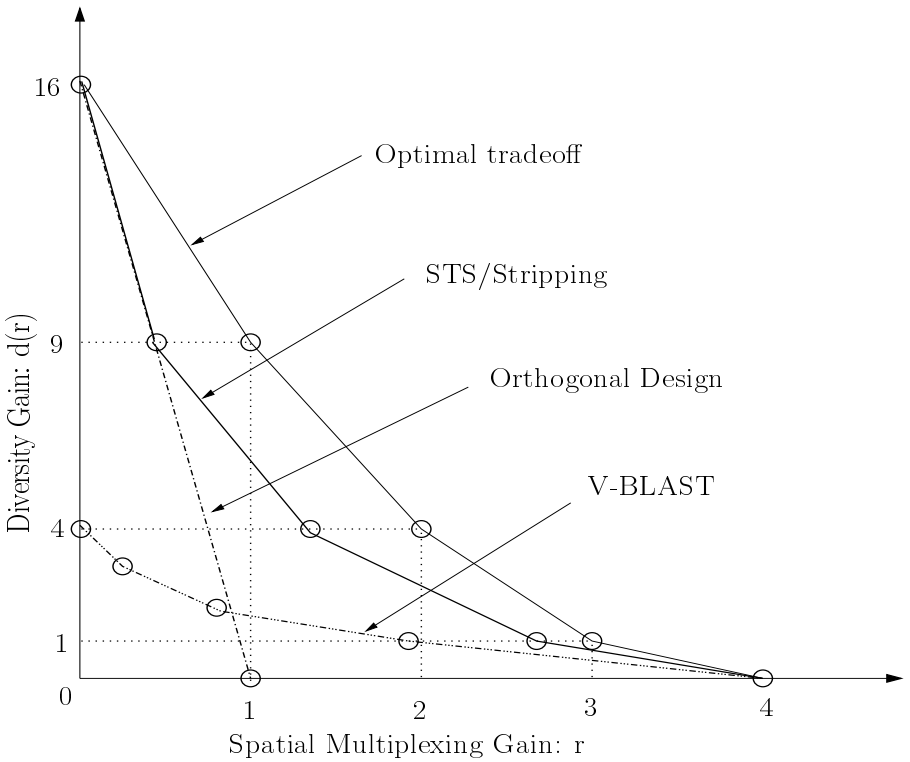

Figure 3.3: Diversity vs. multiplexing tradeoff of different schemes. $N_{tx} = N_{rx} = 4$, $L = 1$.

- To improve the performance of the scheme, and to limit the error propagation, we can substitute the stream-wise decision feedback by a Viterbi decoder. If a binary channel code is used, we can also couple the stream-wise DFE equalizer with a PSP channel decoder.

- STS combined with the Stripping DFE Rx and SNR adaptive QAM constellation outperforms the popular schemes of orthogonal design and V-BLAST (see fig. 3.3, $N_{tx} = N_{rx} = 4$, $L = 1$). In fact, the performances of these two schemes have been studied in [9] for the case of flat channel. The orthogonal design achieves maximum diversity but is limited to a multiplexing rate of 1 (the multiplexing rate that can be achieved is even smaller then 1 for $N_{tx} > 2$). Whereas the V-BLAST can achieve the maximum rate but has poor diversity. The STS/Stripping achieves better diversity vs. multiplexing tradeoff for

any rate or diversity. In particular it achieves the two extreme points of r^*_{max} and d^*_{max}.

3.5 Conventional MIMO DFE Receiver

The different streams in the Stripping receiver enjoy different diversity gains. For fixed non-adaptive rates as it is the case in the conventional design of STC (section 1.4) the performance is dominated by the stream that experiences the lowest diversity. To avoid this situation we propose a new receiver that treats the different streams equally. The considered Rx is the classical MIMO decision feedback equalizer, in which the symbol vectors $\boldsymbol{b}_k$ are processed sequentially in time (see fig. 3.4).

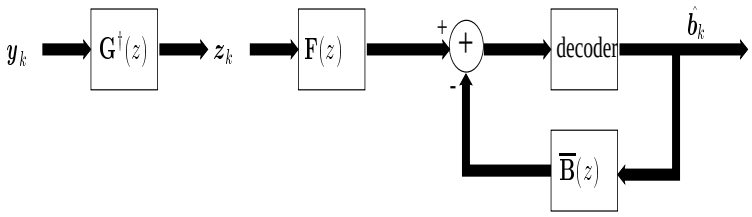

Figure 3.4: Convetional MIMO DFE receiver

The DFE output is then

$$\widehat{\mathbf{b}}_k \;=\; -\;\underbrace{\overline{\mathbf{B}}(q)}_{\text{feedback}}\;\mathbf{b}_k + \;\underbrace{\mathbf{F}(q)}_{\text{feedforward}}\;\mathbf{z}_k\,, \tag{3.42}$$

where the feedback filter $\overline{\mathbf{B}}(z) = \sum_{i\geq 1} \mathbf{B}_i z^{-i}$ is such that $\mathbf{B}(z) = I + \overline{\mathbf{B}}(z)$ is causal, monic and minimum phase. We shall consider the MSE as filter design criterion.

3.5.1 Conventional MMSE MIMO DFE Rx

As for the Stripping Rx (section. 3.2) the ZF and MMSE design hold. We detail the MMSE design below.

The linear MMSE estimate satisfies

$$\mathbf{b}_k \;=\; \widehat{\mathbf{b}}_k - \widetilde{\mathbf{b}}_k \;=\; \mathbf{S}_{\mathbf{bz}}(q)\,\mathbf{S}_{\mathbf{zz}}^{-1}(q)\,\mathbf{z}_k - \widetilde{\mathbf{b}}_k\,. \tag{3.43}$$

The development is the same as in section 3.2.2 but using the minimum and maximum phase factorization of $\mathbf{R}(z) = \mathbf{G}^{\dagger}(z)\mathbf{G}(z) + \frac{1}{\rho}\,I$ (see [52]). Let $\mathbf{B}(z)$ be the unique causal, monic minimum phase factor of $\mathbf{R}(z)$, then

$$\mathbf{R}(z) \;=\; \mathbf{B}^{\dagger}(z)\,\mathbf{M}\,\mathbf{B}(z). \tag{3.44}$$

where $\mathbf{M}$ is a constant positive definite hermitian matrix.
Then $\mathbf{b}_k \;=\; \mathbf{B}^{-1}(q)\,\mathbf{M}^{-1}\,\mathbf{B}^{-\dagger}(q)\,\mathbf{z}_k - \widetilde{\mathbf{b}}_k$.
By choosing $\mathbf{F}(q) = \mathbf{M}^{-1}\mathbf{B}^{-\dagger}(q)$, we get

$$\begin{array}{rcl} \mathbf{F}(q)\,\mathbf{z}_k & = & \mathbf{M}^{-1}\,\mathbf{B}^{-\dagger}(q)\,\mathbf{z}_k \\ & = & \mathbf{B}(q)\,\mathbf{b}_k + \mathbf{B}(q)\,\widetilde{\mathbf{b}}_k \\ & = & \mathbf{B}(q)\,\mathbf{b}_k + \mathbf{e}_k \\ & = & \mathbf{b}_k + \overline{\mathbf{B}}(q)\,\mathbf{b}_k + \mathbf{e}_k\,, \end{array} \tag{3.45}$$

where $\mathbf{S}_{\mathbf{ee}}(z) \;=\; \mathbf{B}(z)\mathbf{R}^{-1}(z)\mathbf{B}^{\dagger}(z) \;=\; \sigma_v^2\,\mathbf{M}^{-1}$.
$\overline{\mathbf{B}}(z) \;=\; \mathbf{B}(z) - I$ is tightly related to the MIMO prediction error filter $\mathbf{P}(z)$ of the spectrum $\mathbf{R}(z)$, $\mathbf{P}^{\dagger}(z)\mathbf{R}(z)\mathbf{P}(z) \;=\;$ Constant Matrix. Indeed, $\mathbf{P}(z) = \mathbf{B}^{-1}(z)$ obviously. The following Theorem gives $\mathbf{B}(z)$ in the case of MIMO flat channel.

Theorem 4: For MIMO flat channel the feedback filter is

$$\mathbf{B}(z) = \mathbf{T}(z)^{\dagger}\,\mathbf{L}^{H}\,\mathbf{T}(z)\,, \tag{3.46}$$

for which corresponds

$$\mathbf{M} = \mathbf{Q}^{H}\mathbf{D}\mathbf{Q}\,, \tag{3.47}$$

where $\mathbf{L}$ and $\mathbf{D}$ results from the LDU decomposition of $\mathbf{H}^{H}\mathbf{H} + \frac{1}{\rho}I = \mathbf{L}\,\mathbf{D}\,\mathbf{L}^{H}$.

Proof :
We need to show that
$\mathbf{B}(z) = \mathbf{T}(z)^{\dagger}\,\mathbf{L}^{H}\,\mathbf{T}(z) = \mathbf{Q}^{H}\,\mathbf{D}(z)^{\dagger}\,\mathbf{L}^{H}\,\mathbf{D}(z)\,\mathbf{Q}$
is minimum phase causal monic filter and satisfies $\mathbf{B}^{-\dagger}(z)\mathbf{R}(z)\mathbf{B}^{-1}(z) = \mathbf{M}$.

$\mathbf{L}^{H}$ is upper triangular, then due to the diagonal structure of $\mathbf{D}(z)$,

$\mathbf{D}(z)^\dagger \mathbf{L}^H \mathbf{D}(z)$ is monic causal filter. $\mathbf{Q}$ is unitary, hence $\mathbf{B}(z)$ in also causal monic filter.
$\det \mathbf{B}(z) = \det \mathbf{L}^H = 1$, this shows that $\mathbf{B}(z)$ is a minimum phase causal monic filter. To complete the proof of the theorem it is sufficient to verify that $\mathbf{B}^{-\dagger}(z)\mathbf{R}(z)\mathbf{B}^{-1}(z) = \mathbf{Q}^H\mathbf{D}\mathbf{Q} = \mathbf{M}$. □

Conventional Unbiased MMSE MIMO DFE Rx :
$\mathbf{F}(q)\,\mathbf{z}_k - \overline{\mathbf{B}}(z)\,\mathbf{b}_k$ is a biased estimate of $\mathbf{b}_k$, since

$$\begin{aligned}\mathbf{F}(q)\,\mathbf{z}_k - \overline{\mathbf{B}}(q)\,\mathbf{b}_k &= [\mathbf{M}^{-1}\,\mathbf{B}^{-\dagger}(q)\,\mathbf{G}^\dagger(q)\mathbf{G}(q) - \overline{\mathbf{B}}(z)]\mathbf{b}_k + \mathbf{M}^{-1}\,\mathbf{B}^{-\dagger}(q)\mathbf{G}^\dagger(q)\boldsymbol{v}_k \\ &= [\mathbf{I} - \tfrac{1}{\rho}\,\mathbf{M}^{-1}\,\mathbf{B}^{-\dagger}(q)]\,\mathbf{b}_k + \mathbf{M}^{-1}\,\mathbf{B}^{-\dagger}(q)\mathbf{G}^\dagger(q)\boldsymbol{v}_k \\ &= (\mathbf{I} - \tfrac{1}{\rho}\,\mathbf{M}^{-1})\,\mathbf{b}_k + \tilde{\mathbf{e}}_k\,,\end{aligned} \tag{3.48}$$

where $\tilde{\mathbf{e}}_k = \mathbf{M}^{-1}\,\mathbf{B}^{-\dagger}(q)\mathbf{G}^\dagger(q)\boldsymbol{v}_k - \frac{1}{\rho}\,\mathbf{M}^{-1}\,(\mathbf{B}^{-\dagger}(q) - \mathbf{I})\mathbf{b}_k$.
After some manipulations, the covariance of $\tilde{\mathbf{e}}$ is written
$C_{\tilde{\mathbf{e}}\tilde{\mathbf{e}}} = \sigma_v^2\,\mathbf{M}^{-1}(\mathbf{I} - \frac{1}{\rho}\,\mathbf{M}^{-1})$.
The feedforward UMMSE filter is

$$\mathbf{F}^U(q) = (\mathbf{I} - \frac{1}{\rho}\,\mathbf{M}^{-1})^{-1}\,\mathbf{M}^{-1}\mathbf{B}^{-\dagger}(q)(\mathbf{M} - \frac{1}{\rho}\,\mathbf{I})^{-1}\,\mathbf{P}^\dagger(q)\,, \tag{3.49}$$

whereas the corresponding feedback filter is

$$\mathbf{B}^U(q) = (\mathbf{I} - \frac{1}{\rho}\,\mathbf{M}^{-1})^{-1}(\mathbf{P}^{-1}(q) - \mathbf{I})\,. \tag{3.50}$$

The capacity of such a Tx system with UMMSE DFE Rx, assuming perfect feedback and joint decoding of the components of $\mathbf{b}_k$, is after some simple manipulations

$$C = \frac{1}{2\pi j}\oint \frac{dz}{z}\ln\det(\rho\,\mathbf{M})\,. \tag{3.51}$$

In order to show that C is equal to the capacity of the MIMO channel, let us notice that for a minimum/maximum phase monic MIMO filter $A(z)$ ($A_0 = I$), $\frac{1}{2\pi j}\oint \frac{dz}{z}\log\det(A(z)) = 0$. This leads to

$$\begin{aligned} C &= \tfrac{1}{2\pi j}\oint \tfrac{dz}{z}\ln\det(\rho\,\mathbf{B}^\dagger(z)\,\mathbf{M}\,\mathbf{B}(z)) \\ &= \tfrac{1}{2\pi j}\oint \tfrac{dz}{z}\ln\det(I + \rho\,\mathbf{H}^\dagger(z)\,\mathbf{H}(z))\,. \end{aligned} \tag{3.52}$$

Hence this decoding strategy preserves the capacity.

3.5.2 Conventional MMSE ZF MIMO DFE Rx

As we have done for the MMSE, the MMSE ZF design can be determined similarly to section 3.2, where again for this design to hold we need to have $N_s = \min\{N_{tx}, N_{rx}\}$.
We assume in below that $N_{rx} \geq N_{tx}$, then $N_s = N_{tx}$. Under the assumption that detected symbols are correct (perfect feedback), we get

$$\begin{aligned} \widehat{\mathbf{b}}_k &= \mathbf{F}(q)\mathbf{z}_k - \overline{\mathbf{B}}(q)\mathbf{b}_k \\ &= \mathbf{b}_k + \mathbf{e}_k \,, \end{aligned} \tag{3.53}$$

where $\mathbf{S_{ee}}(z) = \sigma_v^2 \mathbf{M}^{-1}$, $\mathbf{B}(z) = \mathbf{T}(z)^\dagger \mathbf{L}^H \mathbf{T}(z)$, $\mathbf{M} = \mathbf{Q}^H \mathbf{D} \mathbf{Q}$, and $\mathbf{L}$, $\mathbf{D}$ result from the LDU decomposition of $\mathbf{H}^H \mathbf{H} = \mathbf{L}\,\mathbf{D}\,\mathbf{L}^H$.

For the detection of the symbol vector $\boldsymbol{b}_k$ different choices are possible. For example a V-BLAST-like detector can be used, however such a processing degrades performance. The optimal choices in this case is the weighted minimum distance detector which has an acceptable complexity especially for small number of transmit antennas and small constellation size. The complexity can be further reduced by the use of sphere decoding.

Diversity Considerations:
Theorem 5: In the case of flat channel and $N_{rx} \geq N_{tx}$, the use of a weighted minimum distance detector allows the MMSE ZF DFE Rx to achieve diversity gain of $N_{tx}.(N_{rx} - \frac{N_{tx}-1}{2})$.

Proof : see appendix 3.F.

In the case of the MMSE MIMO DFE Rx we can not analyze the coding gain as done in the proof of Theorem 5. In fact, for this Rx the noise $\mathbf{e}_k$ contains a part of the interference. The interference is non-Gaussian, hence $\mathbf{e}_k$ is non-Gaussian.
However, the MMSE MIMO DFE makes a compromise between interference cancellation and noise enhancement, its performances are then better than those of the MMSE ZF MIMO DFE. We conclude that the MMSE MIMO DFE achieves at the least the same diversity gain as the MMSE ZF MIMO DFE.

3.5.3 Decoding Strategy

Previously in Theorem 5 we have shown that the MMSE ZF MIMO DFE achieves a high diversity gain of $N_{tx}.(N_{rx} - \frac{N_{tx}-1}{2})$. However, the problem of the DFE Rx is error propagation, it degrades the error probability or the coding gain (this corresponds to a translation of the error probability curve to the right). To reduce this effect, PSP can be used to robustify the receiver by saving several survivors (possibilities) that are the more likely as has been done in [53]. PSP typically uses a binary convolutional channel code, coupled with a Viterbi decoder at the receiver. For decoding, only a reduced number of survivors are saved, they are used as feedback in the equalizer and hence increase the number of distances to be evaluated. The number of survivors is chosen in a manner to keep the complexity acceptable.
Another possibility of binary coding is to allow inter-block coding, the decoding progress is then done serially in one block but in parallel in the different blocks, for symbols that have the same index k. For the approach to be smoothly combined with the Conventional MIMO DFE Rx, it is desirable that the symbol components of the vector symbol $\boldsymbol{b}_k$ belong to the same stream and that consecutive $\boldsymbol{b}_k$ belong to different streams. To this end, a new type of stream assignment (layering) should be introduced. In this case, the frame of data to be transmitted gets partitioned into consecutive blocks. Each stream has one diagonal set of symbols in any given block, and hence stream i is composed of diagonal i in every block (for a frequency-flat channel). Hence, every block contains only one vector symbol (diagonal) $\boldsymbol{b}_k$ belonging to a particular stream. The non-iterative reception gets performed by running the DFE in parallel over each block and decoding each consecutive stream sequentially, before using it in the feedback for the detection of the next stream. This approach also allows to take advantage of time diversity by distributing the blocks over different realization. This strategy also ensures a high reliability of the feedback and hence reduces error propagation.
In [53], simulations are done to evaluate the performance of PSP but for a case where no linear precoding is used. This approach is a pure binary channel code approach as diversity is exploited only by binary CC. The performances obtained show that the DFE coupled with a PSP exploits all the available diversity but with reduced coding gain when compared to an iterative decoder. This degradation is due to the reduced number of survivors and can hence be removed by increasing this number. These results still

apply in our case but we have to point out that the linear precoding that we use robustifies the coding part when being compared with the approach proposed in [53]. It also exploits the diversity and allows to dedicate the binary channel code to the exploitation of the multi-block diversity and to improve the coding gain. The next chapter covers these advantages but for Rx with an iterative decoder.

3.6 Stripping vs. Conventional MIMO DFE

The Stripping approach allows the use of conventional SISO decoders for the detection/decoding of each stream, reducing the problem to the design of encoders for equalized streams that experience a known diversity but that are non-symmetrical in the sense that the earlier the stream is canceled, the less diversity it experiences. The non-symmetry of the Stripping Rx constrains the Tx to adapt the binary channel coding and constellations to each stream, in order to compensate the deficiency of the spatial diversity by the time diversity and coding gains, introduced by the constellation and binary channel code.
In the case of the conventional MIMO DFE, the binary channel code and the constellation are unique, but the binary CC have to be correctly chosen to allow inter-block coding and/or Per-Survivor-Processing.
On the other hand, the Stripping MIMO DFE Rx is very convenient for high multiplexing rates. In this case the constellation size grows exponentially with the SNR. The per stream SISO decoder maintains an acceptable complexity in this case. However, this is not the case of the Conventional MIMO DFE where the joint detection of the components of $\mathbf{b}_k$ leads to high complexity.

3.7 Diversity vs. Multiplexing Tradeoff of the Conventional MIMO DFE an Open Problem

In section 3.5.2, we have shown that the diversity gain achieved by the Conventional MIMO DFE with a MMSE ZF design and for $N_{rx} \geq N_{tx}$ is $N_{tx}.(N_{rx} - \frac{N_{tx}-1}{2}) \leq N_{tx}.N_{rx}$.

The diversity gain corresponds to the diversity achieved for a multiplexing $r = 0$ in the curve of the diversity vs. multiplexing tradeoff.
A second point is the trivial ($r = \min\{N_{tx}, N_{rx}\}$, $d = 0$), since the STS scheme achieves a full multiplexing rate.
However, the general problem of the diversity vs. multiplexing tradeoff achieved by the Conventional MIMO DFE Rx for the STS scheme, in a frequency selective channel environment is an open problem.

The $\mathbf{Q}$ matrix can be seen as the generator matrix of a lattice code, we can then use elements introduced in [37] to handle the problem for the MMSE ZF design and flat channel.
For the frequency selective channel, a preliminary problem have to be solved. In fact, we need first to characterize $\mathbf{M}$ as has been done in the flat case.
Finally for the MMSE design, a compromise between noise enhancement and interference cancellation is done, the noise is then no more Gaussian. This fact have to be handled and we suspect that it could be the case using techniques for lattice code analysis used in [37]. We also believe that the Conventional MIMO DFE MMSE Rx for the STS scheme has the potential to achieve the optimal diversity vs. multiplexing tradeoff.

3.8 Conclusion

In this chapter we presented two non-iterative Rx. The Stripping MIMO DFE detects the streams successively, it allows to use the well studied SISO binary CC techniques to improve the performances if needed. It achieves a high diversity vs. multiplexing tradeoff, in particular the maximum diversity and maximum rate. This Rx is particularly suitable for SNR adaptive rate coding. However, for a fixed rate and symmetrical streams the Conventional MIMO DFE is more adapted. It achieves a high diversity gain and can be combined with Per-Survivor-Processing to limit the error propagation.
The use of PSP suggests the use of an iterative decoding scheme to improve the performances, this is the topic of the next chapter.
The Conventional MIMO DFE performances in term of diversity vs. multiplexing tradeoff haven't been evaluated in this chapter. They can be studied by using elements relative to lattice codes introduced in [37].

APPENDIX

The appendix starts by presenting a preliminary result on SIMO frequency selective channel. Theorem 6 describes the behavior of the outage capacity of such a channel. The proof of this theorem provides important tools that will be used later in the generalization of the diversity vs. multiplexing tradeoff to the MIMO frequency selective channel.

3.A Outage Capacity Behavior of SIMO Frequency Selective Channel

Theorem 6: The outage capacity of a $N_{rx} \times 1$ SIMO channel with L_s resolvable paths satisfies:

$$P_{out}(r \ln \rho) \doteq \rho^{-L_s(1-r)} \doteq \rho^{-d_{out}(r)}\,, \tag{3.54}$$

where $d_{out}(r) = L_s(1-r)$ and $R = r \ln \rho$ $(0 \leq r \leq 1)$ is the data rate.

Proof :

$\mathbf{g}(z) = \sum_{l=0}^{L-1} \mathbf{g}_l z^{-l}$ is a $N_{rx} \times 1$ frequency selective fading channel. $\mathbf{g}(z)$ contains L_s resolvable source of diversity

$$\underline{\mathbf{g}} = \mathbf{U}_g\, \mathbf{s}\,, \tag{3.55}$$

where $\underline{\mathbf{g}} = \begin{bmatrix} \mathbf{g}_0 \\ \vdots \\ \mathbf{g}_{L-1} \end{bmatrix}$ represents the vectorized channel impulse response. $\mathbf{U}_g$ is a $(LN_{rx}) \times L_s$ $(L_s \leq L\,.\,N_{rx})$ constant full column rank matrix (see model in section 6.5). $\mathbf{s} = [s_1, \ldots, s_{L_s}]^T$ contains the resolvable diversity source gains (path gains). $\mathbf{s}$ is assumed to follow a Gaussian distribution $\mathbf{s} \sim \mathcal{CN}(0, \mathbf{I}_{L_s})$. The instantaneous capacity of the channel is

$$C(\mathbf{g}) = \frac{1}{2\pi j} \oint \frac{dz}{z} \ln(1 + \rho \mathbf{g}^\dagger(z)\mathbf{g}(z)) = \frac{1}{2\pi j} \oint \frac{dz}{z} \ln \mathbf{S}(z), \tag{3.56}$$

$\mathbf{S}(z) = 1 + \rho \mathbf{g}^\dagger(z)\mathbf{g}(z)$ is the normalized psdf of the received signal (normalized w.r.t. to the noise power). Using the spectral factorization $\mathbf{S}(z) =$

$\sigma^2 A(z)\, A^\dagger(z)$, where $A(z)$ is a the minimum phase causal monic factor

$$A(z) = 1 + \sum_{l=1}^{L-1} A_l z^{-l} = \prod_{l=1}^{L-1} (1 - p_l z^{-1}) \qquad |p_l| < 1\,, \quad \text{for} \quad l = 1, \ldots, L-1\,. \tag{3.57}$$

For this factorization to exist $\mathbf{S}(z)$ should have no zeros on the unit circle, which is the case here.
The instantaneous capacity is then

$$C(\mathbf{g}) = \ln \sigma^2 + \frac{1}{2\pi j} \oint \frac{dz}{z} \ln A(z)\, A^\dagger(z)\,. \tag{3.58}$$

$\frac{1}{2\pi j} \oint \frac{dz}{z} \ln A(z)\, A^\dagger(z) = 0$, in fact if we derive $C(\mathbf{g})$ w.r.t. A_l $(1 \le l \le L-1)$ we get

$$\frac{\partial C(\mathbf{g})}{\partial A_l} = \frac{1}{2\pi j} \oint \frac{dz}{z} z^{-l} A^{-1}(z)\,. \tag{3.59}$$

$A(z)$ is causal minimum phase then its inverse is causal, and $z^{-l} A^{-1}(z)$ is strictly causal and hence $\frac{\partial C(\mathbf{g})}{\partial A_l} = 0$.
We conclude that $C(\mathbf{g})$ is constant w.r.t. A_l, $1 \le l \le L-1$, in particular for $A_l = 0$, $1 \le l \le L-1$

$$C(\mathbf{g}) = \ln \sigma^2\,. \tag{3.60}$$

The close form of σ^2 is

$$\sigma^2 = \frac{\frac{1}{2\pi j} \oint \frac{dz}{z} \mathbf{S}(z)}{\frac{1}{2\pi j} \oint \frac{dz}{z} A(z)\, A^\dagger(z)} = \frac{1 + \rho ||\underline{\mathbf{g}}||^2}{\sum_{l=0}^{L-1} |A_l|^2}\,. \tag{3.61}$$

From eq. (3.57) we notice that $A_l = \sum_{1 \le i_1 < i_2 < \ldots < i_l \le L-1} (-1)^l p_{i_1} p_{i_2} \ldots p_{i_l}$, the norm $|A_l|$ is hence upper bounded as follows

$$\begin{aligned} |A_l| &\le \sum_{1 \le i_1 < i_2 < \ldots < i_l \le L-1} |p_{i_1}|\, |p_{i_2}|\, \ldots\, |p_{i_l}| \\ &< \sum_{1 \le i_1 < i_2 < \ldots < i_l \le L-1} 1 \\ &= \binom{l}{L-1}\,. \end{aligned} \tag{3.62}$$

We can then lower bound σ^2 by

$$\sigma^2 \geq \frac{1+\rho||\underline{\mathbf{g}}||^2}{\gamma_L}\,, \tag{3.63}$$

where $\gamma_L = \sum_{l=0}^{L-1} \begin{pmatrix} l \\ L-1 \end{pmatrix}^2$. For data rate $R = r\ln\rho$ $(0 \leq r \leq 1)$, the outage capacity is upper bounded as follows

$$\begin{aligned}
P_{out}(r\ln\rho) &= P\left(C(\mathbf{g}) < r\ln\rho\right) \\
&= P\left(\sigma^2 < \rho^r\right) \\
&\leq P(\rho^{1-r}||\underline{\mathbf{g}}||^2 < \gamma_L - \rho^{-r}) \\
&= \mathrm{E}\{1_{\rho^{1-r}||\underline{\mathbf{g}}||^2-\gamma_L+\rho^{-r}<0}\} \\
&\leq \min_{\lambda>0}\, \mathrm{E}\{e^{-\lambda(\rho^{1-r}||\underline{\mathbf{g}}||^2-\gamma_L+\rho^{-r})}\} \\
&= \min_{\lambda>0} \frac{e^{\lambda(\gamma_L-\rho^{-r})}}{\det(\mathbf{I}_{L_s}+\lambda\rho^{1-r}\mathbf{U}_g^H\mathbf{U}_g)} \\
&\leq \frac{e^{\gamma_L-\rho^{-r}}}{\det(\mathbf{I}_{L_s}+\rho^{1-r}\mathbf{U}_g^H\mathbf{U}_g)}, \qquad (\lambda=1) \\
&\doteq \rho^{-L_s(1-r)}\,,
\end{aligned} \tag{3.64}$$

where in the fifth and the sixth inequalities we use the Chernoff upper bound and in the last inequality we use the fact that $\mathbf{U}_g$ is full column rank (the L_s paths are resolvable).
Eq. (3.64) gives an upper bound on the outage probability.
We derive now a lower bound.

A lower bound on the capacity can be found by exploiting the concavity of the log function

$$C(\mathbf{g}) \leq \ln\left(\frac{1}{2\pi j}\oint \frac{dz}{z}\mathbf{S}(z)\right) = \ln\left(1+\rho||\underline{\mathbf{g}}||^2\right)\,. \tag{3.65}$$

Then

$$\begin{aligned}
P_{out}(\rho) = P\left(C(\mathbf{g}) < r\ln\rho\right) &\geq P\left(1+\rho||\underline{\mathbf{g}}||^2 < \rho^r\right) \\
&= P(\rho||\underline{\mathbf{g}}||^2 < \rho^r - 1)\,.
\end{aligned} \tag{3.66}$$

Let $\mathbf{U}_g^H\mathbf{U}_g = \mathbf{V}\mathbf{D}\mathbf{V}^H$, $\mathbf{V}$ unitary and $\mathbf{D} = \mathrm{diag}\,(d_l, i = 1,\ldots,L_s)$, be the eigendecomposition of $\mathbf{U}_g^H\mathbf{U}_g$. We denote $\mathbf{t} = [t_1,\ldots,t_{L_s}]^T = \mathbf{V}^H\mathbf{s}$, then

$||\underline{\mathbf{g}}||^2 = \sum_{l=1}^{L_s} d_l|t_l|^2$ and the set $\{(\rho d_1|t_1|^2 < \frac{\rho^r-1}{L_s}), \ldots, (\rho d_{L_s}|t_{L_s}|^2 < \frac{\rho^r-1}{L_s})\}$ is a subset of $\{\rho \sum_{l=1}^{L_s} d_l|s_l|^2 < \rho^r - 1\}$. We can now write

$$\begin{aligned} P_{out}(\rho) &\geq \prod_{l=1}^{L_s} P\left(\rho d_l|t_l|^2 < \tfrac{\rho^r-1}{L_s}\right) \\ &= \prod_{l=1}^{L_s} \int_0^{\frac{\rho^r-1}{d_l L_s \rho}} e^{-x} dx \\ &\geq \prod_{l=1}^{L_s} \int_0^{\frac{\rho^r-1}{d_l L_s \rho}} e^{-\frac{\rho^r-1}{d_l L_s \rho}} dx \\ &= \prod_{l=1}^{L_s} \left(e^{-\frac{\rho^r-1}{d_l L_s \rho}} \frac{\rho^r-1}{d_l L_s \rho}\right) \\ &\doteq \rho^{-L_s(1-r)} . \end{aligned} \tag{3.67}$$

By combining 3.64 and 3.67 we then show that

$$P_{out}(r \ln \rho) \doteq \rho^{-L_s(1-r)} \doteq \rho^{-d_{out}(r)} , \tag{3.68}$$

where $d_{out}(r) = L_s(1-r)$. □

In the same way as what is done in appendix 3.E, we can show that the DFE receiver of a SIMO channel can achieve the diversity vs. multiplexing tradeoff defined by $d_{out}(r)$.

An important intermediate result we have derived during the proof, gives us a useful bounds that we will use in the next appendices

$$\ln\left(\frac{1+\rho||\underline{\mathbf{g}}||^2}{\gamma_L}\right) \leq \frac{1}{2\pi j}\oint \frac{dz}{z} \ln(1+\rho \mathbf{g}^\dagger(z)\mathbf{g}(z)) \leq \ln\left(1+\rho||\underline{\mathbf{g}}||^2\right) . \tag{3.69}$$

Similarly, for any SIMO channel we can derive the following bounds

$$\ln\left(\frac{\frac{1}{2\pi j}\oint \frac{dz}{z}\mathbf{g}^\dagger(z)\mathbf{g}(z)}{\gamma_L}\right) \leq \frac{1}{2\pi j}\oint \frac{dz}{z} \ln(\mathbf{g}^\dagger(z)\mathbf{g}(z)) \leq \ln\left(\frac{1}{2\pi j}\oint \frac{dz}{z}\mathbf{g}^\dagger(z)\mathbf{g}(z)\right) , \tag{3.70}$$

where $\gamma_L = \sum_{l=0}^{L-1} \begin{pmatrix} l \\ L-1 \end{pmatrix}^2$ and L is the length of the impulse response. For the lower bound to exist, we need to verify that $\mathbf{g}(z)$ have no zeros on the unit circle.

3.B Proof of Lemma 1

Recall that

$$C_n^{MMSE\,DFE} = -\frac{1}{2\pi j}\oint \frac{dz}{z}\ln([\mathbf{V}_n^H \rho\mathbf{R}(z)\mathbf{V}_n]^{-1})_{11}\,, \tag{3.71}$$

where $\rho\mathbf{R}(z) = \mathbf{I}_{N_{tx}} + \rho\mathbf{Q}^H\mathbf{D}^\dagger(z)\,\mathbf{H}^\dagger(z)\mathbf{H}(z)\mathbf{D}(z)\mathbf{Q}$ and $\mathbf{H}(z) = \sum_{i=0}^{L-1}\mathbf{H}_i z^{-i}$.
$\mathbf{H}(z)\mathbf{D}(z)\mathbf{Q}$ can be rewritten as $\bar{\mathbf{H}}\,\bar{\mathbf{D}}(z)\,\mathbf{Q}$ where $\bar{\mathbf{H}} = [\mathbf{H}_0, \mathbf{H}_1, \ldots, \mathbf{H}_{L-1}]$,
$\bar{\mathbf{D}}(z) = [\mathbf{D}^T(z), z^{-1}\mathbf{D}^T(z), \ldots, z^{-L+1}\mathbf{D}^T(z)]^T$ and
$\mathbf{D}(z) = \mathrm{diag}\,(1, z^{-L}, z^{-2L}, \ldots, z^{-(N_{tx}-1)L})$.
Let $\bar{\mathbf{H}}^H\bar{\mathbf{H}} = \mathbf{U}\mathbf{S}\mathbf{U}^H$ be the eigendecomposition of $\bar{\mathbf{H}}^H\bar{\mathbf{H}}$ where the diagonal values of $\mathbf{S} = \mathrm{diag}\,\{s_1, s_2, \ldots, s_{N_{tx}L}\}$ are sorted in the increasing order.
We denote $\mathbf{U}_n = [\mathbf{u}_{N_{tx}(L-1)+n}, \mathbf{u}_{N_{tx}(L-1)+n+1}, \ldots, \mathbf{u}_{N_{tx}L}]$,
$\overline{\mathbf{U}}_n = [\mathbf{u}_1, \mathbf{u}_2, \ldots, \mathbf{u}_{N_{tx}(L-1)+n-1}]$, and rewrite

$$\mathbf{V}_n^H\rho\mathbf{R}(z)\mathbf{V}_n = \mathbf{V}_n^H\mathbf{Q}^H\bar{\mathbf{D}}^\dagger(z)\mathbf{U}\,(\frac{1}{L}\mathbf{I}_{N_{tx}L} + \rho\mathbf{S})\mathbf{U}^H\bar{\mathbf{D}}(z)\mathbf{Q}\mathbf{V}_n\,. \tag{3.72}$$

To bound the capacity $C_n^{MMSE\,DFE}$ we distinguish two cases:

Case 1: $n < N_{tx}$

The ordering of the diagonal values of $\mathbf{S}$ allows us to bound $\mathbf{I}_{N_{tx}L} + \rho\mathbf{S}$

$$\begin{gathered}\text{block-diag}(\mathbf{0}_{(N_{tx}(L-1)+n-1)\,\times\,(N_{tx}(L-1)+n-1)}, (\tfrac{1}{L} + \rho s_{N_{tx}(L-1)+n})\,\mathbf{I}_{N_{tx}-n+1}\,) \leq \\ (\tfrac{1}{L}\mathbf{I}_{N_{tx}L} + \rho\mathbf{S}) \leq \\ \text{block-diag}((\tfrac{1}{L} + \rho s_{N_{tx}(L-1)+n})\,\mathbf{I}_{N_{tx}(L-1)+n}, (\tfrac{1}{L} + \rho s_{N_{tx}(L-1)+n} + x)\mathbf{I}_{N_{tx}-n})\,,\end{gathered} \tag{3.73}$$

where $\text{block-diag}(\mathbf{A},\mathbf{B}) = \begin{bmatrix}\mathbf{A} & \mathbf{0}\\ \mathbf{0} & \mathbf{B}\end{bmatrix}$, and $x \geq \rho(s_{N_{tx}L} - s_{N_{tx}(L-1)+n}) \geq 0$.
Then

$$\begin{gathered}\tfrac{1}{L(\frac{1}{L}+\rho s_{N_{tx}(L-1)+n})}[\mathbf{I}_{N_{tx}-n+1} + \tfrac{x}{L(\frac{1}{L}+\rho s_{N_{tx}(L-1)+n})}\mathbf{V}_n^H\mathbf{Q}^H\bar{\mathbf{D}}^\dagger(z)\mathbf{U}_{n+1}\,\mathbf{U}_{n+1}^H\bar{\mathbf{D}}(z)\mathbf{Q}\mathbf{V}_n]^{-1} \leq \\ [\mathbf{V}_n^H\rho\mathbf{R}(z)\mathbf{V}_n]^{-1} \leq \\ \tfrac{1}{\frac{1}{L}+\rho s_{N_{tx}(L-1)+n}}[\mathbf{V}_n^H\mathbf{Q}^H\bar{\mathbf{D}}^\dagger(z)\mathbf{U}_n\,\mathbf{U}_n^H\bar{\mathbf{D}}(z)\mathbf{Q}\mathbf{V}_n]^{-1}\,.\end{gathered} \tag{3.74}$$

Using the matrix inversion lemma, we can show that for $x \to +\infty$ we have

$$\lim_{x\to+\infty}[\mathbf{I}_{N_{tx}-n+1}+\frac{x}{1+L\rho s_{N_{tx}(L-1)+n}}\mathbf{V}_n^H\mathbf{Q}^H\bar{\mathbf{D}}^\dagger(z)\mathbf{U}_{n+1}\,\mathbf{U}_{n+1}^H\bar{\mathbf{D}}(z)\mathbf{Q}\mathbf{V}_n]^{-1}= \mathbf{P}^\perp_{\mathbf{V}_n^H\mathbf{Q}^H\bar{\mathbf{D}}^\dagger(z)\mathbf{U}_{n+1}}, \tag{3.75}$$

where $\mathbf{V}_n^H\mathbf{Q}^H\bar{\mathbf{D}}^\dagger(z)\mathbf{U}_{n+1}$ is $(N_{tx}-n+1)(N_{tx}-n)$ matrix, $\mathbf{P}^\perp_{\mathbf{A}}=\mathbf{I}-\mathbf{P}_{\mathbf{A}}$ and $\mathbf{P}_{\mathbf{A}}$ is the orthogonal projection on $\mathbf{A}$. We get finally

$$\begin{aligned}\frac{1}{L(\frac{1}{L}+\rho s_{N_{tx}(L-1)+n})}\mathbf{P}^\perp_{\mathbf{V}_n^H\mathbf{Q}^H\bar{\mathbf{D}}^\dagger(z)\mathbf{U}_{n+1}} \le [\mathbf{V}_n^H\rho\mathbf{R}(z)\mathbf{V}_n]^{-1} \le \\ \frac{1}{\frac{1}{L}+\rho s_{N_{tx}(L-1)+n}}[\mathbf{V}_n^H\mathbf{Q}^H\bar{\mathbf{D}}^\dagger(z)\mathbf{U}_n\,\mathbf{U}_n^H\bar{\mathbf{D}}(z)\mathbf{Q}\mathbf{V}_n]^{-1},\end{aligned} \tag{3.76}$$

Let us denote $\beta_n=-\frac{1}{2\pi j}\oint\frac{dz}{z}\ln\{\mathbf{P}^\perp_{\mathbf{V}_n^H\mathbf{Q}^H\bar{\mathbf{D}}^\dagger(z)\mathbf{U}_{n+1}}\}_{11}$ and $\alpha_n=-\frac{1}{2\pi j}\oint\frac{dz}{z}\ln\{[\mathbf{V}_n^H\mathbf{Q}^H\bar{\mathbf{D}}^\dagger(z)\mathbf{U}_n\,\mathbf{U}_n^H\bar{\mathbf{D}}(z)\mathbf{Q}\mathbf{V}_n]^{-1}\}_{11}$. We can now bound the capacity by

$$\ln(\frac{1}{L}+\rho s_{N_{tx}(L-1)+n})+\alpha_n \le C_n^{MMSE\,DFE} \le \ln(\frac{1}{L}+\rho s_{N_{tx}(L-1)+n})+\ln L+\beta_n\,, \tag{3.77}$$

where α_n and β_n are independent of ρ and $\mathbf{S}$.

The bounds can be further refined, in fact

$$\mathbf{P}^\perp_{\mathbf{V}_n^H\mathbf{Q}^H\bar{\mathbf{D}}^\dagger(z)\mathbf{U}_{n+1}}=\prod_{i=N_{tx}(L-1)+n+1}^{N_{tx}L}\mathbf{P}^\perp_{\mathbf{V}_n^H\mathbf{Q}^H\bar{\mathbf{D}}^\dagger(z)\mathbf{u}_i}\,. \tag{3.78}$$

On the other hand $\mathbf{I}_{N_{tx}-n+1}\ge\mathbf{e}_1^{N_{tx}-n+1}(\mathbf{e}_1^{N_{tx}-n+1})^H$, where $\mathbf{e}_i^{N_{tx}-n+1}$ is the $(N_{tx}-n+1)\times 1$ vector with 1 at the i^{th} position and all other entries are zeros. Then

$$\begin{aligned}\{\mathbf{P}^\perp_{\mathbf{V}_n^H\mathbf{Q}^H\bar{\mathbf{D}}^\dagger(z)\mathbf{U}_{n+1}}\}_{11} &\ge \textstyle\prod_{i=N_{tx}(L-1)+n+1}^{N_{tx}L}(\mathbf{e}_1^{N_{tx}-n+1})^H\mathbf{P}^\perp_{\mathbf{V}_n^H\mathbf{Q}^H\bar{\mathbf{D}}^\dagger(z)\mathbf{u}_i}\,\mathbf{e}_1^{N_{tx}-n+1}\\ &= \textstyle\prod_{i=N_{tx}(L-1)+n+1}^{N_{tx}L}\{\mathbf{P}^\perp_{\mathbf{V}_n^H\mathbf{Q}^H\bar{\mathbf{D}}^\dagger(z)\mathbf{u}_i}\}_{11}\,,\end{aligned} \tag{3.79}$$

hence

$$\begin{aligned}\beta_n &\leq \sum_{i=N_{tx}(L-1)+n+1}^{N_{tx}L} -\frac{1}{2\pi j}\oint \frac{dz}{z}\ln\{\mathbf{P}^{\perp}_{\mathbf{V}_n^H\mathbf{Q}^H\bar{\mathbf{D}}^{\dagger}(z)\mathbf{u}_i}\}_{11} \\ &= \sum_{i=N_{tx}(L-1)+n+1}^{N_{tx}L} -\frac{1}{2\pi j}\oint \frac{dz}{z}\ln\left(1-\frac{\{\mathbf{V}_n^H\mathbf{Q}^H\bar{\mathbf{D}}^{\dagger}(z)\mathbf{u}_i\mathbf{u}_i^H\bar{\mathbf{D}}(z)\mathbf{Q}\mathbf{V}_n\}_{11}}{\mathbf{u}_i^H\bar{\mathbf{D}}(z)\mathbf{Q}\mathbf{V}_n\mathbf{V}_n^H\mathbf{Q}^H\bar{\mathbf{D}}^{\dagger}(z)\mathbf{u}_i}\right) \\ &= \sum_{i=N_{tx}(L-1)+n+1}^{N_{tx}L} \frac{1}{2\pi j}\oint \frac{dz}{z}\ln\frac{\mathbf{u}_i^H\bar{\mathbf{D}}(z)\mathbf{Q}\mathbf{V}_n\mathbf{V}_n^H\mathbf{Q}^H\bar{\mathbf{D}}^{\dagger}(z)\mathbf{u}_i}{\mathbf{u}_i^H\bar{\mathbf{D}}(z)\mathbf{Q}\mathbf{V}_{n+1}\mathbf{V}_{n+1}^H\mathbf{Q}^H\bar{\mathbf{D}}^{\dagger}(z)\mathbf{u}_i}\,. \end{aligned} \tag{3.80}$$

Using intermediate results derived in appendix 3.A (eq. (3.70)), we can show that

$$\begin{aligned}&\tfrac{1}{2\pi j}\oint\tfrac{dz}{z}\ln\{\mathbf{u}_i^H\bar{\mathbf{D}}(z)\mathbf{Q}\mathbf{V}_n\mathbf{V}_n^H\mathbf{Q}^H\bar{\mathbf{D}}^{\dagger}(z)\mathbf{u}_i\}\leq \\ &\ln\{\tfrac{1}{2\pi j}\oint\tfrac{dz}{z}\mathbf{u}_i^H\bar{\mathbf{D}}(z)\mathbf{Q}\mathbf{V}_n\mathbf{V}_n^H\mathbf{Q}^H\bar{\mathbf{D}}^{\dagger}(z)\mathbf{u}_i\} = \\ &\ln\{\mathbf{u}_i^H(\tfrac{N_{tx}-n+1}{N_{tx}}\mathbf{I}_{N_{tx}L})\mathbf{u}_i\} = \ln(\tfrac{N_{tx}-n+1}{N_{tx}})\,.\end{aligned} \tag{3.81}$$

For $\bar{\mathbf{H}}$ with Gaussian i.i.d. elements, $\mathbf{u}_i$ follows a uniform distribution over the Grassmann manifold. The zeros of $\mathbf{u}_i^H\bar{\mathbf{D}}(z)\mathbf{Q}\mathbf{V}_{n+1}\mathbf{V}_{n+1}^H\mathbf{Q}^H\bar{\mathbf{D}}^{\dagger}(z)\mathbf{u}_i$ have then a continuous distribution over the complex plane. The probability of a zero to be on the unit circle is then 0 [54, 55]. This allows us to use the lower bound of eq. (3.70),

$$\begin{aligned}&\tfrac{1}{2\pi j}\oint\tfrac{dz}{z}\ln\{\mathbf{u}_i^H\bar{\mathbf{D}}(z)\mathbf{Q}\mathbf{V}_{n+1}\mathbf{V}_{n+1}^H\mathbf{Q}^H\bar{\mathbf{D}}^{\dagger}(z)\mathbf{u}_i\}\geq \\ &\ln\{\tfrac{\frac{1}{2\pi j}\oint\frac{dz}{z}\mathbf{u}_i^H\bar{\mathbf{D}}(z)\mathbf{Q}\mathbf{V}_{n+1}\mathbf{V}_{n+1}^H\mathbf{Q}^H\bar{\mathbf{D}}^{\dagger}(z)\mathbf{u}_i}{\gamma_{N_{tx}L}}\} = \ln(\tfrac{N_{tx}-n}{N_{tx}\gamma_{N_{tx}L}})\,,\end{aligned} \tag{3.82}$$

hence

$$\beta_n \leq (N_{tx}-n)\ln\left(\frac{\gamma_{N_{tx}L}(N_{tx}-n+1)}{N_{tx}-n}\right)\,, \tag{3.83}$$

where $\gamma_{N_{tx}L} = \sum_{l=0}^{N_{tx}L-1}\begin{pmatrix} l \\ N_{tx}L-1\end{pmatrix}^2$, and $N_{tx}L-1$ is the degree of $\mathbf{u}_i^H\bar{\mathbf{D}}(z)\mathbf{Q}\mathbf{V}_{n+1}$.

On the other hand we have that $[\mathbf{V}_n^H\mathbf{Q}^H\bar{\mathbf{D}}^{\dagger}(z)\mathbf{U}_n\,\mathbf{U}_n^H\bar{\mathbf{D}}(z)\mathbf{Q}\mathbf{V}_n]_{11}^{-1} = \left((\mathbf{e}_n^{N_{tx}})^H\mathbf{Q}^H\bar{\mathbf{D}}^{\dagger}(z)\mathbf{U}_n\mathbf{P}^{\perp}_{\mathbf{U}_n^H\bar{\mathbf{D}}(z)\mathbf{Q}\mathbf{V}_{n+1}}\mathbf{U}_n^H\bar{\mathbf{D}}(z)\mathbf{Q}\mathbf{e}_n^{N_{tx}}\right)^{-1}$. This result can be derived using the QR decomposition of $\mathbf{U}_n^H\bar{\mathbf{D}}(z)\mathbf{Q}\mathbf{V}_n\mathbf{J}$, where $\mathbf{J}$ is the $(N_{tx}-n+1)\times(N_{tx}-n+1)$ matrix with ones on the anti-diagonal and zeros elsewhere.

We have now that
$\alpha_n = \frac{1}{2\pi j}\oint \frac{dz}{z} \ln\left((\mathbf{e}_n^{N_{tx}})^H \mathbf{Q}^H \bar{\mathbf{D}}^\dagger(z) \mathbf{U}_n \mathbf{P}^\perp_{\mathbf{U}_n^H \bar{\mathbf{D}}_{(z)} \mathbf{Q} \mathbf{V}_{n+1}} \mathbf{U}_n^H \bar{\mathbf{D}}(z) \mathbf{Q} \mathbf{e}_n^{N_{tx}} \right)$.
Similarly to what have been done for β_n we can show that

$$\begin{aligned}
\alpha_n &\geq \tfrac{1}{2\pi j}\oint \tfrac{dz}{z} \ln\{(\mathbf{e}_n^{N_{tx}})^H \mathbf{Q}^H \bar{\mathbf{D}}^\dagger(z) \mathbf{U}_n \mathbf{e}_1^{N_{tx}-n+1} (\mathbf{e}_1^{N_{tx}-n+1})^H \mathbf{U}_n^H \bar{\mathbf{D}}(z) \mathbf{Q} \mathbf{e}_n^{N_{tx}}\} \\
&\quad + \tfrac{1}{2\pi j}\oint \tfrac{dz}{z} \ln\{(\mathbf{e}_1^{N_{tx}-n+1})^H \mathbf{P}^\perp_{\mathbf{U}_n^H \bar{\mathbf{D}}_{(z)} \mathbf{Q} \mathbf{V}_{n+1}} \mathbf{e}_1^{N_{tx}-n+1}\} \\
&= \tfrac{1}{2\pi j}\oint \tfrac{dz}{z} \ln\{(\mathbf{e}_n^{N_{tx}})^H \mathbf{Q}^H \bar{\mathbf{D}}^\dagger(z) \mathbf{u}_{N_{tx}(L-1)+n} \mathbf{u}^H_{N_{tx}(L-1)+n} \bar{\mathbf{D}}(z) \mathbf{Q} \mathbf{e}_n^{N_{tx}}\} \\
&\quad + \sum_{i=n+1}^{N_{tx}} \frac{1}{2\pi j}\oint \frac{dz}{z} \ln\{\mathbf{P}^\perp_{\mathbf{U}_n^H \bar{\mathbf{D}}_{(z)} \mathbf{Q} \mathbf{e}_i^{N_{tx}}}\}_{11} \\
&\geq \ln(\tfrac{1}{N_{tx}\gamma_{N_{tx}L}}) + (N_{tx}-n) \ln\left(\tfrac{N_{tx}-n}{(N_{tx}-n+1)\gamma_{N_{tx}L}}\right) .
\end{aligned} \tag{3.84}$$

Finally the capacity is bounded by

$$\begin{aligned}
&\ln(\tfrac{1}{N_{tx}\gamma_{N_{tx}L}}) + (N_{tx}-n) \ln\left(\tfrac{N_{tx}-n}{(N_{tx}-n+1)\gamma_{N_{tx}L}}\right) \leq \\
C_n^{MMSE\,DFE} - \ln(\tfrac{1}{L} + \rho s_{N_{tx}(L-1)+n}) &\leq (N_{tx}-n) \ln\left(\tfrac{\gamma_{N_{tx}L}(N_{tx}-n+1)}{N_{tx}-n}\right) + \ln L .
\end{aligned} \tag{3.85}$$

Case 2: $n = N_{tx}$

In this case

$$C_{N_{tx}}^{MMSE\,DFE} = \frac{1}{2\pi j}\oint \frac{dz}{z} \ln((\mathbf{e}_{N_{tx}}^{N_{tx}})^H \mathbf{Q}^H \bar{\mathbf{D}}^\dagger(z) \mathbf{U} \, (\frac{1}{L}\mathbf{I}_{N_{tx}L} + \rho \mathbf{S}) \mathbf{U}^H \bar{\mathbf{D}}(z) \mathbf{Q} \mathbf{e}_{N_{tx}}^{N_{tx}}) , \tag{3.86}$$

due to the ordering of the diagonal $(\frac{1}{L}\mathbf{I}_{N_{tx}L} + \rho\mathbf{S})$, we can bound it by

$$(\frac{1}{L} + \rho s_{N_{tx}L}) \mathbf{e}_{N_{tx}L}^{N_{tx}L} (\mathbf{e}_{N_{tx}L}^{N_{tx}L})^H \leq \frac{1}{L}\mathbf{I}_{N_{tx}L} + \rho\mathbf{S} \leq (\frac{1}{L} + \rho s_{N_{tx}L}) \mathbf{I}_{N_{tx}L} . \tag{3.87}$$

This allows to bound the capacity by

$$\begin{aligned}
&\tfrac{1}{2\pi j}\oint \tfrac{dz}{z} \ln((\mathbf{e}_{N_{tx}}^{N_{tx}})^H \mathbf{Q}^H \bar{\mathbf{D}}^\dagger(z) \mathbf{u}_{N_{tx}L} \mathbf{u}^H_{N_{tx}L} \bar{\mathbf{D}}(z) \mathbf{Q} \mathbf{e}_{N_{tx}}^{N_{tx}}) \leq \\
&\qquad C_{N_{tx}}^{MMSE\,DFE} - \ln(\tfrac{1}{L} + \rho s_{N_{tx}L}) \leq \ln L .
\end{aligned} \tag{3.88}$$

Again using results derived in appendix 3.A, we end to the following bounds

$$\ln(\frac{1}{N_{tx}\gamma_{N_{tx}L}}) \leq C_{N_{tx}}^{MMSE\,DFE} - \ln(\frac{1}{L} + \rho s_{N_{tx}L}) \leq \ln L . \tag{3.89}$$

3.C Proof of Theorem 1

Case $N_{rx} \leq N_{tx}$: In this case $p = m = N_{rx}$ and $q = N_{tx}$. From the capacity decomposition we have that $C = \sum_{i=1}^{N_{tx}} C_i^{MMSE\,DFE}$. Eq. (3.31) and eq. (3.32) lead then to

$$e^C \doteq \rho^{\sum_{i=1}^{N_{rx}} (1-\alpha_i)^+}\,, \tag{3.90}$$

and the outage capacity is

$$\begin{aligned} P_{out}(R) &= P\left(C < r \ln \rho\right) \\ &\doteq P\left(\sum_{i=1}^{N_{rx}} (1-\alpha_i)^+ < r\right)\,. \end{aligned} \tag{3.91}$$

Using the Wishart distribution expression, and as has been done in [9], it is possible to show that

$$P_{out}(R) \doteq \int_{\mathcal{A}} \prod_{i=1}^{N_{rx}} \rho^{-(2i-1+LN_{tx}-N_{rx})\alpha_i} d\boldsymbol{\alpha}\,, \tag{3.92}$$

where $\mathcal{A} = \{\boldsymbol{\alpha} : \sum_{i=1}^{N_{rx}} (1-\alpha_i)^+ < r, \alpha_1 \geq \alpha_2 \geq \ldots \geq \alpha_{N_{rx}}\} \cap \mathbf{R}^{+N_{rx}}$, and $\boldsymbol{\alpha} = (\alpha_1, \ldots, \alpha_{N_{rx}})$.
By applying the Varadhan's lemma [56] we obtain

$$\begin{aligned} d_{out}(r) &= -\lim_{\rho \to +\infty} \frac{\ln P_{out}(r \ln \rho)}{\ln \rho} \\ &= \lim_{t \to +\infty} \frac{1}{t} \ln \int_{\mathcal{A}} \prod_{i=1}^{N_{rx}} e^{-t(2i-1+LN_{tx}-N_{rx})\alpha_i} d\boldsymbol{\alpha} \\ &= \inf_{\boldsymbol{\alpha} \in \mathcal{A}} \sum_{i=1}^{N_{rx}} (2i-1+LN_{tx}-N_{rx})\alpha_i\,. \end{aligned} \tag{3.93}$$

The solution of the last equation can be found in [9] and turns out to be the piecewise-linear function connecting the points $(k, d_{out}(k))$, $k = 0, 1, \ldots, N_{rx}$, where

$$d_{out}(k) = (LN_{tx} - k)(N_{rx} - k)\,. \tag{3.94}$$

Case $N_{rx} > N_{tx}$ *:* We observe that capacity satisfies

$$\begin{aligned} C &= \mathrm{E}_{\mathbf{H}} \tfrac{1}{2\pi j} \oint \tfrac{dz}{z} \ln\det(I + \rho\,\mathbf{H}(z)\mathbf{H}^{\dagger}(z)) \\ &= \mathrm{E}_{\mathbf{H}} \tfrac{1}{2\pi j} \oint \tfrac{dz}{z} \ln\det(I + \rho\,\mathbf{H}(z)\mathbf{H}^{H}(z)) \\ &= \mathrm{E}_{\mathbf{H}} \tfrac{1}{2\pi j} \oint \tfrac{dz}{z} \ln\det(I + \rho\,\mathbf{H}^{T}(z)\mathbf{H}^{*}(z)) \,. \end{aligned} \tag{3.95}$$

In the second equality we replace † by H because the integral is done on the unit circle. We conclude that the capacity is the same as for a new virtual channel $\mathbf{H}^T(z)$. As a consequence the result of the first case, $N_{rx} \leq N_{tx}$, holds also here after interchanging N_{rx} and N_{tx}.

The two cases can be summarized by taking $d_{out}(k) = (Lq-k)(p-k)$ for $k = 0, 1, \ldots, p$. □

3.D Proof of Theorem 2

Lemma 3 allows us to write

$$P_{out}^{SIC}(r\ln\rho) \doteq \min_{r=\sum_{k=1}^{p} r_k} \sum_{i=1}^{p} P\left(C_i^{ZF} < r_i \ln\rho, C_1^{ZF} \geq r_1 \ln\rho, \ldots, C_{i-1}^{ZF} \geq r_{i-1}\ln\rho\right) \doteq$$

$$\min_{r=\sum_{k=1}^{p} r_k} \sum_{i=1}^{p} P\left((1-\alpha_{m-p+i})^{+} < r_i, (1-\alpha_{m-p+1})^{+} \geq r_1, \ldots, (1-\alpha_{m-p+i-1})^{+} \geq r_{i-1}\right) . \tag{3.96}$$

By C_i^{ZF} we denote $C_i^{MMSEZFDFE}$.
Let
$\mathcal{A}_i = \{\boldsymbol{\alpha} : (1-\alpha_{m-p+i})^{+} < r_i, (1-\alpha_{m-p+1})^{+} \geq r_1, \ldots, (1-\alpha_{m-p+i-1})^{+} \geq r_{i-1}, \alpha_1 \geq \alpha_2 \geq \ldots \geq \alpha_m\} \cap \mathbf{R}^{+m}$, where $\boldsymbol{\alpha} = (\alpha_1, \ldots, \alpha_m)$.
Each term of the sum can be written similarly as in appendix 3.C

$$P\left((1-\alpha_{m-p+i})^{+} < r_i, (1-\alpha_{m-p+1})^{+} \geq r_1, \ldots, (1-\alpha_{m-p+i-1})^{+} \geq r_{i-1}\right) \doteq \int_{\mathcal{A}_i} \prod_{k=1}^{m} \rho^{-(2k-1+n-m)\alpha_k} d\boldsymbol{\alpha} \,. \tag{3.97}$$

We denote $n = \max\{N_{rx}, N_{tx}L\}$.
Using Varadhan's lemma we can show that if $r_i \geq \max_{0\leq k\leq i-1} r_k$ (this condition

is always verified for the minimum outage as we will see in the optimization)

$$\begin{aligned}\int_{\mathcal{A}_i}\prod_{k=1}^{m}\rho^{-(2k-1+n-m)\alpha_k}d\boldsymbol{\alpha} &\doteq \rho^{-\inf\limits_{\boldsymbol{\alpha}\in\mathcal{A}_i}\sum\limits_{k=1}^{m}(2k-1+n-m)\alpha_k} \\ &\doteq \rho^{-(m-p+i)(n-p+i)(1-r_i)}\,.\end{aligned} \tag{3.98}$$

Hence, under the condition $r_i \geq \max\limits_{0\leq k\leq i-1} r_k$ we get

$$\begin{aligned}P\left(C_i^{ZF} < r_i\ln\rho, C_1^{ZF}\geq r_1\ln\rho,\ldots,C_{i-1}^{ZF}\geq r_{i-1}\ln\rho\right) &\doteq P\left(C_i^{ZF} < r_i\ln\rho\right) \\ &\doteq \rho^{-(m-p+i)(n-p+i)(1-r_i)}\,.\end{aligned} \tag{3.99}$$

C_i^{ZF} is positive quantity, then for $R_i = 0$

$$P\left(C_i^{ZF} < 0, C_1^{ZF}\geq r_1\ln\rho,\ldots,C_{i-1}^{ZF}\geq r_{i-1}\ln\rho\right) = 0 \doteq \rho^{-\infty}\,. \tag{3.100}$$

Now if we transmit on N_s streams, $r_i = 0$ for $i = 1,\ldots,p-N_s$, then

$$\begin{aligned}&\sum_{i=p-N_s+1}^{p} P\left(C_i^{ZF} < r_i\ln\rho, C_{p-N_s+1}^{ZF}\geq r_{p-N_s+1}\ln\rho,\ldots,C_{i-1}^{ZF}\geq r_{i-1}\ln\rho\right) \doteq \\ &\max_{i=p-N_s+1,\ldots,p}\rho^{-(m-p+i)(n-p+i)(1-r_i)} \doteq \rho^{-\min_{i=p-N_s+1,\ldots,p}\ (m-p+i)(n-p+i)(1-r_i)}\,.\end{aligned} \tag{3.101}$$

The number of streams is then also an argument of the optimization of the outage

$$\begin{aligned}d_{out}^{SIC}(r) &= -\lim_{\rho\to\infty}\frac{\ln P_{out}^{SIC}(r\ln\rho)}{\ln\rho} \\ &= \max_{N_s=1,\ldots,p}\ \min_{r=\sum_{k=p-N_s+1,\ldots,p}r_k}\ \min_{i=p-N_s+1}^{p}(m-p+i)(n-p+i)(1-r_i)\,.\end{aligned} \tag{3.102}$$

The coefficient $(m-p+i)(n-p+i)$ that multiplies $1-r_i$ represents the diversity of each stream i. We observe that the diversity is an increasing function of i. The optimal solution that maximizes $d_{out}^{SIC}(r)$ has to allocate more rate to the stream that has the more diversity in order to maximize the minimum of $(m-p+i)(n-p+i)(1-r_i)$. We can then conclude that the optimal solution satisfies $r_1 \leq r_2 \leq \ldots \leq r_p$.
Let P_k denotes the point where we start transmitting on k streams $(p-k+1,\ldots,p)$. At this point $r_{p-k+1} = 0^+$. For the optimal solution the value of

$d_{out}^{SIC}(r)$ at this point is $(m-p+p-k+1)(n-p+p-k+1) = (m-k+1)(n-k+1)$. The optimization of this point constrains that

$$(m-k+1)(n-k+1) = (m-k+2)(n-k+2)(1-r_{p-k+2}) = \ldots = mn(1-r_p)\,, \tag{3.103}$$

the multiplexing rate at this point is then

$$r_k^t = k-1-(m-k+1)(n-k+1)\sum_{i=2}^{k}\frac{1}{(m-k+i)(n-k+i)}\,. \tag{3.104}$$

We use a variable change $k-1 \to k$. The optimal solution for $d_{out}^{SIC}(r)$ turns out to be the piecewise-linear function connecting the points $(b_k, d_{out}^{SIC}(b_k))$, $k = 0, \ldots, p$, where

$$\begin{array}{rcll} r_k^t & = & k-(m-k)(n-k)\displaystyle\sum_{i=1}^{k}\frac{1}{(m-k+i)(n-k+i)} & ,\ k=0,\ldots,p-1 \\ r_k^t & = & p & ,\ k=p \end{array} \tag{3.105}$$

and

$$\begin{array}{rcll} d_{out}^{SIC}(r_k^t) & = & (m-k)(n-k) & ,\ k=0,\ldots,p-1 \\ d_{out}^{SIC}(r_k^t) & = & 0 & ,\ k=p \end{array} \tag{3.106}$$

For the corresponding optimal rate allocation, and for $r \in [r_k^t,\, r_{k+1}^t]\,(0 \le k \le p-1)$, only $k+1$ streams are used. With rates r_i, $p-k \le i \le p$

$$\begin{gathered} (m-k)(n-k)(1-r_{p-k}) = (m-k+1)(n-k+1)(1-r_{p-k+1}) = \ldots = mn(1-r_p) \\ \sum_{i=p-k}^{p} r_i = r \end{gathered} \tag{3.107}$$

□

3.E Proof of Theorem 3

We consider the Stripping MMSE ZF DFE Rx described in subsection 3.2.1. After streams $1, \ldots, i-1$ have been detected and canceled, the symbols of the actual processed i^{th} stream are detected sequentially. We denote by P_e^i the probability of erroneous detection of the i^{th} stream, and by $P_e^i(b_k^i)$

the probability of making an error when detecting the k^{th} symbol of the actual stream (assuming the symbols $1, 2, \ldots, k-1$ were correctly detected). Whenever there is an error on any of the detected symbols, the stream is said to be in error. The error probability on stream i is the union of the probabilities of the events of making an error on the symbols k, where the previous symbols were correctly detected and canceled. These events are disjoint sets, we have then

$$P_e^i = \sum_{k=1}^{T-LN_{tx}+1} P(E_k^i, \bar{E}_1^i, \ldots, \bar{E}_{k-1}^i), \tag{3.108}$$

where E_k^i is the event of making an error on b_k^i, and $\bar{E}_k^i$ is its complement. Obviously $P_e^i \geq P(E_1^i)$, in the other hand, for each i

$$\begin{array}{rcl} P(E_k^i, \bar{E}_1^i, \ldots, \bar{E}_{k-1}^i) & = & P(E_k^i | \bar{E}_1^i, \ldots, \bar{E}_{k-1}^i) P(\bar{E}_1^i, \ldots, \bar{E}_{k-1}^i) \\ & \leq & P(E_k^i | \bar{E}_1^i, \ldots, \bar{E}_{k-1}^i)\,, \end{array} \tag{3.109}$$

hence

$$P_e^i \leq \sum_{k=1}^{T-LN_{tx}+1} P(E_k^i | \bar{E}_1^i, \ldots, \bar{E}_{k-1}^i) \tag{3.110}$$

For the ZF design and for perfect feedback, the noise experienced by the sequence of symbols, that belong to the same stream, is an AWGN (see subsection 3.2.1). The condition $\bar{E}_1^i, \ldots, \bar{E}_{k-1}^i$ is equivalent to correct feedback, then $P(E_k^i | \bar{E}_1^i, \ldots, \bar{E}_{k-1}^i) = P(E_1^i)$, $k = 2, 3$, $T - LN_{tx} + 1$. Finally if we denote $P(E_1^i)$ by $P_e^i(b_1^i)$ we have

$$P_e^i(b_1^i) \leq P_e^i \leq (T - LN_{tx} + 1) P_e^i(b_1^i)\,. \tag{3.111}$$

We conclude that $P_e^i \doteq P_e^i(b_1^i)$.
Eq. (3.7) allows us to write the output of the linear filter

$$\widehat{b}_1^i = b_1^i + e_1^i\,, \tag{3.112}$$

where e_1^i is a centered white Gaussian noise of variance
$\sigma_{e^i}^2 = \sigma_v^2\, \Sigma_{ii} = \sigma_b^2 (\mathrm{SNR}_i^{MMSEZF})^{-1}$. b_1^i comes from a QAM constellation of size ρ^{r_i}, $(0 < r_i < 1)$ with minimum distance d_i such as $d_i^2 = \frac{3\sigma_b^2}{2(\rho^{r_i}-1)}$ (see section 2.5.2).

For the processed stream 1, let $b_1^{1\prime}$ be one of the nearest neighbors of b_1^1, the PEP is

$$\begin{aligned} P(b_1^1 \to b_1^{1\prime}) &\doteq P(\tfrac{1}{\sigma_{e^1}^2} d_1^2 \leq 1) \\ &\doteq P(\mathrm{SNR}_1^{MMSEZF} \rho^{-r_1} \leq 1) \\ &\doteq P(\mathrm{SNR}_1^{MMSEZF} \leq \rho^{r_1}) \\ &\doteq P(1 + \mathrm{SNR}_1^{MMSEZF} \leq \rho^{r_1}) \\ &\doteq P(\ln(1 + \mathrm{SNR}_1^{MMSEZF}) \leq r_1 \ln \rho) \\ &\doteq P(C_1^{ZF} \leq r_1 \ln \rho)\,, \end{aligned} \tag{3.113}$$

where in the first equation we used a result derived in equation (21) of [9]. For QAM constellation there is at most four nearest neighbors to b_1^1, the overall error event is upper bounded by the union of all the error events corresponding to the nearest neighbors. We can then write

$$\begin{aligned} P_e^1 &\doteq (T - LN_{tx} + 1) P(b_1^1 \to b_1^{1\prime}) \\ &\doteq P(C_1^{ZF} \leq r_1 \ln \rho)\,, \end{aligned} \tag{3.114}$$

Similarly we can show that the overall error probability for a given rate allocation satisfies

$$\begin{aligned} P_e &\doteq \sum_{i=1}^{p} P_e^i \\ &\doteq \sum_{i=1}^{p} P\left(C_i^{ZF} < r_i \ln \rho, C_1^{ZF} \geq r_1 \ln \rho, \ldots, C_{i-1}^{ZF} \geq r_{i-1} \ln \rho\right)\,, \end{aligned} \tag{3.115}$$

where the right hand side of the second equation is the same as the outage probability for a given rate allocation. The optimization of P_e w.r.t. the rate allocation gives the same solution as the outage one

$$d^{*,SIC}(r) = d_{out}^{SIC}(r)\,. \tag{3.116}$$

□

3.F Proof of Theorem 5

To prove Theorem 5 we have to study the error probability.
Similarly to what has been done in appendix 3.E we can show that the error

probability verifies

$$P_e \leq (T - N_{tx} + 1)P_e^1 \,, \tag{3.117}$$

where P_e^1 is the probability to make an error on the first symbol. P_e^1 is upper bounded by

$$P_e^1 \leq \sum_{\mathbf{b}_1 \neq \mathbf{b}_1^{'}} P(\mathbf{b}_1 \rightarrow \mathbf{b}_1') \,, \tag{3.118}$$

where $P(\mathbf{b}_1 \rightarrow \mathbf{b}_1')$ is the probability to transmit $\mathbf{b}_1$ and to detect $\mathbf{b}_1'$.
For a fixed rate, the number of terms in the sum (3.118) is finite. As has been done in section 1.4, the diversity gain is then given by the worst diversity gain between the $P(\mathbf{b}_1 \rightarrow \mathbf{b}_1')$'s.

Consider a weighted minimum distance detector, $P(\mathbf{b}_1 \rightarrow \mathbf{b}_1')$ is the probability that $||\widehat{\mathbf{b}}_1 - \mathbf{b}_1||^2_{\mathbf{M}} \geq ||\widehat{\mathbf{b}}_1 - \mathbf{b}_1'||^2_{\mathbf{M}}$. Denote $\Delta\mathbf{b} = \mathbf{b}_1' - \mathbf{b}_1$, $||\widehat{\mathbf{b}}_1 - \mathbf{b}_1||^2_{\mathbf{M}} - ||\widehat{\mathbf{b}}_1 - \mathbf{b}_1'||^2_{\mathbf{M}} = -\Delta\mathbf{b}^H\mathbf{M}\Delta\mathbf{b} + 2\Re\{\Delta\mathbf{b}^H\mathbf{M}\mathbf{e}_1\}$. $\nu = 2\Re\{\Delta\mathbf{b}^H\mathbf{M}\mathbf{e}_1\}$ has a Gaussian distribution $\nu \sim \mathcal{N}(0, 2\sigma_v^2\Delta\mathbf{b}^H\mathbf{M}\Delta\mathbf{b})$

$$\begin{aligned} P(\mathbf{b}_1 \rightarrow \mathbf{b}_1'|\mathbf{H}) &= P(\nu \geq \Delta\mathbf{b}^H\mathbf{M}\Delta\mathbf{b}|\mathbf{H}) \\ &= Q_G\left(\sqrt{\frac{\Delta\mathbf{b}^H\mathbf{M}\Delta\mathbf{b}}{2\sigma_v^2}}\right) \\ &\leq e^{-\frac{\Delta\mathbf{b}^H\mathbf{M}\Delta\mathbf{b}}{4\sigma_v^2}} \\ &= e^{-\frac{\Delta\mathbf{b}^H\mathbf{Q}^H\mathbf{D}\mathbf{Q}\Delta\mathbf{b}}{4\sigma_v^2}} \\ &= e^{-\frac{\Delta\mathbf{c}^H\mathbf{D}\Delta\mathbf{c}}{4\sigma_v^2}} \,, \end{aligned} \tag{3.119}$$

where $Q_G(.)$ is the Gaussian tail function, $\Delta\mathbf{c} = \mathbf{Q}\Delta\mathbf{b}$, and the third inequality corresponds to the Chernoff bound.
We use the MMSE ZF DFE with $N_{rx} \geq N_{tx}$. $\mathbf{D}$ is identifiable from the QR factorization of $\mathbf{H} = \mathbf{U}\mathbf{R}$. In fact, $\mathbf{U}$ is a $N_{rx} \times N_{tx}$ unitary matrix and $\mathbf{R}$ is a $N_{tx} \times N_{tx}$ upper triangular matrix, then $\mathbf{L}\mathbf{D}\mathbf{L}^H = \mathbf{R}^H\mathbf{R}$ and $\mathbf{D}_i = |\mathbf{R}_{ii}|^2$. Denote $\overline{\mathbf{H}}_i = [\mathbf{h}_1, \ldots, \mathbf{h}_{i-1}]$ and $\overline{\mathbf{h}}_i = (\mathbf{I}_{N_{rx}} - P_{\overline{\mathbf{H}}_i})\mathbf{h}_i$ the projection of $\mathbf{h}_i$ over the orthogonal complement of $\overline{\mathbf{H}}_i$. Then $|\mathbf{R}_{ii}| = ||\overline{\mathbf{h}}_i||$ and
$\mathbf{D}_i = ||\overline{\mathbf{h}}_i||^2 = \overline{\mathbf{h}}_i^H\overline{\mathbf{h}}_i$.
The dependence between $\overline{\mathbf{h}}_i$, $i = 1, \ldots, N_{tx}$, comes only from the directions, hence the norms $||\overline{\mathbf{h}}_i||, i = 1, \ldots, N_{tx}$, are independent.

$\mathbf{D}_i$, $i = 1, \ldots, N_{tx}$ have then independent Chi-square distributions with $2(N_{rx} - i + 1)$, $i = 1, \ldots, N_{tx}$, degrees of freedom. The error probability is then

$$\begin{aligned} P(\mathbf{b}_1 \to \mathbf{b}_1') = \mathrm{E}_{\mathbf{H}} P(\mathbf{b}_1 \to \mathbf{b}_1'|\mathbf{H}) &\leq \prod_{i=1}^{N_{tx}} \left(\int e^{-\frac{|\Delta \mathbf{c}_i|^2 \mathbf{D}_i}{4\sigma_v^2}} f_i(\mathbf{D}_i) d\mathbf{D}_i \right) \\ &= \prod_{i=1}^{N_{tx}} \left(1 + \frac{|\Delta \mathbf{c}_i|^2}{4\sigma_v^2} \right)^{-(N_{rx}-i+1)} \\ &\leq \prod_{i=1}^{N_{tx}} \left(\frac{|\Delta \mathbf{c}_i|^2}{4\sigma_v^2} \right)^{-(N_{rx}-i+1)} , \end{aligned} \tag{3.120}$$

where $f_i(.)$, $i = 1, \ldots, N_{tx}$ are the pdf of the Chi-square distributions with $2(N_{rx} - i + 1)$, $i = 1, \ldots, N_{tx}$, degrees of freedom.

We have shown in subsection 2.5.2 that due to the choice of the precoding matrix, $\mathbf{Q}$, and for a uniform QAM constellations with $(2M)^2$ points, the following property is verified for any possible $\Delta \mathbf{c}$: $\frac{|\Delta \mathbf{c}_i|^2}{\sigma_b^2} > 0$ for $i = 1, \ldots, N_{tx}$.

We get finally that

$$P(\mathbf{b}_1 \to \mathbf{b}_1') \leq c_g \rho^{-N_{tx}(N_{rx} - \frac{N_{tx}-1}{2})} . \tag{3.121}$$

where $c_g = \min_{\Delta \mathbf{c} \neq 0} \prod_{i=1}^{N_{tx}} \left(\frac{|\Delta \mathbf{c}_i|^2}{4\sigma_b^2} \right)^{-(N_{rx}-i+1)}$.

The SNR exponent $N_{tx}(N_{rx} - \frac{N_{tx}-1}{2})$ corresponds to the diversity gain. □

Chapter 4

Iterative Rx

The STS scheme based on linear precoding was introduced in chapter 2. STS allows to attain full diversity without loss in ergodic capacity. However STS cannot provide high coding gain. Hence, practical transmission systems have to resort to binary channel coding. Threading is an example of a MIMO transmission system in which spatial diversity gets exploited via channel coding only. Practical symbol constellations however only allow the exploitation of a limited diversity order by the binary channel coding. Hence powerful yet simple MIMO Tx schemes can be obtained by combining the coding gain and diversity exploitation of classical binary channel codes with linear precoding to exploit the remaining diversity degrees. A typical design would use channel coding to exploit temporal fading with linear precoding to exploit space-frequency fading.

4.1 Introduction

Recent schemes [22, 23, 24] based on constellation rotating, succeed to exploit all the diversity without rate loss but require ML decoding leading to an exponential (in N_{tx}, size of the block and constellation size) complexity that limits its use. Constellation rotating doesn't enhance the coding gain and can even worsen it. For practical applications it has to be coupled with a binary channel code, it leads then to the potential use of a turbo decoding approach, which reduces the complexity. Unfortunately, the structures of these schemes lead to the calculation of a different equalizers, one by symbol, and make complex the use of turbo decoder. On the other hand, the turbo decoding approach was proposed in [57] as a decoder for the Threading scheme. Taking advantage of the presence of the binary channel code to exploit diversity, this scheme, even if it succeeds to achieve a good performance, is limited by the binary channel code ability to exploit diversity.
We propose to combine binary channel coding and the linear precoding of STS to use a turbo decoder with interference cancellation. The binary channel code can also be used to exploit the block diversity, this chapter proposes a practical scheme to this end, analyses the performances and is supported by numerical examples.
The results presented in this chapter are to be published in [58].

4.2 Combining Linear Precoding and Binary Channel Coding

Linear precoding was introduced to exploit the transmit diversity, leading to a maximum diversity gain. This gain corresponds to the slope of the error probability vs. SNR curve (in logarithmic scale), but in order to achieve this regime (fast decaying error probability P_e) we need an SNR such that $\rho >> 4\left(\frac{1}{coding gain}\right)^{\frac{1}{N_{tx}}} = \frac{2(4M^2-1)N_{tx}}{3}$ (subsection 2.5.2). This SNR range is out of scope for practical systems. For lower SNR values, it will be important to improve the position of the P_e curve by increasing the coding gain via binary channel coding, see fig. 4.1. The use of a binary channel code increases the minimum distance of the encoded sequence, the by a using a good interleaver, the coding gain: $C_g = \min_{\mathbf{C}\neq\mathbf{C}'} \det\left((\mathbf{C}-\mathbf{C}')(\mathbf{C}-\mathbf{C}')^H\right)$ is increased. The choice of the interleaver should maximize C_g, however this

chapter does not deal with this problem and use a random interleaver. In fact the minimum of $\det\left((\mathbf{C}-\mathbf{C}')(\mathbf{C}-\mathbf{C}')^H\right)$ is achieved for errors with small distance (or Frobenius norm), the matrix $\mathbf{C}-\mathbf{C}'$ is hence sparse, and taking into account that the determinant is maximized for orthogonal $\mathbf{C}-\mathbf{C}'$ rows, using the random interleaver ensures orthogonal or near orthogonal rows and consequently optimal or near optimal performance.
For channel decoding, we consider an iterative decoder that combines a SISO decoder with a MIMO linear filter and Interference Canceler (IC), pictured in fig. 4.3. This decoder structure was first used for CDMA [59], and was then proposed for the MIMO reception [60, 61, 57]. It is the analog to the turbo detection when the mapping, Linear precoding and the channel (resp. the binary channel coding) are seen as Inner coding (resp. Outer coding). This decoder structure exhibits good performance for small size constellations and exploits the diversity when a LMMSE front-end equalizer is used [61]. In the sequel we give a short overview of iterative channel decoding with interference cancellation.

4.2.1 Encoding

Fig. 4.1 shows the encoding operation. The binary channel encoder output is followed by the interleaver, the output is then mapped into symbols before serial-to-parallel conversion. Fig. 4.2 clarifies how the S/P conversion is done, the entries in the array indicating the index of the symbols at the output of the mapper. The symbols vector $\boldsymbol{b}_k$ is then filtered by $\mathbf{T}(z)$.
If the iterative decoder would succeed canceling all the interference (genie aided decoder), each symbol would be interfered only by noise. Performance would then reach the matched filter bound, which corresponds to full diversity exploitation. The binary channel coder and interleaver are in this case only used to lower the error probability (increase coding gain). Now, by considering the overall channel and the binary channel code as the two constituents of a serial turbo code, then a lower error probability can be obtained by increasing the minimum distance. Therefore a good choice for the interleaver for large frame sizes is to choose a random interleaver.

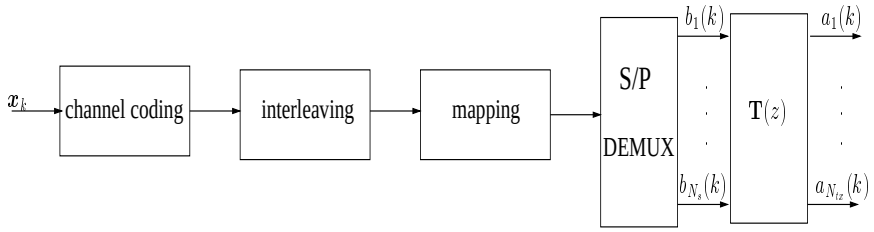

Figure 4.1: Encoder for space-time spreading.

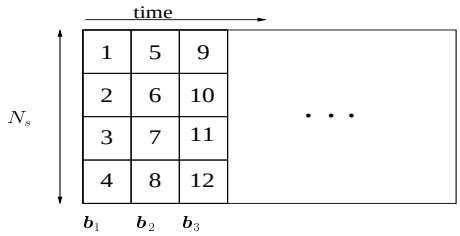

Figure 4.2: Serial-to-parallel converted space-time block before precoding for $N_s = 4$.

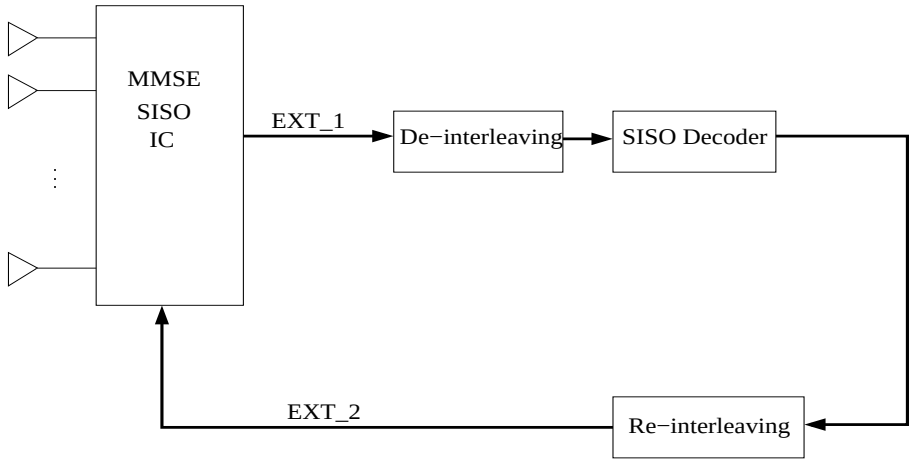

Figure 4.3: Iterative decoder with interference cancellation.

4.2.2 Iterative Decoding

In this section we propose an iterative decoding strategy for a general block fading channel. We consider an iterative decoding scheme with IC, see fig. 4.3. The first block of the scheme contains the IC operation followed by a MIMO linear equalizer, and symbol-to-bit demapping and de-interleaving. The second block of the decoder is the maximum-a-posteriori (MAP) soft-Input soft-Output (sIsO, to distinguish from SISO) decoder of the binary channel code (for instance, we use a convolutional code and the corresponding BCJR SISO decoder [62]) followed by the interleaver and the bit-to-symbol mapper. These two blocks exchange information in the form of Log-Likelihood Ratios (LLRs) during iterations, the overall decoder can be seen as an application of the belief propagation principle, also known as the sum-product algorithm [59],[60]. We assume that the residual interference plus noise at the output of the equalizer follows a Gaussian distribution. This is clearly an approximation, however it tends to be valid for large systems (large N_{tx} and/or delay spread), see [59] for the case of CDMA.
Recall that the overall channel $\mathbf{H}(q)\,\mathbf{T}(q)$ is denoted by $\mathbf{G}(q)$.
As linear equalizer we use the Ubiased MMSE (UMMSE) design, where

$$\mathbf{f}_n^{(i)}(z) = \frac{1}{\frac{1}{2\pi j}\oint \frac{dz}{z}\rho \mathbf{G}_{:,n}^{\dagger}(z)\mathbf{R}^{(i)}(z)^{-1}\mathbf{G}_{:,n}(z)}\mathbf{G}_{:,n}^{\dagger}(z)\mathbf{R}^{(i)}(z)^{-1} \tag{4.1}$$

is the equalizer filter for $\mathbf{T}(z)$, stream (input) number n of the MIMO system at iteration i, $\mathbf{R}^{(i)}(z) = \sigma_v^2 I + \sum_{n=1}^{N_{tx}} \tilde{\sigma}_{b_n}^{2\,(i-1)}\mathbf{G}_{:,n}(z)\mathbf{G}_{:,n}^{\dagger}(z)$ is the spectrum of the noise plus residual interference and $\tilde{\sigma}_{b_n}^{2\,(i)} = \mathrm{E}\,|\tilde{b}_n^{(i)}(k)|^2 = \mathrm{E}\,|b_n(k) - \hat{b}_n^{(i)}(k)|^2$ is the variance of the residual interference of stream n. $\hat{b}_n^{(i)}(k) = E(b_n(k)\,|\,\mathrm{EXT}_2^{(i)})$ is the MMSE estimate of $b_n(k)$ based on the information contained in $\mathrm{EXT}_2^{(i)}$. For the residual interference spectrum we assume that the residual interference $\tilde{b}_n(k)$ is temporally and spatially white and decorrelated from the noise. This approximation is again valid for large systems (and hence works better when linear precoding is used).
Finally, the equalizer output at iteration (i) for stream n at time k is

$$s_n^{(i)}(k) = \mathbf{f}_n^{(i)}(q)\,\left(\boldsymbol{y}_k - \mathbf{G}(q)\hat{\boldsymbol{b}}_k^{(i-1)}\right) + \hat{b}_n^{(i-1)}(k)\,. \tag{4.2}$$

Due to the unbiasedness of $\mathbf{f}_n^{(i)}$, $\hat{b}_n^{(i-1)}(k)$ does not appear in $s_n^{(i)}(k)$. Let's denote the bit-to-symbol mapping by $\mu : \mathbb{F}_2^P \to \mathcal{A}$, where $\mathbb{F}_2$ is the binary

alphabet and $P = \log_2(|\mathcal{A}|)$ is the number of coded (and interleaved) bits per symbol: $b_n(k) = \mu(x^1_{n,k}, \ldots, x^P_{n,k})$. The extrinsic information of the p^{th} bit of the binary mapping of the k^{th} symbol of stream n, evaluated at the output of the IC at the $(i)^{th}$ iteration is

$$\begin{aligned} \mathrm{EXT}_2^{(i)}(x^p_{n,k}) &= \log \frac{P(x^p_{n,k}=1|s^{(i)}_{n,k},\mathbf{G})}{P(x^p_{n,k}=0|s^{(i)}_{n,k},\mathbf{G})} \\ &= \log \frac{\sum_{b_{n,k}\in\mathcal{A}|x^p_{n,k}=1} P(s^{(i)}_{n,k}|b_{n,k},\mathbf{G}) \ \exp\left(\sum_{p'=1,\neq p}^{P} \mathrm{EXT}_1^{(i-1)}(x^{p'}_{n,k})\right)}{\sum_{b_{n,k}\in\mathcal{A}|x^p_{n,k}=0} P(s^{(i)}_{n,k}|b_{n,k},\mathbf{G}) \ \exp\left(\sum_{p'=1,\neq p}^{P} \mathrm{EXT}_1^{(i-1)}(x^{p'}_{n,k})\right)}, \end{aligned} \tag{4.3}$$

where the probability $P(s^{(i)}_{n,k}|b_{n,k},\mathbf{G})$ is evaluated by assuming that $\bar{v}^{(i)}_{n,k} = s^{(i)}_{n,k} - b_{n,k}$ is an AWGN.
After de-interleaving, the EXT_1 information sequence is used as a priori LLR input to the MAP decoder of the binary channel code which is a convolutional code in our case. Using the forward-backward BCJR algorithm, the a posteriori LLR is computed and the extrinsic information is defined as $\mathrm{EXT}_2^{(i)} = \mathrm{MAP}(\mathrm{EXT}_1^{(i)}) - \mathrm{EXT}_1^{(i)}$. Experimentally we observed that the number of iterations needed for the convergence of this algorithm is small, typically 3 or 4 iterations.
Remarks:
• For a flat channel with $N_s = N_{tx}$ we can show by induction that: $\tilde{\sigma}^{2\,(i)}_{b_n} = \tilde{\sigma}^{2\,(i)}_b$, $n = 1, \ldots N_{tx}$, and that $\mathbf{f}^{(i)}_n(z) = \frac{N_{tx}/\rho}{\mathrm{tr}\{\mathbf{H}^H\mathbf{R}\mathbf{H}\}}\mathbf{T}^{\dagger}_{:,n}(z)\mathbf{H}^H\mathbf{R}$, $\mathbf{R} = \left(\sigma_v^2 I + \tilde{\sigma}^{2\,(i-1)}_b \mathbf{H}\mathbf{H}^H\right)^{-1}$. This simplifies the equalization: the joint equalizer for all streams consists of a channel equalizer followed by the matched filter of the precoder (= precoder inverse since $\mathbf{T}(z)$ is paraunitary). Even if these results cannot be generalized to the frequency selective channel case, experiments show that performance does not degrade when using the suboptimal approach. This approach consists in averaging the $\tilde{\sigma}^{2\,(i)}_{b_n}$'s over streams and using a MIMO equalizer of the frequency selective channel followed by the matched filter of the precoder.
• The stream equalizer can be designed using criteria other than UMMSE, typically Zero-Forcing or channel Matched Filter. These two alternative designs lead to performance loss. Especially the MF design leads to an error floor and therefore doesn't exploit diversity.

4.2.3 Complexity Comparison with Threading

Whereas the proposed STS strategy differs from V-BLAST by the insertion of the time-invariant precoder filter $\mathbf{T}(z)$, in Threading [57] $\mathbf{T}(z)$ is replaced by a periodically time-varying cyclic shift matrix $\mathbf{Z}^{k \bmod N_{tx}}$ where $\mathbf{Z}$ is the elementary circulant shift matrix. When comparing STS to Threading, in the encoding part, precoding with $\mathbf{T}(z)$ leads to an additional complexity $\mathcal{O}(\log_2(N_{tx}))$ per symbol period. $\mathcal{O}(\log_2(N_{tx}))$ results from the multiplication of $\boldsymbol{b}_k$ by $\mathbf{Q}$ which has a DFT-like structure (see section 2.5.1). This is a negligible increase compared to the remaining operations such as binary channel coding and pulse shaping. At the receiver side the additional complexity comes from the inverse operation, namely the matched filter $\mathbf{T}^{\dagger}(z)$, with same negligible complexity increase.

4.3 Multi-Block Time Diversity

In the usual SISO fading channel problem, time diversity of the channel (*i.e.* the variation from block to block) is used to improve performance. We can exploit block fading for the MIMO channel as well. Below, we discuss how to exploit the diversity sources with STS.

We consider a block-fading environment with F i.i.d. blocks.

Case of STS:
In the STS approach, space-frequency diversity is exploited in each block by the linear precoding. The problem of additionally exploiting temporal diversity (from block to block) is then reduced to the SISO channel fading problem.
If we denote by d_F the diversity exploited in this latter problem, the overall diversity exploited by STS is then $d^{STS} = d_F\, N_{tx}\, N_{rx}\, L$.
In order to exploit temporal diversity, we need to first use a block interleaver on the ensemble of fading blocks (see fig. 4.4), and then apply a random interleaver within each block. Using a genie-aided reasoning, the temporal diversity that can be achieved is limited by the fundamental Singleton Bound (SB) [63]

$$d_F \leq 1 + \lfloor F_d(1 - \frac{r}{|\mathcal{A}|}) \rfloor \leq F_d\,, \tag{4.4}$$

where r is the rate of the binary channel code, $\lfloor . \rfloor$ denotes the flooring operation, and F_d ($= F$ here) is the number of diversity branches. The diversity

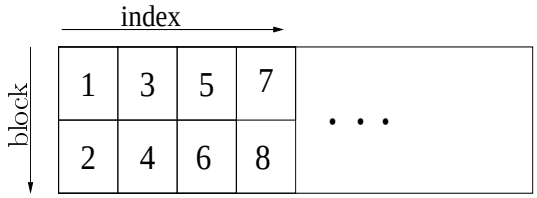

Figure 4.4: Block interleaver for F=2.

exploited by STS is hence bounded by

$$d^{STS} = d_F \, N_{tx} \, N_{rx} \, L \leq \left(1 + \lfloor F(1 - \frac{r}{|\mathcal{A}|}) \rfloor\right) N_{tx} \, N_{rx} \, L \, . \tag{4.5}$$

Table 4.1 gives the SB and the temporal diversity exploited by a set of channel convolutional codes with $r = \frac{1}{2}$ and for different symbol constellations and different number F_d of diversity branches.

d_F or d_s		BPSK			QPSK		
States	Generators	F_d=2	4	8	2	4	8
Singleton Bound		2	3	5	2	4	7
4	(5,7)	2	3	4	2	3	3
8	(15,17)	2	3	4	2	3	4
16	(23,35)	2	3	5	2	3	4
32	(53,75)	2	3	5	2	3	4
64	(133,171)	2	3	5	2	3	5

Table 4.1: Block diversity for some popular rate 1/2 binary convolutional codes mapped onto BPSK and QPSK (with Gray labeling). Code generators are expressed in octal notation [12].

Case of Threading:
In the case of Threading, no linear precoding is used to help the binary channel code to exploit all the diversity sources. The number of diversity branches is here $F_d = FN_{tx}$[60]. By applying the same reasoning as before, the (source) diversity d_s exploited by the binary channel code is bounded by

$$d_s \leq 1 + \lfloor FN_{tx}(1 - \frac{r}{|\mathcal{A}|}) \rfloor \leq FN_{tx} \, . \tag{4.6}$$

The overall exploited diversity is then $d^{Thr} = d_s \, N_{rx} \, L$. The overall diversity

exploited by Threading is then

$$d^{Thr} \leq \left(1 + \lfloor FN_{tx}(1 - \frac{r}{|\mathcal{A}|})\rfloor\right) N_{rx}\, L\,. \tag{4.7}$$

Comparison:
From table 4.1 we can see that for $r = \frac{1}{2}$ and using convolutional code the effectively exploited diversity degree d_s, in the Threading case, is far from the available one (FN_{tx}).
For example, for $N_{tx} = N_{rx} = 4$, $F = 2$, $L = 1$, (5,7) code and QPSK constellation, the binary CC exploits all the diversity branches in the STS case $d_F = 2$, $F_d = F = 2$, and only $d_s = 3$ over $F_d = N_{tx}F = 8$ branches for the Threading case. The total exploited diversity by each technique are then $d^{STS} = 32 > d^{Thr} = 12$. The only way to exploit higher diversity in the Threading case are then by lowering the rate and increasing the constellation size. This leads to high decoding complexity and low performance in comparison with the case of STS.
Remarks:
- Using the SB we can explain why the proposed STS achieves full diversity for a single block MIMO channel. In fact, prefiltering the QAM constellation increases the constellation size at the channel input from $|\mathcal{A}|$ to $|\mathcal{A}|^{N_{tx}}$. Therefore the SB becomes: $1 + \lfloor N_{tx}(1 - \frac{1}{|\mathcal{A}|^{N_{tx}}})\rfloor = 1 + \lfloor N_{tx} - 2^{n_t - P\,2^{n_t}}\rfloor$ where $n_t = \log_2(N_{tx}) \geq 1$ as $N_{tx} \geq 2$ and $P = \log_2(|\mathcal{A}|) \geq 1$. These two last conditions imply that $n_t - P\,.\,2^{n_t} < 0$ and hence $0 \leq 2^{n_t - P\,.\,2^{n_t}} < 1$. Finally $\lfloor N_{tx} - 2^{n_t - P\,2^{n_t}}\rfloor = N_{tx} - 1$ and the SB equals N_{tx}. The bound on the achievable diversity by STS is then $N_{rx}N_{tx}$.
- Two other recent approaches are the Complex Field Coding approach of Giannakis [22] and the Universal Coding approach of El Gamal [23, 24]. These approaches, similar to earlier work by Belfiore [31], correspond to linear dispersive block codes with block length equal to N_{tx}. As a result, each transmitted symbol sees a different SINR and symbol-independent equalization or residual interference variance in a turbo detection approach do not apply. That's why these authors consider other ML detection approximations in the form of sphere decoding.

4.4 Performance Analysis

We compare the performance of STS and Threading via simulation. We use for both a rate 1/2, (5,7) four states convolutional code, to take advantage of the availability of computationally efficient sIsO decoders (BCJR). Performance is evaluated in terms of frame error rate (FER) as a function of E_b/N_0 ($SNR = R\,E_b/N_0, R = rN_s \log_2 |\mathcal{A}|, \rho = SNR/N_s$). We run simulations for an input frame of 512 information bits for $N_{tx} = 2, 4$, and 1024 for $N_{tx} = 8$. We fix the number of decoding iterations to 5. We use QPSK with Gray labeling.

4.4.1 Comparison of Threading and STS

In fig. 4.5, for $F = 1, 2, 4$ blocks, we see that STS (solid lines) succeeds in exploiting more diversity than Threading (dash-dot) except for $F = 1$ block. *E.g.* for $F = 2$, the asymptotic slope for ML decoding would be equal, for Threading, to $d_s N_{rx} = 3 \times 2 = 6$ and for STS to $d_F N_{tx} N_{rx} = 3 \times 2 \times 2 = 12$. In fig. 4.6, the slopes roughly double when delay spread L doubles. In fig. 4.7, when the number of antennas double, STS and Threading differentiate even for $F = 1$ block and the slopes again increase when the number of antennas further double in fig. 4.8. The increase in the number of antennas (N_{rx}) also leads to an array gain and hence a translation of the curves to the left.

Case of a channel with $N_{rx} < N_{tx}$
In fig. 4.9, we consider the case $2 = N_{rx} < N_{tx} = 4$. For STS, we vary the number of streams N_s by varying the number of inputs to $\mathbf{T}(z)$. With $N_s = 2$, STS achieves the same diversity in a 2×4 MIMO system with $F = 1$ as in a square 2×2 MIMO system with $F = 2$: we observe equivalence between N_{tx}/N_{rx} and F.
We also consider the Space-Time Orthogonal Design (STOD) of Tarokh [21] which leads to the leftmost curve, but at rate 0.75b/s/Hz. We see that at 2 b/s/Hz (the two middle curves), STS (solid) with $N_s = 2$ ("half rate": $\frac{N_s}{N_{tx}} = \frac{1}{2}$) and QPSK performs much better than Threading (dash-dot) with $N_s = 4$ ("full rate") and BPSK.

4.4.2 Use of Walsh Hadamard (WH) matrix as Precoding matrix

In fig. 4.10, we compare the performance of the STS scheme when using our optimized precoding matrix ($Q = Q_s$, solid lines), with the case where we use the normalized Walsh Hadamard matrix as precoding matrix ($Q = Q_{WH}$, dash-dot lines). The normalization is done such that $Q_{WH} = \alpha \mathbf{M}_{WH}$, where $\mathbf{M}_{WH}$ is the Walsh Hadamard matrix with entries equal to ± 1 and $Q_{WH}^H Q_{WH} = \mathbf{I}$. The comparison is done for different number of antennas. We observe then that the two precoding matrices yield the same performance. Consequetly, when using a turbo detector we can replace the optimized precoding matrix by the WH matrix. These results in a reduction of complexity and a possible and simple adaptation of the CDMA systems to MIMO high rate transmission.

4.5 Conclusion

The STS scheme proposed in chapter 2 can be seen as an Inner Code that exploits the multiple antennas diversity and needs to be coupled to an Outer Code to operate in the range of interest for practical systems. In this chapter we have proposed to combine binary channel coding with our linear precoding in order to enhance the performance and to use low complexity turbo decoder. The presence of the binary CC also allows to exploit time diversity (multi-block diversity). Simulations confirm the theoretical results and clearly show the advantage of our technique over existing high rate MIMO systems (Threading, STOD).

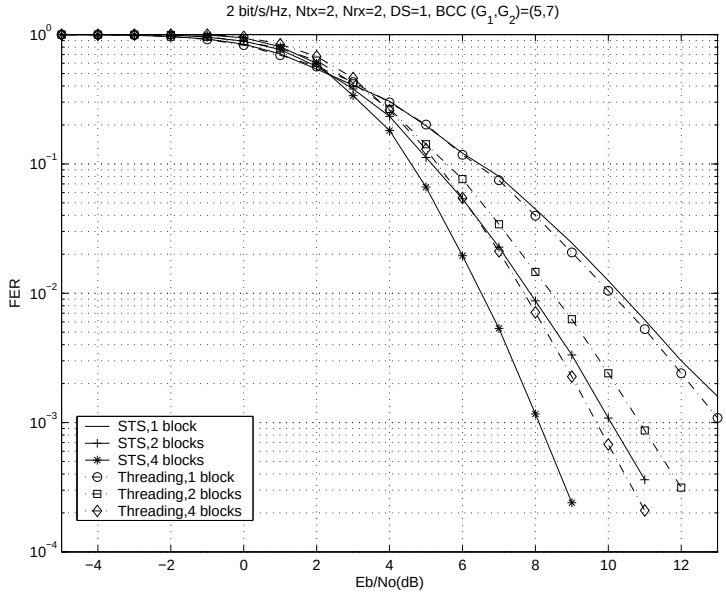

Figure 4.5: STS/Threading for $(N_{tx}, N_{rx}) = (2, 2)$, $L = 1$, $F = 1, 2, 4$.

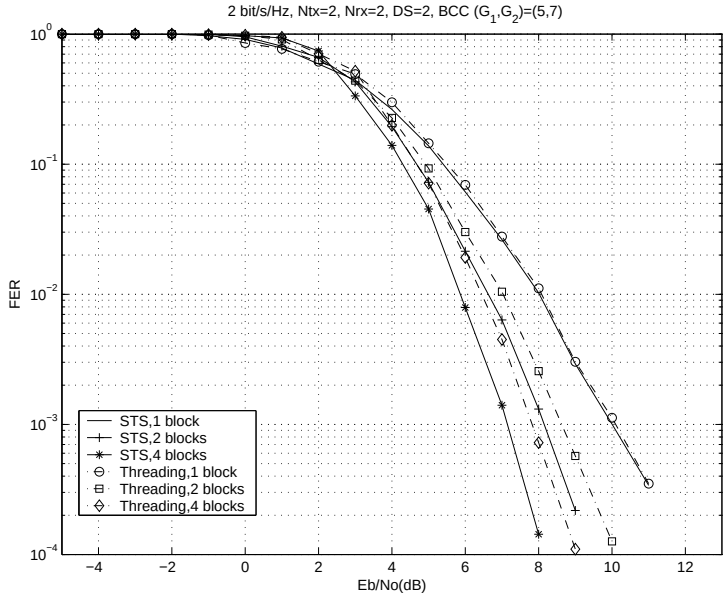

Figure 4.6: STS/Threading for $(N_{tx}, N_{rx}) = (2, 2)$, $L = 2$, $F = 1, 2, 4$.

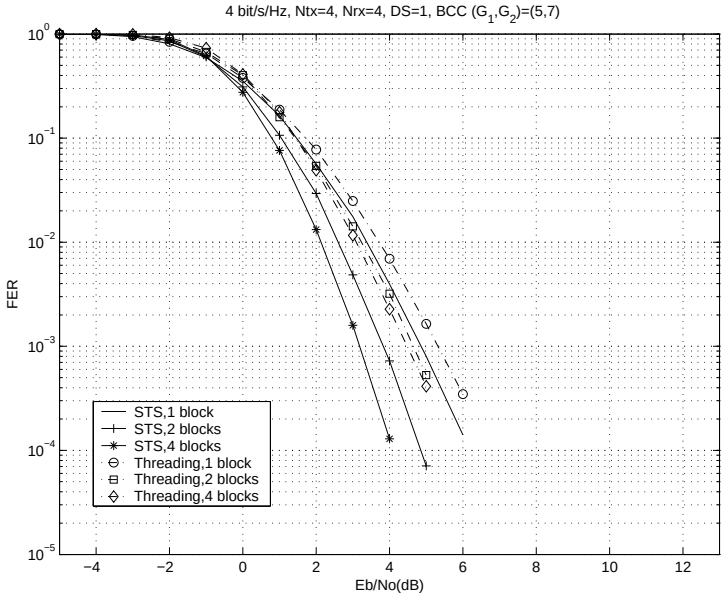

Figure 4.7: STS/Threading for $(N_{tx}, N_{rx}) = (4, 4)$, $L = 1$, $F = 1, 2, 4$.

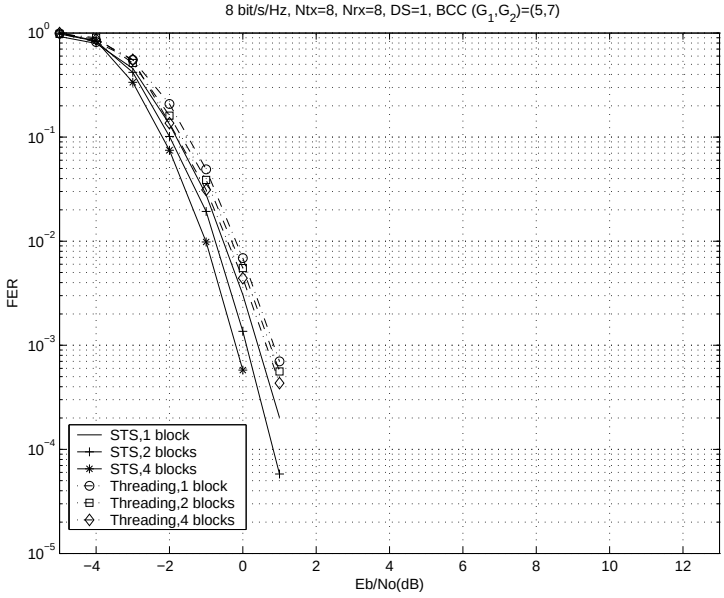

Figure 4.8: STS/Threading for $(N_{tx}, N_{rx}) = (8, 8)$, $L = 1$, $F = 1, 2, 4$.

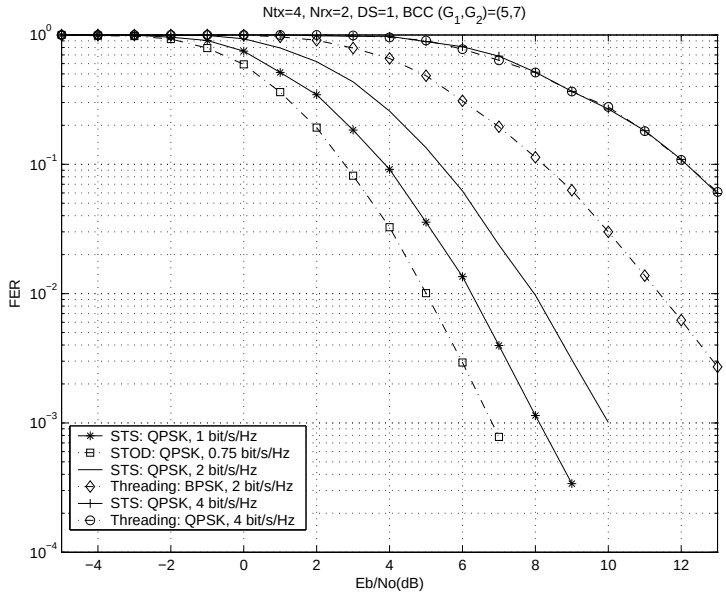

Figure 4.9: STS ($N_s = 1, 2, 4$) vs. Threading (QPSK, BPSK) and STOD for $(N_{tx}, N_{rx}) = (4, 2)$, $L = 1$ and $F = 1$.

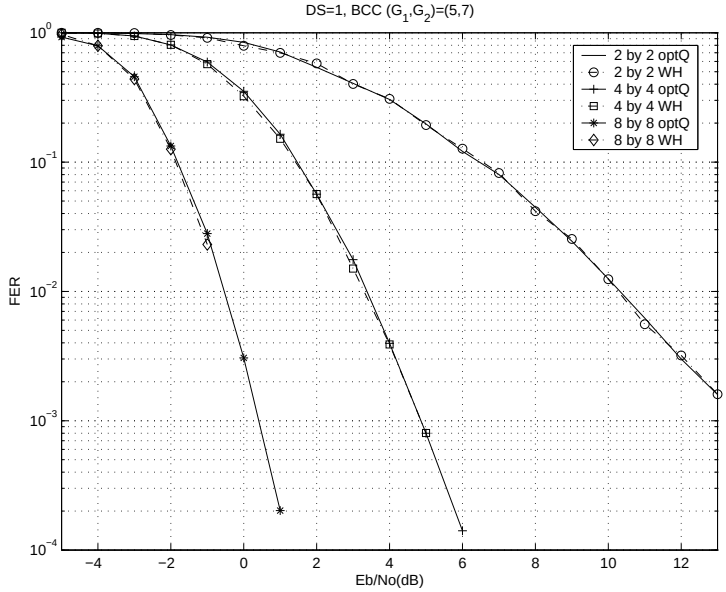

Figure 4.10: Two choice of the precoding matrix: optimized Q vs. Walsh Hadamard for $L = 1$ and $F = 1$.

Part II

Partial CSI at TX

Chapter 5

On MIMO Capacity with Partial CSI at Tx

The maximum achievable capacity for a MIMO channel corresponds to the waterfilling solution provided that the transmitter has a perfect knowledge of the channel. In practice, the available knowledge may only be partial due to the time selectivity of the channel and delay of the feedback from the receiver. However, exploiting the partial knowledge leads to a significant improvement when compared to the capacity without any channel knowledge. In this chapter we analyze the MIMO capacity with partial knowledge of the channel under practical frequency flat channel models.

5.1 Introduction

Space-time coding techniques assume the MIMO channel to be Rayleigh flat fading (subsection 1.1.1) with i.i.d. components. In practice this assumption may not always be valid, since for physical reasons the channel components may be correlated [64]. This correlation corresponds to partial knowledge that can be fed back to the transmitter. When the partial channel state information is present at the transmitter, it is advantageous to use it to optimize the precoder at the transmission [65, 66]. This **precoder will basically be a cascade of space-time coder and a decorrelating beamformer**.

In this chapter, we investigate the achievable capacity given the available CSI at Tx. We assume that, in addition to the channel correlations, the transmitter has more information about the channel: knowledge of slowly varying channel parameters, or knowledge of the channel up to the amplitude and phase shifts that arise when the roles of transmitter and receiver are reversed. We demonstrate how the partial CSI leads to an improvement of the communication capacity when compared to the capacity without CSI. However, the additional improvement when compared to knowing only the channel correlations is demonstrated to be small. We note that similar results (for different channel models) have also been published in [65].

Results presented in this chapter were published in [67, 68, 69].

5.2 Channel Models and Assumptions

The channel is flat ($L = 1$), and the covariance matrix at the transmitter is defined as $\Sigma = \mathrm{E}\{\mathbf{H}^H\mathbf{H}\}$. We use normalization $\mathrm{tr}\{\mathbf{\Sigma}\} = 1$.

The ergodic capacity given in (1.9) is reformulated as

$$C = \mathrm{E}_{\mathbf{H}} \ln\det(\mathbf{I} + \frac{P}{\sigma_v^2}\mathbf{H}\mathbf{S}\mathbf{H}^H) = \mathrm{E}_{\mathbf{H}} \ln\det(\mathbf{I} + \rho N_{tx}\mathbf{H}\mathbf{S}\mathbf{H}^H)\,, \qquad (5.1)$$

where $\rho = \frac{P}{N_{tx}\sigma_v^2}$ and $\mathbf{S_{XX}} = P\mathbf{S}$ is a covariance matrix of the transmitted Gaussian signals maximizing the above expression, under the power constraint $\mathrm{tr}\{\mathbf{S}\} \leq 1$.

5.2.1 Pathwise Channel Model

The pathwise model [70] of the channel matrix in the case of frequency flat fading is

$$\mathbf{H} = \sum_{l=1}^{L_p} c_l \mathbf{a}_l \mathbf{b}_l^T, \tag{5.2}$$

where L_p is the number of multipaths and c_l, $i = 1, \ldots, L_p$ denotes the complex multipath amplitudes. We assume that the amplitudes c_l are i.i.d. circular symmetrical complex Gaussian distributed with mean 0 and variance 1. The $N_{rx} \times 1$ vectors $\mathbf{a}_i$ are the steering vectors of the receive antenna array and the $N_{tx} \times 1$ vectors $\mathbf{b}_l$ are the steering vectors of the transmitting antenna array. Due to the i.i.d. assumption of the complex amplitudes, it is assumed that the multipath variances are included in the vectors $\mathbf{b}_i$. We also normalize $||\mathbf{a}_i||^2 = 1 \; \forall i$. Generally all c_l, $\mathbf{a}_l$ and $\mathbf{b}_l$ are random variables. The complex amplitudes c_l model the fast fading channel parameters while the steering vectors model the slowly fading channel parameters.

The channel matrix may also be given as

$$\mathbf{H} = \mathbf{ACB}, \tag{5.3}$$

where $\mathbf{A} = [\mathbf{a}_1, \ldots, \mathbf{a}_{L_p}]$, $\mathbf{B} = [\mathbf{b}_1, \ldots \mathbf{b}_{L_p}]^T$ and $\mathbf{C} = \text{diag}\{c_1, \ldots, c_{L_p}\}$. If for every channel usage the receiver knows the realization of the channel and the slowly fading parameters remain constant over a sufficient time interval, the slowly fading parameters may be obtained at the receiver [71], and fed back to the transmitter. This information then corresponds to partial channel state information at the transmitter.

We investigate the ergodic capacity of the channel given in (5.3) when $\mathbf{A}$ and $\mathbf{B}$ are fixed.

5.2.2 Channel Models for Limited Reciprocity

Assume that the physical channel is reciprocal between uplink and downlink, and the transmitter knows the uplink channel $\mathbf{W}^T$. This case can arise for example in the time division duplex mode of the UMTS standard, where both the uplink and the downlink share the same bandwidth. The overall channel in downlink including the cabling and electronic devices for both ends is therefore

$$\mathbf{H} = \mathbf{D}_1 \mathbf{W} \mathbf{D}_2, \tag{5.4}$$

where $\mathbf{D}_1$ and $\mathbf{D}_2$ are diagonal matrices. These matrices reflect the amplitude and phase shifts that arise when the roles of transmitter and receiver are reversed in case of no or limited calibration. We use three different models for the matrices $\mathbf{D}_1$ and $\mathbf{D}_2$

Model 1 Only phase shifts: Diagonal elements contain i.i.d. phases ($\mathbf{D}_1 = \text{diag}\{e^{j\phi_1^1}, \ldots, e^{j\phi_{N_{rx}}^1}\}$ and $\mathbf{D}_2 = \text{diag}\{e^{j\phi_1^2}, \ldots, e^{j\phi_{N_{tx}}^2}\}$, where ϕ_l^i are i.i.d. and uniformly distributed on $[0, 2\pi]$)

Model 2 Case of complete absence of calibration: Diagonal elements of D_1 and D_2 are i.i.d. zero mean complex circularly symmetrical Gaussian with variance 1.

Model 3 Case of imperfect calibration: The diagonal matrices are given by $\mathbf{D}_1 = \sqrt{1-\epsilon_1^2}\mathbf{I} + \epsilon_1\mathbf{DN}_1$ and $\mathbf{D}_2 = \sqrt{1-\epsilon_2^2}\mathbf{I} + \epsilon_2\mathbf{DN}_2$, where ϵ_i are small and $\mathbf{DN}_1$ and $\mathbf{DN}_2$ are diagonal matrices with i.i.d. diagonal elements that are zero mean complex circularly symmetrical Gaussian with variance 1.

5.3 Results for Pathwise Channel Model

In the case of pathwise model, the ergodic capacity for a given transmit covariance matrix $P\mathbf{S}$ is

$$C = \mathrm{E}_{\mathbf{C}} \ln \det \left[\mathbf{I} + \rho N_{tx} \mathbf{ACBSB}^H \mathbf{C}^H \mathbf{A}^H\right]. \tag{5.5}$$

For arbitrary SNR (ρ), the optimal $\mathbf{S}$ can be given by direct numerical solution as described later in this chapter. In the following, we calculate approximations for low and high SNR scenarios.

5.3.1 Low SNR

When $\rho << 1$, we may approximate (5.5) by

$$\begin{aligned} C &\approx \mathrm{Etr}\left\{\rho N_{tx} \mathbf{ACBSB}^H \mathbf{C}^H \mathbf{A}^H\right\} \\ &= \rho N_{tx} \mathrm{Etr}\left\{\mathbf{BSB}^H \mathbf{C}^H \mathbf{A}^H \mathbf{AC}\right\} \\ &= \rho N_{tx} \mathrm{tr}\left\{\mathbf{BSB}^H \mathrm{diag}\{\mathbf{A}^H \mathbf{A}\}\right\} \\ &= \rho N_{tx} \mathrm{tr}\left\{\mathbf{SB}^H \mathbf{B}\right\}. \end{aligned} \tag{5.6}$$

Note that $\text{diag}\{\mathbf{A}^H\mathbf{A}\} = \mathbf{I}$ due to the normalization. Write $\mathbf{B}^H\mathbf{B} = \mathbf{U}\mathbf{\Lambda}\mathbf{U}^H$ according to the eigenvector decomposition, and let $\mathbf{S}' = \mathbf{U}^H\mathbf{S}\mathbf{U}$. Note that $\text{tr}\{\mathbf{S}'\} = \text{tr}\{\mathbf{S}\} = 1$.
Now

$$\text{tr}\left\{\mathbf{S}\mathbf{B}^H\mathbf{B}\right\} = \text{tr}\left\{\mathbf{S}'\mathbf{\Lambda}\right\}. \tag{5.7}$$

For any $\mathbf{\Lambda}$, the matrix $\mathbf{S}'$ maximizing (5.7) is given by

$$\mathbf{S}' = \text{diag}\{0, \ldots, 0, 1, 0, \ldots, 0\}, \tag{5.8}$$

where the only nonzero diagonal element is in the position corresponding to the largest diagonal element of $\mathbf{\Lambda}$ (if there is no unique maximum, we can choose a position of any of the "maximum" elements).

We have thus shown that for $\rho << 1$, the optimal transmit covariance matrix maximizing (5.5) is given by

$$\mathbf{S} = \mathbf{u}\mathbf{u}^H, \tag{5.9}$$

where $\mathbf{u}$ is the eigenvector corresponding to the maximum eigenvalue of the channel covariance matrix

$$\mathbf{\Sigma} = \mathbf{B}^H\mathbf{B}. \tag{5.10}$$

The optimal covariance matrix thus depends only on the channel covariance matrix at the transmitter.

We note that in this case, the capacity with no CSI ($\mathbf{S} = \frac{1}{N_{tx}}\mathbf{I}$) is given by

$$\rho \sum_{i=1}^{N_{tx}} \lambda_i, \tag{5.11}$$

where λ_i are the eigenvalues of the matrix given in (5.10). Hence the ratio between the capacity with partial CSI and the capacity with no CSI is given by

$$1 \leq \frac{\max\{\lambda_i\}}{N_{tx}^{-1}\sum_{i=1}^{N_{tx}} \lambda_i} \leq N_{tx}. \tag{5.12}$$

As a conclusion, the gain obtained by using the partial CSI at Tx can be very significant.

5.3.2 High SNR

When $\rho >> 1$, giving a general solution is not possible, because the optimal covariance matrix $\mathbf{S}$ depends on the dimensions N_{rx} , N_{tx} and L_p, more specifically on the minimum dimension. We now derive the solution for two different possibilities for the minimum dimension.

1. $L_p \leq \min\{N_{tx}, N_{rx}\}$,

$$\begin{aligned} C &= \ln\det\left[\mathbf{I}_{L_p} + \rho N_{tx}\mathbf{B}\mathbf{S}\mathbf{B}^H\mathbf{C}^H\mathbf{A}^H\mathbf{A}\mathbf{C}\right] \\ &\approx \mathrm{E}_{\mathbf{C}}\left\{\ln\det\left[\rho N_{tx}\mathbf{B}\mathbf{S}\mathbf{B}^H\mathbf{C}^H\mathbf{A}^H\mathbf{A}\mathbf{C}\right]\right\} \\ &= \ln\det\left[\rho N_{tx}\mathbf{B}\mathbf{S}\mathbf{B}^H\right] + \mathrm{E}_{\mathbf{C}}\ln\det\left[\mathbf{C}^H\mathbf{A}^H\mathbf{A}\mathbf{C}\right] . \end{aligned} \tag{5.13}$$

   Therefore the solution is given by

$$\mathbf{S} = \frac{1}{L_p}\mathbf{U}\mathbf{U}^H, \tag{5.14}$$

   where $\mathbf{U}$ is the matrix of the eigenvectors of $\mathbf{\Sigma}$ corresponding to the nonzero eigenvalues.

2. $N_{tx} \leq \min\{N_{rx}, L_p\}$, using the same reasonning presented above, we get that

$$C \approx \ln\det\{\mathbf{S}\} + \text{constant}. \tag{5.15}$$

   Hence the solution is given by

$$\mathbf{S} = \frac{1}{N_{tx}}\mathbf{I}\,. \tag{5.16}$$

In these cases, the difference between the capacity with CSI and the one with no CSI is given by

$$\min\{N_{tx}, L_p\}\ln\frac{N_{tx}}{\min\{N_{tx}, L_p\}}. \tag{5.17}$$

Therefore, when $\rho >> 1$, the gain obtained by using partial CSI is important especially for large number of transmit and receive antennas and small number of multipaths.

When N_{rx} is the minimum dimension, it is not possible to isolate $\mathbf{S}$ from the random part of the channel, because the approximation used in the previous cases gives

$$C \approx \mathrm{E}_{\mathbf{C}}\ln\det\left[\rho N_{tx}\mathbf{A}\mathbf{C}\mathbf{B}\mathbf{S}\mathbf{B}^H\mathbf{C}^H\mathbf{A}^H\right]. \tag{5.18}$$

Since N_{rx} is the minimum dimension, this expression can not be further decomposed.

5.3.3 Waterfilling Solution for the Channel Covariance Matrix

Since ln det is a concave on the set of positive definite matrices, the ergodic capacity for any transmit covariance matrix $\mathbf{S}$ may be upper bounded by

$$\begin{aligned} C &= \mathrm{E}_{\mathbf{C}}\left\{\ln\det\left[\mathbf{I}+\rho N_{tx}\mathbf{ACBSB}^H\mathbf{C}^H\mathbf{A}^H\right]\right\} \\ &\leq \ln\det\left[\mathbf{I}+\rho N_{tx}\mathbf{SB}^H\,\mathrm{E}_{\mathbf{C}}\{\mathbf{C}^H\mathbf{A}^H\mathbf{AC}\}\mathbf{B}\right] \\ &= \ln\det\left[\mathbf{I}+\rho N_{tx}\mathbf{SB}^H\mathbf{B}\right]. \end{aligned} \tag{5.19}$$

The optimal $\mathbf{S}$ maximizing this upper bound corresponds to the waterfilling solution applied to $\rho N_{tx}\mathbf{\Sigma}$ [2]. The waterfilling solution matches the solutions given in equations (5.9),(5.14) and (5.16) for $\rho << 1$ and $\rho >> 1$.

5.3.4 Optimal Solution

As mentioned above, ln det is concave on the set of positive definite matrices. The set of positive semidefinite matrices with trace equal to 1 is a connex set. Therefore, the optimum transmit covariance matrix can be calculated by using numerical methods. In practice, the objective function has to be formed by averaging over sufficient number of Monte Carlo realizations. Note that the averaging preserves the concavity of the objective function. We demonstrate the usage of numerical methods in section 5.5. The applied method is based on projected gradient descent algorithm [72].

5.3.5 Solution for Separable Spatial Channel Model

The MIMO channel is often modeled as a separable spatial channel model introduced in subsection 1.1.2. It can be shown that the pathwise channel model converges in distribution to the separable spatial model with appropriate covariance matrices, as the number of multipaths tends to infinity [73]. The ergodic capacity for this channel model in case $\mathbf{\Sigma}_1 = \mathbf{I}$ has been considered *e.g.* in [74, 75, 66, 76, 7, 6]. It has been shown that for this case the optimal transmit covariance matrix $\mathbf{S}$ has the same eigenvectors as $\mathbf{\Sigma}_2$. The capacity achieving power allocation (the eigenvalues of optimal $\mathbf{S}$) has to be calculated using numerical methods (*e.g.* gradient descend algorithm). The method used in [66] to show that the eigenvectors of $\mathbf{S}$ correspond to those of $\mathbf{\Sigma}_2$ is complex. Here we provide a simpler proof of that fact. Let

$\mathbf{\Sigma}_2 = \mathbf{U}\mathbf{D}\mathbf{U}^H$ be the eigenvector decomposition of $\mathbf{\Sigma}_2$. The ergodic capacity for the covariance matrix $\mathbf{S}$ is then given by

$$\mathrm{E}_{\mathbf{W}} \ln\det[\mathbf{I} + \rho N_{tx} \mathbf{\Sigma}_1^{\frac{1}{2}} \mathbf{W}\mathbf{U}\mathbf{D}^{\frac{1}{2}}\mathbf{U}^H\mathbf{S}\mathbf{U}\mathbf{D}^{\frac{1}{2}}\mathbf{U}^H\mathbf{W}^H\mathbf{\Sigma}_1^{\frac{H}{2}}]\,. \tag{5.20}$$

Since for any $N_{tx} \times N_{tx}$ unitary matrix $\mathbf{U}$, the distribution of $\mathbf{W}$ is the same as the distribution of $\mathbf{W}\mathbf{U}$. $\mathbf{W}$ has also the same distribution as $\mathbf{W}\mathbf{\Phi}$, where $\mathbf{\Phi} = \mathrm{diag}\{e^{j\phi_1}, e^{j\phi_2}, \ldots, e^{j\phi_{N_{tx}}}\}$ with ϕ_i i.i.d. and uniformly distributed on $[0, 2\pi)$ is a unitary matrix. The ergodic capacity can then be written as

$$\mathrm{E}_\phi \, \mathrm{E}_W \ln\det\left[\mathbf{I} + \rho N_{tx} \mathbf{\Sigma}_1^{\frac{1}{2}} \mathbf{W}\mathbf{\Phi}\mathbf{D}^{\frac{1}{2}}\mathbf{S}'\mathbf{D}^{\frac{1}{2}}\mathbf{\Phi}^H\mathbf{W}^H\mathbf{\Sigma}_1^{\frac{H}{2}}\right], \tag{5.21}$$

where $\mathbf{S}' = \mathbf{U}^H\mathbf{S}\mathbf{U}$. Note that $\mathrm{tr}(\mathbf{S}') = \mathrm{tr}(\mathbf{S})$. Since $\ln\det$ is concave,

$$\begin{aligned} &\mathrm{E}_\phi \, \mathrm{E}_W \ln\det\left[\mathbf{I} + \rho N_{tx} \mathbf{\Sigma}_1^{\frac{1}{2}} \mathbf{W}\mathbf{\Phi}\mathbf{D}^{\frac{1}{2}}\mathbf{S}'\mathbf{D}^{\frac{1}{2}}\mathbf{\Phi}^H\mathbf{W}^H\mathbf{\Sigma}_1^{\frac{H}{2}}\right] \\ &\leq \mathrm{E}_W \ln\det\left[\mathbf{I} + \rho N_{tx} \mathbf{\Sigma}_1^{\frac{1}{2}} \mathbf{W}\, \mathrm{E}_\phi\{\mathbf{\Phi}\mathbf{D}^{\frac{1}{2}}\mathbf{S}'\mathbf{D}^{\frac{1}{2}}\mathbf{\Phi}^H\}\mathbf{W}^H\mathbf{\Sigma}_1^{\frac{H}{2}}\right] \\ &= \mathrm{E}_W \ln\det\left[\mathbf{I} + \rho N_{tx} \mathbf{\Sigma}_1^{\frac{1}{2}} \mathbf{W}\mathbf{D}\mathrm{diag}\{\mathbf{S}'\}\mathbf{W}^H\mathbf{\Sigma}_1^{\frac{H}{2}}\right]. \end{aligned} \tag{5.22}$$

The equality is achieved iff $\mathbf{S}'$ is a diagonal matrix, and the result follows. This result can even be generalized to any stochastic $\mathbf{W}$ with decorrelated columns.

5.4 Results for Channel Models with Limited Reciprocity

In the case of limited reciprocity, the ergodic capacity for the transmit covariance matrix $P\mathbf{S}$ is

$$C = \mathrm{E} \ln\det\left[I + \rho N_{tx} \mathbf{D}_1 \mathbf{W}\mathbf{D}_2\mathbf{S}\mathbf{D}_2^H\mathbf{W}^H\mathbf{D}_1^H\right], \tag{5.23}$$

where the expectation is calculated with respect to $\mathbf{D}_1$ and $\mathbf{D}_2$.

It is straightforward, using the technique described in subsection 5.3.5, to show that in the case of Model 1 or Model 2 (only phases or Gaussian zero mean diagonal entries), the optimal transmit covariance matrix has to be diagonal: $\mathbf{S} = \mathbf{D}_S$.

For the Model 1, the optimum solution may be derived by numerically maximizing

$$C = \ln \det \left[\mathbf{I} + \rho N_{tx} \mathbf{W} \mathbf{D}_S \mathbf{W}^H \right], \tag{5.24}$$

which is a concave on $\mathbf{D}_S$. We note that for given $\mathbf{D}_S$, (5.24) is an upper bound of the ergodic capacity for Model 2.

For Model 2, the optimal solution can be found by using numerical methods described in subsection 5.3.4, with simpler optimization as it has to be done only for a diagonal matrix.

For Model 3, optimization is performed as described in subsection 5.3.4.

In addition to the optimal solutions, sub-optimal solutions may be derived by considering the upper bound on ergodic capacity as it has been done in the case of pathwise model in subsection 5.3.3. For Models 1 and 2, this leads to waterfilling on

$$\mathbf{M} = \rho N_{tx} \mathrm{diag}\{\mathbf{W}^H \mathbf{W}\}, \tag{5.25}$$

for $N_{tx} \leq N_{rx}$.
When for $N_{tx} > N_{rx}$ we have to take in account the rank of the channel, it leads then to waterfilling on $\mathbf{M}$ where we force now the $N_{tx} - N_{rx}$ minimum diagonal values to zero.
For Model 3, this approach leads to waterfilling on

$$\rho N_{tx} \left((1 - \epsilon_1^2) \mathbf{W}^H \mathbf{W} + \epsilon_1^2 \mathrm{diag}\{\mathbf{W}^H \mathbf{W}\} \right). \tag{5.26}$$

For Model 2, a tighter upper bound is given by (5.24). Therefore, a better solution may be given by applying the optimal solution for Model 1. For Model 3, waterfilling on $\rho N_{tx} \mathbf{W}^H \mathbf{W}$ can also be used.

Min-Max Problem

In previous we assumed implicitly that the transmitter can see different realizations of $\mathbf{D}_1$ and $\mathbf{D}_2$ (and therefore code on different realizations). Without this assumption considering the ergodic capacity is meaningless. Below we assume that the transmitter can see only one realization of the channel, and depending on the way of encoding this leads to either a success or failure of the transmission. In a deterministic point of view (one realization, non-statistic problem), the transmitter should encode in a way to ensure

successful decoding at Rx. This corresponds to an infinite failure cost. The problem can be solved in a deterministic way by maximizing the worst case of the capacity over all possible values of $\mathbf{D}_1$, $\mathbf{D}_2$. The formulation of the Min-Max Problem is then

$$\max_{\mathbf{S}:\mathrm{tr}\{\rho N_{tx}\mathbf{S}\}\leq P} \min_{\mathbf{D}_1,\mathbf{D}_2} \ln\det\left[\mathbf{I}+\rho N_{tx}\mathbf{D}_1\mathbf{W}\mathbf{D}_2\mathbf{S}\mathbf{D}_2^H\mathbf{W}^H\mathbf{D}_1^H\right]. \tag{5.27}$$

As $\mathbf{0}$ is a possible value for $\mathbf{D}_1$, $\mathbf{D}_2$ in Models 2 and 3, it is therefore easy to see that the minimum capacity is zero for all values of $\mathbf{S}$, and the Min-Max Problem formulation is not useful for Models 2 and 3. Below let's focus on the case of Model 1 (diagonals of phases).

We will derive Upper and Lower Bounds on (5.27) ($LB \leq (5.27) \leq UB$), and show that we obtain equality between the UB and LB (and hence with (5.27)), which leads to the optimality of the LB (equivalently UB) solution. The UB is obtained by

$$\begin{aligned}(5.27) &= \max_{\mathbf{S}:\mathrm{tr}\{\rho N_{tx}\mathbf{S}\}\leq P} \min_{\mathbf{D}_2} \ln\det\left[\mathbf{I}+\rho N_{tx}\mathbf{W}\mathbf{D}_2\mathbf{S}\mathbf{D}_2^H\mathbf{W}^H\right] \\ &\leq \max_{\mathbf{S}:\mathrm{tr}\{\rho N_{tx}\mathbf{S}\}\leq P} \mathrm{E}_{\mathbf{D}_2} \ln\det\left[\mathbf{I}+\rho N_{tx}\mathbf{W}\mathbf{D}_2\mathbf{S}\mathbf{D}_2^H\mathbf{W}^H\right] \\ &\leq \max_{\mathbf{S}:\mathrm{tr}\{\rho N_{tx}\,\mathrm{diag}\{\mathbf{S}\}\}\leq P} \ln\det\left[\mathbf{I}+\rho N_{tx}\mathbf{W}\,\mathrm{diag}\{\mathbf{S}\}\mathbf{W}^H\right] = UB\,,\end{aligned} \tag{5.28}$$

the expectation $\mathrm{E}_{\mathbf{D}_2}$, is done over all the possible values of $\mathbf{D}_2$, this give a larger capacity than $\min_{\mathbf{D}_2} \ln\det\left[\mathbf{I}+\rho N_{tx}\mathbf{W}\mathbf{D}_2\mathbf{S}\mathbf{D}_2^H\mathbf{W}^H\right]$ and hence shows the first inequality. The second inequality follows from the concavity of ln det. The LB is obtained by doing the maximization in (5.27) over the subset of diagonals ($\mathbf{S}=\mathbf{D}_S$)

$$\begin{aligned}(5.27) &\geq \max_{\mathbf{S}:\mathrm{tr}\{\rho N_{tx}\mathbf{D}_S\}\leq P} \min_{\mathbf{D}_2} \ln\det\left[\mathbf{I}+\rho N_{tx}\mathbf{W}\mathbf{D}_2\mathbf{D}_S\mathbf{D}_2^H\mathbf{W}^H\right] \\ &\geq \max_{\mathbf{S}:tr\{\rho N_{tx}\mathbf{D}_S\}\leq P} \ln\det\left[\mathbf{I}+\rho N_{tx}\mathbf{W}\mathbf{D}_S\mathbf{W}^H\right] = LB.\end{aligned} \tag{5.29}$$

It is easy to see that the expressions of the upper and the lower bounds are the same. We conclude then that $LB = UB = (5.27)$, and that the solution of (5.27) matches the solution of LB, hence it is diagonal and corresponds to the same solution of the outage capacity optimization (5.24).

Models 2 and 3 can be adapted to the Min-Max Problem by modifying the distributions of $\mathbf{D}_1$ and $\mathbf{D}_2$ in order to avoid the zero capacity solution. For example by choosing a truncated Gaussian distribution that takes into account the most likely values or by choosing other bounded distributions.

5.5 Simulation Results

5.5.1 Pathwise Model

We first present results of a simulation study for pathwise model. In the simulations, we used Uniform Linear Arrays (ULAs) with half wavelength inter element spacing both at the transmitter and the receiver side. The path variances were generated randomly from exponential distribution with mean 1. At the receiver, the Directions of Arrival (DOA) were generated from uniform distribution on the interval $[-\pi, \pi]$. At the transmitter side, the directions of departure were generated from Gaussian distribution with mean 0° (array broadside) and standard deviation $\sigma = 5^\circ$. In all the simulations the trace of the channel covariance matrix at the transmitter was normalized to be equal to 1.

We compare seven different cases.

1. Instantaneous waterfilling: waterfilling solution for every realization of the channel. This assume perfect CSI at Tx and gives hence an upper bound for the ergodic capacity with any transmit covariance matrix.

2. Optimum: solution obtained by the numerical method described in subsection 5.3.4.

3. Approximate waterfilling: waterfilling on the channel covariance matrix (subsection 5.3.3).

4. Separable model: solution based on the separable spatial channel model.

5. Large SNR: large SNR approximation in (5.14) or (5.16) depending on the dimensions.

6. Beamforming: optimal solution for low SNR in (5.9).

7. No channel knowledge: $\mathbf{S} = \frac{1}{N_{tx}}\mathbf{I}$.

In the first experiment, the number of paths is small (poor scattering environment). We use $N_{tx} = N_{rx} = 4$ and $L_p = 2$. Figure 5.1 presents the result averaged over 100 Monte-Carlo realizations for the angles, and for each set of angles, 1000 Monte-Carlo realizations for the path amplitudes. The results show that the approximate waterfilling gives nearly optimal results, especially for small values of ρ. It can also be seen that the difference between the high SNR approximation and optimum solution decreases as ρ increases. The capacity for the transmit covariance matrix which is optimized for separable channel model is very low.
In the second experiment the number of paths is changed to 10 (rich scattering environment). In this case the capacity obtained with the solution of the separable channel model is much better than in the previous experiment. This is due to the fact that the pathwise channel model converges in distribution to the separable spatial channel model as L_p tends to infinity [73].

5.5.2 Limited Reciprocity

We consider now the case of limited reciprocity, with $N_{rx} = N_{tx} = 4$ for all simulations. The presented results are averaged over 100 realizations for $\mathbf{W}$, for which every element was generated independently from $\mathcal{CN}(0, 1)$ distribution. For every realization of $\mathbf{W}$, the capacities were averaged over 1000 Monte-Carlo realizations for $\mathbf{D}_1$ and $\mathbf{D}_2$. For Model 3, we use $\epsilon_1^2 = \epsilon_2^2 = 0.1$.

Simulation results are presented in fig. 5.3, 5.4 and 5.4. It can be seen that for Model 1 and Model 2, approximated waterfilling gives near optimal results. Therefore, as in the case of pathwise model, waterfilling on the covariance matrix seen from the transmitter is almost sufficient. Similar conclusion can be done from the observation of the result for Model 3.

5.6 Conclusion

We studied the ergodic capacity of two models for partial channel knowledge: the pathwise channel model with knowledge of the slow varying parameters at the transmitter and the limited reciprocity channel model. The simulation studies and the theoretical results show that waterfilling on the channel

covariance matrix at the transmitter leads to almost optimal capacity. As a conclusion we can state that the additional information obtained seems not to be very significant. To achieve closely optimal capacity, only the covariance matrix information is required at the transmitter.
The simulation results for the pathwise model also show that the use of separable spatial channel model to optimize the transmit covariance matrix results in loss of performance especially for small number of multipaths. Beamforming used in the multipath environment gives close to optimum performance for low and middle range SNRs.
We also introduced the Min-Max Problem for the limited reciprocity model, the solution of this problem in case of phases ambiguities leads to the same solution as the ergodic capacity maximization problem.

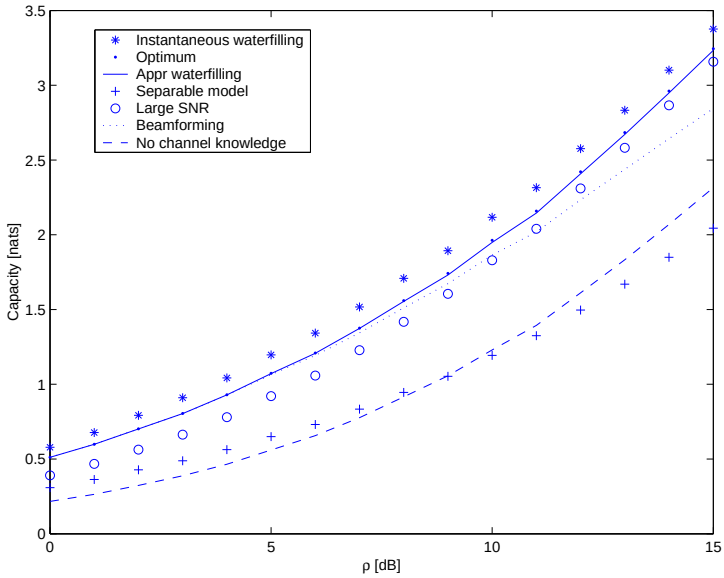

Figure 5.1: Result for $N_{tx} = N_{rx} = 4$, $L_p = 2$.

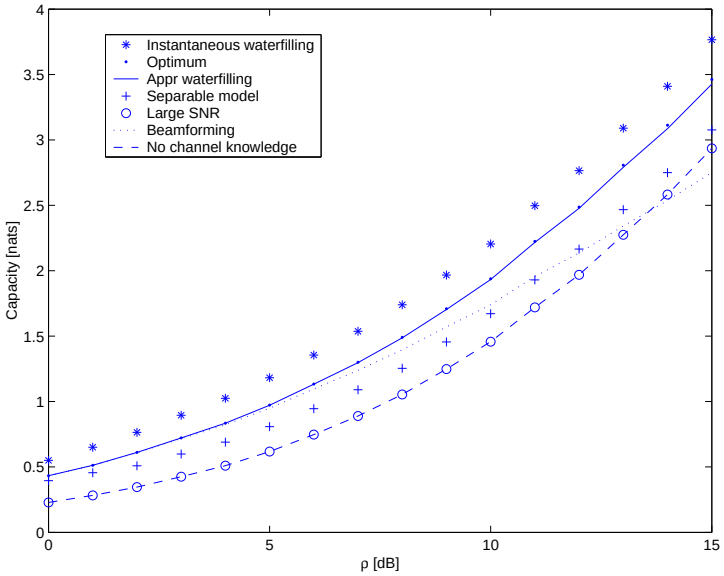

Figure 5.2: Result for $N_{tx} = N_{rx} = 4$, $L_p = 10$.

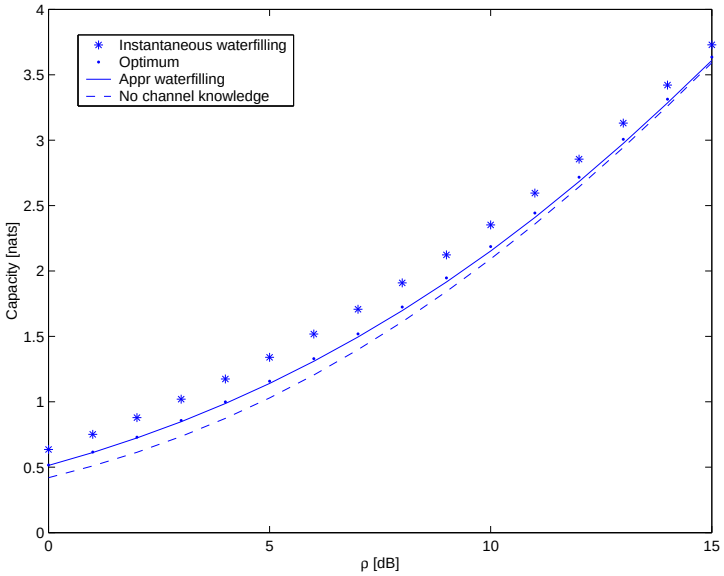

Figure 5.3: Results for limited reciprocity, $N_{rx} = N_{tx} = 4$, Model 1.

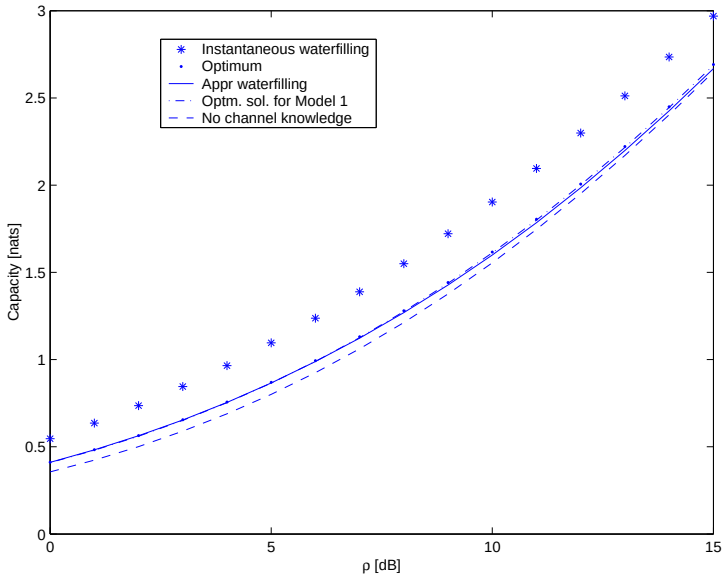

Figure 5.4: Results for limited reciprocity, $N_{rx} = N_{tx} = 4$, Model 2.

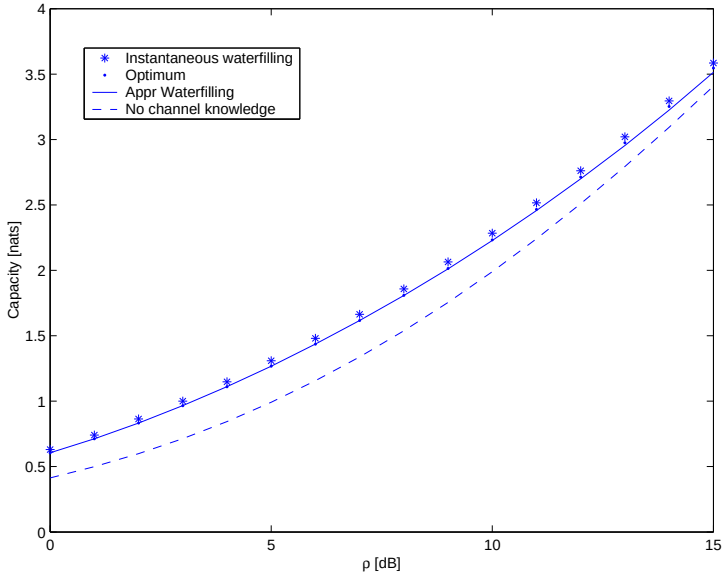

Figure 5.5: Results for limited reciprocity, $N_{rx} = N_{tx} = 4$, Model 3.

Part III

Absence of CSI at RX

Chapter 6

Mutual Information without CSI at Rx

In this chapter, we analyze the Mutual Information (MI) between the input and the output of a MIMO system in the absence of CSI at Rx and Tx. To that end we consider two popular models. The first one is the block fading model and the second one is the time selective channel. We assume that some training/pilot symbols are inserted at the beginning of each burst. We show that the average MI over a transmission burst can be decomposed into symbol position dependent contributions. The MI component at a certain symbol position optimally combines semi-blind information up to that symbol position (with perfect input recovery up to that position) with blind information from the rest of the burst. We also analyze the asymptotic regime for which we can formulate optimal channel estimates and evaluate the capacity loss with respect to the known channel case. Asymptotically, the decrease in MI involves Fisher information matrices corresponding to channel estimation problems. Finally we suggest to exploit correlations in the channel model in order to improve estimation performance and minimize capacity loss.

6.1 Introduction

In the previous parts of this thesis the channel was assumed to be perfectly known at the receiver. This assumption is considered in general in order to decorrelate the problem of the Tx and the Rx design from the channel estimation consequences. In fact, for cases where the channel remains constant over a large burst (we consider a transmission by burst), we can always use enough training sequence to allow a good estimation quality of the channel, with neglectible loss in capacity. However, in cases where the burst is of limited length or for time selective channels were the channel varies over the burst, the assumption of perfect CSI at the Rx is no more valid [77, 78, 79]. To stay in the conventional schemes used in practical system, we assume that some training/pilot symbols are inserted in the beginning of each burst. Our study focuses on the MI between the transmitted burst and the received signal. The capacity is the average of the MI over the burst, maximized w.r.t. the input distribution. We assume that the Tx have no CSI and consider two channel models, the block fading model and the time selective model (high Doppler spead).
In the usual block fading model, the data gets transmitted over a number of bursts such that the channel is constant over a burst but fading independently between bursts. For such a channel model, the capacity has been previously studied in [80, 81]. The capacity in these works is achieved by optimizing the distribution of the all burst input, which has a length equals to the coherence interval of the channel. A burst with such a distribution and size may be difficult to code and decode. In our work we consider a practical point view where blocks of a small size have independent distributions.
The second model that we consider is the time selective channel model (high Doppler speed). The channel is assumed to be constant over small blocks, of size the number of transmit antennas, and varies along the burst as a Gaussian stationary process.

This chapter begins with a preliminary section where we present the general flat fading channel model and derive a serial decomposition of the MI. This decomposition suggests to use a semi-blind channel estimation. The following section studies the asymptotic behavior of the capacity for block fading channel and large burst length. We then show that the optimal channel estimator, in order to reduce the capacity loss, is the semi-blind MMSE one. The time selective channel model is also studied and we derive bounds

on the capacity. Finally a correlated MIMO channel model is introduced in other to improve the performance by exploiting the channel structure.

Results presented in this chapter were published in [82, 83].

6.2 Mutual Information Decomposition

6.2.1 General Flat Fading Model

We consider transmission over flat fading MIMO channel for a particular burst of T symbol periods. The received signal at time index k is

$$\mathbf{y}_k = \mathbf{H}^{(k)}\mathbf{x}_k + \mathbf{v}_k \, . \tag{6.1}$$

The channel can be a block fading model, except that we shall refer to a block as burst. In this case, the channel is constant over the burst $\mathbf{H}^{(k)} = \mathbf{H}\,,\ \forall k$.
Another model, used in this chapter, is the time selective model when the channel varies over the burst. Its instantaneous value is then dependent on the index k.
We assume the use of a training sequence (TS) of length N_{TS} pilot symbol vectors. The length of the transmitted data, also called "*blind*" in the estimation terminology, is then N_B so that $N_{TS} + N_B = T$.
We can decompose the burst signal into training and data parts $\mathbf{X} = [\mathbf{X}^{TS}, \mathbf{X}^B]$, $\mathbf{Y} = [\mathbf{Y}^{TS}, \mathbf{Y}^B]$ and $\mathbf{V} = [\mathbf{V}^{TS}, \mathbf{V}^B]$. $\mathbf{Y}$ and $\mathbf{V}$ are $N_{rx} \times T$ matrices where $\mathbf{X}$ is $N_{tx} \times T$.
We assume also that the transmitter can code over different bursts, so that the instantaneous capacity is replaced by the ergodic capacity in the block fading model (see subsection 1.2.2).
In the following, we derive preliminary results on MI which are valid for the two channel models.

6.2.2 MI Decomposition

As stated in [79], using the chain rule [84], the MI between the input and the output of flat channel satisfies

$$\begin{aligned} I(\mathbf{Y}^{TS}, \mathbf{Y}^B; \mathbf{X}^B | \mathbf{X}^{TS}) &= I(\mathbf{Y}^{TS}; \mathbf{X}^B | \mathbf{X}^{TS}) + I(\mathbf{Y}^B; \mathbf{X}^B | \mathbf{X}^{TS}, \mathbf{Y}^{TS}) \\ &= I(\mathbf{Y}^B; \mathbf{X}^B | \mathbf{X}^{TS}, \mathbf{Y}^{TS}) \, , \end{aligned} \tag{6.2}$$

where $I(\mathbf{Y}^{TS};\mathbf{X}^{B}|\mathbf{X}^{TS}) = 0$ due to the independence between $\mathbf{X}^{B}$ and $(\mathbf{Y}^{TS},\mathbf{X}^{TS})$.

Consider now a partition of $\mathbf{X}^{B}$ in Q blocks $\mathbf{X}^{B} = [\mathbf{X}_1,\ldots,\mathbf{X}_Q]$.
$\mathbf{X}_i$, $i = 1,\ldots,Q$ are assumed to be independent from block to block; this corresponds to the usual case of block-wise coding across bursts in STC schemes. Furthermore, we assume that the $\mathbf{V}_i$'s are independent between blocks. The block lengths $T_i, i = 1,\ldots,Q$ where $\sum_i^Q T_i = N_B$, are identical for STC schemes. More generally, we assume in the following that they can be different, but bounded by a constant.

We define for $k \geq i$, $\mathbf{X}_i^k = [\mathbf{X}_i,\mathbf{X}_{i+1},\ldots,\mathbf{X}_k]$ and $\mathbf{Y}_i^k = [\mathbf{Y}_i,\mathbf{Y}_{i+1},\ldots,\mathbf{Y}_k]$.
Then

$$\begin{aligned} I(\mathbf{Y}^{B};\mathbf{X}^{B}|\mathbf{X}^{TS},\mathbf{Y}^{TS}) &= I(\mathbf{Y}_1^{Q};\mathbf{X}_1,\mathbf{X}_2^{Q}|\mathbf{X}^{TS},\mathbf{Y}^{TS}) \\ &= I(\mathbf{Y}_1^{Q};\mathbf{X}_1|\mathbf{X}^{TS},\mathbf{Y}^{TS}) + I(\mathbf{Y}_1^{Q};\mathbf{X}_2^{Q}|\mathbf{X}^{TS},\mathbf{Y}^{TS},\mathbf{X}_1) \\ &= I(\mathbf{Y}_1^{Q};\mathbf{X}_1|\mathbf{X}^{TS},\mathbf{Y}^{TS}) + I(\mathbf{Y}_2^{Q};\mathbf{X}_2^{Q}|\mathbf{X}^{TS},\mathbf{Y}^{TS},\mathbf{X}_1,\mathbf{Y}_1) \\ &\quad + \underbrace{I(\mathbf{Y}_1;\mathbf{X}_2^{Q}|\mathbf{X}^{TS},\mathbf{Y}^{TS},\mathbf{X}_1)}_{=0}, \end{aligned} \tag{6.3}$$

where
$I(\mathbf{Y}_1;\mathbf{X}_2^{Q}|\mathbf{X}^{TS},\mathbf{Y}^{TS},\mathbf{X}_1) = h(\mathbf{Y}_1|\mathbf{X}^{TS},\mathbf{Y}^{TS},\mathbf{X}_1) - h(\mathbf{Y}_1|\mathbf{X}^{TS},\mathbf{Y}^{TS},\mathbf{X}_1,\mathbf{X}_2^{Q})$,
$h(.)$ is the entropy measure.
Considering the fact that $\mathbf{X}_2^{Q}$ is independent of $\mathbf{Y}_1$ conditioned on $(\mathbf{X}^{TS},\mathbf{Y}^{TS},\mathbf{X}_1)$, we have $h(\mathbf{Y}_1|\mathbf{X}^{TS},\mathbf{Y}^{TS},\mathbf{X}_1,\mathbf{X}_2^{Q}) = h(\mathbf{Y}_1|\mathbf{X}^{TS},\mathbf{Y}^{TS},\mathbf{X}_1)$ and finally $I(\mathbf{Y}_1;\mathbf{X}_2^{Q}|\mathbf{X}^{TS},\mathbf{Y}^{TS},\mathbf{X}_1) = 0$.
Iterating the equation for $i = 2,\ldots,Q$, we get

$$\begin{aligned} I(\mathbf{Y}^{B};\mathbf{X}^{B}|\mathbf{X}^{TS},\mathbf{Y}^{TS}) &= \underset{Q-1}{\sum_{i=1}^{Q}} I(\mathbf{Y}_i^{Q};\mathbf{X}_i|\mathbf{X}^{TS},\mathbf{Y}^{TS},\mathbf{X}_1^{i-1},\mathbf{Y}_1^{i-1}) \\ &= \underbrace{\sum_{i=1} I(\mathbf{Y}_{i+1}^{Q};\mathbf{X}_i|\mathbf{X}^{TS},\mathbf{Y}^{TS},\mathbf{X}_1^{i-1},\mathbf{Y}_1^{i-1})}_{=0} \\ &\quad + \sum_{i=1}^{Q} I(\mathbf{Y}_i;\mathbf{X}_i|\mathbf{X}^{TS},\mathbf{X}_1^{i-1},\underbrace{\mathbf{Y}^{TS},\mathbf{Y}_1^{i-1},\mathbf{Y}_{i+1}^{Q}}_{=\overline{\mathbf{Y}}_i}) \\ &= \sum_{i=1}^{Q} I(\mathbf{Y}_i;\mathbf{X}_i|\mathbf{X}^{TS},\mathbf{X}_1^{i-1},\overline{\mathbf{Y}}_i)\,, \end{aligned} \tag{6.4}$$

where $\overline{\mathbf{Y}}_i$ contains all the received signal except $\mathbf{Y}_i$. In order to show that $I(\mathbf{Y}_{i+1}^{Q};\mathbf{X}_i|\mathbf{X}^{TS},\mathbf{Y}^{TS},\mathbf{X}_1^{i-1},\mathbf{Y}_1^{i-1}) = 0$ for every i, we used the same arguments as the one used for eq. (6.3).

Eq. (6.4) shows clearly the way of processing to achieve the capacity: for every block, we use the already detected blocks as a (Data-Aided (DA)) training sequence (in addition to the actual training), and use the not yet detected blocks as blind information.
We can also reorganize the MI as follows

$$\begin{aligned} I(\mathbf{Y}^B;\mathbf{X}^B|\mathbf{X}^{TS},\mathbf{Y}^{TS}) &= \sum_{i=1}^{Q} I(\mathbf{Y}_i^Q;\mathbf{X}_i|\mathbf{X}^{TS},\mathbf{Y}^{TS},\mathbf{X}_1^{i-1},\mathbf{Y}_1^{i-1}) \\ &= \underbrace{\sum_{i=1}^{Q} I(\mathbf{Y}_i;\mathbf{X}_i|\mathbf{X}^{TS},\mathbf{Y}^{TS},\mathbf{X}_1^{i-1},\mathbf{Y}_1^{i-1})}_{I1} \\ &+ \underbrace{\sum_{i=1}^{Q-1} I(\mathbf{Y}_{i+1}^Q;\mathbf{X}_i|\mathbf{X}^{TS},\mathbf{Y}^{TS},\mathbf{X}_1^{i-1},\mathbf{Y}_1^{i})}_{I2} . \end{aligned} \tag{6.5}$$

The MI can then be seen as the sum of two parts,
$I(\mathbf{Y}^B;\mathbf{X}^B|\mathbf{X}^{TS},\mathbf{Y}^{TS}) = I1 + I2$ where:
$I1$ is the rate that we can achieve by using only the already processed blocks for side information (DA training).
$I2$ is the additional amount of rate that can be achieved by exploiting the blind information contained in the not yet detected blocks (future blocks).

Before we continue this chapter, we define the average MI as $I_{avg}(T) = \frac{1}{T} I(\mathbf{Y}^B;\mathbf{X}^B|\mathbf{X}^{TS},\mathbf{Y}^{TS})$. The capacity equals $I_{avg}(T)$ optimized w.r.t. to the input distribution (under the power constraint).

6.3 Asymptotic Behavior of the Capacity for Block Fading Channel

For block fading model the channel is constant over the burst ($\mathbf{H}^{(k)} = \mathbf{H}$, $\forall k$).
In the following, we want to show that the average MI goes to the coherent MI $I(\mathbf{y};\mathbf{x}|\mathbf{H})$ for large T (large burst length) and fixed N_{TS}. The blocks lengths $T_i, i = 1,\ldots,Q$ are bounded by a constant, then when T grows, Q also grows. Hence, Q is an increasing and unbounded function of T, we denote it by $Q(T)$.

The coherent MI is $I(\mathbf{y};\mathbf{x}|\mathbf{H}) = \lim_{T\to\infty} \frac{1}{T} I(Y;\mathbf{X}|\mathbf{H})$. An upper bound is given by

$$\begin{array}{rcl} I_{avg}(T) & = & \frac{1}{T}(h(\mathbf{X}^B) - h(\mathbf{X}^B|\mathbf{X}^{TS},\mathbf{Y}^{TS},\mathbf{Y}^B)) \\ & \leq & \frac{1}{T}(h(\mathbf{X}^B) - h(\mathbf{X}^B|\mathbf{X}^{TS},\mathbf{Y}^{TS},\mathbf{Y}^B,\mathbf{H})) \\ & = & \frac{1}{T}(h(\mathbf{X}^B) - h(\mathbf{X}^B|\mathbf{Y}^B,\mathbf{H})) \\ & = & \frac{1}{T}(I(\mathbf{Y};\mathbf{X}|\mathbf{H}) - I(\mathbf{Y}^{TS};\mathbf{X}^{TS}|\mathbf{H}))\,. \end{array} \tag{6.6}$$

$I(\mathbf{Y}^{TS};\mathbf{X}^{TS}|\mathbf{H})$ is a positive quantity, we conclude that

$$\lim_{T\to\infty} I_{avg}(T) \leq I(\mathbf{y};\mathbf{x}|\mathbf{H})\,. \tag{6.7}$$

Written in term of the entropy the MI is

$$I(\mathbf{Y}_i;\mathbf{X}_i|\mathbf{X}^{TS},\mathbf{X}_1^{i-1},\overline{\mathbf{Y}}_i) = h(\mathbf{X}_i) - h(\mathbf{X}_i|\mathbf{X}^{TS},\mathbf{X}_1^{i-1},\overline{\mathbf{Y}}_i,\mathbf{Y}_i)\,. \tag{6.8}$$

Let $\widehat{\mathbf{H}}^{(i)} = \widehat{\mathbf{H}}(\mathbf{X}^{TS},\mathbf{X}_1^{i-1},\overline{\mathbf{Y}}_i)$ be an estimate of the channel based on $(\mathbf{X}^{TS},\mathbf{X}_1^{i-1},\overline{\mathbf{Y}}_i)$. $\widehat{\mathbf{H}}^{(i)}$ is hence a reduced statistic of $(\mathbf{X}^{TS},\mathbf{X}_1^{i-1},\overline{\mathbf{Y}}_i)$. Since reducing the conditioning increases the entropy, we have

$$\begin{array}{rcl} I(\mathbf{Y}_i;\mathbf{X}_i|\mathbf{X}^{TS},\mathbf{X}_1^{i-1},\overline{\mathbf{Y}}_i) & \geq & h(\mathbf{X}_i) - h(\mathbf{X}_i|\widehat{\mathbf{H}}(\mathbf{X}^{TS},\mathbf{X}_1^{i-1},\overline{\mathbf{Y}}_i,\mathbf{Y}_i),\mathbf{Y}_i) \\ & = & h(\mathbf{X}_i) - h(\mathbf{X}_i|\mathbf{Y}_i,\widehat{\mathbf{H}}(\mathbf{X}^{TS},\mathbf{X}_1^{i-1},\overline{\mathbf{Y}}_i)) \\ & = & I(\mathbf{Y}_i;\mathbf{X}_i|\widehat{\mathbf{H}}^{(i)})\,. \end{array} \tag{6.9}$$

If we choose $\widehat{\mathbf{H}}^{(i)} = \widehat{\mathbf{H}}(\mathbf{X}^{TS},\mathbf{X}_1^{i-1},\overline{\mathbf{Y}}_i)$ to be the optimal estimate of the channel (statistic of reduced dimension), it satisfies $\lim_{i\to\infty} \widehat{\mathbf{H}}^{(i)} = \mathbf{H}$ *almost surely.*
We have then

$$\begin{array}{rcl} \lim_{T\to\infty} I_{avg}(T) & \geq & \lim_{T\to\infty} \frac{1}{T} \sum_{i=1}^{Q(T)} I(\mathbf{Y}_i;\mathbf{X}_i|\widehat{\mathbf{H}}^{(i)}) \\ & = & \lim_{T\to\infty} \frac{1}{T} \sum_{i=1}^{Q(T)} I(\mathbf{Y}_i;\mathbf{X}_i|\mathbf{H}) \\ & = & \lim_{T\to\infty} \frac{1}{T} I(\mathbf{Y}^B;\mathbf{X}^B|\mathbf{H}) \\ & = & I(\mathbf{y};\mathbf{x}|\mathbf{H})\,, \end{array} \tag{6.10}$$

where in the third inequality we used the independence between blocks given the true channel value.

Combining (6.7) and (6.10) we conclude that

$$\lim_{T\to\infty}\frac{1}{T}I(\mathbf{Y}^B;\mathbf{X}^B|\mathbf{X}^{TS},\mathbf{Y}^{TS}) = I(\mathbf{y};\mathbf{x}|\mathbf{H})\,. \tag{6.11}$$

This means that, as T grows, adopting the detection method per block, and the associated channel estimation allows to reach the capacity of the system with perfect CSI at Rx.
Remark1: As T grows, the use of detected blocks only to estimate the channel allows to achieve asymptotically the MI I_{avg} of the system. But for finite T, it is necessary to also use the blind information to reach it.
Remark2: The MI expression of eq. (6.4) does not make any difference between training and past detected symbols. Then for a fixed T, and when all the entries of $\mathbf{X}$ (training and data) are i.i.d., it is easy to see that the average MI I_{avg} of the system is maximized when the number of the training symbols N_{TS} is as small as possible (*i.e.* allows semi-blind identifiability of the channel).

6.3.1 Channel Estimation for Block Fading Model

The ergodic capacity C of the system is the maximum of $I_{avg}(T)$ over all input distributions, under a given power constraint. We have

$$\tfrac{1}{T}\sum_{i=1}^{Q} I(\mathbf{Y}_i;\mathbf{X}_i|\widehat{\mathbf{H}}^{(i)}) \le C \le \max_{p(\mathbf{X}^B),tr(R_{\mathbf{X}^B})\le N_B N_{tx}\sigma_x^2} \frac{1}{T}I(\mathbf{Y}^B;\mathbf{X}^B|\mathbf{H})\,. \tag{6.12}$$

For an AWGN with power σ_v^2 and in the absence of CSI at Tx, the max in the upper bound of the ergodic capacity is attained for a centered white Gaussian input with covariance $\sigma_x^2\mathbf{I}_{N_{tx}}$ (subsection 1.2.2). Hence,

$$\frac{1}{T}\sum_{i=1}^{Q} I(\mathbf{Y}_i;\mathbf{X}_i|\widehat{\mathbf{H}}^{(i)}) \le C \le \frac{T-N_{TS}}{T}\,\mathrm{E}\ln\det(I+\frac{\sigma_x^2}{\sigma_v^2}\mathbf{H}\,\mathbf{H}^H). \tag{6.13}$$

The received signal is

$$\begin{aligned} \mathbf{Y}_i &= \mathbf{H}\,\mathbf{X}_i + \mathbf{V}_i \\ &= \widehat{\mathbf{H}}^{(i)}\,\mathbf{X}_i + \widetilde{\mathbf{H}}^{(i)}\,\mathbf{X}_i + \mathbf{V}_i \\ &= \widehat{\mathbf{H}}^{(i)}\,\mathbf{X}_i + \mathbf{V}_i + \mathbf{Z}_i\,, \end{aligned} \tag{6.14}$$

where $\mathbf{Z}_i = \widetilde{\mathbf{H}}^{(i)}\,\mathbf{X}_i$.
The MI satisfies

$$\begin{aligned} I(\mathbf{Y}_i, \mathbf{X}_i|\widehat{\mathbf{H}}^{(i)}) &= h(\mathbf{Y}_i|\widehat{\mathbf{H}}^{(i)}) - h(\mathbf{Y}_i|\mathbf{X}_i, \widehat{\mathbf{H}}^{(i)}) \\ &= h(\mathbf{Y}_i|\widehat{\mathbf{H}}^{(i)}) - h(\mathbf{V}_i + \mathbf{Z}_i|\mathbf{X}_i, \widehat{\mathbf{H}}^{(i)})\,. \end{aligned} \tag{6.15}$$

Assume $\widehat{\mathbf{H}}^{(i)}$ to satisfy the Pythagorean Theorem (PT), *i.e.* $\widehat{\mathbf{H}}$ is decorrelated with $\widetilde{\mathbf{H}}$. For a Gaussian $\mathbf{X}$ it was shown in [79] that a lower bound for $I(\mathbf{Y}_i, \mathbf{X}_i|\widehat{\mathbf{H}}^{(i)})$ is given by considering $\mathbf{Z}_i$ as an independent and white Gaussian noise, with covariance $\sigma_z^2\, I$, where
$\sigma_z^2 = \frac{1}{T_i N_{rx}} \mathrm{tr}\ \mathrm{E}(\mathbf{Z}_i \mathbf{Z}_i^H) = \sigma_x^2 \frac{\mathrm{tr}\ \mathrm{E}(\widetilde{\mathbf{H}}^{(i)} \widetilde{\mathbf{H}}^{(i)\,H})}{N_{rx}} = N_{tx} \sigma_x^2 \sigma^2_{\widetilde{\mathbf{H}}^{(i)}}$ and
$\sigma^2_{\widetilde{\mathbf{H}}^{(i)}} = \frac{\mathrm{tr}\ \mathrm{E}(\widetilde{\mathbf{H}}^{(i)} \widetilde{\mathbf{H}}^{(i)\,H})}{N_{rx}\, N_{tx}}$.
A lower bound is

$$\begin{aligned} C &\geq \tfrac{1}{T} \textstyle\sum_{i=1}^{Q} I(\mathbf{Y}_i; \mathbf{X}_i|\widehat{\mathbf{H}}^{(i)}) \\ &\geq \tfrac{1}{T} \textstyle\sum_{i=1}^{Q} T_i\, \mathrm{E} \ln \det(I + \frac{\sigma_x^2}{\sigma_v^2 + N_{tx} \sigma_x^2 \sigma^2_{\widetilde{\mathbf{H}}^{(i)}}} \widehat{\mathbf{H}}^{(i)} \widehat{\mathbf{H}}^{(i)\,H})\,. \end{aligned} \tag{6.16}$$

Let $\sigma^2_{\widehat{\mathbf{H}}^{(i)}} = \frac{\mathrm{tr}\ \mathrm{E}(\widehat{\mathbf{H}}^{(i)} \widehat{\mathbf{H}}^{(i)\,H})}{N_{rx}\, N_{tx}}$ and $\overline{\mathbf{H}}^{(i)} = \frac{\widehat{\mathbf{H}}^{(i)}}{\sigma_{\widehat{\mathbf{H}}^{(i)}}}$. Then because the channel estimator satisfies the Pythagorean Theorem, we have
$\sigma^2_{\widehat{\mathbf{H}}^{(i)}} + \sigma^2_{\widetilde{\mathbf{H}}^{(i)}} = \sigma_H^2$. Now

$$\begin{aligned} C &\geq \tfrac{1}{T} \textstyle\sum_{i=1}^{Q} T_i\, \mathrm{E} \ln \det(I + \frac{\sigma_x^2(\sigma_H^2 - \sigma^2_{\widetilde{\mathbf{H}}^{(i)}})}{\sigma_v^2 + N_{tx} \sigma_x^2 \sigma^2_{\widetilde{\mathbf{H}}^{(i)}}} \overline{\mathbf{H}}^{(i)} \overline{\mathbf{H}}^{(i)\,H}) \\ &= C_{LB}\,. \end{aligned} \tag{6.17}$$

The expectation is over the distribution of $\overline{\mathbf{H}}^{(i)}$, which remains close to that of $\mathbf{H}$. Then the given capacity lower bound C_{LB} depends primarily on the

Mean Square Error (MSE) of the channel estimator $\widehat{\mathbf{H}}^{(i)}$. Since C_{LB} is a decreasing function of the MSE, the optimum estimator is the Minimum Mean Square Error(MMSE) estimator

$$\begin{aligned} \widehat{\mathbf{H}}^{(i)}_{MMSE} &= \widehat{\mathbf{H}}^{(i)}_{MMSE}(\mathbf{X}^{TS}, \mathbf{X}_1^{i-1}, \overline{\mathbf{Y}}_i) \\ &= \mathrm{E}(\mathbf{H}|\mathbf{X}^{TS}, \mathbf{X}_1^{i-1}, \overline{\mathbf{Y}}_i)\,, \end{aligned} \tag{6.18}$$

which is an unbiased estimator of $\mathbf{H}$. The performance of any unbiased estimator can be bounded by the Cramér-Rao lower bound as

$$R_{\widetilde{\mathbf{h}}^{(i)}\widetilde{\mathbf{h}}^{(i)}} = \mathrm{E}\,\widetilde{\mathbf{h}}^{(i)}\widetilde{\mathbf{h}}^{(i)\,T} \geq J^{-(i)}\,, \tag{6.19}$$

where $\mathbf{h} = [\Re(\mathrm{vec}(\mathbf{H}))^T\ \Im(\mathrm{vec}(\mathbf{H}))^T]^T$ and $\mathrm{vec}(\mathbf{H}) = [\mathbf{h}_1^T, \ldots, \mathbf{h}_{N_{tx}}^T]^T$ denotes $\mathbf{H}$ written in a vector form. $J^{(i)}$ is the Bayesian Fischer Information Matrix (FIM) for the a posteriori distribution of $\mathbf{H}$, and is in this case

$$\begin{aligned} J^{(i)} &= -\mathrm{E}\,\frac{\partial}{\partial \mathbf{h}}\left(\frac{\partial \ln p(\mathbf{H}|\mathbf{X}^{TS}, \mathbf{X}_1^{i-1}, \overline{\mathbf{Y}}_i)}{\partial \mathbf{h}}\right)^T \\ &= \underbrace{-\mathrm{E}\,\frac{\partial}{\partial \mathbf{h}}\left(\frac{\partial \ln p(\mathbf{X}^{TS}, \mathbf{Y}^{TS}, \mathbf{X}_1^{i-1}, \mathbf{Y}_1^{i-1}|\mathbf{H})}{\partial \mathbf{h}}\right)^T}_{J^{(i)}_{DA\,training}}, \end{aligned} \tag{6.20}$$

$$\underbrace{-\mathrm{E}\,\frac{\partial}{\partial \mathbf{h}}\left(\frac{\partial \ln p(\mathbf{Y}_{i+1}^{N_B}|\mathbf{H})}{\partial \mathbf{h}}\right)^T}_{J^{(i)}_{blind}} \underbrace{-\mathrm{E}\,\frac{\partial}{\partial \mathbf{h}}\left(\frac{\partial \ln p(\mathbf{H})}{\partial \mathbf{h}}\right)^T}_{J^{(i)}_{prior}}. \tag{6.21}$$

We have $\sigma^2_{\widetilde{\mathbf{H}}^{(i)}} \geq \frac{\mathrm{tr}\,J^{-(i)}}{N_{tx}\,N_{rx}}$. This is an absolute lower bound on the channel estimation MSE. The MMSE estimator achieves this bound asymptotically ($N_B \to \infty$).

6.4 Capacity Behavior and Bounds for Time Selective Channel

In the following we seek to study the behavior of the capacity for time selective channels. We first derive theoretical bounds on MI. Then we analyze the capacity behavior for the differential encoding case, where the input blocks

are constrained to be unitary, and generalize the analysis to the general unconstrained input case.

The channel is assumed to be constant over a block of N_{tx} symbol periods. Further variation of the channel during this block is included in the thermal noise. If we fix $T_i = N_{tx}\ \forall i$, then $\mathbf{Y}_i = [\mathbf{y}_{i\,N_{tx}+1}, \ldots, \mathbf{y}_{(i+1)\,N_{tx}}]$and $\mathbf{X}_i = [\mathbf{x}_{i\,N_{tx}+1}, \ldots, \mathbf{x}_{(i+1)\,N_{tx}}]$.The blocks $\mathbf{X}_i$ are assumed to be i.i.d..
We denote by $L(L = T/N_{tx})$ the total number of blocks, and integrate the pilot symbols with the already detected symbols. The i^{th} term of the MI is then

$$I(\mathbf{Y}_i; \mathbf{X}_i | \mathbf{X}_1^{i-1}, \overline{\mathbf{Y}}_i) = I^{(i)}\,, \tag{6.22}$$

$I^{(i)}$ can be written in term of the entropy as

$$I(\mathbf{Y}_i; \mathbf{X}_i | \mathbf{X}_1^{i-1}, \overline{\mathbf{Y}}_i) = h(\mathbf{X}_i) - h(\mathbf{X}_i | \mathbf{X}_1^{i-1}, \overline{\mathbf{Y}}_i)\,. \tag{6.23}$$

The entropy increases when the conditioning is reduced, hence

$$h(\mathbf{X}_i | \overline{\mathbf{X}}_i, \overline{\mathbf{Y}}_i) \leq h(\mathbf{X}_i | \mathbf{X}_1^{i-1}, \overline{\mathbf{Y}}_i) \leq h(\mathbf{X}_i | \mathbf{X}_1^{i-1}, \mathbf{Y}_1^{i-1})\,. \tag{6.24}$$

Upper and lower bounds of the MI can then be found as

$$I(\mathbf{Y}_i; \mathbf{X}_i | \mathbf{X}_1^{i-1}, \mathbf{Y}_1^{i-1}) \leq I^{(i)} \leq I(\mathbf{Y}_i; \mathbf{X}_i | \overline{\mathbf{X}}_i, \overline{\mathbf{Y}}_i). \tag{6.25}$$

The channel is assumed to be a stationary Gaussian process. The conditioned joint probability of $\mathbf{X}_i$ and $\mathbf{Y}_i$ is then

$$p(\mathbf{Y}_i, \mathbf{X}_i | \mathbf{X}_1^{i-1}, \mathbf{Y}_1^{i-1}) = \int_{\mathbf{H}^{(i)}} p(\mathbf{Y}_i, \mathbf{X}_i | \mathbf{H}^{(i)}) p(\mathbf{H}^{(i)} | \mathbf{X}_1^{i-1}, \mathbf{Y}_1^{i-1})\,. \tag{6.26}$$

Let $h^{(i)} = \mathrm{vec}(\mathbf{H}^{(i)})$, $h_1^{i-1} = [{h^{(1)}}^T, \ldots, {h^{(i-1)}}^T]^T$, $\boldsymbol{r}_h = \mathrm{E}\,(h^{(i)} {h^{(i)}}^H)$, $\boldsymbol{r}^{(i)} = \mathrm{E}\,(h_1^{i-1} {h^{(i)}}^H)$ and $\boldsymbol{R}^{(i)} = \mathrm{E}\,(h_1^{i-1} h_1^{i-1\,H})$. Then $Y_1^{N_{tx}(i-1)} = \mathcal{X}^{i-1} h_1^{i-1} + V_1^{i-1}$, where Y_1^{i-1}, V_1^{i-1} correspond to $\mathbf{Y}_1^{i-1}, \mathbf{V}_1^{i-1}$ written in vector form.
We denote by $\mathcal{X}^{i-1} = [\bigoplus_{k=1}^{i-1} \mathbf{X}_k^T] \otimes \mathbf{I}_{N_{rx}} = {\mathcal{X}_{\mathcal{D}}}^{i-1} \otimes \mathbf{I}_{N_{rx}}$.
Since $h^{(i)}$ and $(Y_1^{N_{tx}(i-1)} | \mathbf{X}_1^{i-1})$ are mutually Gaussian, then $(h^{(i)} | Y_1^{N_{tx}(i-1)}, \mathbf{X}_1^{i-1})$ has a Gaussian distribution with mean

$$\widehat{\mathbf{h}}^{(i)} = {\boldsymbol{r}^{(i)}}^H \mathcal{X}^{i-1\,H} (\sigma_v^2 I + \mathcal{X}^{i-1} \boldsymbol{R}^{(i)} \mathcal{X}^{i-1\,H})^{-1}\, Y_1^{N_{tx}(i-1)}\,, \tag{6.27}$$

and covariance

$$\mathrm{E}\,(\widetilde{\mathbf{h}}^{(i)}\widetilde{\mathbf{h}}^{(i)\,H}) = \boldsymbol{r}_h - \boldsymbol{r}^{(i)\,H}\mathcal{X}^{i-1\,H}(\sigma_v^2 I + \mathcal{X}^{i-1}\boldsymbol{R}^{(i)}\mathcal{X}^{i-1\,H})^{-1}\mathcal{X}^{i-1}\boldsymbol{r}^{(i)}\,. \tag{6.28}$$

The MI is then:

$$I(\mathbf{Y}_i;\mathbf{X}_i|\mathbf{X}_1^{i-1},\mathbf{Y}_1^{i-1}) = I(\mathbf{Y}_i;\mathbf{X}_i|\widehat{\mathbf{h}}^{(i)})\,. \tag{6.29}$$

This MI corresponds to a channel with an instantaneous value $\widehat{\mathbf{H}}^{(i)}$ and an additive noise $\widetilde{\mathbf{V}}_i = \widetilde{\mathbf{H}}^{(i)}\,\mathbf{X}_i + \mathbf{V}_i$, $\mathbf{Y}_i = \widehat{\mathbf{H}}^{(i)}\,\mathbf{X}_i + \widetilde{\mathbf{V}}_i$.
The noise $\widetilde{\mathbf{V}}_i$ depends on $\mathbf{X}_i$ and $\mathbf{X}_1^{i-1}$(the statistics of $\widetilde{\mathbf{H}}^{(i)}$ are function of $\mathbf{X}_1^{i-1}$).
The same results can be stated for $I(\mathbf{Y}_i;\mathbf{X}_i|\overline{\mathbf{X}}_i,\overline{\mathbf{Y}}_i)$, where now $\overline{\mathbf{X}}_i$ (resp. $\overline{\mathbf{Y}}_i$) plays the role of $\mathbf{X}_1^{i-1}$(resp. $\mathbf{Y}_1^{i-1}$).

6.4.1 Case of Differential Encoding

We study this case because it leads to channel estimate statistics that are independent of the inputs. This allows us to derive close-form formulas for the bounds on the capacity.

We consider a time selective fading channel with spatially i.i.d. Gaussian elements, *i.e.*

$$\mathrm{E}\,\mathbf{H}_{lp}^{(i)}\mathbf{H}_{mn}^{(k)\,*} = s(i-k)\delta_{l-m,p-n}\,. \tag{6.30}$$

The channel covariance is hence $\boldsymbol{R}^{(i)} = \boldsymbol{R}_s^{(i)} \otimes \mathbf{I}_{N_{tx}N_{rx}}$, $\boldsymbol{r}^{(i)} = r_s^{(i)} \otimes \mathbf{I}_{N_{tx}N_{rx}}$ and $\boldsymbol{r}_h$ equals $s(0)\mathbf{I}_{N_{rx}N_{tx}} = \sigma_h^2\mathbf{I}_{N_{rx}N_{tx}}$, with $(\boldsymbol{R}_s^{(i)})_{lp} = s(l-p)$ and $(r_s^{(i)})_l = s(l)$ $(1 \le l,p \le i-1)$.
For differential encoding schemes $\mathbf{X}_i/\sqrt{N_{tx}\sigma_x^2}$ is unitary, then $(h^{(i)}|Y_1^{N_{tx}(i-1)},\mathbf{X}_1^{i-1})$ follows a Gaussian distribution with mean

$$\widehat{\mathbf{h}}^{(i)} = (\{r_s^{(i)\,H}(\sigma_v^2\mathbf{I}_{i-1} + N_{tx}\sigma_x^2\boldsymbol{R}_s^{(i)})^{-1}\}) \otimes \mathbf{I}_{N_{tx}N_{rx}}\,\mathcal{X}^{i-1\,H}\,Y_1^{N_{tx}(i-1)}\,, \tag{6.31}$$

and covariance

$$\mathrm{E}\,(\widetilde{\mathbf{h}}^{(i)}\widetilde{\mathbf{h}}^{(i)\,H}) = \sigma^2_{\widetilde{\mathbf{h}}^{(i)}}\mathbf{I}_{N_{tx}N_{rx}}\,, \tag{6.32}$$

where $\sigma^2_{\widetilde{\mathbf{h}}^{(i)}} = (s(0) - r_s^{(i)\,H}(\sigma_v^2/(N_{tx}\sigma_x^2)\mathbf{I}_{i-1} + \boldsymbol{R}_s^{(i)})^{-1}r_s^{(i)})$.
Due to the unitary character of the input, the equivalent noise $\widetilde{\mathbf{V}}_i$ is independent of the input $\mathbf{X}_i$ and follows a centered white Gaussian distribution

of covariance $\sigma^2_{\tilde{v}_i}\mathbf{I}_{N_{tx}N_{rx}}$, with $\sigma^2_{\tilde{v}_i} = \sigma^2_v + N_{tx}\sigma^2_x\sigma^2_{\tilde{\mathbf{h}}^{(i)}}$. $\sigma^2_{\tilde{\mathbf{h}}^{(i)}}$ corresponds to the estimation error of $\mathbf{H}^{(i)}_{lp}$ from the already transmitted and decoded signal blocks. Due to the stationarity of the process $\mathbf{X}_i$ and $\mathbf{Y}_i$, $\sigma^2_{\tilde{\mathbf{h}}^{(i)}}$ is a decreasing function of (i) and tends to a limit value $\lim_{i\to\infty}\sigma^2_{\tilde{\mathbf{h}}^{(i)}} = \sigma^2_{\tilde{\mathbf{h}}^{\infty}}$. The approximation $\sigma^2_{\tilde{\mathbf{h}}^{(i)}} \approx \sigma^2_{\tilde{\mathbf{h}}^{\infty}}$ is valid for $i >> L_{coh}$, where L_{coh} is the coherence time of the channel. This approximation corresponds to the steady-state. It is considered to be valid for all the data symbols if the TS is long enough: $N_{TS} >> N_{tx}L_{coh}$.
$\sigma^2_{\tilde{\mathbf{h}}^{\infty}}$ is the infinite horizon mean square prediction error variance of $\mathbf{H}_{lp}$

$$\sigma^2_{\tilde{\mathbf{h}}^{\infty}} = e^{\int_{-1/2}^{1/2}\ln(S(f)+\frac{\sigma^2_v}{N_{tx}\sigma^2_x})df} - \frac{\sigma^2_v}{N_{tx}\sigma^2_x}\,, \tag{6.33}$$

where $S(f) = \sum_k s(k)e^{-j2\pi kf}$.
For $i >> L_{coh}$, $I(\mathbf{Y}_i;\mathbf{X}_i|\widehat{\mathbf{h}}^{(i)})$ is independent of the index i.

Let $\mathcal{C}_{\mathcal{U}}(\rho)$ be the ergodic capacity of a $N_{rx}\times N_{tx}$ AWGN and Rayleigh flat block fading channel. The channel has i.i.d. elements of Gaussian distribution $\mathcal{CN}(0,1)$, and the Rx has perfect CSI (and none at Tx). For $\mathcal{C}_{\mathcal{U}}(\rho)$, the input blocks of size $N_{tx}\times N_{tx}$ are constrained to be unitary and follow the same distribution as in the differential encoding case, and finally the additive white Gaussian noise follows the distribution $\mathcal{CN}(0,\frac{1}{N^2_{tx}\rho})$.
Then

$$\frac{1}{N_{tx}}I(\mathbf{Y}_i;\mathbf{X}_i|\widehat{\mathbf{h}}^{(i)}) = \mathcal{C}_{\mathcal{U}}(\rho^{eff})\,, \tag{6.34}$$

where

$$\begin{aligned}\rho^{eff} &= \frac{1}{N_{tx}}\frac{\sigma^2_x(\sigma^2_h-\sigma^2_{\tilde{\mathbf{h}}^{\infty}})}{\sigma^2_v+N_{tx}\sigma^2_x\sigma^2_{\tilde{\mathbf{h}}^{\infty}}}\\ &= \rho\frac{1-\frac{\sigma^2_{\tilde{\mathbf{h}}^{\infty}}}{\sigma^2_h}}{1+N^2_{tx}\rho\frac{\sigma^2_{\tilde{\mathbf{h}}^{\infty}}}{\sigma^2_h}}\,,\end{aligned} \tag{6.35}$$

and $\rho = \frac{\sigma^2_x\sigma^2_h}{N_{tx}\sigma^2_v}$.

Hence, the lack of CSI at the receiver results in a loss of SNR of $10\log_{10}\left(\frac{1-\frac{\sigma^{2\infty}_{\widetilde{\mathbf{h}}}}{\sigma^2_h}}{1+N^2_{tx}\rho\frac{\sigma^{2\infty}_{\widetilde{\mathbf{h}}}}{\sigma^2_h}}\right)$ dB.

We can also see that this loss increases with the SNR ($= N_{tx}\rho$) and with the normalized channel estimation error $\frac{\sigma^{2\infty}_{\widetilde{\mathbf{h}}}}{\sigma^2_h}$. For large SNR ($\rho >> \frac{\sigma^2_h}{N^2_{tx}\sigma^{\infty\,2}_{\widetilde{\mathbf{h}}}}$) the capacity gets saturated at $\mathcal{C}^{\infty}_{\mathcal{U}} = \mathcal{C}_{\mathcal{U}}\left(\frac{\sigma^2_h}{\sigma^2_{\widetilde{\mathbf{h}}^{\infty,o}}N^2_{tx}} - \frac{1}{N^2_{tx}}\right)$, where $\sigma^2_{\widetilde{\mathbf{h}}^{\infty,o}}$ is $\sigma^2_{\widetilde{\mathbf{h}}^{\infty}}$ in the absence of noise.

The same development can be done for the upper bound. The steady-state of the upper bound is considered to be valid under the both conditions $i >> L_{coh}$ and $L - i >> L_{coh}$.

The upper and lower bounds of $I^{(i)}$ are then

$$\frac{1}{N_{tx}}\mathcal{C}_{\mathcal{U}}\left(\rho\frac{1-\frac{\sigma^{\infty\,2}_{\widetilde{\mathbf{h}}}}{\sigma^2_h}}{1+N^2_{tx}\rho\frac{\sigma^{\infty\,2}_{\widetilde{\mathbf{h}}}}{\sigma^2_h}}\right) \leq I^{(i)} \leq \frac{1}{N_{tx}}\mathcal{C}_{\mathcal{U}}\left(\rho\frac{1-\frac{\sigma^{2\infty}_{\widetilde{\mathbf{h}},m}}{\sigma^2_h}}{1+N^2_{tx}\rho\frac{\sigma^{2\infty}_{\widetilde{\mathbf{h}},m}}{\sigma^2_h}}\right), \tag{6.36}$$

where $\sigma^{2\infty}_{\widetilde{\mathbf{h}},m} = [\int_{-1/2}^{1/2}\frac{df}{S(f)+\frac{\sigma^2_v}{N_{tx}\sigma^2_x}}]^{-1} - \frac{\sigma^2_v}{N_{tx}\sigma^2_x}$ is the infinite horizon mean square interpolation error variance of $\mathbf{H}_{lp}$.

Under the constraint of unitary input distribution, the capacity equals the average MI. For large T this average MI satisfies

$$\begin{aligned} I^{\infty}_{avg} &= \lim_{T\to\infty} I_{avg}(T) \\ &= \lim_{L\to\infty}\frac{1}{LN_{tx}}\sum_{i=1}^{L} I^{(i)} \\ &= \frac{1}{N_{tx}}\lim_{(i,L-i)\to\infty} I^{(i)}, \end{aligned} \tag{6.37}$$

Hence it is bounded by

$$\mathcal{C}_{\mathcal{U}}\left(\rho\frac{1-\frac{\sigma^{\infty\,2}_{\widetilde{\mathbf{h}}}}{\sigma^2_h}}{1+N^2_{tx}\rho\frac{\sigma^{\infty\,2}_{\widetilde{\mathbf{h}}}}{\sigma^2_h}}\right) \leq I^{\infty}_{avg} \leq \mathcal{C}_{\mathcal{U}}\left(\rho\frac{1-\frac{\sigma^{2\infty}_{\widetilde{\mathbf{h}},m}}{\sigma^2_h}}{1+N^2_{tx}\rho\frac{\sigma^{2\infty}_{\widetilde{\mathbf{h}},m}}{\sigma^2_h}}\right). \tag{6.38}$$

The distance of the capacity w.r.t. the upper bound (resp. lower bound), depends on how much significant is the information on the channel provided by the blind part of the signal (*i.e.*, the non decoded signal at time (i): $\mathbf{Y}_{i+1}^{L}$).

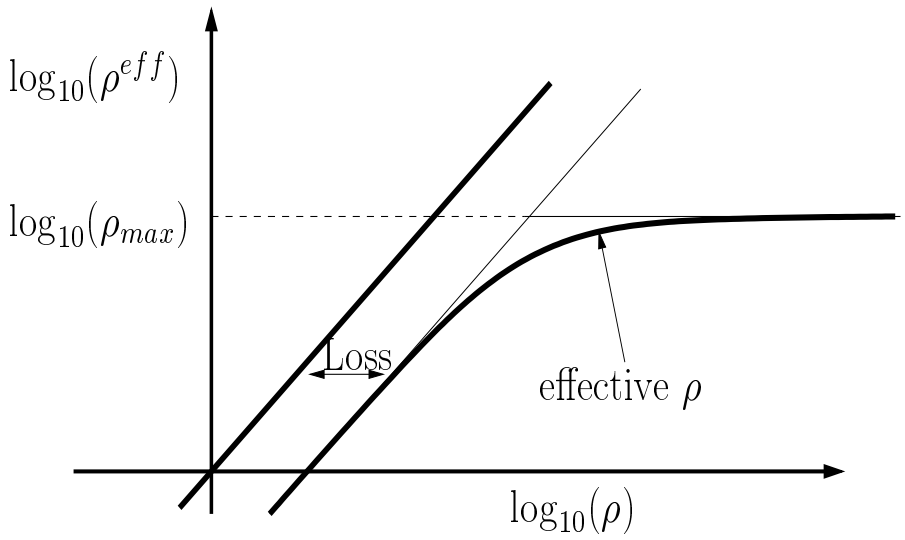

Figure 6.1: Effective SNR for time selective channel

Fig 6.1 and 6.2 show the behavior of the effective SNR and the capacity as functions of the input SNR. We can see that the lack of CSI at Rx results in a proportional loss for medium SNR and a saturation for high SNR range. This behavior is valid for relatively small $\frac{N_{tx}^2 \sigma^2_{\widetilde{\mathbf{h}}^{\infty,o}}}{\sigma_h^2}$ (otherwise the medium SNR part of fig. 6.2 disappears).

6.4.2 General Case

We will now give upper and lower bounds on the achievable ergodic capacity. The inputs $\mathbf{X}_i$ are i.i.d. with unconstrained distribution. We assume the same channel model as in the previous subsection, then $\mathrm{E}\,(\widetilde{\mathbf{h}}^{(i)}\widetilde{\mathbf{h}}^{(i)\,H}) = [s(0)\mathbf{I}_{N_{tx}} - (r_s^{(i)\,H} \otimes \mathbf{I}_{N_{tx}})\mathcal{X}_{\mathcal{D}}{}^{i-1\,H}(\sigma_v^2 I + \mathcal{X}_{\mathcal{D}}{}^{i-1}\boldsymbol{R}_s^{(i)}\mathcal{X}^{i-1\,H})^{-1}\mathcal{X}_{\mathcal{D}}{}^{i-1}(r_s^{(i)} \otimes \mathbf{I}_{N_{tx}})] \otimes \mathbf{I}_{N_{rx}} = Cov_{\widetilde{\mathbf{h}}}^{(i)} \otimes \mathbf{I}_{N_{rx}}$. This shows that the rows of $\widetilde{\mathbf{H}}^{(i)}$ are i.i.d. with covariance $Cov_{\widetilde{\mathbf{h}}}^{(i)}$.

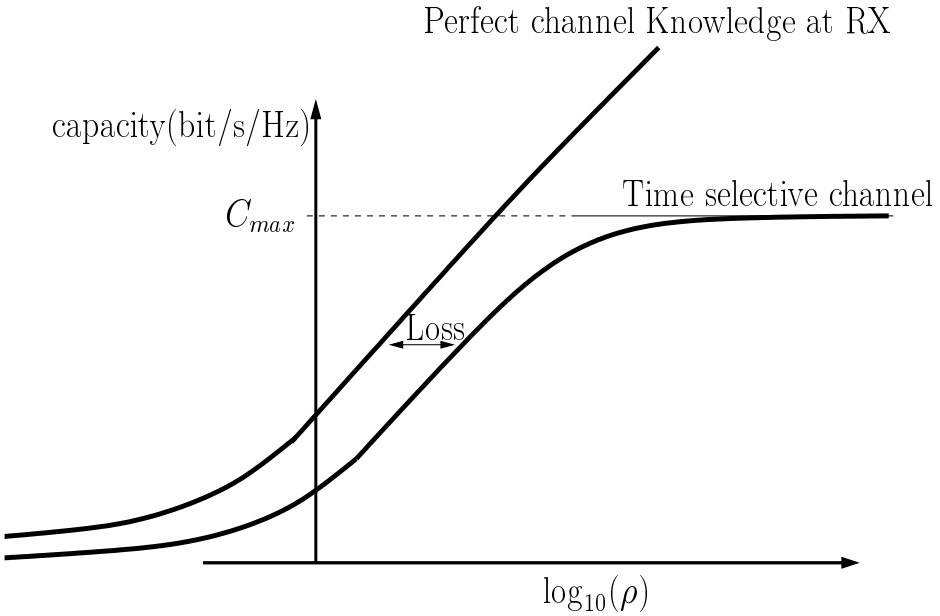

Figure 6.2: Capacity behavior of time selective channel

We define $\sigma^2_{\widetilde{\mathbf{h}}^{(i)}} = \frac{1}{N_{tx}}\mathrm{tr}\{Cov^{(i)}_{\widetilde{\mathbf{h}}}\}$, as in subsection 6.3.1. A lower bound to $I(\mathbf{Y}_i;\mathbf{X}_i|\widehat{\mathbf{h}}^{(i)})$ is given by

$$\begin{aligned} I(\mathbf{Y}_i;\mathbf{X}_i|\widehat{\mathbf{h}}^{(i)}) &\geq N_{tx}\,\mathrm{E}\ln\det(I + \frac{\sigma_x^2(\sigma_h^2-\sigma^2_{\widetilde{\mathbf{h}}^{(i)}})}{\sigma_v^2+N_{tx}\sigma_x^2\sigma^2_{\widetilde{\mathbf{h}}^{(i)}}}\overline{\mathbf{H}}^{(i)}\overline{\mathbf{H}}^{(i)\,H}) \\ &= C^{(i)}_{LB}\,. \end{aligned} \tag{6.39}$$

In appendix 6.A, it is shown that an upper bound to $I(\mathbf{Y}_i;\mathbf{X}_i|\overline{\mathbf{X}}_i,\overline{\mathbf{Y}}_i) = I(\mathbf{Y}_i;\mathbf{X}_i|\widehat{\mathbf{h}}^{(i)}_m)$ is

$$\begin{aligned} I(\mathbf{Y}_i;\mathbf{X}_i|\widehat{\mathbf{h}}^{(i)}_m) \leq\; & N_{tx}\,\mathrm{E}\ln\det(I + \frac{\sigma_x^2(\sigma_h^2-\sigma^2_{\widetilde{\mathbf{h}}^{(i)}_{,m}})}{\sigma_v^2+N_{tx}\sigma_x^2\sigma^2_{\widetilde{\mathbf{h}}^{(i)}_{,m}}}\overline{\mathbf{H}}^{(i)}_m\overline{\mathbf{H}}^{(i)\,H}_m) \\ & -N_{rx}\,\mathrm{E}\ln\det(\frac{\mathbf{X}_i^H Cov^{(i)}_{\widetilde{\mathbf{h}}_{,m}}\mathbf{X}_i+\sigma_v^2\mathbf{I}_{N_{tx}}}{\sigma_v^2+N_{tx}\sigma_x^2\sigma^2_{\widetilde{\mathbf{h}}^{(i)}_{,m}}}) = C^{(i)}_{UB}\,, \end{aligned} \tag{6.40}$$

and in appendix 6.B, we show that

$$0 \leq -\,\mathrm{E}\ln\det\Big(\frac{\mathbf{X}_i^H Cov^{(i)}_{\widetilde{\mathbf{h}},m}\,\mathbf{X}_i+\sigma_v^2\mathbf{I}_{N_{tx}}}{\sigma_v^2+N_{tx}\sigma_x^2\sigma^2_{\widetilde{\mathbf{h}}^{(i)}_{,m}}}\Big) \leq -\,\mathrm{E}\ln\det\Big(\frac{\mathbf{X}_i^H Cov^{(i)}_{\widetilde{\mathbf{h}},m}\,\mathbf{X}_i}{N_{tx}\sigma_x^2\sigma^2_{\widetilde{\mathbf{h}}^{(i)}_{,m}}}\Big).$$

This additional term behaves like a measure of the deviation of the distribution of $\mathbf{X}_i$ w.r.t. the unitary matrices manifold. In fact, for $\mathbf{X}_i$ unitary this quantity is zero. Another observation is that the white Gaussian noise case is the worse one: it is then natural that the additional term in the upper bound is positive.

Summarizing, we have shown that

$$C_{LB}^{(i)} \leq I^{(i)} \leq C_{UB}^{(i)}\,. \tag{6.41}$$

For large SNR ($>> \frac{\sigma_h^2}{N_{tx}\sigma^{\infty\,2}_{\widetilde{\mathbf{h}}}}$) the distribution of $\widehat{\mathbf{H}}^{(i)}$ (resp. $\widehat{\mathbf{H}}^{(i),m}$) is independent of the index i and $Cov^{(i)}_{\widetilde{\mathbf{h}}} = \sigma^2_{\widetilde{\mathbf{h}}^{\infty,o}}\mathbf{I}_{N_{tx}}$,
$\mathrm{E}(\widehat{\mathbf{h}}^{(i)}\widehat{\mathbf{h}}^{(i)\,H}) = (\sigma_h^2 - \sigma^2_{\widetilde{\mathbf{h}}^{\infty,o}})\mathbf{I}_{N_{tx}N_{rx}}$
(resp. $Cov^{(i)}_{\widetilde{\mathbf{h}},m} = \sigma^2_{\widetilde{\mathbf{h}}^{\infty,o}_{,m}}\mathbf{I}_{N_{tx}}$, $\mathrm{E}(\widehat{\mathbf{h}}^{(i)}_m\widehat{\mathbf{h}}^{(i)\,H}_m) = (\sigma_h^2 - \sigma^2_{\widetilde{\mathbf{h}}^{\infty,o}_{,m}})\mathbf{I}_{N_{tx}N_{rx}}$).

6.5 Correlated MIMO Channel Model

In order to improve channel estimation and reduce capacity loss, it is advantageous to exploit the correlations in the channel, if present. So consider the frequency-flat MIMO channel: $\mathbf{H}$ ($N_{rx} \times N_{tx}$), $\boldsymbol{h} = \mathrm{vec}(\mathbf{H})$. The correlated channel model we suggest is

$$\boldsymbol{h} = \mathbf{U}_h\ \boldsymbol{s}\,, \tag{6.42}$$

where the elements of $\boldsymbol{s}$ are taken to be i.i.d. Gaussian for a stochastic model, and the correlations are captured by $\mathbf{U}_h$.

This model applies for channel models we have used in the previous chapters:
Separable spatial correlation model
$\mathbf{H} = R_r^{1/2}\ \mathbf{W}\ R_t^{H/2} \Rightarrow \mathbf{U}_h = R_t^{H/2} \otimes R_r^{1/2}$ and $\boldsymbol{s} = \mathrm{vec}(\mathbf{W})$.

Path-wise channel model
$\mathbf{H} = \sum_i s_i \, \boldsymbol{a}_i \, \boldsymbol{b}_i^H \;\; \Rightarrow \;\; \mathbf{U}_h = [\boldsymbol{b}_1^* \otimes \boldsymbol{a}_1, \;\; \boldsymbol{b}_2^* \otimes \boldsymbol{a}_2, \; \cdots] \, .$

The model $\boldsymbol{h} = \mathbf{U}_h \; \boldsymbol{s}$ is straightforwardly extendible to the non-zero delay-spread case.

6.6 Observations

To approach capacity, channel estimation should exploit prior information on the channel plus data (decision) aided information and blind information. In fact, the symbol-wise decomposition of MI involves, for each symbol position in a burst, a channel estimate that is based on: prior channel distribution information, training and detected inputs up to that symbol position, and blind information in the remaining channel outputs.
The MI decomposition can be extended to channels with physical delay spread, or artificial delay introduced by precoding (STS of Part I). In this cases it suggests the use of conventional MIMO DFE Rx like the one proposed in chapter 3. Such a Rx have to be coupled with symbol-wise semi-blind channel estimator.
Estimation methods that combine the training and blind information are called semi-blind. In the next chapter we propose a new family of semi-blind methods that model the undetected symbols as Gaussian, in which the blind information is called Gaussian information.

For the block fading model, in order to have asymptotically (in burst length) negligible capacity loss (w.r.t. to perfect CSI at Rx case), enough training symbols are required to have identifiability of the parameters that cannot be identified blindly. In general, blind information improves identifiability and reduces training data requirements.
The recursive MI decomposition may suggest a practical approach for channel estimation. However, simpler practical approaches would pass through the bursts iteratively. In the first iteration the semi-blind channel estimation uses the undetected symbols as blind information, whereas in the next iterations it is the soft decision on that data that are used as blind information. This can be realized by coupling an iterative Rx like the one studied in chapter 4 with a channel estimator.

These results extend to the time selective channel model case. In the steady-state, channel estimation should be based on the semi-infinite past detected symbols, and semi-infinite future blind information.

The exploitation of prior channel information channel, for example channel correlations, reduces the (effective) number of degrees of freedom in the channel: the training requirements is then reduced. Hence, channel with i.i.d. entries, while optimal from an outage capacity point of view (highest diversity gain), is the worst case from the channel estimation point of view. Prior channel information (and $\mathbf{U}_h$ in the channel model) gets estimated by considering the data in multiple bursts jointly, assuming the parameters are invariant across a large set of bursts.
Finally, the proposed channel model is useful for the introduction of partial CSI at the Tx (see chapter 5). Indeed, if the transmitter can know the channel correlations summarized in $\mathbf{U}_h$ in $\boldsymbol{h} = \mathbf{U}_h\ \boldsymbol{s}$ and only lacks knowledge of the fast fading parameters $\boldsymbol{s}$, the channel capacity is closer to that of perfect CSI.

6.7 Conclusion

The study of the MI of a burst transmission over fading channels, with no CSI at Rx and Tx, suggests sequential detection of symbols or blocks in the case when STC scheme is used. At a given symbol (block), the channel is re-estimated based on TS, past detected and future non-detected symbols. The actual symbol is detected and included in the data aided part (TS plus detected symbols) to be used in next the iterations for channel estimation.
For a block fading model, where the channel is constant over the burst duration, this way of processing ensures that the MI attains the capacity with perfect CSI at Rx for large burst lengths.
However, in the case of time selective model, where the channel is continuously varying, the capacity saturates for high SNR. Bounds on the capacity in this case are given in term of the prediction/smoothing estimation error variance of the channel.
The estimation suggested by the MI decomposition combines the data aided information and the blind information. Such semi-blind methods are proposed in the next chapter.

APPENDIX

6.A Appendix A

We would like to find an upper bound to

$$I(\mathbf{Y}_i;\mathbf{X}_i|\widehat{\mathbf{h}}_m^{(i)}) = h(\mathbf{Y}_i|\widehat{\mathbf{h}}_m^{(i)}) - h(\mathbf{Y}_i|\mathbf{X}_i,\widehat{\mathbf{h}}_m^{(i)})\,, \tag{6.43}$$

where $\mathbf{Y}_i = \widehat{\mathbf{H}}_m^{(i)}\,\mathbf{X}_i + \widetilde{\mathbf{V}}_i^{(m)}$.
The entropy $h(\mathbf{Y}_i|\widehat{\mathbf{h}}_m^{(i)})$ is maximized for white Gaussian $\mathbf{X}_i$ and $\widetilde{\mathbf{V}}_i^{(m)}$, then

$$\begin{aligned} h(\mathbf{Y}_i|\widehat{\mathbf{h}}_m^{(i)}) &\leq N_{tx}\,\mathrm{E}\ln\det \pi e\left((N_{tx}\sigma_x^2\sigma^2_{\widetilde{\mathbf{h}}^{(i)}_{,m}} + \sigma_v^2)\mathbf{I}_{N_{rx}} + \sigma_x^2\widehat{\mathbf{H}}_m^{(i)}\widehat{\mathbf{H}}_m^{(i)\,H}\right) \\ &= N_{tx}\,\mathrm{E}\ln\det(\mathbf{I}_{N_{rx}} + \frac{\sigma_x^2(\sigma_h^2-\sigma^2_{\widetilde{\mathbf{h}}^{(i)}_{,m}})}{\sigma_v^2+N_{tx}\sigma_x^2\sigma^2_{\widetilde{\mathbf{h}}^{(i)}_{,m}}}\overline{\mathbf{H}}_m^{(i)}\overline{\mathbf{H}}_m^{(i)\,H}) \\ &\quad + N_{rx}N_{tx}\ln(N_{tx}\sigma_x^2\sigma^2_{\widetilde{\mathbf{h}}^{(i)}_{,m}} + \sigma_v^2)\,, \end{aligned} \tag{6.44}$$

where $\overline{\mathbf{H}}_m^{(i)} = \dfrac{\widehat{\mathbf{H}}_m^{(i)}}{\sqrt{\sigma_h^2-\sigma^2_{\widetilde{\mathbf{h}}^{(i)}_{,m}}}}$.
The entropy $h(\mathbf{Y}_i|\mathbf{X}_i,\widehat{\mathbf{h}}_m^{(i)})$ equals $h(\widetilde{\mathbf{V}}_i^{(m)}|\mathbf{X}_i,\widehat{\mathbf{h}}_m^{(i)})$ with $\widetilde{\mathbf{V}}_i^{(m)} = \widetilde{\mathbf{H}}_m^{(i)}\,\mathbf{X}_i + \mathbf{V}_i$.
Since $(\widetilde{\mathbf{V}}_i^{(m)}|\mathbf{X}_i,\widehat{\mathbf{h}}_m^{(i)})$ has a Gaussian distribution, we can write

$$\begin{aligned} h(\mathbf{Y}_i|\mathbf{X}_i,\widehat{\mathbf{h}}_m^{(i)}) &= h(\widetilde{\mathbf{H}}_m^{(i)}\,\mathbf{X}_i + \mathbf{V}_i|\mathbf{X}_i,\widehat{\mathbf{h}}_m^{(i)}) \\ &= N_{rx}\,\mathrm{E}\ln\det(\mathbf{X}_i^H Cov^{(i)}_{\widetilde{\mathbf{h}},m}\mathbf{X}_i + \sigma_v^2\mathbf{I}_{N_{tx}})\,, \end{aligned} \tag{6.45}$$

Finally we have

$$\begin{aligned} I(\mathbf{Y}_i;\mathbf{X}_i|\widehat{\mathbf{h}}_m^{(i)}) \leq\; & N_{tx}\,\mathrm{E}\ln\det(I + \frac{\sigma_x^2(\sigma_h^2-\sigma^2_{\widetilde{\mathbf{h}}^{(i)}_{,m}})}{\sigma_v^2+N_{tx}\sigma_x^2\sigma^2_{\widetilde{\mathbf{h}}^{(i)}_{,m}}}\overline{\mathbf{H}}_m^{(i)}\overline{\mathbf{H}}_m^{(i)\,H}) \\ & - N_{rx}\,\mathrm{E}\ln\det(\frac{\mathbf{X}_i^H Cov^{(i)}_{\widetilde{\mathbf{h}},m}\mathbf{X}_i+\sigma_v^2\mathbf{I}_{N_{tx}}}{\sigma_v^2+N_{tx}\sigma_x^2\sigma^2_{\widetilde{\mathbf{h}}^{(i)}_{,m}}})\,. \end{aligned} \tag{6.46}$$

6.B Appendix B

In this appendix we seek to show that

$$0 \leq -\,\mathrm{E}\ln\det\left(\frac{\mathbf{X}_i^H Cov^{(i)}_{\widetilde{\mathbf{h}},m}\mathbf{X}_i+\sigma_v^2\mathbf{I}_{N_{tx}}}{\sigma_v^2+N_{tx}\sigma_x^2\sigma^2_{\widetilde{\mathbf{h}}^{(i)},m}}\right) \leq -E\ln\det\left(\frac{\mathbf{X}_i^H Cov^{(i)}_{\widetilde{\mathbf{h}},m}\mathbf{X}_i}{N_{tx}\sigma_x^2\sigma^2_{\widetilde{\mathbf{h}}^{(i)},m}}\right).$$

We first notice that the function

$$f(\sigma_x^2\sigma^2_{\widetilde{\mathbf{h}}^{(i)},m}) = E_{\mathbf{X}_i}\ln\det\left(\frac{N_{tx}\sigma_x^2\sigma^2_{\widetilde{\mathbf{h}}^{(i)},m}\frac{Cov^{(i)}_{\widetilde{\mathbf{h}},m}}{\sigma^2_{\widetilde{\mathbf{h}}^{(i)},m}}\frac{\mathbf{X}_i\mathbf{X}_i^H}{N_{tx}\sigma_x^2}+\sigma_v^2\mathbf{I}_{N_{tx}}}{\sigma_v^2+N_{tx}\sigma_x^2\sigma^2_{\widetilde{\mathbf{h}}^{(i)},m}}\right)$$

is a decreasing one.

The quantities $\overline{\mathbf{X}\mathbf{X}}_i = \frac{\mathbf{X}_i\mathbf{X}_i^H}{N_{tx}\sigma_x^2}$ and $\overline{Cov}^{(i)}_{\widetilde{\mathbf{h}},m} = \frac{Cov^{(i)}_{\widetilde{\mathbf{h}},m}}{\sigma^2_{\widetilde{\mathbf{h}}^{(i)},m}}$ are normalized and independent of $\sigma_x^2\sigma^2_{\widetilde{\mathbf{h}}^{(i)},m}$, then

$$\begin{aligned}
\frac{\partial f(\sigma_x^2\sigma^2_{\widetilde{\mathbf{h}}^{(i)},m})}{\partial\sigma_x^2\sigma^2_{\widetilde{\mathbf{h}}^{(i)},m}} &= \frac{N_{tx}\sigma_v^2}{\sigma^2_{\widetilde{\mathbf{h}}^{(i)},m}(N_{tx}\sigma_x^2\sigma^2_{\widetilde{\mathbf{h}}^{(i)},m}+\sigma_v^2)} \\
&\quad -\frac{\sigma_v^2}{\sigma^2_{\widetilde{\mathbf{h}}^{(i)},m}}E_{\mathbf{X}_i}\mathrm{tr}\{[N_{tx}\sigma_x^2\sigma^2_{\widetilde{\mathbf{h}}^{(i)},m}\overline{Cov}^{(i)}_{\widetilde{\mathbf{h}},m}\overline{\mathbf{X}\mathbf{X}}_i+\sigma_v^2\mathbf{I}_{N_{tx}}]^{-1}\} \\
&\leq \frac{N_{tx}\sigma_v^2}{\sigma^2_{\widetilde{\mathbf{h}}^{(i)},m}(N_{tx}\sigma_x^2\sigma^2_{\widetilde{\mathbf{h}}^{(i)},m}+\sigma_v^2)} \\
&\quad -\frac{\sigma_v^2}{\sigma^2_{\widetilde{\mathbf{h}}^{(i)},m}}\mathrm{tr}\{[\sigma_x^2\sigma^2_{\widetilde{\mathbf{h}}^{(i)},m}\overline{Cov}^{(i)}_{\widetilde{\mathbf{h}},m}E_{\mathbf{X}_i}\overline{\mathbf{X}\mathbf{X}}_i+\sigma_v^2\mathbf{I}_{N_{tx}}]^{-1}\} \\
&\leq \frac{N_{tx}\sigma_v^2}{\sigma^2_{\widetilde{\mathbf{h}}^{(i)},m}(N_{tx}\sigma_x^2\sigma^2_{\widetilde{\mathbf{h}}^{(i)},m}+\sigma_v^2)} \\
&\quad -\frac{\sigma_v^2}{\sigma^2_{\widetilde{\mathbf{h}}^{(i)},m}}\frac{N_{tx}}{\mathrm{tr}\{N_{tx}\sigma_x^2\sigma^2_{\widetilde{\mathbf{h}}^{(i)},m}\overline{Cov}^{(i)}_{\widetilde{\mathbf{h}},m}E_{\mathbf{X}_i}\overline{\mathbf{X}\mathbf{X}}_i+\sigma_v^2\mathbf{I}_{N_{tx}}\}} \\
&= 0.
\end{aligned} \tag{6.47}$$

The second equality can be shown by writing the eigenvector decomposition of $(N_{tx}\sigma_x^2\sigma^2_{\widetilde{\mathbf{h}}^{(i)},m}\overline{Cov}^{(i)}_{\widetilde{\mathbf{h}},m}\overline{\mathbf{X}\mathbf{X}}_i+\sigma_v^2\mathbf{I}_{N_{tx}})$ and exploiting the concavity of $g(x)=-x^{-1}$. The third inequality also exploit the concavity of $g(x)=-x^{-1}$ to show that $-\mathrm{tr}\mathbf{M}^{-1}$ is upper bounded by $-N_{tx}(\mathrm{tr}\mathbf{M})^{-1}$ for any hermitian positive definite $N_{tx}\times N_{tx}$ matrix $\mathbf{M}$.

We have shown that $f(\sigma_x^2\sigma^2_{\widetilde{\mathbf{h}}^{(i)},m})$ is a decreasing function over $[0,\infty)$, which allows us to write

$$f(\infty) = \ln\det(\overline{Cov}^{(i)}_{\widetilde{\mathbf{h}},m}) + E_{\mathbf{X}_i}\ln\det(\overline{\mathbf{X}\mathbf{X}}_i) \leq f(\sigma_x^2\sigma^2_{\widetilde{\mathbf{h}}^{(i)},m}) \leq f(0) = 0\,. \tag{6.48}$$

This shows that

$$0 \leq -E\ln\det(\frac{\mathbf{X}_i^H Cov^{(i)}_{\widetilde{\mathbf{h}},m}\mathbf{X}_i + \sigma_v^2\mathbf{I}_{N_{tx}}}{\sigma_v^2 + N_{tx}\sigma_x^2\sigma^2_{\widetilde{\mathbf{h}}^{(i)},m}}) \leq -E\ln\det(\frac{\mathbf{X}_i^H Cov^{(i)}_{\widetilde{\mathbf{h}},m}\mathbf{X}_i}{N_{tx}\sigma_x^2\sigma^2_{\widetilde{\mathbf{h}}^{(i)},m}}). \tag{6.49}$$

Chapter 7

Semi-Blind Estimation for MIMO Channels

As we have seen in the previous chapter, the mutual information analysis suggests the use of semi-blind techniques for the channel estimation. In fact, the high number of coefficients in the MIMO channel response (number of Tx antennas times number of Rx antennas times delay spread) allows to achieve high diversity and to improve the outage capacity. But, at the same time, it represents a challenge for channel estimation as it imposes the use of a longer training sequence (TS) leading to a rate loss. In this chapter, we augment the TS artificially by including the blind part (unknown symbols) information and the non pure training information. This allows to reduce the TS length needed for channel estimation and hence to save rate. We use semi-blind approaches that exploit both training and blind information. Though these techniques present a larger complexity than that of training base techniques, their complexity remains however very reasonable. For the flat channel case, the technique we present achieves the Cramér-Rao Bound. In the frequency-selective channel case, we use a quadratic semi-blind criterion that combines a training-based least-squares criterion with a blind criterion based on linear prediction.

7.1 Introduction

The formidable capacity increase realizable with the multi-antenna systems has been shown [2, 81] to be proportional to the minimum of the antenna array dimensions for channel with i.i.d. fading entries. At least, this is the case when the receiver has perfect CSI. This condition is fairly straightforward to approach in SISO systems by inserting pilot/training data in the transmission, with acceptable capacity decrease [77]. For MIMO systems of large dimensions, the training overhead for good channel estimation quality becomes far from negligible, especially for higher Doppler speeds such as in mobile communications. The effect of channel estimation errors on the MI has been analyzed in [78, 79]. In order to reduce this degradation due to pure TS estimation, semi-blind approach have to be used. In fact, in the previous chapter, we have seen that semi-blind channel estimation is suggested by the MI decomposition. Using such an approach coupled with a DFE processing at the Rx, allows to achieve high performances and reduces the capacity loss.

Most of semi-blind techniques exploit the existence of signal and noise subspaces when $N_{rx} > N_{tx}$. In fact, the presence of these subspaces has led to the development of a large number of blind channel estimation techniques over the last decade[85, 86, 87, 88]. Some of these techniques are relatively simple due to the modeling of the unknown input symbols as either deterministic unknowns of uncorrelated random variables, other are more complex and exploit the finite alphabet nature. The uncorrelated case is also called the Gaussian case because (only) second-order statistics are exploited. However, most of these blind techniques are not robust in the sense that they often require a precise knowledge of the channel length(s). Moreover, if transmission zeros can be handled, they are required to be minimum-phase. Furthermore, the blind techniques leave channel ambiguities, which can range from a simple scalar ambiguity factor for SIMO channels or certain MIMO channels, to instantaneous or even convolutive mixtures of the sources for other MIMO channels. On the other hand, all current standardized communication systems employ some form of known inputs to allow channel estimation. The channel estimation performance in those cases can always be improved by a semi-blind approach which exploits both training and blind information. The training information allows to resolve the blind ambiguities and robustifies the channel estimates. The purpose of this chapter is to introduce semi-blind techniques whose complexity is not immensely much higher than that of training based techniques.

In the case of SIMO channels, [85] introduces a simple semi-blind technique, whose blind criterion is based on the Subchannel Response Matching (SRM) method. The SRM method is also known as the Cross-Relation (CR) method. In the SRM approach, we use a simple parameterization of the noise subspace that is linear in the channel parameters. A blind criterion is then obtained by expressing orthogonality between this parameterized noise subspace and the data. For use in a semi-blind approach, the data covariance matric should be denoised. This leads to a simple quadratic semi-blind criterion. However, a linear parameterization of the noise subspace in terms of the channel parameters exists only in the SIMO case [89].

The present chapter is structured in two parts. The first one deals with the flat channel case. It begins by an analysis of the ML estimator, the Fischer information matrix and the asymptotic behavior of the Cramér-Rao bound (CRB) for large blind part length. Inspired by the CRB analysis, we propose the Gaussian Semi-Blind (GSB) approach and detail its characteristic. In the end of this part we introduce the Deterministic Semi-Blind (DSB) approach.
The second part of this chapter considers the frequency selective channel case. To exploit the blind information in this case we use a parameterization of the channel based on the MIMO linear predictor. We introduce some linear prediction basis, in particular the estimation of the MIMO linear predictor. We show then how to use this quantity to derive quadratic criteria for the GSB and DSB approaches. Identifiability conditions of these methods are also derived and an augmented TS part technique proposed. We end this chapter by presenting some numerical examples.

Results presented in this chapter were published in [90, 91].

7.2 MIMO Flat Channel

In this case, the discrete time received signal is

$$\mathbf{y}_k = \mathbf{H}\mathbf{x}_k + \mathbf{v}_k \,, \tag{7.1}$$

where $\mathbf{x}_k \sim \mathcal{CN}(0, \sigma_x^2 \mathbf{I}_{N_{tx}})$ and $\mathbf{v}_k \sim \mathcal{CN}(0, \sigma_v^2 \mathbf{I}_{N_{rx}})$. The received signal frame contains two parts:

- Training Sequence of N_{TS} pilot symbol vectors. The training received signal follows a non-zero mean Gaussian distribution:
  $\mathbf{y}_k^{TS}/\mathbf{H} \sim \mathcal{CN}(\mathbf{H}\mathbf{x}_k^{TS}, \sigma_v^2 \mathbf{I}_{N_{rx}})$.

- Blind part of N_B data symbol vectors. These follow a zero mean Gaussian distribution: $\mathbf{y}_k/\mathbf{H} \sim \mathcal{CN}(0, \sigma_v^2 \mathbf{I}_{N_{rx}} + \sigma_x^2 \mathbf{H}\mathbf{H}^H)$.

In the following, we assume the noise power σ_v^2 to be known by the receiver. We analyze the ML estimator, the Fischer information matrix and the asymptotic behavior of CRB for large blind part length. We then propose the GSB and DSB approaches.

7.2.1 Maximum Likelihood Channel Estimator

The ML channel estimator maximizes the log likelihood probability (LL) of the total received signal

$$\widehat{\mathbf{H}}_{ML} \triangleq \arg\max_{\mathbf{H}} LL(\mathbf{H}), \tag{7.2}$$

with

$$\begin{aligned}
LL(\mathbf{H}) &\triangleq \ln p(\mathbf{Y}/\mathbf{H}) \\
&= cnst. \\
&- \sigma_v^{2^{-1}} \sum_{k=1}^{N_{TS}} (\mathbf{y}_k^{TS} - \mathbf{H}\mathbf{x}_k^{TS})^H (\mathbf{y}_k^{TS} - \mathbf{H}\mathbf{x}_k^{TS}) \\
&- \sum_{k=1}^{N_B} \mathbf{y}_k^H (\sigma_v^2 \mathbf{I}_{N_{rx}} + \sigma_x^2 \mathbf{H}\mathbf{H}^H)^{-1} \mathbf{y}_k \\
&- N_B \ln\det(\sigma_v^2 \mathbf{I}_{N_{rx}} + \sigma_x^2 \mathbf{H}\mathbf{H}^H) \\
&= cnst. \\
&+ \underbrace{-\sigma_v^{2^{-1}} \mathrm{tr}\{(\mathbf{Y}^{TS} - \mathbf{H}\mathbf{X}^{TS})^H (\mathbf{Y}^{TS} - \mathbf{H}\mathbf{X}^{TS})\}}_{LL_{TS}(\mathbf{H})} \\
&+ \underbrace{-N_B \mathrm{tr}\{\mathbf{R}^{-1}(\mathbf{H})\hat{\mathbf{R}}\} - N_B \ln\det \mathbf{R}(\mathbf{H})}_{LL_B(\mathbf{H})},
\end{aligned} \tag{7.3}$$

where $\mathbf{Y}^{TS} = \left[\mathbf{y}_1^{TS} \ \ldots \mathbf{y}_{N_{TS}}^{TS}\right]$, $\hat{\mathbf{R}} = \frac{1}{N_B} \sum_{k=1}^{N_B} \mathbf{y}_k \mathbf{y}_k^H$ and $\mathbf{R}(\mathbf{H}) = \sigma_v^2 \mathbf{I}_{N_{rx}} + \sigma_x^2 \mathbf{H}\mathbf{H}^H$. The $LL_{TS}(\mathbf{H})$ and $LL_B(\mathbf{H})$ terms are the log likelihood of the blind and the training parts, respectively. *cnst.* denotes constant scalar.

7.2.2 Information Matrix Issues

Let the singular value decomposition (SVD) of the channel be:

$$\mathbf{H} = \mathbf{UDQ} = \mathbf{WQ} \tag{7.4}$$

where $\mathbf{U}$(resp. $\mathbf{Q}$) is a $N_{rx} \times \min\{N_{rx}, N_{tx}\}$ (resp. $\min\{N_{rx}, N_{tx}\} \times N_{tx}$) unitary matrix, i.e $\mathbf{U}^H\mathbf{U} = \mathbf{I}$ (resp. $\mathbf{QQ}^H = \mathbf{I}$). Let $\mathbf{W} = \mathbf{W}(\alpha)$ and $\mathbf{Q} = \mathbf{Q}(\beta)$ be two bijective real parameterizations: $\mathbf{H} = \mathbf{H}(\alpha, \beta)$. The blind part contains no information on $\mathbf{Q}$. The Fischer information matrix is then

$$\begin{aligned} J(\mathbf{H}) &= -\mathrm{E}_{\mathbf{Y}} \frac{\partial}{\partial \mathbf{h}} \left(\frac{\partial \ln p(\mathbf{Y}/\mathbf{H})}{\partial \mathbf{h}} \right)^T \\ &= J_B(\mathbf{H}) + J_{TS}(\mathbf{H}) \\ &= M_1 \, J_B(\alpha) \, M_1^T + J_{TS}(\mathbf{H}) \,, \end{aligned} \tag{7.5}$$

where

$$M_1 = \frac{\partial \, \alpha^T}{\partial \, \mathbf{h}} = \frac{\partial \, \mathbf{w}^T}{\partial \, \mathbf{h}} \frac{\partial \, \alpha^T}{\partial \, \mathbf{w}} = (\mathsf{M}(\mathbf{Q}^H) \otimes \mathbf{I}_{N_{rx}}) \frac{\partial \, \alpha}{\partial \, \mathbf{w}} \,, \tag{7.6}$$

$$\mathbf{h} = [\Re(\mathrm{vec}(\mathbf{H}))^T \; \Im(\mathrm{vec}(\mathbf{H}))^T]^T \,, \tag{7.7}$$

$$\mathbf{w} = [\Re(\mathrm{vec}(\mathbf{W}))^T \; \Im(\mathrm{vec}(\mathbf{W}))^T]^T \,, \tag{7.8}$$

and

$$\mathsf{M}(\mathbf{M}) = \begin{bmatrix} \Re(\mathbf{M}) & -\Im(\mathbf{M}) \\ \Im(\mathbf{M}) & \Re(\mathbf{M}) \end{bmatrix} \,, \tag{7.9}$$

for any matrix $\mathbf{M}$.
$\mathrm{E}_{\mathbf{Y}}(f)$ denotes the expectation of f w.r.t. $\mathbf{Y}$. $J_B(\mathbf{H})$ and $J_{TS}(\mathbf{H})$ are the Fischer information matrices of the blind and the training parts. $J_{TS}(\mathbf{H})$ can be evaluated easily as

$$J_{TS}(\mathbf{H}) = \frac{2}{\sigma_v^2} \mathsf{M}\left(\mathbf{X}^{TS} \mathbf{X}^{TS\,H} \right) \otimes \mathbf{I}_{N_{rx}} \,. \tag{7.10}$$

The MSE error of any unbiased channel estimate satisfies

$$\mathrm{E}||\tilde{\mathbf{H}}||^2 \geq \mathrm{E}_{\mathbf{H}} \, CRB = \mathrm{tr}\, \mathrm{E}_{\mathbf{H}} J^{-1}(\mathbf{H}) \,, \tag{7.11}$$

where $CRB = \mathrm{tr}\,(J^{-1}(\mathbf{H}))$ is the Cramér-Rao Bound on the estimate of the channel for a given channel realization. We use $\mathrm{E}_{\mathbf{H}}$ to average over a possible statistical distribution of the channel.

For the design of the TS, the following theorem gives a useful result:

Theorem 1 : For statistical channel $\mathbf{H} = \mathbf{WQ}$ with $\mathbf{Q}$ uniformly distributed over the Grassmann manifold, the minimum of $\mathrm{E}_{\mathbf{H}}\, CRB$ is achieved by a white training sequence: $\mathbf{X}^{TS}\,\mathbf{X}^{TS^H} \propto \mathbf{I}$.
Proof : see appendix 7.A.

Asymptotic Behavior If $\left(\mathbf{X}^{TS}\mathbf{X}^{TS^H}\right)^{-1}$ exists (persistently exciting training sequence), and $N_B >> \rho\, N_{TS}$, then the Cramér-Rao Bound satisfies

$$\mathrm{E}_{\mathbf{H}}\, CRB = \mathrm{tr}\ \mathrm{E}_{\mathbf{H}}\ \left\{ J_{TS}^{-1}(\mathbf{H})\ \mathbf{P}^{\perp}_{J_{TS}^{-\frac{1}{2}}(H)M_1} \right\} + O(\frac{1}{N_B})\,, \tag{7.12}$$

where $O(\frac{1}{N_B})$ denotes a quantity of the order of $\frac{1}{N_B}$. The CRB is dominated by the part of the channel resulting from the projection on the orthogonal complement of $J_{TS}^{-\frac{1}{2}}(H)M_1$. This corresponds to the channel part that cannot be identified blindly, and hence gets identified only by the training.

Semi-Blind Method In view of the above results, we propose the following method:

1- Estimate $\mathbf{U}$ and $\mathbf{D}$ from the Blind Part:
$$\hat{\mathbf{U}}\hat{\mathbf{D}} = \hat{\mathbf{W}} = \arg\max_{\mathbf{W}}\ LL_B(\mathbf{W})$$

2- Estimate $\mathbf{Q}$ from the Training Sequence Part:
$$\hat{\mathbf{Q}} = \arg\max_{\mathbf{Q}}\ LL_{TS}(\mathbf{Q}/\mathbf{W} = \hat{\mathbf{W}})$$

3- Form $\widehat{\mathbf{H}} = \hat{\mathbf{W}}\ \hat{\mathbf{Q}}$.

This method is further described in the following section.

7.2.3 Gaussian Semi-Blind Approach

The approach just described above belongs to the Gaussian category because the blind information it exploits involves symbol's second-order statistics. It is also semi-blind since blind and training based parts get combined.

Blind Part Solution We write the eigenvector decompositions of the true and the estimated covariance matrices of the signal as

$$\begin{aligned} \mathbf{R} &= \mathbf{U}\,(\sigma_v^2\mathbf{I}_{\min\{N_{tx},N_{rx}\}} + \sigma_x^2 D^2)\mathbf{U}^H + \sigma_v^2\mathbf{U}^\perp\mathbf{U}^{\perp H} \\ \hat{\mathbf{R}} &= \mathbf{U}_e\mathbf{S}_e\mathbf{U}_e^H\,, \end{aligned} \tag{7.13}$$

where the subscript e denotes sample estimates, and $\mathbf{U}^\perp$ provides an orthonormal basis for the orthogonal complement of $\mathbf{U}$.
The blind LL part, up to a constant, is then

$$LL_B(\mathbf{H}) = -N_B \mathrm{tr}\{\mathbf{R}^{-1}\hat{\mathbf{R}}\} - N_B \ln\det(\sigma_v^2\mathbf{I} + \sigma_x^2 D^2)\,. \tag{7.14}$$

Theorem 2: The solution of the blind part is:

- $\hat{\mathbf{U}}$ corresponds to the $\min\{N_{tx}, N_{rx}\}$ dominant eigenvectors in $\mathbf{U}_e$
- $\hat{\mathbf{D}}$ matches the $\min\{N_{tx}, N_{rx}\}$ dominant eigenvalues of $\frac{1}{\sigma_x}\,(\lfloor \mathbf{S}_e - \sigma_v^2\mathbf{I}_{N_{rx}}\rfloor_+)^{1/2}$
- $\hat{\mathbf{W}} = \hat{\mathbf{U}}\hat{\mathbf{D}}$

where $\lfloor . \rfloor_+$ denotes the positive semi-definite part of its Hermitian argument.
Proof : see appendix 7.B.

Training Part Solution Given the $\hat{\mathbf{W}}$ estimate, the TS LL part (up to a constant) becomes

$$\begin{aligned} \sigma_v^2\, LL_{TS}(\mathbf{Q}/\mathbf{W}=\hat{\mathbf{W}}) &= -\mathrm{tr}\{(\mathbf{Y}^{TS} - \hat{\mathbf{W}}\mathbf{Q}\mathbf{X}^{TS})^H\,(\mathbf{Y}^{TS} - \hat{\mathbf{W}}\mathbf{Q}\mathbf{X}^{TS})\} \\ &= 2\Re\,\mathrm{tr}\{\mathbf{X}^{TS}\mathbf{Y}^{TS\,H}\hat{\mathbf{W}}\mathbf{Q}\} - \mathrm{tr}(\hat{\mathbf{W}}^H\hat{\mathbf{W}}\mathbf{Q}\mathbf{X}^{TS}\mathbf{X}^{TS\,H}\mathbf{Q}^H)\,. \end{aligned} \tag{7.15}$$

Due to the quadratic constraint ($\mathbf{Q}\mathbf{Q}^H = \mathbf{I}$), the solution is non trivial in general. However, for optimal training $\mathbf{X}^{TS}\,\mathbf{X}^{TS\,H} = \beta^{TS}\,\mathbf{I}$, $\beta^{TS} > 0$, $\hat{\mathbf{W}}^H\hat{\mathbf{W}}\mathbf{Q}\mathbf{X}^{TS}\mathbf{X}^{TS\,H}\mathbf{Q}^H = \beta^{TS}\hat{\mathbf{W}}^H\hat{\mathbf{W}}$, and the TS LL part is then (up to a constant)

$$LL_{TS}(\mathbf{Q}/\mathbf{W}=\hat{\mathbf{W}}) = 2\,\sigma_v^{-2}\,\Re\,\mathrm{tr}\{\mathbf{X}^{TS}\mathbf{Y}^{TS\,H}\hat{\mathbf{W}}\mathbf{Q}\}\,. \tag{7.16}$$

Theorem 3 : For white training sequence, $\mathbf{X}^{TS}\,\mathbf{X}^{TS\,H} \propto \mathbf{I}$, the solution for the training part is

$$\hat{\mathbf{Q}} = \mathbf{V}\,\mathbf{S}^H\,, \tag{7.17}$$

where $\mathbf{S}$ and $\mathbf{V}$ denote the unitary factors of the SVD of $\mathbf{X}^{TS}\mathbf{Y}^{TS\,H}\hat{\mathbf{W}} = \mathbf{S}\,\Sigma\,\mathbf{V}^H$.
Proof : The maximization of (7.16) corresponds to a subspace rotation problem that is solved in [90, 92].

7.2.4 Deterministic Semi-Blind Approach

In this subsection, we do not exploit the correlations of the inputs. We only exploit the subspace. The use of this approach is restricted to the case when a noise subspace of the spatial covariance matrix exists, *i.e.* $N_{rx} > N_{tx}$. The blind information expresses then the orthogonality of the channel to the noise subspace: $\mathbf{U}^{\perp,H}\mathbf{H} = 0$. Using a weighted least squares approach we combine the blind and training parts in a quadratic criterion

$$\min_{\mathbf{H}} \left(\sigma_v^{-2} ||\mathbf{Y}^{TS} - \mathbf{H}\mathbf{X}^{TS}||_F^2 \; + \; N_B ||\hat{\mathbf{U}}^{\perp\,H}\mathbf{H}^H||_F^2 \right) . \tag{7.18}$$

This can be seen as a special case of the approach detailed in subsection 7.3.2, for flat channel.

7.3 MIMO Frequency Selective Channel

We generalize our channel model given in section 1.1 to the case where the SIMO subchannels from the different sources (antennas) have different lengths. The (vector) impulse response from source n has length N_n, and the first non-zero vector impulse response sample occurs at discrete time zero. Without loss of generality, we consider that $L = N_1 \geq N_2 \geq \cdots \geq N_{N_{tx}}$. Let $N = \sum_{n=1}^{N_{tx}} N_n$. The Rx signal can then be represented as

$$\begin{aligned}
\mathbf{y}_k &= \sum_{l=0}^{L-1} \mathbf{H}_l\, \mathbf{x}_{k-l} + \mathbf{v}_k \\
\mathbf{y}_k &= \sum_{n=1}^{N_{tx}} \sum_{l=0}^{N_n-1} \mathbf{h}_n(l) x_n(k-l) + \mathbf{v}_k \\
&= \sum_{n=1}^{N_{tx}} \mathbf{H}^{n,N_n} A^{n,N_n}(k) + \mathbf{v}_k \\
&= \mathbf{H}^N \mathbf{X}^N(k) + \mathbf{v}_k \;,
\end{aligned} \tag{7.19}$$

$$\text{with } \mathbf{H}^{n,N_n} = [\mathbf{h}_n(0)\cdots\mathbf{h}_n(N_n{-}1)]\,, \mathbf{H}^N = \left[\mathbf{H}^{1,N_1}\cdots\mathbf{H}^{N_{tx},N_{N_{tx}}}\right], \text{ and}$$
$$X^{n,N_n}(k) = [x_n(k)\cdots x_n(k{-}N_n{+}1)]^T\,, \mathbf{X}^N(k) = \left[X^{1,N_1\,T}(k)\cdots X^{N_{tx},N_{N_{tx}}\,T}(k)\right]^T. \tag{7.20}$$

In the case of frequency selective channel the TS and Blind parts interfere, the training and blind LL parts are hence no longer separable. To continue to express the LL separately, we assume the use of a cyclic prefix and neglect the effect of the interference with the training signal when evaluating the blind LL. This is correct asymptotically in the length of the blind part N_B for $N_B >> \max(N_{TS}, L)$, and leads, up to a constant, to

$$\begin{aligned} LL_B(\mathbf{H}) &= -\sum_{k=0}^{N_B-1}[\mathbf{y}^H(f_k)(\sigma_v^2\mathbf{I}_{N_{rx}} + \sigma_x^2\,\mathbf{H}(f_k)\,\mathbf{H}^H(f_k))^{-1}\mathbf{y}(f_k) \\ &+ \ln\det(\sigma_v^2\mathbf{I}_{N_{rx}} + \sigma_x^2\,\mathbf{H}(f_k)\,\mathbf{H}^H(f_k))] \\ &= -\sum_{k=0}^{N_B-1}[\mathrm{tr}(\mathbf{R}^{-1}(f_k)\mathbf{y}(f_k)\mathbf{y}^H(f_k)) + \ln\det\mathbf{R}^{-1}(f_k)] \\ &= -\sum_{k=0}^{N_B-1}[\mathrm{tr}(\mathbf{R}^{-1}(f_k)\hat{\mathbf{R}}(f_k)) + \ln\det\mathbf{R}^{-1}(f_k)]\,, \end{aligned} \tag{7.21}$$

where $\mathbf{y}(f_k)$ and $\mathbf{H}(f_k)$ are the DFT of the sequence $\mathbf{y}_i$ and $\mathbf{H}_i$ at the normalized frequency $f_k = \frac{k}{N_B}$, and $\hat{\mathbf{R}}(f_k) = \mathbf{y}(f_k)\mathbf{y}^H(f_k)$ is a highly noisy estimate of $\mathbf{R}(f_k)$.
The maximization of $LL_B(\mathbf{H})$ leads to covariance matching. The problem is then how to do covariance matching of $\hat{\mathbf{R}}(f_k)$ with acceptable complexity. First, in order to take advantage of the a priori knowledge of the finite channel length (only $\mathbf{R}(k)$, $k = -L+1, -L+2, \ldots, L-2, L-1$ are nonzero, where $\mathbf{R}(k)$ sequence is the inverse DFT of $\mathbf{R}(f_k)$), covariance matching is done in the time domain: this should allow to reduce the complexity.
In order to be able to do the covariance matching, we have to use an appropriate parameterization of the channel to characterize the channel from the correlation sequence $\hat{\mathbf{R}}(k)$.
$\mathbf{P}_K(z) = \mathbf{I} + \sum_{i=1}^{K-1}\mathbf{P}_i z^{-i}$ is a predictor for the channel $\mathbf{H}(z)$ if $\mathbf{P}_K(z)\mathbf{H}(z) = \mathbf{H}_0$. For $N_{rx} \geq N_{tx}$ the channel predictor generically exists and is FIR for $N_{rx} > N_{tx}$. This constitutes an appropriate parameterization of the channel

$$\mathbf{H}(z) = \mathbf{P}^{-1}(z)\mathbf{U}\mathbf{D}\mathbf{Q} = \mathbf{P}^{-1}(z)\mathbf{W}\mathbf{Q}\,. \tag{7.22}$$

For $N_{rx} > N_{tx}$ and $K \geq \left\lceil \frac{L-N_{tx}}{N_{rx}-N_{tx}} \right\rceil$ the predictor can be evaluated from $\hat{\mathbf{R}}(k)$, $k = 0, \ldots, K-1$. This fixes the channel up to a unitary matrix $\mathbf{Q}$: $\hat{\mathbf{H}}(z) = \hat{\mathbf{P}}_K^{-1}(z)\hat{\mathbf{W}}\mathbf{Q}$ ($\mathbf{R}(z) - \sigma_v^2\,\mathbf{I} = \mathbf{P}_K^{-1}(z)\mathbf{W}\mathbf{W}^H\mathbf{P}_K^{-\dagger}(z)$).
However, unlike in the flat channel case, there is no trivial method to estimate $\mathbf{Q}$ by ML.
By reducing the exploitation of $\mathbf{P}(z)\,\mathbf{H}(z) = \mathbf{H}_0$ or
$\mathbf{P}(q)\,\mathbf{H}_k = \mathbf{H}_0\,\delta_{k0}$ to $\mathbf{W}^{\perp,H}\,\mathbf{H}_0 = 0$ and $\mathbf{P}(q)\,\mathbf{H}_k = 0$, $k > 0$, and combining it with the training part in a weighted least squares approach, then the result is a simple quadratic criterion.
In the following we will start by introducing some notions on MIMO linear prediction, in particular how to estimate the predictor from the blind received signal. We then present the GSB and DSB approaches and study there identifiability conditions. In the end of this section we present the Augmented TS approaches, that exploit the received signal containing the mixture of the TS and the blind part.

7.3.1 MIMO Linear Prediction

The use of linear prediction quantities has first been proposed in [86] for a SIMO context. However linear prediction is applicable equally well to both the SIMO and MIMO cases as long as $N_{rx} > N_{tx}$ [87]. Two favours can be obtained, depending on whether the transmitted symbols are modeled as deterministic unknowns or as uncorrelated random sequences (in the deterministic case, for the purpose of linear prediction, some considerations are more straightforward if the symbols are considered as stationary sequences with unknown correlation).
Consider the problem of predicting $\mathbf{y}_k$ from $\mathbf{Y}_{L_p}(k-1) = [\mathbf{y}_{k-1}^T \cdots \mathbf{y}_{k-L_p}^T]^T$, for noiseless received signal (L_p is the prediction depth). The prediction error can be written as

$$\widetilde{\mathbf{y}}_k|_{\mathbf{Y}_{L_p}(k-1)} = \mathbf{y}_k - \widehat{\mathbf{y}}_k|_{\mathbf{Y}_{L_p}(k-1)} = \mathbf{P}_{L_p}\mathbf{Y}_{L_p+1}(k)\,, \tag{7.23}$$

with $\mathbf{P}_{L_p} = [\boldsymbol{P}_{L_p,0}\ \boldsymbol{P}_{L_p,1} \cdots \boldsymbol{P}_{L_p,L_p}]$, $\boldsymbol{P}_{L_p,0} = I_{N_{rx}}$. Minimizing the prediction error variance leads to the following optimisation problem

$$\min_{\mathbf{P}_{L_p}} \mathbf{P}_{L_p} R_{YY} \mathbf{P}_{L_p}^H \;=\; \sigma^2_{\widetilde{\mathbf{y}},L_p}\,. \tag{7.24}$$

Hence

$$\mathbf{P}_{L_p} R_{YY} \;=\; \left[\sigma^2_{\widetilde{\mathbf{y}},L_p} \;\; 0\cdots 0\right] . \tag{7.25}$$

Let $\underline{L} \;=\; \left\lceil \frac{N-N_{tx}}{N_{rx}-N_{tx}} \right\rceil$.
$\underline{L}+1$ corresponds to the minimum size for R_{YY} to be full column rank. This is the generalization of the condition in [93] for SIMO case, we don't provide a demonstration but simulations confirm this choice for random frequency selective channels with Gaussian i.i.d. components.
The rank profile of $\sigma^2_{\widetilde{y},L_p}$ behaves as a function of L_p generically (for an irreducible and column reduced MIMO channel) like

$$\text{rank}\left(\sigma^2_{\widetilde{\mathbf{y}},L_p}\right) \begin{cases} = N_{tx} & , L_p \geq \underline{L} \\ = N_{rx} - \underline{m} \in \{N_{tx}+1, .., N_{rx}\} & , L_p = \underline{L}-1 \\ = N_{rx} & , L_p < \underline{L}-1 \, , \end{cases} \tag{7.26}$$

where $\underline{m} = \underline{L}(N_{rx} - N_{tx}) - N + N_{tx} \in \{0, 1, \ldots, N_{rx}-1-N_{tx}\}$ represents the degree of singularity of $R_{YY,\underline{L}}$.
For $L_p \geq \underline{L}$, $\widetilde{\mathbf{y}}_k|\mathbf{Y}_{L_p(k-1)} = \mathbf{H}_0\mathbf{x}_k$ and $\sigma^2_{\widetilde{\mathbf{y}},L_p} = \sigma^2_x \mathbf{H}_0\mathbf{H}_0^H = \sigma^2_x \mathbf{W}\mathbf{W}^H$. For such L_p, let $\mathbf{U}_i$ be the eigenvectors of $\sigma^2_{\widetilde{\mathbf{y}},L_p}$ in order of decreasing eigenvalue. Then $\mathbf{U}_{1:N_{tx}} = [\mathbf{U}_1 \cdots \mathbf{U}_{N_{tx}}]$ has the same column space as $\mathbf{H}_0$ and $\overline{\mathbf{P}}(z) = \mathbf{U}^H_{N_{tx}+1:N_{rx}} \mathbf{P}(z)$ satisfies $\overline{\mathbf{P}}(z)\mathbf{H}(z) = 0$ ($\overline{\mathbf{P}}(z)$ represents a parameterization of the noise subspace). Note that $\mathbf{P}(z)$ changes if the symbols are correlated (hence $\mathbf{P}(z)$ contains information about the symbol correlation) whereas $\overline{\mathbf{P}}(z)$ is insensitive to such correlation. To obtain the noise-free prediction quantities, we need to denoise an estimated covariance matrix via $\widehat{R}^d_{YY} = \widehat{R}_{YY} - \widehat{\sigma^2_v}\, I$ (partial denoising) or
$\widehat{R}^d_{YY} = \lfloor \widehat{R}_{YY} - \widehat{\sigma^2_v}\, I \rfloor_+$ (full denoising). In the case of partial denoising, we used a generalized version (to covariance windowing) of the MIMO Levinson algorithm, which applies in the nonsingular indefinite case. Singular components appear then as negative semi-definite. In the case of full denoising, we determine the prediction quantities directly from the normal equations, with a generalized inverse $R^{\#} = VD^{\#}V^H$ where $R = VDV^H$ is the eigenvector decomposition of R and $D^{\#}$ is the Moore-Penrose inverse of the singular diagonal matrix D. As in [94], the columns in V corresponding to zeros in D are taken to be all zero, except for a unit diagonal element. In both approaches, the overestimation of L_p leads to consistent estimate in SNR of $\overline{\mathbf{P}}(z)$, whereas for $\mathbf{P}(z)$ we only have consistency in amount M_B of (blind) data samples $\mathbf{y}(k)$. The noiseless uncorrelated symbols case with finite amount of data is

similar to a colored symbols case. Note that the partial and full denoising approaches correspond to resp. the first and second subspace estimates in [95]. Let $\mathbf{h}_i = [\mathbf{h}_i^T(0) \cdots \mathbf{h}_i^T(N_i{-}1)]^T = \mathbf{H}^{i,N_i\,tT}$ where ^{t} denotes transposition of the block entries, and $\mathbf{h} = \mathbf{H}_N^{tT}$. Then a stretch of Rx signal $\mathbf{Y}$ can be written as

$$\mathbf{Y}_M = \mathcal{T}_M(\mathbf{h})\,\mathbf{X} + \mathbf{V}_M = \mathcal{X}\,\mathbf{h} + \mathbf{V}_M\,, \tag{7.27}$$

where $\mathcal{T}_M(\mathbf{h}) = [\mathcal{T}_M(\mathbf{H}^{1,N_1}) \cdots \mathcal{T}_M(\mathbf{H}^{N_{tx},N_{N_{tx}}})]$ and $\mathcal{T}_M(\mathbf{H})$ denotes a block toeplitz convolution matrix with M block rows and $[\mathbf{H}\;0 \cdots 0]$ as first block row. $\mathcal{X}$ is a structured matrix containing the multi-source symbols. Let N_{TS} denote the number of training sequence (TS) symbols per source, considered equal for all sources for most of what follows.

7.3.2 Deterministic Semi-Blind Approach

In the semi-blind approaches, we shall seek a channel estimate $\widehat{\mathbf{h}}$ with possibly overestimated channel lengths $\widehat{N}_i \geq N_i$ and we shall assume that $\widehat{N}_1$ remains the largest $\widehat{N}_i$. In the deterministic symbols setting, we shall work with $\overline{\mathbf{P}}$. $\overline{\mathbf{P}}(z)\,\widehat{\mathbf{h}}_i(z) = 0$ can be written in the time domain as $\mathcal{T}^T_{\widehat{N}_i}(\overline{\mathbf{P}}^t)\,\widehat{\mathbf{h}}_i = 0$. Let $\overline{\mathcal{B}} = \bigoplus_{i=1}^{N_{tx}} \mathcal{T}^T_{\widehat{N}_i}(\overline{\mathbf{P}}^t)$. We can now formulate a semi-blind criterion as

$$\min_{\widehat{\mathbf{h}}} \left\{ \left\| \mathbf{Y}_{TS} - \mathcal{X}_{TS}\,\widehat{\mathbf{h}} \right\|^2 \;+\; \alpha \left\| \overline{\mathcal{B}}\,\widehat{\mathbf{h}} \right\|^2 \right\}, \tag{7.28}$$

where α is a weighting factor, and $\mathbf{Y}_{TS}$: $(N_{TS} - \widehat{N}_1 + 1) \times 1$ is the portion of Rx signal containing only training symbols. A more optimal approach introduces weighting involving the covariance matrix $\overline{C}$ of $\overline{\mathcal{B}}\,\mathbf{h}$ due to the estimation errors in $\overline{\mathbf{P}}$ and leads to

$$\min_{\widehat{\mathbf{h}}} \left\{ \left\| \mathbf{Y}_{TS} - \mathcal{X}_{TS}\,\widehat{\mathbf{h}} \right\|^2 \;+\; \sigma_v^2\,\widehat{\mathbf{h}}^H \overline{\mathcal{B}}^H\,\overline{C}^{\#}\,\overline{\mathcal{B}}\,\widehat{\mathbf{h}} \right\}, \tag{7.29}$$

where a possible pseudo-inverse can be avoided by using an infinitisemal amount of regularization. Inspired by an approximate expression for $\overline{C}$ given in [87], we have taken $\sigma_v^2\,\overline{C}^{\#} = M_B\,I$ so that (7.29) reduces to (7.28) with $\alpha = M_B$.

With overestimated channel lengths, deterministic blind identification leads to an estimate $\widehat{\widehat{\mathbf{H}}}(z) = \mathbf{H}(z)\,\mathbf{S}(z)$ where $\mathbf{S}(z)$: $N_{tx} \times N_{tx}$ is also causal

and polynomial, and the length(number of unknown coefficients of the polynome) of $\mathbf{S}_{in}(z)$ can be shown to be $(\widehat{N}_i - N_n + 1)^+$ where $(x)^+ = \max\{x, 0\}$. Note that this is a generalization of a result in [88] where $\widehat{N}_i = N_i$.

Identifiability conditions :
The channel is identifiable by the DSB approach iff (7.29) has a unique solution, or equivalently iff the Hessian $\mathbf{J} = \mathcal{X}_{TS}^H \mathcal{X}_{TS} + \sigma_v^2 \overline{\mathcal{B}}^H \overline{C}^{\#} \overline{\mathcal{B}}$ is invertible. The fact that the deterministic blind part identifies the channel up to the $\mathbf{S}(z)$ factor is equivalent to that the null space of $\overline{\mathcal{B}}^H \overline{C}^{\#} \overline{\mathcal{B}}$ is generated by
$\mathcal{E} = [\mathcal{Z}_{(\widehat{N}_1 - N_1 + 1)^+}(\mathbf{h}_1^1) \mathcal{Z}_{(\widehat{N}_2 - N_1 + 1)^+}(\mathbf{h}_1^2) \dots \mathcal{Z}_{(\widehat{N}_{N_{tx}} - N_1 + 1)^+}(\mathbf{h}_1^{N_{tx}}) \mathcal{Z}_{(\widehat{N}_1 - N_2 + 1)^+}(\mathbf{h}_2^1)$
$\mathcal{Z}_{(\widehat{N}_2 - N_2 + 1)^+}(\mathbf{h}_2^2) \dots \mathcal{Z}_{(\widehat{N}_{N_{tx}} - N_{N_{tx}} + 1)^+}(\mathbf{h}_{N_{tx}}^{N_{tx}})]$,
where $\mathcal{Z}_M(\mathbf{g})$ is a block toeplitz convolution matrix with M columns and $\mathbf{g}$ as first column, and
$\mathbf{h}_i^k = [0_{(N_{rx} \sum_{n=1}^{k-1} \widehat{N}_n) \times 1} \mathbf{h}_i^T 0_{N_{rx}(\widehat{N}_k - N_i) \times 1} 0_{(N_{rx} \sum_{n=k+1}^{N_{tx}} \widehat{N}_n) \times 1}]^T$.
$\mathbf{J}$ is the sum of two positive hermitian matrices $\mathcal{X}_{TS}^H \mathcal{X}_{TS}$ and $\sigma_v^2 \overline{\mathcal{B}}^H \overline{C}^{\#} \overline{\mathcal{B}}$. Then $\mathbf{J}$ is invertible iff $\mathcal{X}_{TS}^H \mathcal{X}_{TS}$ restricted on the null space of $\overline{\mathcal{B}}^H \overline{C}^{\#} \overline{\mathcal{B}}$ is invertible. This last condition is equivalent to saying that $\mathcal{E}^H \mathcal{X}_{TS}^H \mathcal{X}_{TS} \mathcal{E}$ is invertible or equivently $\mathcal{X}_{TS} \mathcal{E}$ is full column rank. We can show that $\mathcal{X}_{TS} \mathcal{E} = [\mathcal{F}_1 \dots \mathcal{F}_{N_{tx}}]$ and $\mathcal{F}_i = \mathcal{T}_{N_{TS} - \widehat{N}_1 + 1}(\mathbf{H}^{i,N_i}) \mathcal{X}_i$, where we assume that $\widehat{N}_1 = \max_i \widehat{N}_i$ and $\mathcal{X}_i$ is a $(N_{TS} - \widehat{N}_1 + N_i) \times (\sum_{n=1}^{N_{tx}} (\widehat{N}_n - N_i + 1)^+)$ structured matrix containing the multi-source symbols.
For $\mathcal{X}_{TS} \mathcal{E}$ to be full column rank, each $\mathcal{F}_i$ has to be full column rank. Then a necessary condition is $(\sum_{n=1}^{N_{tx}} (\widehat{N}_n - N_i + 1)^+) \leq \text{rank}(\mathcal{T}_{N_{TS} - \widehat{N}_1 + 1}(\mathbf{H}^{i,N_i}))$. In general w.p. 1 [93]
$\text{rank}(\mathcal{T}_{N_{TS} - \widehat{N}_1 + 1}(\mathbf{H}^{i,N_i})) = \min\Big(N_{rx}(N_{TS} - \widehat{N}_1 + 1), (N_{TS} + N_i - \widehat{N}_1)\Big)$. The second condition is on all matrix dimensions *i.e.*
$(\sum_{i,n}^{N_{tx}} (\widehat{N}_n - N_i + 1)^+) \leq N_{rx}(N_{TS} - \widehat{N}_1 + 1)$.
These conditions are necessary but to be sufficient the training has to be chosen so that $\mathcal{X}_i,\ i = 1, \dots, N_{rx}$ are full column rank. On the other hand, the generalization of the result in the [93] to the MIMO case allows us to state that $\text{rank}(\mathcal{T}_{N_{TS} - \widehat{N}_1 + 1}(\mathbf{h}))$ is the minimum number of columns and rows

w.p. 1. Combining these results with a correct choice of TS ensures that the conditions are necessary and sufficient. As a result, the DSB approach has the following identifiability requirements

$$\begin{aligned} &1)\ \forall i\ \sum_{n=1}^{N_{tx}} (\widehat{N}_n - N_i + 1)^+ \leq \min\{N_{rx}(N_{TS} - \widehat{N}_1 + 1), N_{TS} + N_i - \widehat{N}_1\} \\ &2)\ \sum_{i,n=1}^{N_{tx}} (\widehat{N}_n - N_i + 1)^+ \leq N_{rx}(N_{TS} - \widehat{N}_1 + 1)\,. \end{aligned} \tag{7.30}$$

7.3.3 Gaussian Semi-Blind Approach

In the Gaussian case, the blind estimation ambiguity gets reduced to an instantaneous unitary mixture of the sources (which gets even limited to mixtures of subsets of sources with identical channel length N_i). However, there is no trivial method to exploit the unitary caracteristic of the mixture. This leads us to reduce the exploitation of $\mathbf{P}(z)\,\mathbf{H}(z) = \mathbf{H}_0$ or $\mathbf{P}(q)\,\mathbf{H}_k = \mathbf{H}_0\,\delta_{k0}$ to $\overline{\mathbf{P}}_0\mathbf{H}_0 = 0$ ($\Leftrightarrow \mathbf{W}^{\perp,H}\,\mathbf{H}_0 = 0$) and $\mathbf{P}(q)\,\mathbf{H}_k = 0$, $k > 0$. We shall call this the *reduced Gaussian case*, in which all the decorrelation is exploited except between symbols at the same time instant. This can be expressed by $\mathcal{B}\,\mathbf{h} = 0$ where $\mathcal{B} = \bigoplus_{i=1}^{N_{tx}} \begin{bmatrix} \overline{\mathbf{P}}_0\ 0 \\ \overline{\mathcal{T}^T_{\widehat{N}_i}(\mathbf{P}^t)} \end{bmatrix}$ where $\overline{\mathcal{T}^T_{\widehat{N}_i}(\mathbf{P}^t)}$ is $\mathcal{T}^T_{\widehat{N}_i}(\mathbf{P}^t)$ with the first block row removed. The problem of recovering $\mathbf{h}$ from $\overline{\mathcal{T}^T_{\widehat{N}_i}(\mathbf{P}^t)}\,\mathbf{h}_i = 0$ in the SIMO case, with an optimal weighting between the nuller $\overline{\mathbf{P}}(z)$ and the equalizer portions of $\mathbf{P}(z)$, has been addressed in [87]. It involves the covariance matrix of $\overline{\mathcal{T}^T_{\widehat{N}_i}(\mathbf{P}^t)}\,\mathbf{h}_i$ and a simple approximation is also given. This allows us to introduce a semi-blind criterion of the form

$$\min_{\mathbf{h}} \left\{ \|\mathbf{Y}_{TS} - \mathcal{X}_{TS}\,\mathbf{h}\|^2 \ +\ \sigma_v^2\,\mathbf{h}^H\,\mathcal{B}^H\,C^{\#}\,\mathcal{B}\,\mathbf{h} \right\}\ . \tag{7.31}$$

We define $C = M_B^{-1} \bigoplus_{i=1}^{N_{tx}} (I_{N_{rx}} \oplus ((I_{N_{rx}} + \sigma_v^{-2}\sigma^2_{\tilde{\mathbf{y}}}) \otimes I_{N_i - 1}))$, as done is [87].

Let $\mathbf{H}_0$ be the unique solution [87] of

$$\mathbf{P}(z)\,\mathbf{H}(z) = \mathbf{H}_0\,. \tag{7.32}$$

In the reduced Gaussian case, only the signal subspace of $\mathbf{H}_0$ *i.e.* $\mathbf{U}$ is known. The equation in (7.32) is then reduced to $\overline{\mathbf{P}}_0\mathbf{H}_0 = 0$ and $\mathbf{P}(q)\,\mathbf{H}_k = 0,\ k >$. These new conditions fix the channel estimate up to a constant $N_{tx} \times N_{tx}$ matrix: $\widehat{\widehat{\mathbf{H}}}(z) = \mathbf{H}(z)\,\mathbf{S}$. On the other hand, the channel length constraints impose that only elements of $\mathbf{S}_{in}$ with $\widehat{N}_i - N_n \geq 0$ can be non-zero. The reduced Gaussian blind identification leads hence to an estimate $\widehat{\widehat{\mathbf{H}}}(z) = \mathbf{H}(z)\,\mathbf{S}$ where $N_{tx} \times N_{tx}$ $\mathbf{S}$ is a constant matrix with $\mathbf{S}_{in} = 0$ for $\Gamma(\widehat{N}_i - N_n) = 0$. Γ is the step function:

$$\Gamma(k) = \begin{cases} 0 & , k < 0 \\ 1 & , k \geq 0\,. \end{cases} \tag{7.33}$$

Identifiability conditions :
Similary to the DSB approach, the channel is identifiable by the GSB approach iff (7.31) has a unique solution, or equivalently iff the Hessian $\mathbf{J} = \mathcal{X}_{TS}^H\mathcal{X}_{TS} + \sigma_v^2\,\mathcal{B}^H\,C^{\#}\,\mathcal{B}$ is invertible. The fact that the reduced Gaussian blind part identifies the channel up to the $\mathbf{S}$ factor is equivalent to that the null space of $\mathcal{B}^H\,C^{\#}\,\mathcal{B}$ is generated by $\mathcal{E}$ which is a $\left(\left(\sum_{i=1}^{N_{tx}} \widehat{N}_i\right) \times \left(\sum_{i,n} \Gamma(\widehat{N}_i - N_n)\right)\right.$ matrix with columns $\mathbf{h}_i^k = [0_{(N_{rx}\sum_{n=1}^{k-1}\widehat{N}_n)\times 1}\mathbf{h}_i^T 0_{N_{rx}(\widehat{N}_k - N_i)\times 1} 0_{(N_{rx}\sum_{n=k+1}^{N_{tx}}\widehat{N}_n)\times 1}]^T$ for $1 \leq k, i \leq N_{tx}$ and $\Gamma(\widehat{N}_k - N_i) = 1$. For the reasons cited in subsection 7.3.2, $\mathbf{J}$ is invertible iff $\mathcal{X}_{TS}\mathcal{E} = [\mathcal{F}_1 \ldots \mathcal{F}_{N_{tx}}]$ is full column rank, where $\mathcal{F}_i = \mathcal{T}_{N_{TS}-\widehat{N}_1+1}(\mathbf{H}^{i,N_i})\mathcal{X}_i$, and $\mathcal{X}_i$ is a $(N_{TS} - \widehat{N}_1 + N_i) \times (\sum_{n=1}^{N_{tx}} \Gamma(\widehat{N}_n - N_i))$ structured matrix containing the multi-source symbols.

Similary to subsection 7.3.2, we can show that the restricted GSB semi-blind approach has the following identifiability requirements

$$\begin{aligned} &1)\ \forall i \ \sum_{n=1}^{N_{tx}} \Gamma(\widehat{N}_n - N_i) \leq \min\{N_{rx}(N_{TS} - \widehat{N}_1 + 1), N_{TS} + N_i - \widehat{N}_1\} \\ &2)\ \sum_{i,n=1}^{N_{tx}} \Gamma(\widehat{N}_n - N_i) \leq N_{rx}(N_{TS} - \widehat{N}_1 + 1)\,. \end{aligned} \tag{7.34}$$

For both semi-blind methods, if the amount of blind data becomes very large, then the particular structure of the weighting matrix for the blind part be-

comes unimportant. Moreover, the soft-constrained criterion approaches the hard constrained criterion, in which the TS criterion $\|Y_{TS} - \mathcal{X}_{TS}\,\mathbf{h}\|^2$ gets minimized subject to the blind constraints $\overline{\mathcal{B}}\,\widehat{\mathbf{h}} = 0$ or $\mathcal{B}\,\widehat{\mathbf{h}} = 0$.

In practice, σ_v^2 should be overestimated to obtain a good denoising. If σ_v^2 gets that much overestimated that its subtraction cuts away a portion of the signal subspace, then this would lead to a loss of the blindly identifiable (in a deterministic setting) part of $\mathbf{H}(z)$. However, in a semi-blind approach, identifiability is recovered if a blindly identifiable portion got ignored in this way, which means that it would have resulted in a bad blind estimation quality. So even if the denoising is done in an overflow fashion and if the order of $\mathbf{P}(z)/\overline{\mathbf{P}}(z)$ gets reduced w.r.t. its theoretical order, the resulting $\overline{\mathbf{P}}(z)$ still lies in the noise subspace and satisfies $\overline{\mathbf{P}}(z)\,\mathbf{H}(z) = 0/\mathbf{P}(z)\,\mathbf{H}(z) \approx \mathbf{h}(0)$ (though in that case this would not allow identification of the blindly identifiable part of $\mathbf{H}(z)$). So in this way, the badly blindly identifiable parameters also get estimated through the TS.

7.3.4 Augmented Training-Sequence Part

So far, we have considered the classical TS approach, where Y_{TS} denotes the Rx samples in which only TS symbols appear. This is a suboptimal method as it ignores the TS signal that interfers with the unknown symbols. A more efficient method is the augmented TS approach. In this method Y_{TS} collects all Rx samples in which at least one TS symbol appears. In that case, we can write $\mathbf{Y}_{TS} - \mathbf{V} = \mathcal{T}(\mathbf{h})\mathbf{X} = \mathcal{T}_K\mathbf{X}_K + \mathcal{T}_U\mathbf{X}_U$ in which $\mathbf{X}_{K/U}$ collects the known/unknown symbols and $\mathcal{T}_{K/U}$ the corresponding columns of $\mathcal{T}$. The TS part of the semi-blind criterion becomes

$$(\mathbf{Y}_{TS} - \mathcal{X}_K\,\mathbf{h})^H (I + \frac{\sigma_x^2}{\sigma_v^2}\mathcal{T}_U\mathcal{T}_U^H)^{-1}(\mathbf{Y}_{TS} - \mathcal{X}_K\,\mathbf{h})\,, \tag{7.35}$$

where $\mathcal{X}_K\,\mathbf{h} = \mathcal{T}_K\mathbf{X}_K$.
Due to the parameter-dependent weighting, the semi-blind criteria now require at least one iteration.
As has been done previously for DSB and GSB approaches, the channel is identifiable if $\mathcal{X}_K\mathcal{E}$ is full column rank. For each approach (DSBA and GSBA) $\mathcal{E}$ is the same as the non augmented case. However $\mathcal{X}_K\mathcal{E} = [\mathcal{F}_1 \ldots \mathcal{F}_{N_{tx}}]$ is now composed of $\mathcal{F}_i = \mathcal{Z}_{N_{TS}+\widehat{N}_1-N_i}(\mathbf{h}_i)\mathcal{X}_i$, where $\mathcal{Z}_{N_{TS}+\widehat{N}_1-N_i}(\mathbf{h}_i)$ is a block

toeplitz convolution matrix with $N_{TS}+\widehat{N}_1-N_i$ columns and $[\mathbf{h}_i^T 0_{N_{rx}(\widehat{N}_1-N_i)\times 1}]$ as first column. The rank of $\mathcal{Z}_{N_{TS}+\widehat{N}_1-N_i}(\mathbf{h}_i)$ is $N_{TS}+\widehat{N}_1-N_i$ w.p. 1. The condition on the rank of $\mathcal{F}_i$ is then
$(\sum_{n=1}^{N_{tx}}(\widehat{N}_n-N_i+1)^+) \leq N_{TS}+\widehat{N}_1-N_i$ for the DSBA (and
$\sum_{n=1}^{N_{tx}}\Gamma(\widehat{N}_n-N_i) \leq N_{TS}+\widehat{N}_1-N_i$ for GSBA). Under the conditions on the rank $\mathcal{F}_i,\ i=1,\ldots,N_{tx}$, the condition on the number of antennas $N_{rx}>N_{tx}$ ensures that the condition on the all matrix $(\mathcal{X}_K\mathcal{E})$ dimension is fulfilled. The Identifiability conditions for the augmented approaches are then

$$\sum_{n=1}^{N_{tx}}(\widehat{N}_n-N_i+1)^+ \leq N_{TS}+\widehat{N}_1-N_i,\ \forall i \tag{7.36}$$

for DSBA, and

$$\sum_{n=1}^{N_{tx}}\Gamma(\widehat{N}_n-N_i) \leq N_{TS}+\widehat{N}_1-N_i,\ \forall i \tag{7.37}$$

for GSBA.

The augmented approach also allows us to handle the user-wise grouped TS approach (Y_{TS} contains TS symbols from only one user at a time) and the distributed TS approach (Y_{TS} contains only one TS symbol from any user at a time).

7.4 Performance Analysis

In this section we present some numerical examples for the two channel cases, flat and frequency selective.

7.4.1 Flat channel case

Figs. 7.1 to 7.6 consider the flat channel case with a blind part of length $N_B=400$. The channel is 4×2 ($N_{rx}\times N_{tx}$) for figs. 7.1 and 7.2, 4×4 for figs. 7.3 and 7.4, and 2×4 for figs. 7.5 and 7.6. We compare the classical TS approach with the GSB/DSB approaches, and with the Cramér-Rao

Bound (CRB) in terms of normalized mean square estimation error (NMSE). In figs. 7.1, 7.3 and 7.5 the performances are given for different TS lengths with a fixed SNR $\rho = 10\,dB$. For figs. 7.2, 7.4 and 7.6 the performances are given for different SNR with $N_{TS} = 4$. The results show that whenever the condition $N_B >> \rho\, N_{TS}$ is fulfilled, the proposed GSB approach achieves the CRB. The GSB performances show a linear behavior w.r.t. the SNR, and outperform the TS approach by a gap corresponding approximately to the relative reduction of the number of real parameters to be estimated; for $4 \times 2 : \ \frac{16}{4} = 6\,dB$, $4 \times 4 : \ \frac{32}{16} = 3\,dB$ and $2 \times 4 : \ \frac{16}{12} \approx 1\,dB$. The GSB saturates for very high SNR due to the lack of consistency in the SNR of the channel part estimated blindly. This does not appear in the case of the DSB in which all information exploited is consistent in SNR. However, the DSB is suboptimal when $N_{rx} > N_{tx}$ (4×2) and its performance reduces to that of the TS approach for $N_{rx} \leq N_{tx}$.

7.4.2 Frequency selective channel case

We consider the scenarios described in table 7.1.

scen.	(N_1, N_2)	$(\widehat{N}_1, \widehat{N}_2)$	N_{TS}	M_B
1	(3,1)	(3,1)	12	300
2	(3,1)	(3,3)	12	300
3	(3,1)	(3,3)	11	300
4	(4,1)	(4,1)	11	300
5	(3,1)	(3,3)	5	300

Table 7.1: Channel lengths, estimated lengths, training and blind data lengths for different scenarios where $N_{tx} = 2$.

For the first two scenarios we use partial denoising, whereas for the last three we use full denoising. We compare the classical TS approach with the DSB/GSB/DSBA/GSBA approaches and with an "exact" version (*e.g.* DSBe) in which the blind quantities ($\mathbf{P}(z)$) are determined from an exact R_{YY} ($M_B = \infty$). We see that the semi-blind approaches offer significant improvements over TS, especially using the augmented TS part. The performance of the deterministic approaches gets close to that of their exact versions, but not for the Gaussian approaches, which should yield better

performance. For the curves which stay flat in fig. 7.11, the identifiability conditions are not satisfied.

7.5 Conclusion

In this chapter we have seen how the semi-blind approaches can improve the channel estimation. In particular, the GSB achieves even the Cramér-Rao bound on the performances in the flat channel case. However, the GSB saturates for high SNR due to the fact that the estime of the signal subspace structure is only consistent in the length of the blind data. The DSB approach does not suffer from this problem since the noise subspace estimate is consistent in both the length of the blind data and the SNR. In the case of frequency selective channels, the semi-blind approaches allow to reduce the length of the training sequence needed for the idendifiability. This is valid especially for GSB. In general this approach outperforms the DSB. In the frequency selective case, the training part can be further augmented to include the training received signal that interferes with the blind one. This leads to more performant semi-blind approaches, and allows hence to reduce further the length of the training sequence.

APPENDIX

7.A Proof of Theorem 1

The proof is in two steps.
Let $\mathbf{U}^{TS}\mathbf{D}^{TS}\mathbf{U}^{TS\,H}$ be the eigenvector decomposition of $\mathbf{X}^{TS}\mathbf{X}^{TS\,H}$. In the first step we show that $\mathrm{E}_{\mathbf{H}}CRB$ is independent of $\mathbf{U}^{TS}$.
In fact,

$$\begin{aligned}\mathrm{E}_{\mathbf{H}}CRB &= \mathrm{E}_{\mathbf{H}}\mathrm{tr}[(\mathsf{M}(\mathbf{U}^{TS})\otimes\mathbf{I}_{N_{rx}})\,(\tfrac{2}{\sigma_v^2}\mathbf{D}^{TS}\otimes\mathbf{I}_{2\,N_{rx}})\,(\mathsf{M}(\mathbf{U}^{TS\,H})\otimes\mathbf{I}_{N_{rx}})^T \\ &\quad + M_1 J_B(\alpha) M_1^T]^{-1} \\ &= \mathrm{E}_{\mathbf{H}}\mathrm{tr}[\tfrac{2}{\sigma_v^2}\mathbf{D}^{TS}\otimes\mathbf{I}_{2\,N_{rx}} \\ &\quad + ([\mathsf{M}(\mathbf{U}^{TS})\otimes\mathbf{I}_{N_{rx}}]M_1)\,J_B(\alpha)\,([\mathsf{M}(\mathbf{U}^{TS\,H})\otimes\mathbf{I}_{N_{rx}}]M_1)^T]^{-1}\,,\end{aligned} \tag{7.38}$$

where in the second equality we used the unitary character of $\mathbf{U}^{TS}$. M_1 is given in (7.6), then

$$[\mathsf{M}(\mathbf{U}^{TS\,H})\otimes\mathbf{I}_{N_{rx}}]M_1 = [\mathsf{M}(\left(\mathbf{Q}\mathbf{U}^{TS}\right)^H)\otimes\mathbf{I}_{N_{rx}}]\,\frac{\partial\,\alpha^T}{\partial\,\mathbf{w}}\,. \tag{7.39}$$

$\mathbf{U}^{TS}$ is unitary, then $\mathbf{Q}\mathbf{U}^{TS}$ has the same uniform distribution as $\mathbf{Q}$.
On the other hand, $\frac{\partial\,\alpha^T}{\partial\,\mathbf{w}}J_B(\alpha)(\frac{\partial\,\alpha^T}{\partial\,\mathbf{w}})^T$ is independent of $\mathbf{Q}$. We can conclude that the $\mathrm{E}_{\mathbf{H}}CRB$ is independent of $\mathbf{U}^{TS}$. In particular for $\mathbf{U}^{TS}=\mathbf{I}$, we get

$$\mathrm{E}_{\mathbf{H}}\;CRB = \mathrm{E}_{\mathbf{H}}\,\mathrm{tr}\left(M_1\,J_B(\alpha)\,M_1^T + \frac{2}{\sigma_v^2}\mathbf{D}^{TS}\otimes\mathbf{I}_{2\,N_{rx}}\right)^{-1}\,. \tag{7.40}$$

In the second step we seek to show that $\mathrm{E}_{\mathbf{H}}CRB$ is minimized for $\mathbf{D}^{TS}\propto\mathbf{I}$.
We start by showing that $\mathrm{E}_{\mathbf{H}}\;CRB = f(\mathbf{D}^{TS})$ is a convex function over the connex set $\mathbf{D}^{TS}\geq 0$.
Let $\mathbf{D}^{TS}=\mathrm{diag}\,(d_1^{TS},\ldots,d_{N_{tx}}^{TS})$ and $\mathbf{C}$ be the Hessian of $f(\mathbf{D})$

$$\mathbf{C}_{i,n} = \frac{\partial^2 f}{\partial d_i\,\partial d_n}\,. \tag{7.41}$$

By evaluating the Hessian we can show that for any real positive vector $\mathbf{x}=[x_1\cdots x_{N_{tx}}]^T\geq 0$

$$\mathbf{x}^T\mathbf{C}\mathbf{x} = \frac{8}{\sigma_v^4}\,\mathrm{E}_{\mathbf{H}}\mathrm{tr}\left(J^{-2}(\mathbf{H})(\mathbf{X}\otimes\mathbf{I}_{2\,N_{rx}})J^{-1}(\mathbf{H})(\mathbf{X}\otimes\mathbf{I}_{2\,N_{rx}})\right)\geq 0\,. \tag{7.42}$$

where $\mathbf{X} = \text{diag}\,(x_1, \ldots, x_{N_{tx}})$. The positive sign follows from the symmetrical positive definite character of $J(\mathbf{H}) = M_1\, J_B(\alpha)\, M_1^T + \frac{2}{\sigma_v^2}\mathbf{D}^{TS} \otimes \mathbf{I}_{2\,N_{rx}}$.
The Hessians is positive, then $\mathrm{E}_{\mathbf{H}}\, CRB = f(\mathbf{D}^{TS})$ is convex over the connex set $\mathbf{D}^{TS} \geq 0$. By consequence $\mathrm{E}_{\mathbf{H}}\, CRB$ has a global minimum under a power constraint expressed on the trace of $\mathbf{D}^{TS}$: $\text{tr}\mathbf{D}^{TS} \leq P_{constraint}$. The Lagrangian of this optimization problem is expressed as

$$\begin{array}{l} L(\mathbf{D}^{TS}, \lambda) = f(\mathbf{D}^{TS}) + \lambda\,(\text{tr}(\mathbf{D}^{TS}) - P_{constraint}) \\ \frac{\partial\, L}{\partial\, d_i} = -\frac{2}{\sigma_v^2}\,\mathrm{E}_{\mathbf{H}}\text{tr}\,(J^{-2}(\mathbf{H})\,(\mathbf{I}_i \otimes \mathbf{I}_{2\,N_{rx}})) + \lambda = 0\,, \end{array} \tag{7.43}$$

where $\mathbf{I}_i$ is the matrix whose i^{th} diagonal element is 1 and all other entries are zeros.
The solution that minimizes $\mathrm{E}_{\mathbf{H}} CRB$ have to verify
$\mathrm{E}_{\mathbf{H}}\text{tr}\,(J^{-2}(\mathbf{H})\,(\mathbf{I}_i \otimes \mathbf{I}_{2\,N_{rx}})) = \mathrm{E}_{\mathbf{H}}\text{tr}\,(J^{-2}(\mathbf{H})\,(\mathbf{I}_i \otimes \mathbf{I}_{2\,N_{rx}}))$ for any $i \neq k$.
Using the same arguments as those used in the first step of this proof, we can show that for $\mathbf{D}^{TS} \propto \mathbf{I}$ and for any unitary matrix $\mathbf{U}$

$$\mathrm{E}_{\mathbf{H}} J^{-2}(\mathbf{H}) = \mathrm{E}_{\mathbf{H}}[(\mathsf{M}(\mathbf{U}) \otimes \mathbf{I}_{N_{rx}}) J^{-2}(\mathbf{H})(\mathsf{M}(\mathbf{U}) \otimes \mathbf{I}_{N_{rx}})^T]\,. \tag{7.44}$$

For $i \neq k$ and by choosing the permutation matrix $\mathcal{P}_{ik}$, that permute between i and k, we get for $\mathbf{U} = \mathcal{P}_{ik}$

$$\begin{array}{rcl} \mathrm{E}_{\mathbf{H}}\text{tr}\,(J^{-2}(\mathbf{H})\,(\mathbf{I}_i \otimes \mathbf{I}_{2\,N_{rx}})) & = & \mathrm{E}_{\mathbf{H}}\text{tr}\left(J^{-2}(\mathbf{H})\,[(\mathcal{P}_{ik}\mathbf{I}_i\mathcal{P}_{ik}^T) \otimes \mathbf{I}_{2\,N_{rx}}]\right) \\ & = & \mathrm{E}_{\mathbf{H}}\text{tr}\,(J^{-2}(\mathbf{H})\,(\mathbf{I}_k \otimes \mathbf{I}_{2\,N_{rx}}))\,, \end{array} \tag{7.45}$$

this show that $\mathbf{D}^{TS} \propto \mathbf{I}$ minimizes $\mathrm{E}_{\mathbf{H}} CRB$.
Hence, $\mathbf{X}^{TS}\,\mathbf{X}^{TS^H} \propto \mathbf{I}$ achieves the global minimum of $\mathrm{E}_{\mathbf{H}}\, CRB$. □

7.B Proof of Theorem 2

We will first derive the solution for the unitary factor and then for the diagonal factor.
We rewrite the parametric covariance matrix as: $\mathbf{R} = \mathbf{U}_R\mathbf{S}_R\mathbf{U}_R^H$ where $\mathbf{S}_R = \text{diag}\,(s_{R,1}, \ldots, s_{R,N_{rx}})$, in which the $s_{R,i}$ are organized in the increasing order. Similarly, we introduce $\mathbf{S}_e = \text{diag}\,(s_{e,i}, \ldots, s_{e,N_{rx}})$. By construction

we note that

$$\begin{array}{rl} s_{R,i} = \sigma_v^2 & , \, 1 \leq i \leq N_{rx} - N_{tx} \text{ for } N_{rx} > N_{tx} \\ s_{R,i+N_{rx}-\min\{N_{tx},N_{rx}\}} = \sigma_v^2 + \sigma_x^2 {d_i}^2 & , \, 1 \leq i \leq \min\{N_{tx}, N_{rx}\} \, . \end{array} \tag{7.46}$$

Let $\mathbf{O} = \mathbf{U}_R^H \, \mathbf{U}_e$. $\mathbf{O}$ is a $N_{tx} \times N_{tx}$ unitary matrix. We denote $\mu_i = (\mathbf{U}_R^H \hat{\mathbf{R}} \mathbf{U}_R)_{ii} = (\mathbf{O} \mathbf{S}_e \mathbf{O}^H)_{ii}$, $i = 1, \ldots, N_{rx}$. Then, up to a constant,

$$\begin{array}{rcl} LL_B(\mathbf{H}) & = & -N_B \mathrm{tr}\{\mathbf{S}_R^{-1} \mathbf{O} \mathbf{S}_e \mathbf{O}^H\} - N_B \ln \det(\mathbf{S}_R) \\ & = & -N_B \sum_{i=1}^{N_{rx}} \left(\mu_i / s_{R,i} + \ln(s_{R,i}) \right) \, . \end{array} \tag{7.47}$$

It can be shown [96] that $(\mu_i)_{1 \leq i \leq N_{rx}}$ majorizes $(s_{e,i})_{1 \leq i \leq N_{rx}}$, *i.e.* $\sum_{i=1}^{N_{rx}} s_{e,i} = \sum_{i=1}^{N_{rx}} \mu_i$ and $\sum_{i=1}^{k} s_{e,i} \leq \sum_{i=1}^{k} \mu_i \, , \, 1 \leq k \leq N_{rx}$. These properties allow us to use the following result [97]

$$\sum_{i=1}^{N_{rx}} \mu_i / s_{R,i} \geq \sum_{i=1}^{N_{rx}} s_{e,i} / s_{R,i} \, , \tag{7.48}$$

or equivalently

$$-\mathrm{tr}\{\mathbf{O} \mathbf{S}_e \mathbf{O}^H \mathbf{S}_R^{-1}\} \leq -\mathrm{tr}\{\mathbf{S}_e \mathbf{S}_R^{-1}\} \, . \tag{7.49}$$

This shows that $LL_B(\mathbf{H})$ is maximized for $\mathbf{O} = \mathbf{I}_{N_{rx}}$, *i.e.* $\mathbf{U}_R = \mathbf{U}_e$ or, equivalently, $\hat{\mathbf{U}}$ corresponds to the $\min\{N_{tx}, N_{rx}\}$ dominant eigenvectors in $\mathbf{U}_e$.
Let us now evaluate the optimal $\hat{\mathbf{D}} = \mathrm{diag}\,(\hat{d}_1, \ldots, \hat{d}_{\min\{N_{tx},N_{rx}\}})$. $LL_B(\mathbf{H})$ is separable in the $\hat{d}_i$, monotonically increasing for $0 \leq \hat{d}_i \leq \sqrt{\lfloor s_{R,i+N_{rx}-\min\{N_{tx},N_{rx}\}} - \sigma_v^2 \rfloor_+} \, / \sigma_x$, $1 \leq i \leq \min\{N_{tx}, N_{rx}\}$, and monotonically decreasing for $\hat{d}_i \geq \sqrt{\lfloor s_{R,i+N_{rx}-\min\{N_{tx},N_{rx}\}} - \sigma_v^2 \rfloor_+} \, / \sigma_x$, $1 \leq i \leq \min\{N_{tx}, N_{rx}\}$. $LL_B(\mathbf{H})$ is hence maximized for $\hat{d}_i = \sqrt{\lfloor s_{R,i+N_{rx}-\min\{N_{tx},N_{rx}\}} - \sigma_v^2 \rfloor_+} \, / \sigma_x$, $1 \leq i \leq \min\{N_{tx}, N_{rx}\}$, which are the dominant $\min\{N_{tx}, N_{rx}\}$ values of $\frac{1}{\sigma_x} \left(\lfloor \mathbf{S}_e - \sigma_v^2 \mathbf{I}_{N_{rx}} \rfloor_+ \right)^{1/2}$. □

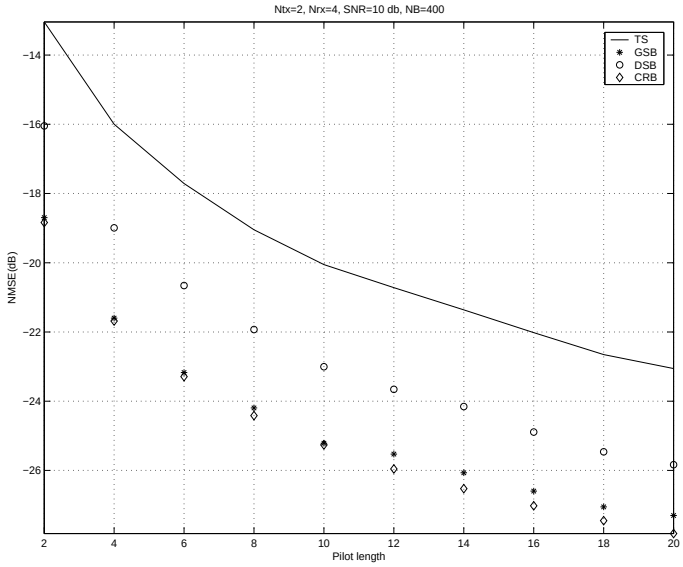

Figure 7.1: Normalized MSE vs N_{TS}: flat channel, $N_{tx} = 2, N_{rx} = 4,\ N_B = 400$, SNR= 10 dB.

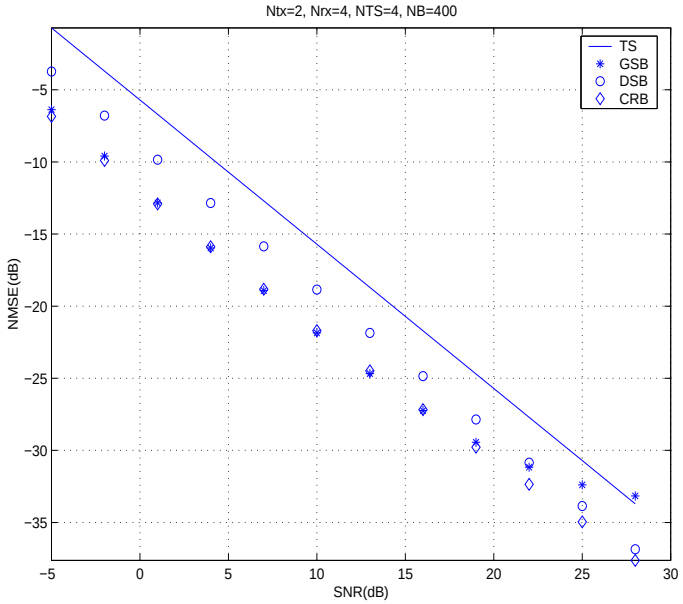

Figure 7.2: Normalized MSE vs SNR: flat channel, $N_{tx} = 2, N_{rx} = 4,\ N_B = 400$, $N_{TS} = 4$.

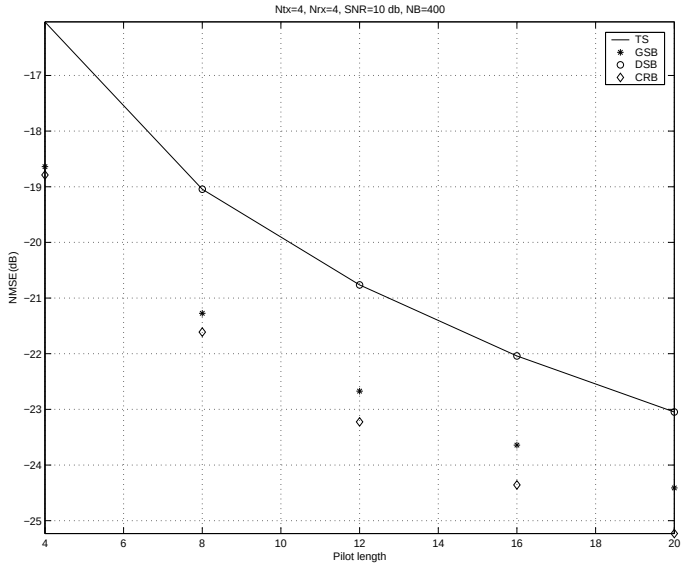

Figure 7.3: Normalized MSE vs N_{TS}: flat channel, $N_{tx} = 4, N_{rx} = 4,\ N_B = 400$, SNR= 10 dB.

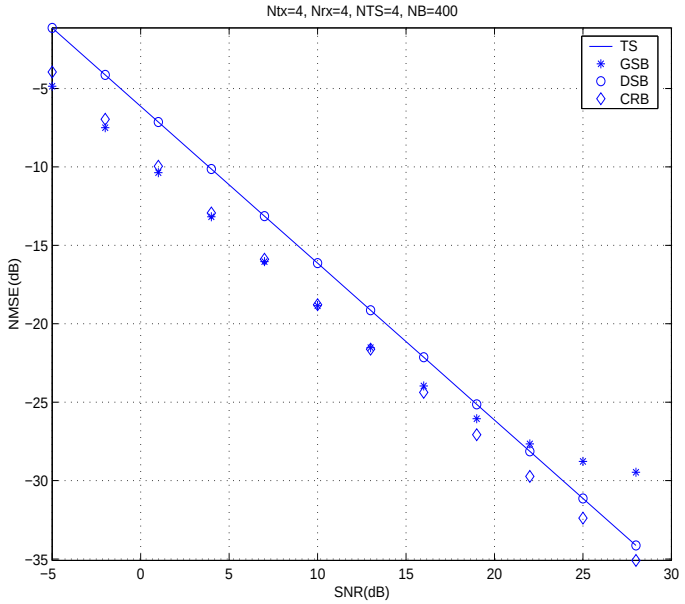

Figure 7.4: Normalized MSE vs SNR: flat channel, $N_{tx} = 4, N_{rx} = 4,\ N_B = 400$, $N_{TS} = 4$.

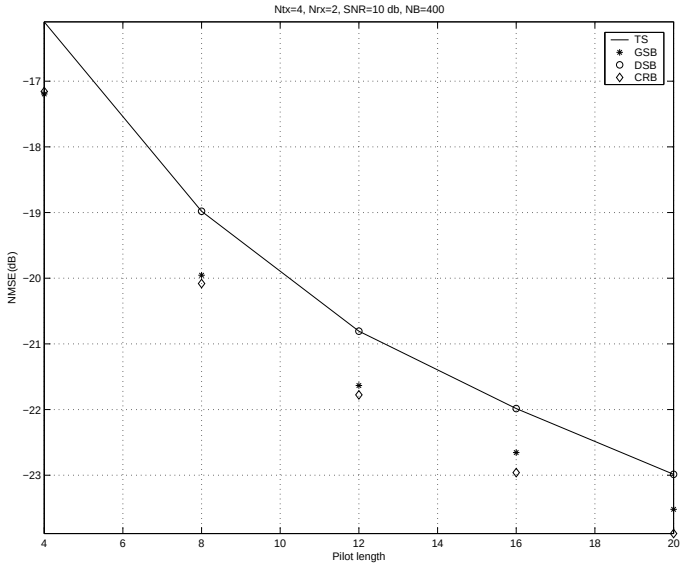

Figure 7.5: Normalized MSE vs N_{TS}: flat channel, $N_{tx} = 4, N_{rx} = 2,\ N_B = 400$, SNR= 10 dB.

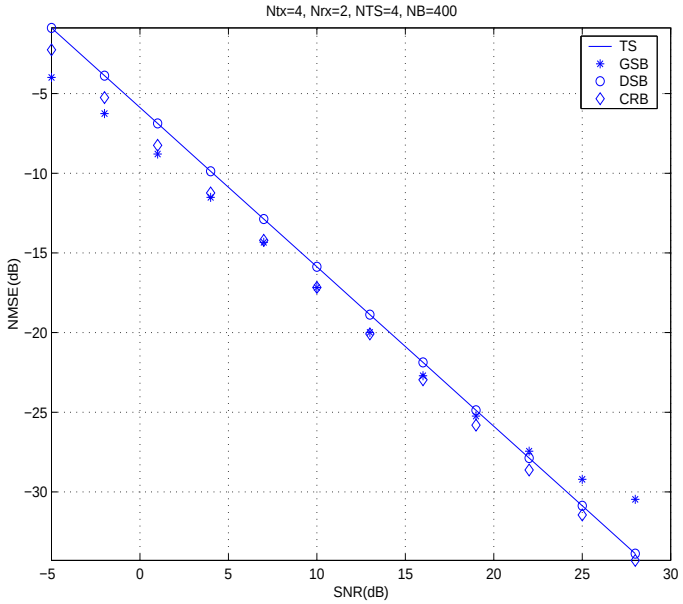

Figure 7.6: Normalized MSE vs SNR: flat channel, $N_{tx} = 4, N_{rx} = 2,\ N_B = 400$, $N_{TS} = 4$.

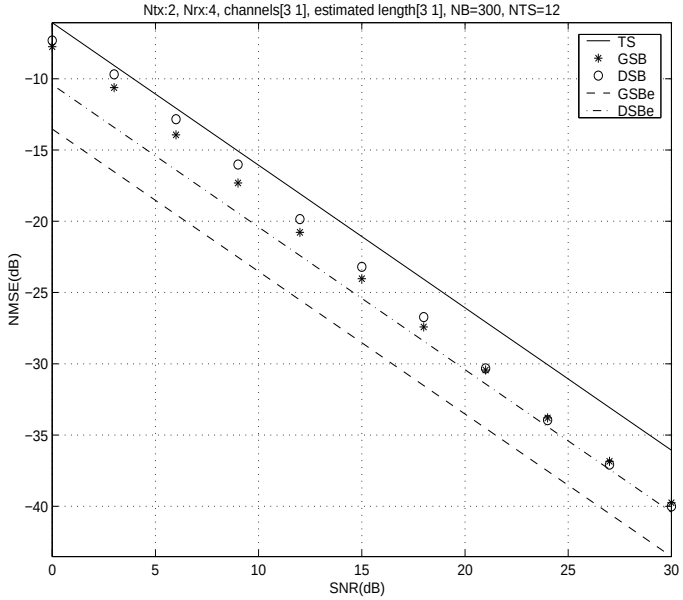

Figure 7.7: Normalized semi-blind channel estimation MSE, scenario 1.

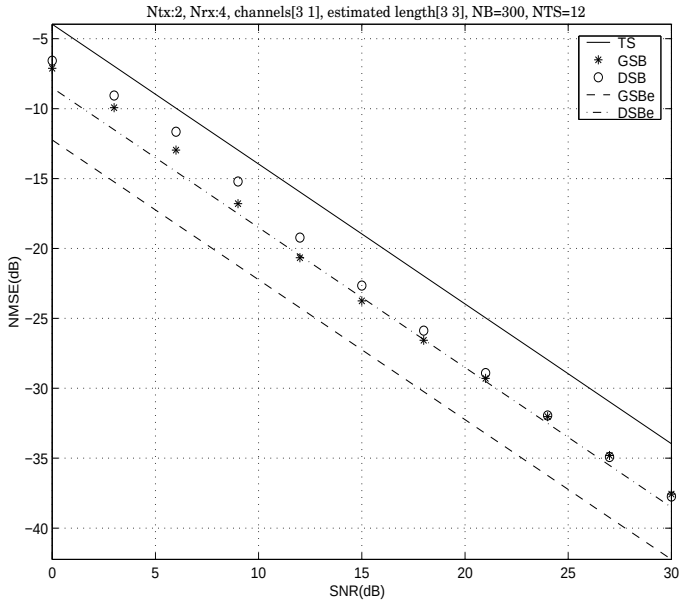

Figure 7.8: Normalized semi-blind channel estimation MSE, scenario 2.

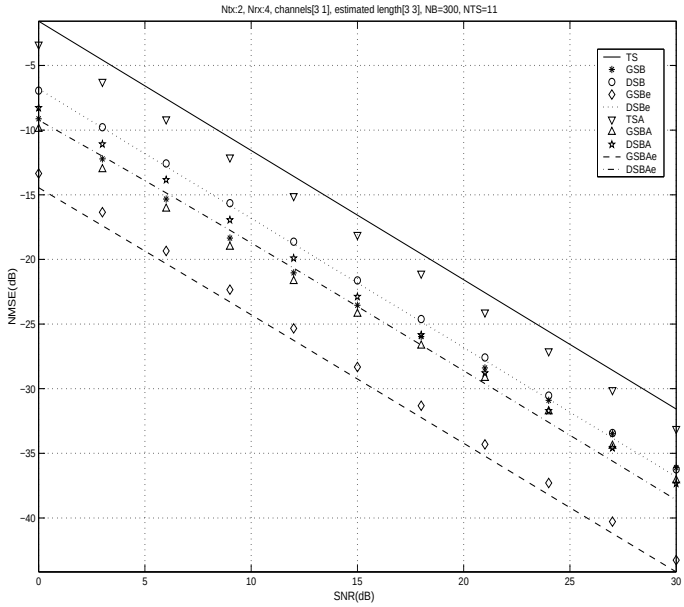

Figure 7.9: Normalized semi-blind channel estimation MSE, scenario 3.

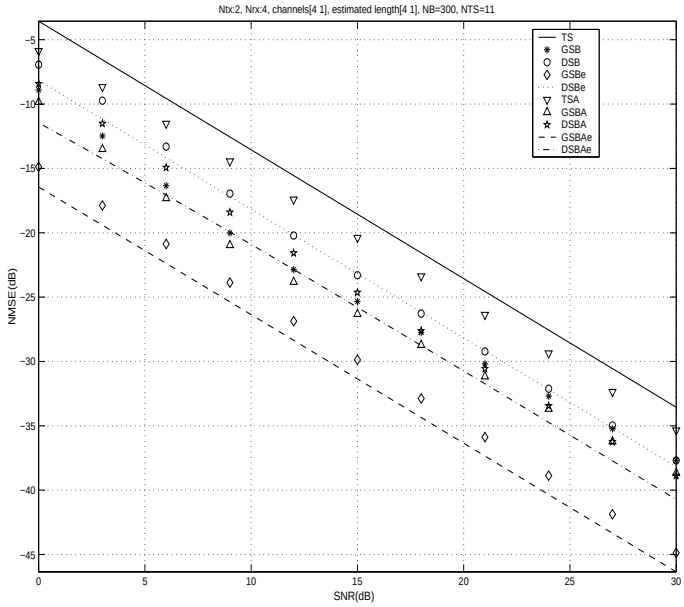

Figure 7.10: Normalized semi-blind channel estimation MSE, scenario 4.

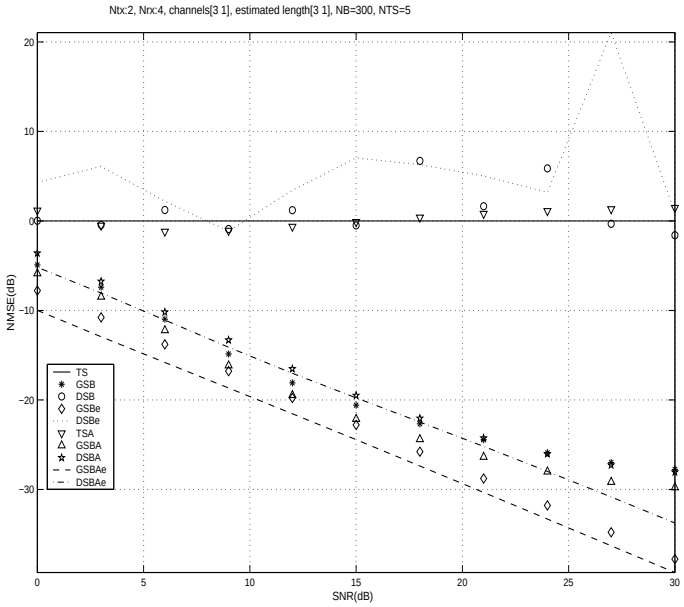

Figure 7.11: Normalized semi-blind channel estimation MSE, scenario 5.

General Conclusion

In this thesis, we have presented various case studies and solutions for coding and signal processing challenges in MIMO systems. This work has been structured in three parts, each one dealing with a particular situation with respect to CSI.

In the first part, the CSI was considered to be absent at the Tx and perfect at the Rx. We focused on the STC at the Tx and the detection processing at the Rx:

- A new STC scheme named STS has been proposed in chapter 2. This scheme uses a paraunitary precoding filter to ensure full diversity and maximum coding gain. STS does not penalize the ergodic capacity and applies in both cases of flat and frequency selective channels. This scheme is the first to exhibit all these properties at once.

- At the Rx, in order to avoid the high complexity of the ML decoder, we proposed three receiver strategies. Two of these strategies are non-iterative and have been studied in chapter 3, whereas the third one is iterative (chapter 4):

  - The Stripping MIMO DFE is a non-iterative Rx that detects and cancels the streams successively. The use of Stripping as a Rx for the STS scheme allows one to decompose the channel into multiple virtual SISO channels with known diversity. This can be exploited to use simple SISO coding techniques. We have theoretically shown that, for independent SNR-adaptive QAM constellation on each stream, the STS combined with the Stripping Rx outperforms the existing schemes in term of the diversity vs. multiplexing tradeoff. In chapter 3 we have also introduced new

techniques to study performances in frequency selective channel environment. This allowed us, in particular, to generalize the diversity vs. multiplexing optimal tradeoff to the MIMO frequency selective channel case.

- The second non-iterative Rx is the Conventional DFE applied to the MIMO case. In contrast to the previous Rx, it is adapted to the use of the same constellation and binary channel code for all streams. We showed that it achieves a high diversity gain and can be coupled with Per Survivor Processing in order to reduce error propagation.
- The last proposed Rx technique is iterative. It performs turbo detection by iterating between the linear equalizer and the binary CC. Using the Singleton Bound,we have shown that STS allows to dedicate the binary channel decoder to improve the coding gain and to exploit the multi-block diversity. Simulation results confirm the advantage of the use of STS over a pure binary channel code approach (Threading) especially for large N_{tx}, in the presence of multi-block diversity, and for $N_{rx} < N_{tx}$.

The second part covered the case of partial CSI at Tx and perfect CSI at Rx (chapter 5). The coding here was basically the cascade of STC schemes, developed in the absence of CSI, and a decorrelator which colors the transmitted signal. We have studied the input color that achieves the ergodic capacity for two channel models, the pathwise and the limited reciprocity. Numerical results showed that a near-optimal solution is obtained by waterfilling on the channel covariance seen from the Tx. Consequently, this covariance matrix was shown to capture almost all the information needed at the Tx.

In the last part, the case of absence of CSI at both Rx and Tx has been studied:

- In chapter 6, we have shown that the capacity of a block fading channel model achieves asymptotically, in the burst length, the one obtained for perfect CSI at the Rx. This is not the case anymore for time selective channel models where the capacity is shown to saturate for high SNR.

- The mutual information decomposition derived in chapter 6 for a block fading model, suggests to use semi-blind estimators that combine training and blind information. In chapter 7 we proposed various semi-blind approaches which improve the channel estimation quality. These techniques have reasonable complexity and lead to gains in performance w.r.t. pure training sequence approaches. In fact, the Gaussian semi-blind approach even achieves the Cramér-Rao bound in the flat channel case. The semi-blind approaches also improve the identifiability conditions and allow to reduce the length of the training sequence.

This work has proposed different schemes and techniques, as well as the analysis of different practical and theoretical situations. On the other hand, our work opened new problems. We list hereafter some research axes arising from this thesis :

- The STS proposed in chapter 2, can be seen as a structured lattice code. From this point of view, elements for lattice code analysis introduced in [37] can be used to study the diversity vs. multiplexing tradeoff achieved by the STS coupled with a ML decoder.

- The Conventional MIMO DFE with a MMSE ZF design (subsection 3.5.2) for $N_{tx} \leq N_{rx}$ and flat channel, achieves the two points ($r = 0$, $d = N_{tx}.(N_{rx} - \frac{N_{tx}-1}{2})$) and ($r = N_{tx}$, $d = 0$) on the diversity vs. multiplexing tradeoff curve. The general problem of the diversity vs. multiplexing tradeoff achieved by the Conventional MIMO DFE Rx with different design (MMSE ZF and MMSE), can be handled by considering the $\mathbf{Q}$ matrix (of the precoder filter) as the generator matrix of a lattice code and using techniques from [37].

- The diversity vs. multiplexing optimal tradeoff analysis proposed so far have focused on channels with i.i.d. components. However, the situation may be very different in reality. Hence, correlated channel models should be considered in order to handle this case.

- Design and simulations of the Conventional MIMO DFE for the STS scheme coupled with a PSP have to be performed in order to compare it with other existing techniques.

- The semi-blind approaches for the estimation of the channel at the Rx can be improved by including partial CSI if available (correlated

channel models in chapter 6). In fact, this will reduce the number of parameters to estimate, and further improve the channel estimation quality.

In the context of MIMO systems, this thesis has combined elements from two fields: signal processing and information theory. The proposed results and the opened perspectives show how the interaction between these two fields can lead to the development of new techniques and solve open problems. Advanced techniques and results from the signal processing framework can have an important impact on the code design. An illustration of this fact is the MIMO convolutive prefilter. Other examples are the the Stripping DFE and the Conventional DFE receivers in the MIMO context. On the other hand, results from the signal processing domain have allowed us to study the diversity vs. multiplexing tradeoff for the Stripping MIMO DFE, and to generalize the optimal tradeoff to frequency selective channels. The techniques associated with these latter results can be of an important contribution to the analysis and design of MIMO systems with frequency selective channels.

Résumé en français

7.3 Introduction

Depuis l'introduction du multiplexage spatial, d'une manière indépendante, par A. Paulraj et Foschini [1] en 1994, l'utilisation d'antennes multiples au transmetteur (Tx) et au récepteur (Rx) est devenue le sujet d'innombrables travaux. Celà est lié à la capacité des systèmes à entrées multiples et à sorties multiples (MIMO) d'offrir une nouvelle dimension spatiale, outre les dimensions temporelle et fréquentielle, d'accroître la capacité ergodique (moyenne) du canal (par un facteur égal au rang du canal), et de diminuer la probabilité de coupure par la contribution d'un nombre de composantes de la diversité égal au nombre de coefficients dans le canal. D'autre part, à l'inverse des canaux à entrée unique et à sortie unique (SISO), les canaux MIMO souffrent de l'interférence entre antennes. Les travaux récents pour exploiter cet important potentiel ont à faire un compromis entre l'augmentation du débit et l'exploitation de la diversité pour combattre l'évanescence du canal et l'interférence, tout en gardant une complexité acceptable.

7.3.1 Modèles des Canaux MIMO

On considère une modulation numérique linéaire sur un canal linéaire avec un bruit Gaussien additif. Le nombre d'antennes à la transmission est N_{tx} et à la réception N_{rx}. Le signal vectoriel $(N_{rx} \times 1)$ reçu à l'instant k est

$$\mathbf{y}_k = \sum_{l=0}^{L-1} \mathbf{H}_l \mathbf{x}_{k-l} + \mathbf{v}_k \tag{7.50}$$

où $\mathbf{x}_k : N_{tx} \times 1$ est le signal transmis, $\mathbf{H}_l : N_{rx} \times N_{tx},\ l = 0, \ldots, L-1$ sont les coefficients matriciels de la réponse impulsionnelle du canal et $\mathbf{v}_k : N_{rx} \times 1$ est le bruit.
En l'absence de connaissance parfaite du canal à la transmission, le canal est modélisé d'une manière statistique. Différents modèles sont couramment utilisés:
Modèle MIMO Rayleigh évanesçant et plat ($L = 1$): Dans ce modèle les différentes composantes du canal ont des distributions i.i.d. centrées Gaussiennes, $(\mathbf{H})_{mk} \sim \mathcal{CN}(0, 1)$ pour $1 \leq m \leq N_{rx}$ et $1 \leq k \leq N_{tx}$.
Modèle MIMO spatialement séparable: Dans ce modèle, le transmetteur dispose d'une connaissance partielle correspondant aux moments de sec-

ond ordre. Le canal dans ce cas est modélisé par

$$\mathbf{H} = \mathbf{\Sigma}_1^{1/2} \mathbf{W} \mathbf{\Sigma}_2^{1/2}, \tag{7.51}$$

où $\mathbf{W}$: $N_{rx} \times N_{tx}$ est une matrice aléatoire de composantes i.i.d. suivant $\mathcal{CN}(0,1)$.
$\mathbf{\Sigma}_1$ (resp. $\mathbf{\Sigma}_2$) est la covariance du canal vue du récepteur (resp. transmetteur).

Modèle MIMO Rayleigh évanesçant et sélectif en fréquence($L > 1$): Ce modèle est la généralisation du cas plat, où les composantes de la réponse impulsionnelle sont indépendantes et Gaussiennes. Chacun des $\mathbf{H}_l$, $l = 0, \ldots, L-1$ a des composantes i.i.d. $(\mathbf{H}_l)_{mk} \sim \mathcal{CN}(0, \sigma_l^2)$ pour $1 \leq m \leq N_{rx}$ et $1 \leq k \leq N_{tx}$. $\sigma_l^2 > 0$, $0 \leq l \leq L-1$, correspondent au profil des puissances du canal.

7.3.2 Capacité du Canal

Dans le cas d'un canal plat avec connaissance parfaite du canal au Tx, la capacité du canal sous la contrainte de puissance (inférieure à P) est

$$C(\mathbf{H}) = \max_{\mathrm{tr}\{\mathbf{S_{XX}}\} \leq P} \ln \det(\mathbf{I}_{N_{rx}} + \frac{1}{\sigma_v^2} \mathbf{H}\, \mathbf{S_{XX}}\, \mathbf{H}^H), \tag{7.52}$$

où $\mathbf{S_{XX}}$ est la covariance du signal à la transmission. La solution de la maximisation correspond au *waterfilling* sur les valeurs propres de $\mathbf{H}^H\mathbf{H}$ (waterfilling spatial) [2].

En l'absence de CSI parfait au Tx d'autres quantités sont définies:

Capacité ergodique: Elle mesure la capacité moyenne

$$C = \max_{\frac{1}{2\pi j} \oint \frac{dz}{z} \mathrm{tr}\{\mathbf{S_{XX}}\} \leq P} \mathrm{E}_{\mathbf{H}} \frac{1}{2\pi j} \oint \frac{dz}{z} \ln \det(\mathbf{I}_{N_{rx}} + \frac{1}{\sigma_v^2} \mathbf{H}(z)\, \mathbf{S_{XX}}(z)\, \mathbf{H}^\dagger(z)), \tag{7.53}$$

où $\mathbf{S_{XX}}(z)$ est la transformée en z de la séquence d'autocorrélation de $\mathbf{x}$.
Pour un canal MIMO avec un modèle Rayleigh évanesçant et plat, Telatar a montré [2] que la capacité ergodique est atteinte pour une entrée blanche ($\mathbf{S_{XX}}(z) = \sigma_x^2 \mathbf{I}_{N_{tx}}$, $\sigma_x^2 = \frac{P}{N_{tx}}$)

$$C = \mathrm{E}_{\mathbf{H}} \ln \det(\mathbf{I}_{N_{rx}} + \rho \mathbf{H}\mathbf{H}^H), \tag{7.54}$$

où $\rho = \frac{P}{N_{tx}\sigma_v^2}$.
Ce résultat est aussi valable pour un modèle de canal MIMO Rayleigh évanesçant et sélectif en fréquence

$$C = \mathrm{E}_{\mathbf{H}} \frac{1}{2\pi j} \oint \frac{dz}{z} \ln\det(\mathbf{I}_{N_{rx}} + \rho\, \mathbf{H}(z)\mathbf{H}^{\dagger}(z))\,. \tag{7.55}$$

Capacité de coupure: La capacité ergodique n'a de sens que dans le cas où le transmetteur peut coder sur une multitude de réalisations du canal. Dans le cas où Tx ne peut voir qu'une réalisation du canal, et pour un SNR et un débit R donné, on définit la probabilité de coupure qui exprime la probabilité que le débit dépasse la capacité instantanée du canal

$$\begin{aligned} P_{out}(R) &= P(C(\mathbf{H}) < R) \\ &= P(\tfrac{1}{2\pi j} \oint \tfrac{dz}{z} \ln\det(\mathbf{I}_{N_{rx}} + \rho \mathbf{H}(z)\, S_{\mathbf{XX}}(z)\, \mathbf{H}^{\dagger}(z)) < R)\,, \end{aligned} \tag{7.56}$$

où $S_{\mathbf{XX}}(z)$ est normalisée pour avoir $(\frac{1}{2\pi j} \oint \frac{dz}{z} \mathrm{tr} S_{\mathbf{XX}}(z) = N_{tx})$.
Pour un niveau de probabilité de coupure α $(0 \leq \alpha \leq 1)$ donné, la capacité de coupure est définie comme

$$C_{out}(\alpha) = (P_{out})^{-1}(\alpha)\,. \tag{7.57}$$

7.3.3 Codage Spatio-Temporel pour des Systèmes MIMO

On considère une transmission des symboles codés sur une durée de T périodes symbole. Le code espace-temps est représenté par une matrice $N_{tx} \times T$, de forme: $\mathbf{C} = \frac{1}{\sigma_x}[\mathbf{x}_1, \mathbf{x}_2, \ldots, \mathbf{x}_T]$. Le canal est MIMO plat, le signal reçu accumulé est

$$\mathbf{Y} = \sigma_x \mathbf{H}\, \mathbf{C} + \mathbf{V}\,, \tag{7.58}$$

où $\mathbf{Y} = [\mathbf{y}_1, \mathbf{y}_2, \ldots, \mathbf{y}_T]$ et $\mathbf{V} = [\mathbf{v}_1, \mathbf{v}_2, \ldots, \mathbf{v}_T]$ sont des matrices $N_{rx} \times T$.
On considère un modèle MIMO Rayleigh évanesçant et un récepteur maximum de vraisemblance (ML). Tx n'as pas de CSI sur le canal et Rx a un CSI parfait.
La probabilité de transmettre $\mathbf{C}$ et de décider $\mathbf{C}'$ a été bornée [16] par

$$P(\mathbf{C} \to \mathbf{C}') \approx \left(\frac{\rho}{4}\right)^{-r.N_{rx}} \left(\prod_{l=1}^{r} \lambda_l\right)^{-N_{rx}}\,, \tag{7.59}$$

où r et les λ_l, $l = 1, \ldots, r$ sont respectivement le rang et les valeurs propres de $(\mathbf{C} - \mathbf{C}')(\mathbf{C} - \mathbf{C}')^H$.
Cela permet de définir deux critères pour la conception des codes spatio-temporels
Gain de diversité : Il est défini comme le rang minimal possible (r_{min}) sur toutes les combinaisons possibles de $(\mathbf{C} - \mathbf{C}')$.
Gain de codage : Il est défini comme le minimum possible de $\prod_{l=1}^{r_{min}} \lambda_l$ sur toutes les combinaisons de $(\mathbf{C} - \mathbf{C}')$ ayant comme rang r_{min}.

7.3.4 Diversité et Multiplexage comme Définis par Zheng & Tse

Dans [9], Zheng et Tse ont donné une nouvelle définition de la diversité et du multiplexage qui considère un schéma adaptatif en SNR. En effet, un schéma $\mathcal{C}(\rho)$ est une famille de codes de longueur de bloc T(un pour chaque niveau de SNR), qui supporte un débit $R(\rho)$.
Ce schéma atteint un multiplexage spatial r et un gain de diversité d si le débit de donnée vérifie

$$\lim_{\rho \to \infty} \frac{R(\rho)}{\ln(\rho)} = r \,, \tag{7.60}$$

et la probabilité d'erreur vérifie

$$P_e(\rho) \doteq \rho^{-d} \,, \tag{7.61}$$

où $\doteq$ est l'égalité exponentielle, on écrit $f(\rho) \doteq \rho^b$ pour

$$\lim_{\rho \to \infty} \frac{\ln f(\rho)}{\ln(\rho)} = b \,. \tag{7.62}$$

Pour chaque r, $d^*(r)$ est définie comme le sup de l'avantage de diversité atteint sur tous les schémas possibles.
Zheng & Tse ont considéré un canal MIMO avec un modèle Rayleigh évanesçant et plat, et ont montré le résultat suivant.

Courbe optimale du compromis : On a $T \geq N_{rx} + N_{tx} - 1$. La courbe optimale du compromis $d^*(r)$ est donnée par la fonction linéaire par morceaux, qui joints les points$(k, d^*(k))$, $k = 0, 1, \ldots, p$, où

$$d^*(k) = (p - k)(q - k) \,, \tag{7.63}$$

où $p = \min\{N_{rx}, N_{tx}\}$ et $q = \max\{N_{rx}, N_{tx}\}$.

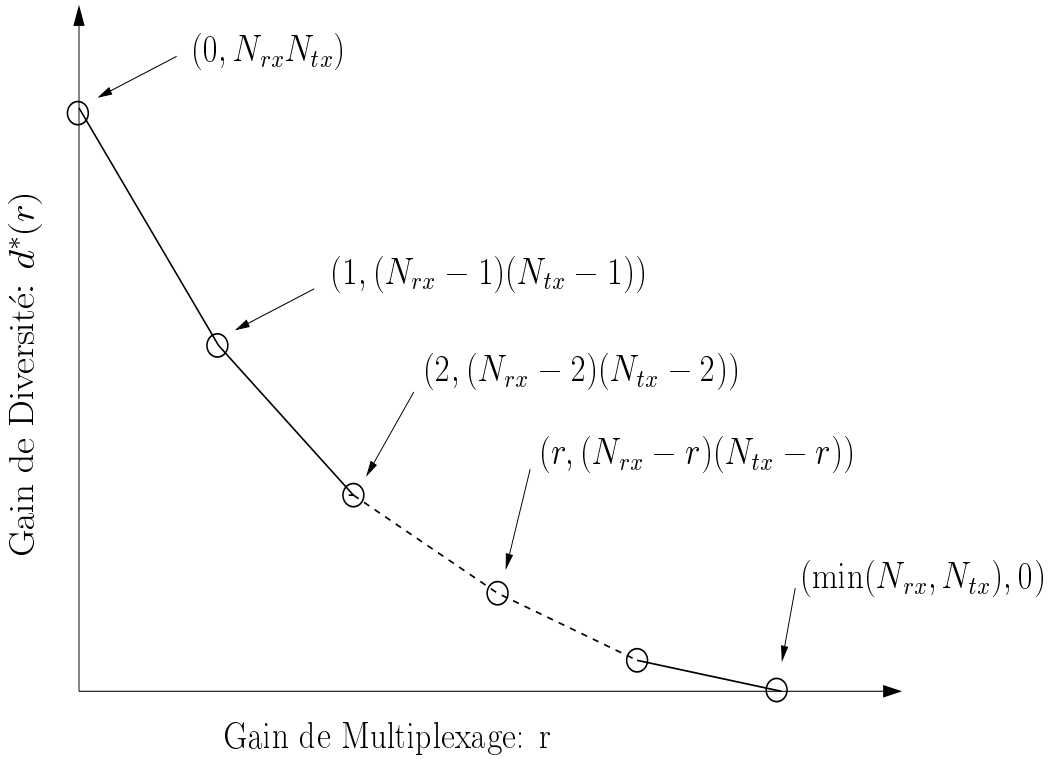

Figure 7.12: Compromis diversité-multiplexage

Partie I: Absence de CSI au Tx

Dans cette première partie du rapport le canal est inconnu à Tx et parfaitement connu au Rx. On commence par introduire notre nouveau schéma de codage spatio-temporel basé sur un précodage linéaire en utilisant un filtre MIMO convolutif. Ce schéma est appelé *étalement spatio-temporel* et désigné par STS. Par la suite on étudie différents récepteurs de complexité limitée qui peuvent être utilisés. Les récepteurs proposés sont de deux catégories: itératifs et non-itératifs.

7.4 Précodage Spatio-Temporel Linéaire et Convolutif

Le schéma général de transmission du STS est décrit dans la figure 7.13. Après un codage correcteur d'erreur et la modulation d'amplitude en quadra-

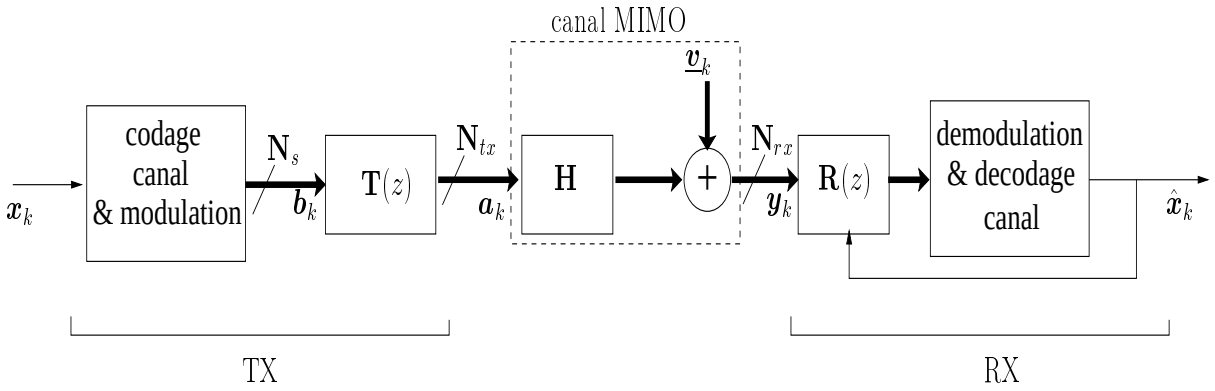

Figure 7.13: Schéma Général de Transmission.

ture (QAM) des symboles, le débit est démultiplexé. Le résultat est un vecteur $\boldsymbol{b}_k$ qui contient N_s symboles par période. $\boldsymbol{b}_k$ passe par la suite dans un filtre MIMO convolutif $\mathbf{T}(z)$, cette opération correspond au précodage spatio-temporel, sa sortie est transmise sur les antennes de transmission au nombre de N_{tx}. Pour chaque composante i, le débit transmis pendant toute la trame $\boldsymbol{b}_{i,k}$, $k = 1, \ldots, T$ est appelé stream.

Pour $\mathbf{T}(z)$ on a choisi une forme qui combine l'étalement spatial $\mathbf{Q}$ et la diversité de délais $\mathbf{D}(z)$

$$\begin{array}{rcl} \mathbf{T}(z) & = & \mathbf{D}(z)\,\mathbf{Q} \\ \mathbf{D}(z) & = & \mathrm{diag}\left\{1,\, z^{-L}, \ldots, z^{-L(N_{tx}-1)}\right\}. \end{array} \tag{7.64}$$

Dans le choix de $\mathbf{Q}$, on a respecté plusieurs critères:

Capacité ergodique Afin de conserver cette quantité, $\mathbf{Q}$ doit être unitaire $\mathbf{Q}^H\mathbf{Q} = I$.

Borne du filtre adapté Pour avoir une borne du filtre adapté (en ignorant l'interférence), qui soit la même pour chacune des composantes des $\boldsymbol{b}_k$, on doit avoir $|\mathbf{Q}_{ik}| = \frac{1}{\sqrt{N_{tx}}}, i, k = 1, \ldots, N_{tx}$.

Gain de codage Pour avoir un gain de codage maximal, la solution proposée est la suivante

$$\mathbf{Q} = \frac{1}{\sqrt{N_{tx}}} \begin{bmatrix} 1 & \theta_1 & \ldots & {\theta_1}^{N_{tx}-1} \\ 1 & \theta_2 & \ldots & {\theta_2}^{N_{tx}-1} \\ \vdots & \vdots & & \vdots \\ 1 & \theta_{N_{tx}} & \ldots & {\theta_{N_{tx}}}^{N_{tx}-1} \end{bmatrix}, \tag{7.65}$$

où les θ_i sont les racines du polynôme $\theta^{N_{tx}} - j = 0\,,\ j = \sqrt{-1}$.

Ces bonnes propriétés de $\mathbf{T}(z)$ sont aussi bien valables pour un canal plat que pour un canal sélectif en fréquence.

7.4.1 Récepteur ML

Un détecteur maximum de vraisemblance peut aussi bien être implémenté en utilisant l'algorithme de Viterbi. Cependant, celui-là est d'une très grande complexité due au nombre d'états qui est $|\mathcal{A}|^{N_{tx}(N_{tx}L-1)}$, où $|\mathcal{A}|$ est la taille de la constellation à l'entrée.

7.5 Rx Non-itératif: Alternatif de Conception

On présente deux possibilités de conceptions: la première est le Stripping MIMO DFE qui fait une détection successive de streams, et la deuxième est le MIMO DFE Conventionnel qui fait une détection conjointe des streams mais successivement dans le temps.

7.5.1 Stripping MIMO DFE

La figure suivante montre un schéma bloc du Stripping MIMO DFE (fig. 7.14). ce récepteur commence par un filtre adapté à la cascade du précodeur

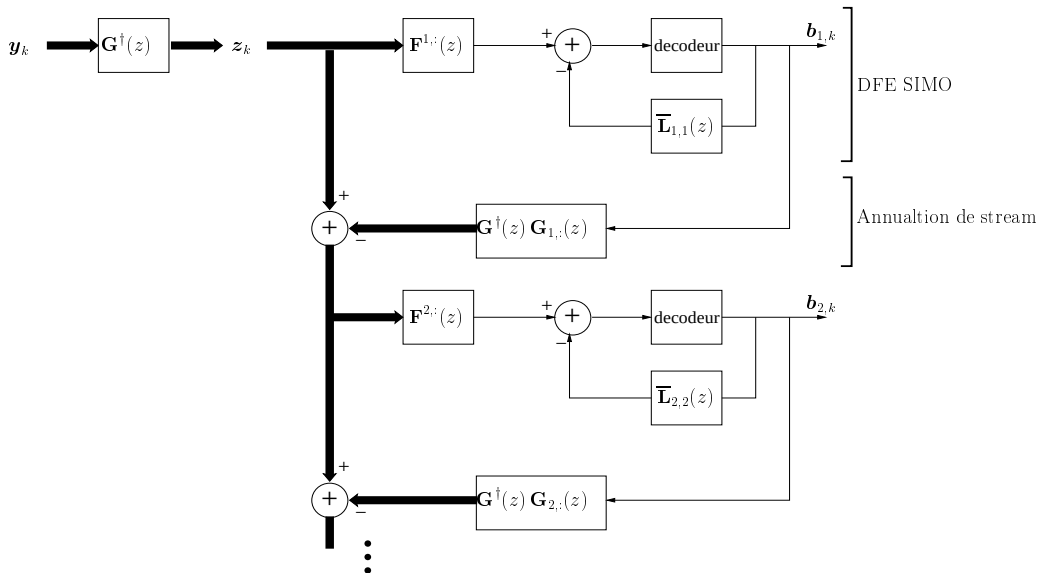

Figure 7.14: Stripping MIMO DFE.

et du canal $\mathbf{G}(z) = \mathbf{H}(z)\,\mathbf{T}(z) = \mathbf{H}(z)\,\mathbf{D}(z)\,\mathbf{Q}$. Pour la détection de chacune des streams i on utilise un égaliseur à retour de décision (DFE), qui fait une détection successive dans le temps des symboles de la même stream i, $\boldsymbol{b}_{i,k}$, $k = 1, \ldots, T$. Il commence par un filtre Feedback $\mathbf{F}^{i,:}(z)$, et le retour de décision se fait avec le filtre Feedforward $\overline{\mathbf{L}}_{i,i}(z)$. Après qu'une stream i soit entièrement détectée, sa contribution est soustraite au signal reçu en utilisant un retour de décision et en filtrant la stream avec le filtre $\mathbf{G}^\dagger(z)\,\mathbf{G}_{i,:}(z)$. Par la suite on passe à la détection du stream $i+1$. La sortie du filtre adapté est

$$\mathbf{z}_k = \mathbf{G}^\dagger(q)\,\boldsymbol{y}_k = \mathbf{G}^\dagger(q)\,\mathbf{G}(q)\,\boldsymbol{b}_k + \mathbf{G}^\dagger(q)\,\boldsymbol{v}_k\,. \tag{7.66}$$

Le Stripping MIMO DFE est de la forme

$$\widehat{\mathbf{b}}_k \;=\; -\;\underbrace{\overline{\mathbf{L}}(q)}_{\text{feedback}}\;\mathbf{b}_k + \;\underbrace{\mathbf{F}(q)}_{\text{feedforward}}\;\mathbf{z}_k\,, \tag{7.67}$$

où

$$\mathbf{I}+\overline{\mathbf{L}}(z)=\mathbf{L}(z)=\begin{bmatrix} L_{11}(z) & 0 & \dots & 0 & 0 \\ L_{21}(z) & L_{22}(z) & 0 & \ddots & 0 \\ \vdots & L_{32}(z) & \ddots & \ddots & \vdots \\ \vdots & \ddots & \ddots & L_{N_s-1,N_s-1}(z) & 0 \\ L_{N_s1}(z) & L_{N_s2}(z) & \dots & L_{N_s,N_s-1}(z) & L_{N_sN_s}(z) \end{bmatrix} \tag{7.68}$$

Le feedback $\overline{\mathbf{L}}(z)=\mathbf{L}(z)-\mathbf{I}$ est strictement causal. Celà veut dire que $\mathbf{L}(z)$ est triangulaire inférieure, avec des éléments diagonaux, $\mathbf{L}_{ii}(z), i=1,\dots,N_{tx}$, causal, monique avec phase minimale. Les éléments de la partie triangulaire inférieure $\mathbf{L}_{ij}(z)$, $i>j$ sont arbitraires (non causal).

Pour la conception du filtre du DFE, différent choix sont possibles, les plus connus sont le MMSE ZF et le MMSE. Le MMSE ZF annule complétement (force à zéro) l'interférence alors que le MMSE fait un compromis entre l'annulation d'interférence et l'amplification du bruit.

On étudie les performances du Stripping MIMO DFE en fonction du compromis diversité-multiplexage.

7.5.2 Compromis Diversité-Multiplexage du Stripping MIMO DFE

On dénote par $C_n^{MMSE\,DFE}$ la capacité instantanée du stream détecté à l'étape n du traitement successif du stripping avec une conception MMSE. De la même façon est définie $C_n^{MMSEZF\,DFE}$ avec une conception MMSE ZF. On présente dans une première étape des résultats préliminaires qui vont être utilisées par la suite.

Décomposition de la capacité :

$$C(\mathbf{H})=\sum_{n=1}^{N_{tx}} C_n^{MMSE\,DFE}\,. \tag{7.69}$$

Bornes sur la capacité des streams :
Les deux lemmes suivants donnent les résultats désirés.
Lemme 1: La capacité du $n^{\text{ème}}$ stream, dans une conception MMSE, est bornée par

$$c_n^1 \le C_n^{MMSE\,DFE} - \ln(1+\rho s_{N_{tx}(L-1)+n}) \le c_n^2\,, \tag{7.70}$$

où

$$c_n^1 = \begin{cases} \ln(\frac{1}{N_{tx}\gamma_{N_{tx}L}}) + (N_{tx}-n)\ln\left(\frac{N_{tx}-n}{(N_{tx}-n+1)\gamma_{N_{tx}L}}\right) & , \ 1 \le n \le N_{tx}-1 \\ \ln(\frac{1}{N_{tx}\gamma_{N_{tx}L}}) & , \ n = N_{tx} \end{cases} \tag{7.71}$$

$$c_n^2 = \begin{cases} (N_{tx}-n)\ln\left(\frac{\gamma_{N_{tx}L}(N_{tx}-n+1)}{N_{tx}-n}\right) & , \ 1 \le n \le N_{tx}-1 \\ 0 & , \ n = N_{tx} \end{cases} \tag{7.72}$$

$(s_n,\ n = 1,\ldots,N_{tx}L)$ sont les valeurs propres de $\bar{\mathbf{H}}^H\bar{\mathbf{H}}$ ordonnées dans un ordre croissant, où $\bar{\mathbf{H}} = [\mathbf{H}_0, \mathbf{H}_1, \ldots, \mathbf{H}_{L-1}]$. $\gamma_{N_{tx}L} = \sum_{l=0}^{N_{tx}L-1} \begin{pmatrix} l \\ N_{tx}L-1 \end{pmatrix}^2$.

Pour la conception MMSEZF le nombre de streams transmises (nombre de colonnes de Q) est fixés à $N_s = \min\{N_{tx}, N_{rx}\}$.

Lemma 2: La capacité du $n^{\text{ème}}$ stream, dans une conception MMSE ZF, est bornée par

$$\ln(1 + e^{c_n^1}\rho s_{N_{tx}L-N_s+n}) \le C_n^{MMSEZFDFE} \le \ln(1 + e^{c_n^2}\rho s_{N_{tx}L-N_s+n}), \tag{7.73}$$

où maintenant

$$c_n^1 = \begin{cases} \ln(\frac{1}{N_{tx}\gamma_{N_{tx}L}}) + (N_s-n)\ln\left(\frac{N_s-n}{(N_s-n+1)\gamma_{N_{tx}L}}\right) & , \ 1 \le n \le N_s-1 \\ \ln(\frac{1}{N_{tx}\gamma_{N_{tx}L}}) & , \ n = N_s \end{cases} \tag{7.74}$$

$$c_n^2 = \begin{cases} (N_s-n)\ln\left(\frac{c_{N_{tx}L}(N_s-n+1)}{N_s-n}\right) & , \ 1 \le n \le N_s-1 \\ 0 & , \ n = N_s \end{cases} \tag{7.75}$$

Encore, $(s_n,\ n = 1,\ldots,N_{tx}L)$ sont les valeurs propres de $\bar{\mathbf{H}}^H\bar{\mathbf{H}}$ ordonnées dans un ordre croissant, où $\bar{\mathbf{H}} = [\mathbf{H}_0, \mathbf{H}_1, \ldots, \mathbf{H}_{L-1}]$.

Avant de présenter les performances du Stripping MIMO DFE, on commence par donner la généralisation du compromis diversité-multiplexing au canaux sélectifs en fréquence pour des longueurs de bloc (trame) $T >> N_{tx}L$.

Théorème 1: On a $T >> N_{tx}L$. La courbe optimale du compromis $d^*(r)$, pour un canal sélectif en fréquence, est donnée par la fonction linéaire par

morceaux, qui joints les points$(k, d^*(k))$, $k = 0, 1, \ldots, p$, où

$$d^*(k) = (p-k)(Lq-k)\,, \tag{7.76}$$

où $p = \min\{N_{rx}, N_{tx}\}$ et $q = \max\{N_{rx}, N_{tx}\}$.

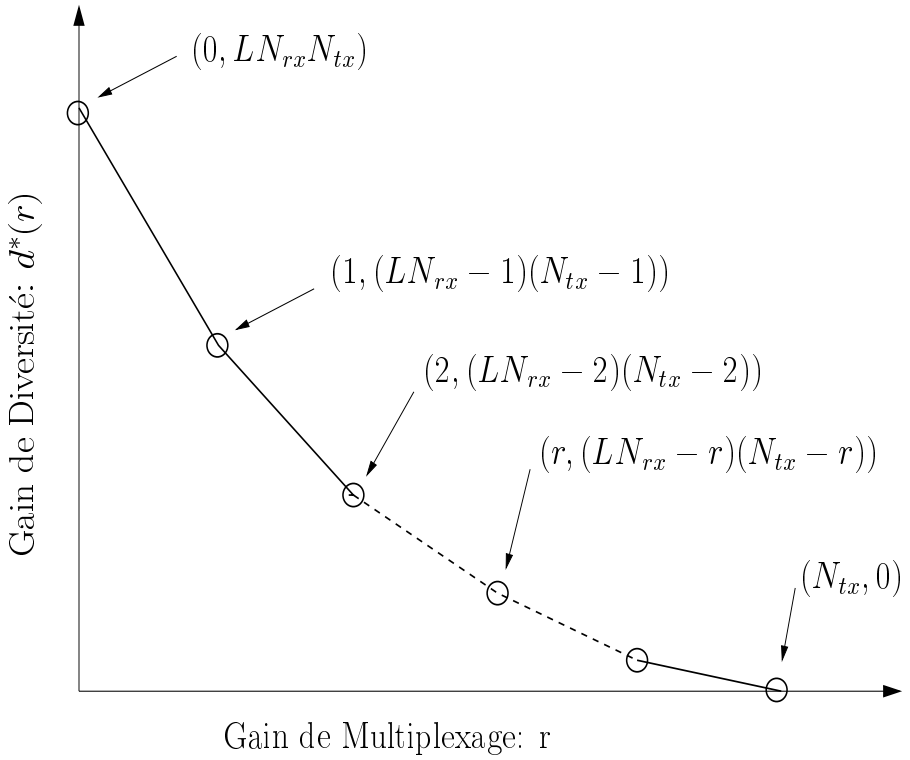

Figure 7.15: Compromis diversité-multiplexage d'un canal sélectif en fréquence

En ce qui concerne le compromis atteint par le récepteur Stripping MIMO DFE appliqué à notre schéma de transmission STS, il est donné par le théorème suivant.

Théorème 2: Pour un bloc de longueur T, $T >> N_{tx}L$, l'utilisation de constellations QAM avec des débits adaptés par stream, permet au récepteur Stripping MIMO DFE avec une conception MMSEZF d'atteindre un compromis de diversité-multiplexage donné par $d^{*,SIC}(r)$.
Où $d^{*,SIC}(r)$ est donnée par la fonction linéaire par morceaux, qui joint les

points $(b_k, d^{*,SIC}(b_k))$, $k = 0, 1, \ldots, p$, où

$$\begin{array}{rcll} r_k^t & = & k - (m-k)(n-k)\displaystyle\sum_{i=1}^{k} \frac{1}{(m-k+i)(n-k+i)} & , \; k = 0, \ldots, p-1 \\ r_k^t & = & p & , \; k = p \end{array} \tag{7.77}$$

et

$$\begin{array}{rcll} d^{*,SIC}(r_k^t) & = & (m-k)(n-k) & , \; k = 0, \ldots, p-1 \\ d^{*,SIC}(r_k^t) & = & 0 & , \; k = p \end{array} \tag{7.78}$$

où $m = \min\{N_{rx}, N_{tx}L\}$, $n = \max\{N_{rx}, N_{tx}L\}$ et $p = \min\{N_{rx}, N_{tx}\}$.

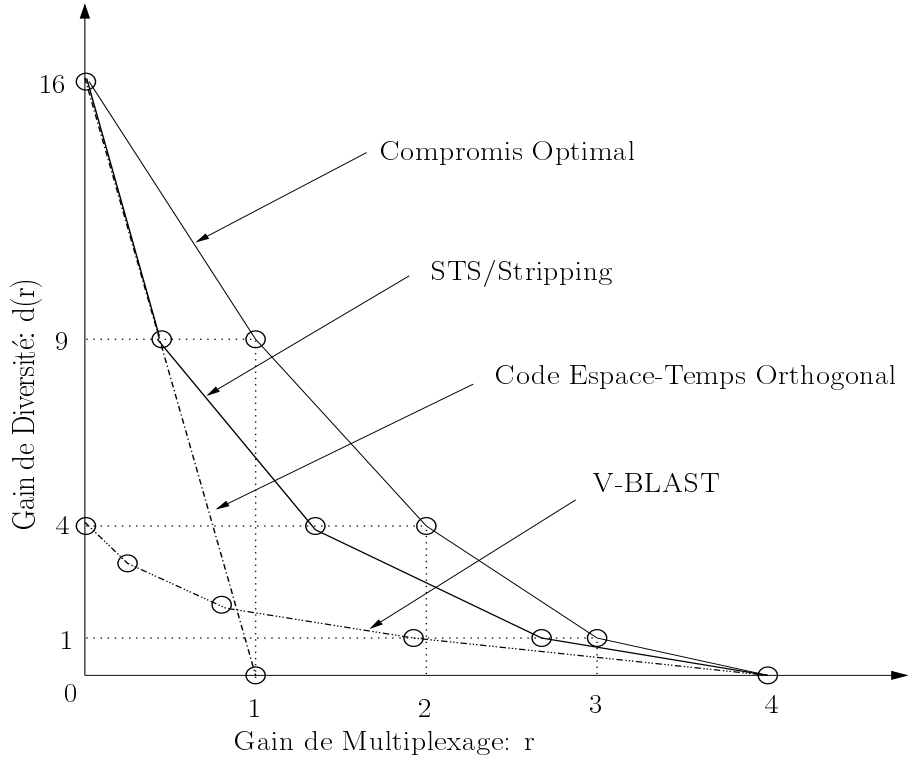

Figure 7.16: Compromis diversité-multiplexage de différentes techniques. $N_{tx} = N_{rx} = 4$, $L = 1$.

Pour l'allocation optimale des débits qui atteint ces points, et pour $r \in [r_k^t, r_{k+1}^t]$, $k = 0, \ldots, p-1$, seules $k+1$ streams sont utilisées.

Les débits non-zéros sont r_i, $p-k \leq i \leq p$, avec

$$\begin{cases} (m-k)(n-k)(1-r_{p-k}) = (m-k+1)(n-k+1)(1-r_{p-k+1}) = \ldots = mn(1-r_p) \\ \sum_{i=p-k}^{p} r_i = r \end{cases} \tag{7.79}$$

7.5.3 MIMO DFE Conventionnel

Le MIMO DFE Conventionnel fait une détection conjointe des streams mais successivement dans le temps. Les vecteurs symboles $\boldsymbol{b}_k$ sont détecté séquentiellement dans le temps (fig. 7.17). La sortie du DFE est

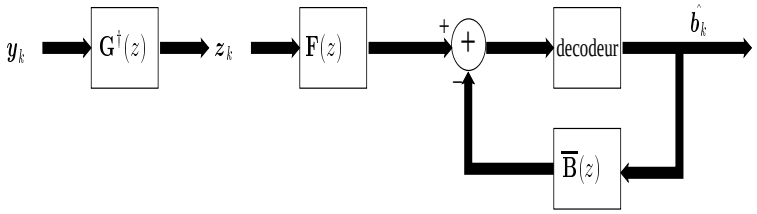

Figure 7.17: MIMO DFE Conventionnel

$$\widehat{\mathbf{b}}_k \;=\; -\underbrace{\overline{\mathbf{B}}(q)}_{\text{feedback}}\;\mathbf{b}_k + \underbrace{\mathbf{F}(q)}_{\text{feedforward}}\;\mathbf{z}_k\,, \tag{7.80}$$

où le filtre feedback $\overline{\mathbf{B}}(z) = \sum_{i\geq 1} \mathbf{B}_i z^{-i}$ est tel que $\mathbf{B}(z) = I + \overline{\mathbf{B}}(z)$ est causal, monique et à phase minimal.

Ici aussi, différents critères sont possibles pour la conception des filtres: MMSE ZF, MMSE et MMSE non-biaisé.

Le théorème suivant donne la performance, en termes de gain de diversité, du MIMO DFE conventionnel avec une conception MMSE ZF.

Théorème 3: Pour un canal plat avec $N_{rx} \geq N_{tx}$, l'utilisation d'un détecteur utilisant un critère de distance minimale pondérée au moment de la prise de décision, permet au MMSE ZF DFE Conventionnel d'atteindre un gain de diversité égal à $N_{tx}.(N_{rx} - \frac{N_{tx}-1}{2})$.

Dans cette section on a présenté deux récepteurs non itératifs. Le Stripping MIMO DFE, pour des streams ayant des débits et des codages différents, permet d'atteindre un bon compromis de diversité-multiplexage. Par contre pour un codage symétrique pour toutes les streams le MIMO DFE Conventionnel est mieux adapté.

7.6 Récepteur Itératif

Dans cette partie on présente un décodeur itératif, qui utilise le principe turbo, et itère entre l'égaliseur linéaire des symboles et le décodeur du codage canal.

7.6.1 Codage

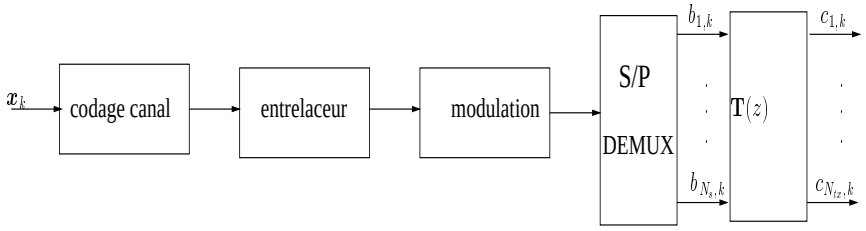

Figure 7.18: Structure de l'encodeur.

Fig. 7.18 montre la structure de l'encodeur. Le codage canal utilisé est un code convolutif afin de pouvoir utiliser le décodeur maximum a posteriori (MAP), implémenté avec l'algorithme BCJR de faible complexité. Le codage canal est suivi par un entrelaceur des bits codés. L'opération suivante est celle de la modulation en des symboles QAM. Par la suite on fait une conversion de série en parallèle, afin de former des vecteurs symboles qui passent dans le filtre MIMO $\mathbf{T}(z)$ correspondant au schéma STS.

7.6.2 Décodage Itératif

Fig. 7.19 montre la structure du décodeur itératif. Le premier bloc de ce récepteur est l'égaliseur linéaire des symboles transmis. Cette égaliseur contient une branche d'annulation d'interférences, l'estimée de l'interférence est faite d'une manière douce en se basant sur l'information extrinsèque obtenue

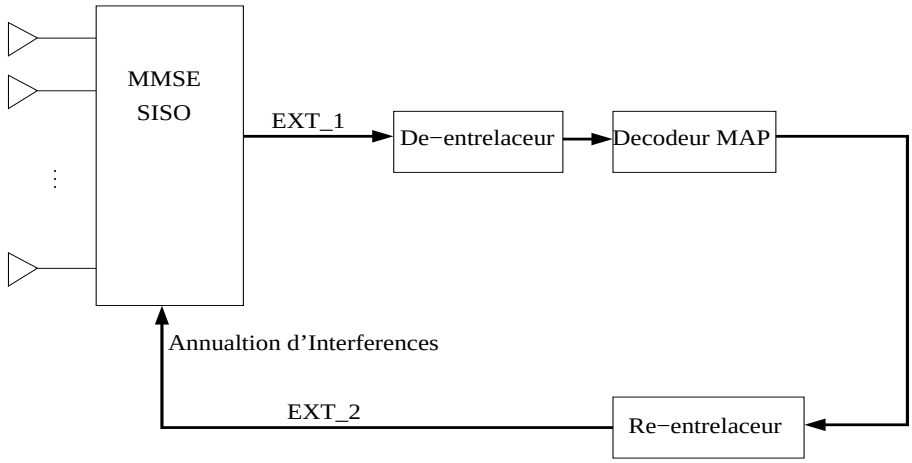

Figure 7.19: Décodage itératif avec annulation d'interférences.

à la sortie du décodeur SISO. La conception de l'égaliseur est faite sur la base d'un critère MMSE qui considère l'interférences résiduelle comme du bruit en plus de celui dans le canal. A la sortie de l'égaliseur on applique une conversion de parallèle en série suivie de l'opération de démodulation et de dé-entrelacement. Par la suite on utilise un décodeur MAP SISO du codeur canal, qui est dans ce cas là le BCJR, afin d'extraire l'information extrinsèque qui sera réinjectée dans l'égaliseur.

7.6.3 Analyse de Performance

On compare les performances du STS et du Threading (pour le Threading $Q = \mathbf{I}$) par simulation. Pour les deux cas on utilise le code convolutif (5,7) à quatre états et de débit 1/2. Les performances sont évaluées en termes de probabilité d'erreur par trame (FER) en fonction du E_b/N_0 ($SNR = RE_b/N_0, R = rN_s \log_2 |\mathcal{A}|, \rho = SNR/N_s$). Les simulations sont pour des trames de 512 bits d'information. Le nombre d'itérations est fixé à 5. On utilise la constellation QPSK.

On permet aussi que le codage puissent être fait sur plusieurs réalisations du canal $F = 1, 2, 4$. Ainsi le nombre de branches de diversité qui doivent être exploitées est $N_{tx}.F$.
Dans les figures 7.20, 7.21, on observe que lorsque le nombre de branches de diversité augmente($N_{tx}.F$), le STS exploite mieux cette diversité que le Threading.

On peut donc conclure que l'utilisation du STS permet de mieux exploiter la diversité, par contre une étude théorique de ce fait n'est pas possible à cause de la difficulté d'analyse des techniques turbo.

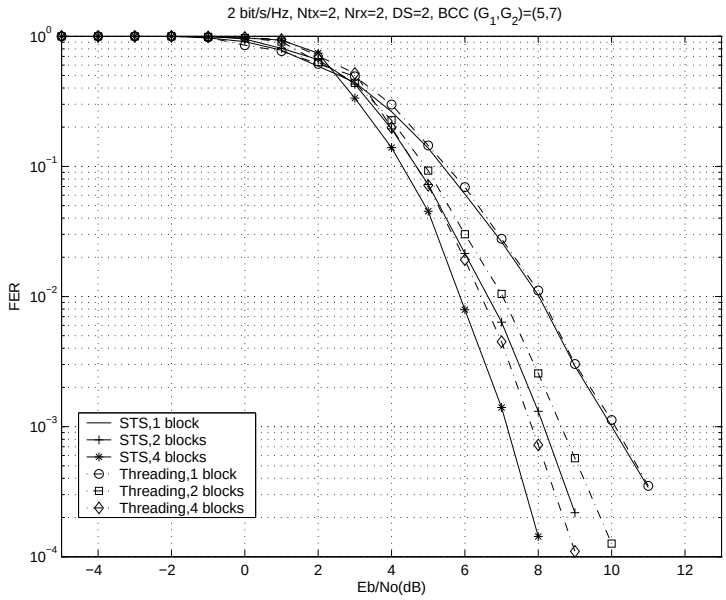

Figure 7.20: STS/Threading pour $(N_{tx}, N_{rx}) = (2, 2)$, $L = 2$, $F = 1, 2, 4$.

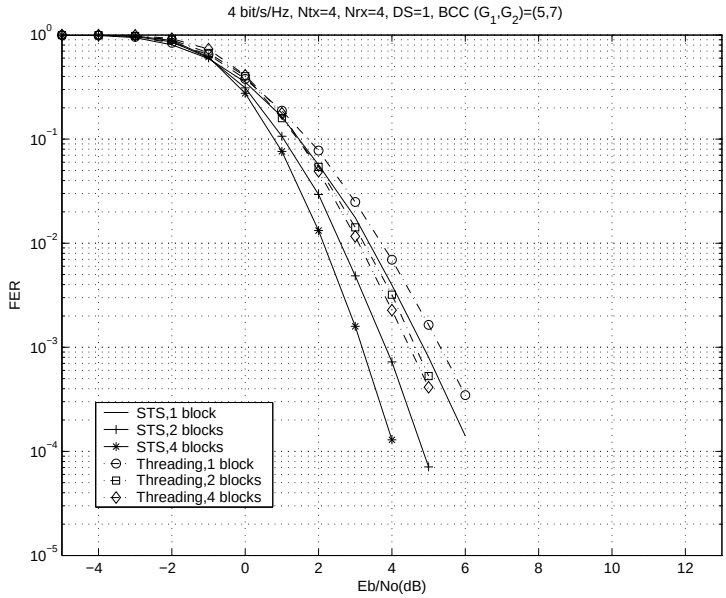

Figure 7.21: STS/Threading pour $(N_{tx}, N_{rx}) = (4, 4)$, $L = 1$, $F = 1, 2, 4$.

Partie II: CSI Partiel au Tx

Le canal ici ne suit plus une distribution Rayleigh, mais le récepteur a une information sur la structure du canal. On considère le cas plat. Le codage ici est fondamentalement la cascade du codeur espace-temps et du décorrélateur. Pour l'optimisation du décodeur on prend comme critère la capacité ergodique.

7.7 Modèles de Canal

On reformule la capacité ergodique du canal

$$C = \mathrm{E}_{\mathbf{H}} \ln\det(\mathbf{I} + \frac{P}{\sigma_v^2}\mathbf{H}\mathbf{S}\mathbf{H}^H) = \mathrm{E}_{\mathbf{H}} \ln\det(\mathbf{I} + \rho N_{tx}\mathbf{H}\mathbf{S}\mathbf{H}^H)\,, \qquad (7.81)$$

où $\rho = \frac{P}{N_{tx}\sigma_v^2}$ et $\mathbf{S_{XX}} = P\mathbf{S}$ est la matrice de covariance du signal transmis Gaussien qui maximise l'expression ci-haut sous la contrainte de puissance $\mathrm{tr}\{\mathbf{S}\} \leq 1$.

7.7.1 Modèle à Chemins

Dans ce cas le canal s'écrit

$$\mathbf{H} = \sum_{l=1}^{L_p} c_l \mathbf{a}_l \mathbf{b}_l^T = \mathbf{ACB} \qquad (7.82)$$

où $\mathbf{A} = [\mathbf{a}_1, \ldots, \mathbf{a}_{L_p}]$, $\mathbf{B} = [\mathbf{b}_1, \ldots \mathbf{b}_{L_p}]^T$ sont connus.
L_p est le nombre de chemins. $\mathbf{C} = \mathrm{diag}\{c_1, \ldots, c_{L_p}\}$, où c_l, $i = 1, \ldots, L_p$ sont les gains complexes des chemins, ils sont modélisés comme Gaussiens de moyenne 0 et de variance 1.

7.7.2 Modèle à Réciprocité Limitée

Dans ce cas là les canaux descendant (de Tx à Rx) et montant (de Rx à Tx) sont les mêmes a part d'un coefficient multiplicatif par antenne. Le canal montant $\mathbf{W}^T$ est connu au Tx, par conséquent le canal descendant peut être modélisé par

$$\mathbf{H} = \mathbf{D}_1\mathbf{W}\mathbf{D}_2, \qquad (7.83)$$

où $\mathbf{D}_1$ et $\mathbf{D}_2$ sont des matrices diagonales. Ces matrice peuvent avoir plusieurs modèles, le plus commun est que les éléments diagonaux soient de pures phases, $\mathbf{D}_1 = \text{diag}\{e^{j\phi_1^1}, \ldots, e^{j\phi_{N_{rx}}^1}\}$ et $\mathbf{D}_2 = \text{diag}\{e^{j\phi_1^2}, \ldots, e^{j\phi_{N_{tx}}^2}\}$, où les ϕ_l^i sont i.i.d. et uniformément distribuées sur $[0, 2\pi]$.

7.8 Résultats

7.8.1 Modèle à Chemins

On dérive ci-dessous différentes solutions possibles.
Bas SNR : Ce cas correspond à $\rho << 1$. Soit $\mathbf{\Sigma} = \text{E}(\mathbf{H}^H\mathbf{H})$ la matrice de covariance du canal vue du Tx.
La solution à bas SNR est aussi appelée la solution beamforming, elle correspond à

$$\mathbf{S} = \mathbf{u}\mathbf{u}^H, \tag{7.84}$$

où $\mathbf{u}$ est le vecteur propre correspondant à la valeur propre maximale de $\mathbf{\Sigma}$.

Haut SNR : Ce cas correspond à $\rho >> 1$. La solution est maintenant

$$\mathbf{S} = \frac{1}{\min\{L_p, N_{tx}\}}\mathbf{U}\mathbf{U}^H, \tag{7.85}$$

où $\mathbf{U}$ est la matrice des vecteurs propres correspondant aux valeurs propres non-nulles de $\mathbf{\Sigma}$.

Waterfilling sur la matrice de covariance du canal (approximé) : Elle correspond au waterfilling sur $\mathbf{\Sigma}$.

Solution optimale : La fonction ln det est une fonction convexe sur l'ensemble connexe des matrices positives définies avec trace égale à 1. Par conséquent la solution optimale peut être calculée par des méthodes numériques en prenant comme fonction de coût la capacité ergodique en remplaçant l'espérance par une moyenne des réalisations Monte Carlo.

Solution pour modèle séparable :

Pour cette solution on applique la même méthode que celle utilisé pour la solution optimale, mais où les réalisations Monte Carlo prennent en compte

le modèle séparable de la section 7.3.1 qui correspond aux covariances du canal à chemins.

7.8.2 Modèle à Réciprocité Limitée

Pour ce modèle les solutions optimale et waterfilling approximé sont aussi applicable.

7.9 Résultats des Simulations

On compare les performances des différentes solutions, ainsi que celles relatives à l'absence de connaissance au Tx $\mathbf{S} = \frac{1}{N_{tx}}\mathbf{I}$, et au cas où on a une connaissance parfaite (borne supérieure des performances). Les résultats des deux modèles, à chemins (fig. 7.22) et à réciprocité limitée (fig. 7.23), montrent que la solution de waterfilling sur la covariance du canal vue du Tx atteint des performances très proches de ceux de la solution optimale.

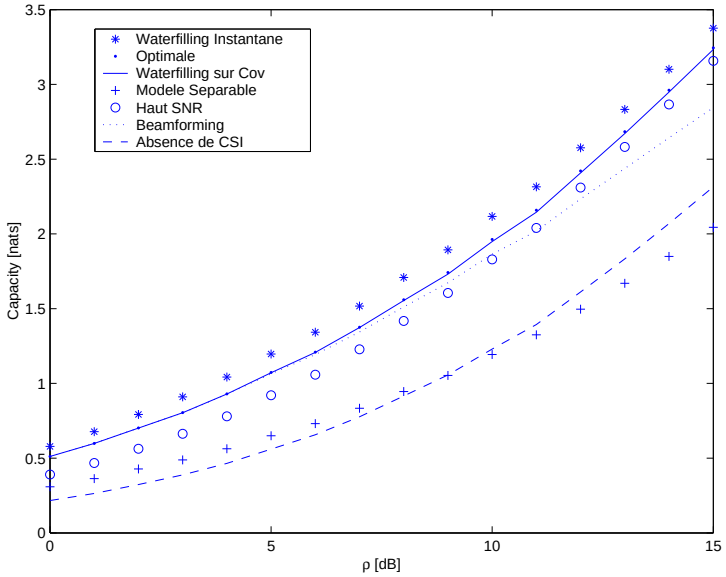

Figure 7.22: Modèle à chemins, $N_{tx} = N_{rx} = 4$, $L_p = 2$.

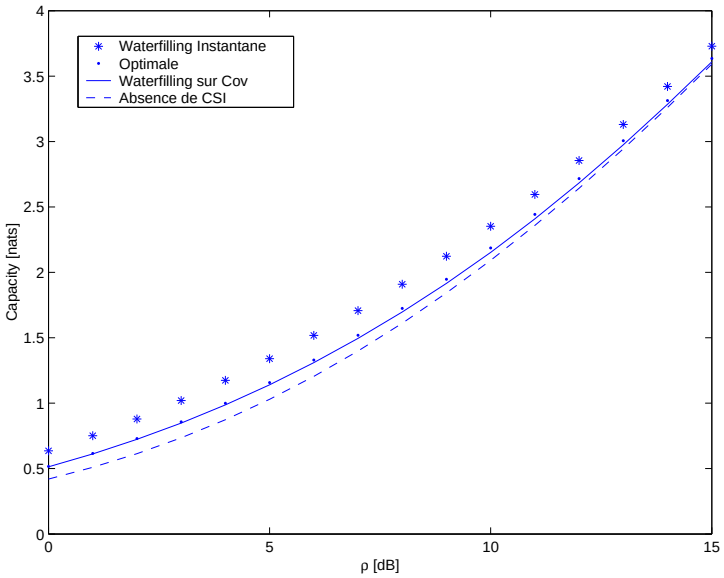

Figure 7.23: Modèle à réciprocité limitée, $N_{rx} = N_{tx} = 4$.

Partie III: Absence de CSI au Rx

7.10 Information Mutuelle en Absence de CSI au Rx

Le modèle de canal qu'on prend ici est plat et peut être sélectif en temps (le canal varie dans le temps)

$$\mathbf{y}_k = \mathbf{H}^{(k)}\mathbf{x}_k + \mathbf{v}_k \ . \tag{7.86}$$

La durée de la trame est T. On divise la trame en partie pilote (séquence d'apprentissage) connue par Rx: $\mathbf{X}^{TS}$ de longueur N_{TS}, et en partie aveugle $\mathbf{X}^B$ qui contient l'information d'une longueur N_B ($N_{TS} + N_B = T$).
Pour $k \geq i$ on définit $\mathbf{X}_i^k = [\mathbf{X}_i, \mathbf{X}_{i+1}, \ldots, \mathbf{X}_k]$.

7.10.1 Décomposition de l'Information Mutuelle

L'information mutuelle entre le signal transmis et celui reçu est

$$I(\mathbf{Y}^{TS}, \mathbf{Y}^B; \mathbf{X}^B | \mathbf{X}^{TS}) = I(\mathbf{Y}^B; \mathbf{X}^B | \mathbf{X}^{TS}, \mathbf{Y}^{TS}). \tag{7.87}$$

L'expansion séquentielle de cette expression donne

$$I(\mathbf{Y}^B; \mathbf{X}^B | \mathbf{X}^{TS}, \mathbf{Y}^{TS}) = \sum_{i=1}^{N_{TS}} I(\mathbf{Y}_i; \mathbf{X}_i | \mathbf{X}^{TS}, \mathbf{X}_1^{i-1}, \overline{\mathbf{Y}}_i) \, , \tag{7.88}$$

où $\overline{\mathbf{Y}}_i = [\mathbf{Y}^{TS}, \mathbf{Y}_1^{i-1}, \mathbf{Y}_{i+1}^{N_{TS}}]$ contient tout le signal reçu à part $\mathbf{Y}_i$.

De cette expression, on peut conclure qu'une manière optimale de traitement est d'utiliser les symboles déjà détectés comme pilote, et le signal future qui correspond aux symboles non encore détectés comme information aveugle pour l'estimation du canal. La combinaison de ces deux parties mène à l'utilisation d'algorithmes semi-aveugles, qui combinent parties pilote et aveugle pour l'estimation de canal.

7.10.2 Comportement Asymptotique des Canaux Evanesçants par Bloc

Dans ce cas $\mathbf{H}^{(k)} = \mathbf{H}$ pour $k = 1, \ldots, T$, l'information mutuelle moyenne est définie comme

$$I_{avg}(T) = \frac{1}{T} I(\mathbf{Y}^B; \mathbf{X}^B | \mathbf{X}^{TS}, \mathbf{Y}^{TS}) \,. \tag{7.89}$$

Pour de long bloc, on obtient la limite suivante

$$\lim_{T \to \infty} I_{avg}(T) = I(\mathbf{y}; \mathbf{x} | \mathbf{H}) \,, \tag{7.90}$$

où $I(\mathbf{y}; \mathbf{x}|\mathbf{H})$ est l'information mutuelle moyenne avec connaissance parfaite du canal au Rx.
Ainsi pour un canal évanesçant par bloc, il n'y pas de perte de capacité asymptotiquement dans la longueur de bloc.

7.11 Estimation Semi-Aveugle des Canaux MIMO

On vient de voir l'importance de l'estimation semi-aveugle du canal dans le traitement au récepteur. Celà est d'autant plus vrai que pour des canaux MIMO le nombre de paramètres à estimer dans le canal est important. Une approche, basée exclusivement sur l'estimation avec des pilotes, nécessite une séquence d'apprentissage d'une longueur importante, ce qui limite l'efficacité spectrale. L'exploitation de la partie semi-aveugle permet de diminuer la longueur de cette séquence nécessaire à l'identification du canal et d'améliorer par conséquent l'efficacité spectrale.
Le canal dans cette section est évanesçant par bloc.

7.11.1 Canal MIMO plat

Le signal transmis est modélisé comme Gaussien $\mathbf{x}_k \sim \mathcal{CN}(0, \sigma_x^2 \mathbf{I}_{N_{tx}})$. On définit $\hat{\mathbf{R}} = \frac{1}{N_B} \sum_{k=1}^{N_B} \mathbf{y}_k \mathbf{y}_k^H$.
Le canal peut être écrit en fonction de sa décomposition en valeurs singulières

$$\mathbf{H} = \mathbf{UDQ} = \mathbf{WQ} \tag{7.91}$$

où $\mathbf{U}$(resp. $\mathbf{Q}$) est une matrice $N_{rx} \times \min\{N_{rx}, N_{tx}\}$ (resp. $\min\{N_{rx}, N_{tx}\} \times N_{tx}$) unitaire, i.e $\mathbf{U}^H\mathbf{U} = \mathbf{I}$ (resp. $\mathbf{Q}\mathbf{Q}^H = \mathbf{I}$).

$\mathbf{W}$ correspond à la partie identifiable en aveugle et $\mathbf{Q}$ à la partie identifiable avec la séquence d'apprentissage seulement.

Les covariances, correcte et estimée, du signal peuvent être réécrites comme

$$\begin{aligned} \mathbf{R} &= \mathbf{U}\,(\sigma_v^2\mathbf{I}_{\min\{N_{tx},N_{rx}\}} + \sigma_x^2 D^2)\mathbf{U}^H + \sigma_v^2\mathbf{U}^{\perp}\mathbf{U}^{\perp H} \\ \hat{\mathbf{R}} &= \mathbf{U}_e\mathbf{S}_e\mathbf{U}_e^H\,. \end{aligned} \tag{7.92}$$

La variance du bruit σ_v^2 est supposée connue au récepteur.
Deux approches peuvent être proposées, l'approche Gaussienne exploite la blancheur du signal transmis, et l'approche déterministique qui n'exploite que le sous-espace bruit.

Approche Semi-Aveugle Gaussienne (GSB)
Pour cette approche on propose un algorithme en deux étapes, la première identifie $\mathbf{W}$ en aveugle seulement, et la deuxième identifie $\mathbf{Q}$ avec la séquence d'apprentissage. La séquence d'apprentissage est choisie tel que $\mathbf{X}^{TS}\,\mathbf{X}^{TS\,H} \propto \mathbf{I}$.

1. Identification de $\mathbf{W}$:
   - $\hat{\mathbf{U}}$ correspond aux $\min\{N_{tx}, N_{rx}\}$ vecteurs propres les plus dominants dans $\mathbf{U}_e$
   - $\hat{\mathbf{D}}$ correspond $\min\{N_{tx}, N_{rx}\}$ valeurs propres les plus dominantes dans $\frac{1}{\sigma_x}\left(\lfloor \mathbf{S}_e - \sigma_v^2\mathbf{I}_{N_{rx}} \rfloor_+\right)^{1/2}$
   - $\hat{\mathbf{W}} = \hat{\mathbf{U}}\hat{\mathbf{D}}$
2. Identification de $\mathbf{Q}$:
$$\hat{\mathbf{Q}} = \mathbf{V}\,\mathbf{S}^H\,, \tag{7.93}$$
où $\mathbf{S}$ et $\mathbf{V}$ sont les parties unitaires de la décomposition en valeurs singulières de $\mathbf{X}^{TS}\mathbf{Y}^{TS\,H}\hat{\mathbf{W}} = \mathbf{S}\,\Sigma\,\mathbf{V}^H$.

Approche Semi-Aveugle Déterministique (DSB)
Dans cette méthode on n'exploite plus les corrélations du signal à l'entrée mais seulement le sous-espace bruit. Pour que ce dernier existe, on doit avoir $N_{rx} > N_{tx}$. L'information aveugle dans ce cas là exprime l'orthogonalité du

canal par rapport au sous-espace bruit $\mathbf{U}^{\perp,H}\mathbf{H} = 0$. En utilisant une approche de minimum d'erreurs quadratiques pondérées on combines la partie aveugle et celle de la séquence d'apprentissage dans un critère quadratique

$$\min_{\mathbf{H}} \left(\sigma_v^{-2} ||\mathbf{Y}^{TS} - \mathbf{H}\mathbf{X}^{TS}||_F^2 \; + \; N_B ||\hat{\mathbf{U}}^{\perp\,H} \mathbf{H}^H||_F^2 \right) . \tag{7.94}$$

De la même manière, des approches semi-aveugles Gaussienne et déterministique peuvent être proposées pour des canaux sélectifs en fréquence dans le cas $N_{rx} > N_{tx}$ [90]. Dans ce types de canaux on utilise la prédiction linéaire afin d'extraire l'information aveugle sur la corrélation du signal et le sous-espace bruit.

7.11.2 Analyse de Performance

La figure 7.24 montre les performances des approches GSB et DSB en comparaison avec l'approche TS, basées seulement sur la séquence d'apprentissage, et la borne de Cramer-Rao (CRB). Le canal est 4×2 et la longueur de la partie aveugle est $N_B = 400$. Le SNR est fixé à 10dB et les performances sont données en erreur quadratique moyenne (MSE) pour différentes longueurs de la séquence d'apprentissage (pilote). On observe que l'utilisation des méthodes semi-aveugles permet de diminuer la longueur de la séquence d'apprentissage nécessaire à une qualité d'estimation donnée. D'autre part, l'approche GSB donne des performances quasi-optimales qui sont proches de la borne de Cramer-Rao.

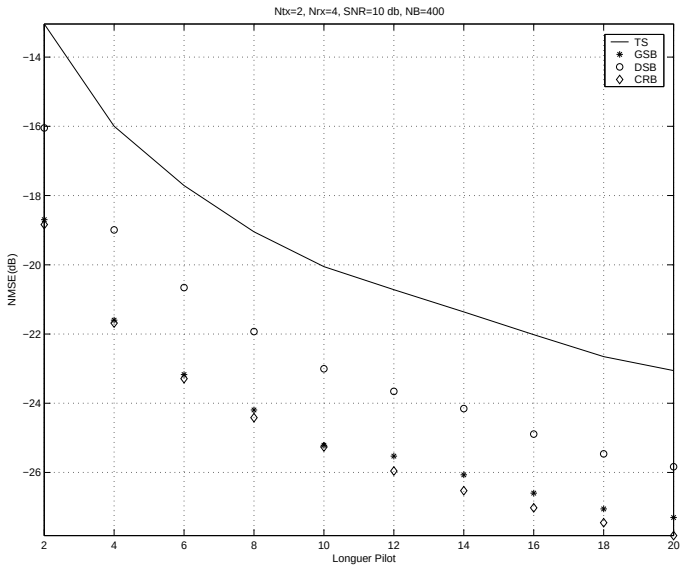

Figure 7.24: MSE vs N_{TS}: canal plat, $N_{tx} = 2, N_{rx} = 4,\ N_B = 400$, SNR= 10 dB.

7.12 Conclusion

Dans cette thèse on a présenté plusieurs études et solutions pour le codage et le traitement de signal dans les systèmes MIMO. Ce travail est structuré en trois parties, chacune traite d'un état particulier de connaissance de canal:

- Dans la première partie le CSI est absent au Tx et parfait au Rx. On a commencé par proposer un schéma de codage espace-temps, le STS, qui est basé sur un filtre de précodage MIMO.
  Au récepteur, et pour éviter d'utiliser le décodeur ML qui a une grande complexité, on a proposé trois stratégies de réception. Le Stripping MIMO DFE est un récepteur non-itératif qui détecte et annule les streams successivement. On a montré théoriquement qu'avec des constellations QAM qui ont des tailles qui dépendent du SNR et du stream, le STS combiné avec le détecteur Stripping MIMO DFE donne des performances, en termes de compromis diversité-multiplexage, meilleures que celles des schémas existants. Le second récepteur non-itératif est le MIMO DFE Conventionnel. Par opposition au premier, il utilise la même constellation pour toute les streams. On montre qu'il at-

teint un bon gain de diversité. Le dernier récepteur à être proposé est itératif. Il utilise une détection turbo en itérant entre l'égaliseur linéaire et le décodeur correcteur d'erreur. Les simulations montrent l'avantage d'utiliser le STS par rapport aux approches basées sur un pur codage correcteur d'erreur (Threading), en particulier pour un nombre important d'antennes de transmission N_{tx}, ou en cas de codage sur plusieurs blocs avec différentes réalisations du canal (diversité temporelle).

- Dans la seconde partie, on a traité le cas de connaissance partielle sur le canal au Tx et parfaite au Rx. Le codage dans ce cas là est fondamentalement la cascade du schéma STC, développé en l'absence de CSI au Tx, et d'un décorrélateur qui colore le signal transmis. On a étudié la couleur de l'entrée qui permet d'atteindre la capacité ergodique pour deux modèles de canaux, le modèle à chemins et le modèle à réciprocité limitée. Les résultats numériques montrent qu'une solution quasi-optimale peut être obtenue par le waterfilling sur la matrice de covariance du canal vue par le Tx.

- Dans la dernière partie on a étudié le cas d'absence de CSI au Rx et Tx. On a montré que la capacité d'un canal évanesçant par bloc atteint asymptotiquement, dans la longueur du bloc, celle obtenue avec connaissance parfaite du canal au Rx. D'autre part, la décomposition de l'information mutuelle motive l'utilisation d'algorithmes semi-aveugles pour l'estimation du canal. Le gain en performance par rapport à une méthode basée exclusivement sur la séquence d'apprentissage peut être important, en particulier l'approche GSB atteint même la borne Cramer-Rao pour un canal plat. Les approches semi-aveugles améliorent aussi l'identifiabilité et permettent de réduire la longueur de la séquence d'apprentissage.

Bibliography

[1] G.J. Foschini. Layered Space-Time Architecture for Wireless Communication in a Fading Environment when Using Multi-Element Antennas. *Bell Labs Tech. J.*, 1(2):41–59, 1996. [2, 13, 18, 172]

[2] I.E. Telatar. Capacity of Multi-antenna Gaussian Channels. *Eur. Trans. Telecom.*, 10(6):585–595, Nov/Dec 1999. [2, 5, 7, 8, 18, 105, 140, 173]

[3] F. Demmerle and W. Wiesbeck. A biconical multibeam antenna for space-division multiple access. *IEEE Transactions on Antennas and Propagation*, 46(6):782–787, 1998. [5]

[4] T. Svantesson. A double-bounce channel model for multi-polarized MIMO systems. In *Proc. VTC 2002 FALL*, Vancouver, Canada, Sept. 2002. [5]

[5] T.L. Marzetta. Fundamental limitations on the capacity of wireless links that use polarimetric antenna arrays. In *Proc. IEEE ISIT 2002*, Lausane, Switzerland, Jun-Jul 2002. [5]

[6] S.H. Simon and A.L. Moustakas. Optimizing MIMO antenna systems with channel covariance feedback. *IEEE Journal on Selected Areas in Communications*, 21(3):406 – 417, Apr. 2003. [9, 105]

[7] A.L. Moustakas and S.H. Simon. Optimizing multiple-input single-output (MISO) communication systems with general Gaussian channels: nontrivial covariance and nonzero mean. *IEEE Trans. Info. Theory*, 49(10):2770 – 2780, Oct. 2003. [9, 105]

[8] A.L. Moustakas and S.H. Simon. Optimizing multi-antenna systems with partial channel knowledge. In *Proc. Seventh International Sym-*

posium on Signal Processing and Its Applications, 2003, Paris, France, Jul. 2003. [9]

[9] L. Zheng and D. Tse. Diversity and multiplexing: a fundamental tradeoff in multiple-antenna channels. *IEEE Trans. Info. Theory*, 49(5):1073 – 1096, May 2003. [9, 16, 44, 54, 55, 59, 75, 80, 175]

[10] R. Gray. *Toeplitz and circulant matrices*. Stanford University, Palo Alto, 1977. [10]

[11] U. Grenander and G. Szego. *Toeplitz forms and their applications*. University of California Press, Berkeley, 1958. [10]

[12] J. Proakis. *Digital Communications*. New York: MacGraw-Hill, 3rd edition, 1995. [11, 90]

[13] J. Ventura-Traveset, G. Caire, E. Biglieri, and G. Taricco. Impact of diversity reception on fading channels with coded modulation. Part I: Coherent detection. *IEEE Transactions on Communications*, 45(5):563–572, May 1997. [11]

[14] J. Ventura-Traveset, G. Caire, E. Biglieri, and G. Taricco. Impact of diversity reception on fading channels with coded modulation. Part II: Differential block detection. *IEEE Transactions on Communications*, 45(6):676 – 686, Jun. 1997. [11]

[15] J. Ventura-Traveset, G. Caire, E. Biglieri, and G. Taricco. Impact of diversity reception on fading channels with coded modulation. Part III: Cochannel Interference. *IEEE Transactions on Communications*, 45(7):809–818, Jul. 1997. [11]

[16] V. Tarokh, N. Seshadri, and A.R. Calderbank. Space-Time Codes for High Data Rates Wireless communication: Performance criterion and code construction. *IEEE Trans. Info. Theory*, 44(2):744–765, March 1998. [13, 18, 26, 28, 174]

[17] M. Lenardi, A. Medles, and D.T.M. Slock. Downlink Intercell Interference Cancellation in WCDMA by Exploiting Excess Codes. In *Proc. SAM 2000*, Boston, Massachusset-USA, 2000. [18]

[18] M. Lenardi, A. Medles, and D.T.M. Slock. Intercell Interference Cancellation at a WCDMA Mobile Terminal by Exploiting Excess Codes. In *Proc. VTC 2001 spring*, Rhodes, Greece, 2001. [18]

[19] M. Lenardi, A. Medles, and D.T.M. Slock. A SINR Maximizing RAKE Receiver for DS-CDMA Dowlinks. In *Proc. 34th Asilomar Conf. on Signals, Systems & Computers*, Pacific Grove, CA, Nov. 2000. [18]

[20] M. Lenardi, A. Medles, and D.T.M. Slock. Comparison of Downlink Transmit Diversity Schemes for RAKE and SINR Maximizing Receivers. In *Proc. ICC*, Helsinki, Finland, Jun. 2001. [18]

[21] V. Tarokh, H. Jafarkhani, and A.R. Calderbank. Space-Time Block Codes from Orthogonal Designs. *IEEE Trans. Info. Theory*, 45(5):1456–1467, July 1999. [18, 26, 92]

[22] X. Ma and G.B. Giannakis. Complex Field Coded MIMO Systems: Performance, Rate, and Tradeoffs. *Wireless Communications and Mobile Computing*, pages 693–717, November 2002. [18, 26, 35, 84, 91]

[23] H. El Gamal and M.O. Damen. Universal space-time coding. *IEEE Trans. Inform. Theory*, 49:1097–1119, May 2003. [18, 26, 84, 91]

[24] M.O. Damen, H. El Gamal, and N.C. Beaulieu. Linear threaded algebraic space-time constellation. *IEEE Trans. Inform. Theory*, 49(10):2372–2388, Oct 2003. [26, 84, 91]

[25] A. Medles and D.T.M. Slock. Linear Convolutive Space-Time Precoding for Spatial Multiplexing MIMO Systems. In *Proc. 39th Annual Allerton Conference on Communication, Control, and Computing*, Monticello, Illinois, Oct. 2001. [26, 27, 45]

[26] A. Medles and D.T.M. Slock. Spatial multiplexing by spatiotemporal spreading of multiple symbol streams. In *Proc. The 5th International Symposium on Wireless Personal Multimedia Communications 2002 (WPMC 2002)*, Honolulu, Hawai, Oct. 2002. [27]

[27] A. Medles and D.T.M. Slock. Miltistream Space-Time Coding by Spatial Spreading, Scrambling and Delay Diversity. In *Proc. ICASSP Conf.*, Orlando, FL, May 2002. [27]

[28] A. Medles and D.T.M. Slock. Linear Space-Time Coding at Full Rate and Full Diversity. In *Proc. IEEE ISIT 2002*, Lausane, Switzerland, Jun-Jul 2002. [27]

[29] G. Caire and G. Colavolpe. On space-time coding for quasi-static multiple-antenna channels. *IEEE Trans. on Inform. Theory*, 49(6):1400–1416, June 2003. [28]

[30] B. Hassibi and B. M. Hochwald. High-Rate Codes that are Linear in Space and Time. *IEEE Trans. Info. Theory*, 48(7):1804 –1824, August 2000. [28]

[31] S. Galliou and J.C. Belfiore. A New Familly of Linear Full-Rate Space-Time Codes Based on Galois Theory. In *Proc. IEEE ISIT 2002*, Lausane, Switzerland, Jun-Jul 2002. [28, 91]

[32] S. Alamouti. A simple transmitter diversity scheme for wireless communications. *IEEE Journal on Selected Areas in Communications*, 16:1451–1458, Oct 1998. [28]

[33] Y. Xin, Z. Wang, and G. Giannakis. Space-Time Diversity Systems Based on Unitary Constellation-Rotating Precoders. In *Proc. ICASSP Conf.*, Salt Lake City, USA, May 2001. [30]

[34] E. Boutillon X. Giraud and J.C. Belfiore. Algebraic Tools to Build Modulation Schemes for Fading Channels. *IEEE Trans. Info. Theory*, 43(3):938–952, May 1997. [33, 35]

[35] J. Boutros, E.Viterbo, C.Rastello, and J.C. Belfiore. Good Lattice Constellations for both Rayleigh Fading and Gaussian Channels. *IEEE Trans. Info. Theory*, 42(2):502–518, March 1996. [33]

[36] M.O. Damen, A.Chkeif, and J.C. Belfiore. Sphere Decoding of Space-Time codes. In *Proc. IEEE ISIT 2000*, Sorrento, Italy, June 2000. [40]

[37] H. EL Gamal, G. Caire, and M.O. Damen. Lattice coding and decoding achieve the optimal diversity-vs-multiplexing tradeoff of MIMO channels. *Submitted to IEEE Trans. Info. Theory*, Nov. 2003. [40, 41, 66, 169]

[38] A. Medles and D.T.M. Slock. Full diversity Spatial Multiplexing Based on SISO Channel Coding, Spatial Spreading and Delay Diversity. In *Proc. Signal Processing Symposium*, Leuven, Belgium, March 2002. [45, 50]

[39] A. Medles and D.T.M. Slock. Spatial multiplexing by spatiotemporal spreading: receiver considerations. In *Proc. IEEE Global Telecommunications Conference, 2002 (GLOBECOM '02)*, Tapei, Taiwan, Nov. 2002. [45]

[40] S. Verdu. *Multiuser detection*. Cambridge University Press, Cambridge, 1998. [46, 50]

[41] R.R. Muller and S. Verdu. Design and analysis of low-complexity interference mitigation on vector channel. *IEEE Journal on Selected Areas in Communications*, 19(8):1429 – 1441, Aug. 2001. [46, 50]

[42] M.K. Varanasi and T. Guess. Optimum decision feedback multiuser equalization with successive decoding achieves the total capacity of the Gaussian multiple-access channel. In *Proc. 31th Asilomar Conf. on Signals, Systems & Computers*, Pacific Grove, CA, Nov. 1997. [46, 50]

[43] D. Mary and D.T.M. Slock. Vectorial DPCM Coding and Application to Wideband Coding of Speech. In *Proc. ICASSP Conf.*, Salt Lake City, USA, May 2001. [46, 49]

[44] Y. A. Rozanov. *Spectral properties of multivariate stationary processes and boundary properties of analytic matrices*, volume 5. Theory Prob. Applics, 1960. Reprinted in Kailath (1970). [46, 51]

[45] G. Ginis and J.M. Cioff. On the Relation Between V-BLAST and the GDFE. *IEEE Communications Letters*, 5(9):364–366, Sept. 2001. [47, 48]

[46] J. M. Cioffi, G. P. Dudevoir, M. Vedat Eyuboglu, and G. D. Forney. MMSE decision-feedback equalizers and coding. Part I: Equalization results . *IEEE Transactions on Communications*, 43(10):2582 – 2594, Oct. 1995. [48, 49]

[47] J. M. Cioffi, G. P. Dudevoir, M. Vedat Eyuboglu, and G. D. Forney. MMSE decision-feedback equalizers and coding. Part II: Coding results.

IEEE Transactions on Communications, 43(10):2595 – 2604, Oct. 1995. [48]

[48] T. Guess and M. Varanasi. A new successively decodable coding technique for intersymbol-interference channels. In *Proc. IEEE ISIT 2000*, Sorrento, Italy, Jun 2000. [50]

[49] M. Kobayashi and G. Caire. A low complexity approach to space-time coding for multipath channels. In *Proc. 6th Int'l Symp. on Wireless Personal Multimedia Communications*, Yokosuka, Japan, Oct 2003. [50]

[50] C.A. Belfiore and J.H. Parks. Decision-feedback equalization. *IEEE Trans. on Communications*, 67:1143–1156, 1979. [50]

[51] S.U.Qureshi. Adaptive equalization. In *Proc. IEEE*, volume 73, pages 1349–1387, Sept. 1985. [50]

[52] T. Kailath, A. H. Sayed, and B. Hassibi. *Linear Estimation*. Prentice Hall, 2000. [61]

[53] G. Caire and G. Colavolpe. On Low-Complexity Space-Time Coding for Quasi-Static Channels. *IEEE Trans. on Inform. Theory*, 49(6):1400–1416, June 2003. [64, 65]

[54] T.S. Rappaport. *Wireless Communications - Principles and Practice*. Prentice Hall, 1996. [73]

[55] R. Schober and W.H. Gerstacker. On the distribution of zeros of mobile channels with application to GSM/EDGE. *IEEE Journal on Selected Areas in Communications*, 19(7):1289–1299, July 2001. [73]

[56] A. Dembo and O. Zeitouni. *Large deviations techniques and applications*. Springer, New York, 2nd edition, 1998. [75]

[57] H. EL Gamal and R. Hammons. A new approach to layered space-time coding and signal processing. *IEEE Trans. Info. Theory*, 47(6):2321–2334, Sept. 2001. [84, 85, 89]

[58] A. Medles and D.T.M. Slock. Linear versus Channel Coding Trade-Offs in Full Diversity Full Rate MIMO Systems. In *Proc. ICASSP Conf.*, Montreal, CAN, May 2004. [84]

[59] J. Boutros and G. Caire. Iterative joint decoding: Unified frame work and asymptotic analysis. *IEEE Trans. on Inform. Theory*, 48(7):1772–1793, July 2002. [85, 87]

[60] G. Caire and A. Guillen i Fabregas. Design of space-time bit-interleaved coded modulation for block fading channels with iterative decoding. In *Proc. 37th Conference on Information Sciences and Systems(CISS 2003)*, Baltimore, USA, March 2003. [85, 87, 90]

[61] G. Caire and A. Guillen i Fabregas. Analysis and design of natural and threaded space-time codes with iterative decoding. In *Proc. 36th Asilomar Conf. on Signals, Systems & Computers*, Pacific Grove, CA, Nov. 2002. [85]

[62] C. Berrou, A. Glavieux, and P. Thitimajshima. Near Shannon limit error-correcting coding and decoding: Turbo-codes. In *Proc. ICC*, Geneva, Switzerland, May 1993. [87]

[63] R. Knopp and P.A. Humblet. On Coding for Block Fading Channels. *IEEE Trans. Info. Theory*, 46(1):189 –205, Jan. 2000. [89]

[64] J. Kermoal, L. Schumacher, K. Pedersen, P. Mogensen, and F. Frederiksen. A stochastic MIMO radio channel model with experimental validation. *IEEE Journal on Selected Areas in Communications*, 20(6):1211–1226, 2002. [100]

[65] M. T. Ivrlac, T. Kurpjuhn, C. Brunner, and W. Utschick. Efficient use of fading correlations in MIMO systems. In *Proc. VTC 2001 FALL*, Atlantic City, NJ, Oct. 2001. [100]

[66] S. A. Jafar, S. Vishwanath, and A. Goldsmith. Channel capacity and beamforming for multiple transmit and multiple receive antennas with covariance feedback. In *Proc. IEEE ICC*, 2001. [100, 105]

[67] A. Medles, S. Visuri, and D.T.M. Slock. On MIMO Capacity with Partial Channel Knowledge at the Transmitter. In *Proc. 36th Asilomar Conf. on Signals, Systems & Computers*, Pacific Grove, CA, Nov. 2002. [100]

[68] A. Medles, S. Visuri, and D.T.M. Slock. On MIMO Capacity for various Types of Partial Channel Knowledge at the Transmitter. In *Proc. 2003*

Information Theory Workshop (ITW 2003), Paris, FRANCE, Apr. 2003. [100]

[69] A. Medles, S. Visuri, and D.T.M. Slock. On the effect of channel knowledge imperfections at the transmitter on the capacity of MIMO systems. In *Proc. Seventh International Symposium on Signal Processing and Its Applications, 2003*, Paris, France, Jul. 2003. [100]

[70] G. G. Raleigh and J. M. Cioffi. Spatio-temporal coding for wireless communication. *IEEE Trans. on Communications*, 46(3):357–366, 1998. [101]

[71] B. Fleury, P. Jourdan, and A. Stucki. High-resolution channel parameter estimation for MIMO applications using the SAGE algorithm. In *Proc. International Zurich Seminar on Broadband Communications*, 2002. [101]

[72] D. Bertsekas. *Nonlinear Programming*. Belmont, MA: Athena Scientific, 1995. [105]

[73] S. Visuri and D. Slock. Colocated antenna arrays: design desiderata for wireless communications. In *Proc. of the Second IEEE Sensor Array and Multichannel Signal Processing Workshop (SAM 2002)*, August 2002. [105, 110]

[74] E. Visotsky and U. Madhow. Space-time transmit precoding with imperfect feedback. *IEEE Transactions on Information Theory*, 47(6):2632–2639, 2001. [105]

[75] S. A. Jafar and A. Goldsmith. On optimality of beamforming for multiple antenna systems with imperfect feedback. In *Proc. of the International Symposium on Information Theory*, Washington D.C., USA, 2001. [105]

[76] E. Jorswieck and H. Boche. On the optimality-range of beamforming for MIMO systems with covariance feedback. In *Proc. Conf. on Information Sciences and Systems*, Princeton University, 2002. [105]

[77] E. Biglieri, J. Proakis, and S. Shamai. Fading channels: information-theoretic and communications aspects. *IEEE Trans. Info. Theory*, 44(6):2619–2692, Oct. 1998. [118, 140]

[78] M. Medard. The effect upon channel capacity in wireless communications of perfect and imperfect knowledge of the channel. *IEEE Trans. Info. Theory*, 46(3):933–946, May 2000. [118, 140]

[79] B. Hassibi and B. M. Hochwald. How Much Training is Needed in Multiple-Antenna Wireless Links? *IEEE Trans. Info. Theory*, 49(10):951–964, Apr. 2003. [118, 119, 124, 140]

[80] L. Zheng and D. Tse. Communication on the Grassmann Manifold: A Geometric Approach to the Non-coherent Multiple Antenna Channel. *IEEE Trans. Info. Theory*, 48(2):359–383, Feb. 2002. [118]

[81] T.L. Marzetta and B.M. Hochwald. Capacity of a mobile multiple-antenna communication link in Rayleigh flat fading . *IEEE Trans. Info. Theory*, 45(1):139–157, Jan. 1999. [118, 140]

[82] A. Medles and D.T.M. Slock. Semiblind Channel Estimaton for MIMO Spatial Multiplexing Systems. In *Proc. 35th Asilomar Conf. on Signals, Systems & Computers*, Pacific Grove, CA, Nov. 2001. [119]

[83] A. Medles and D.T.M. Slock. Mutual Information without channel Knowledge at the Receiver. In *Proc. 4rd Workshop on Signal Processing Advances in Wireless Communications(SPAWC 2003)*, Rome, Italy, Jun 2003. [119]

[84] T.M. Cover and J.A. Thomas. *Elements of Information Theory*. Wiley-Interscience, 1991. [119]

[85] E. de Carvalho and D.T.M. Slock. *Signal Processing Advances in Communications*, volume (1): Trends in Channel Estimation and Equalization, chapter Semi-Blind Methods for FIR Multichannel Estimation. Prentice Hall, 2000. [140, 141]

[86] E. de Carvalho, L. Deneire, and D.T.M. Slock. Blind and Semi-Blind Maximum-Likelihood Techniques for Multi-user Multichannel Identification. In *Proc. European Signal Processing Conf. (EUSIPCO)*, Rhodes, Greece, Sept. 1998. [140, 148]

[87] A. Gorokhov and Ph. Loubaton. Blind Identification of MIMO-FIR Systems: a Generalized Linear Prediction Approach. *EURASIP Signal Processing*, 73:105–124, 1999. [140, 148, 150, 152]

[88] A. Gorokhov and Ph. Loubaton. Subspace based techniques for second-order blind separation of convolutive mixtures with temporally correlated sources. *IEEE Trans. Circuits and Systems*, 44:813–820, Sept. 1997. [140, 151]

[89] A. Aissa-EI-Bey, M. Grebici, K. Abed-Meraim, and A. Belouchrani. Blind system identification using cross-relation methods: further results and developments. In *Proc. Seventh International Symposium on Signal Processing and Its Applications, 2003*, Paris, France, Jul. 2003. [141]

[90] A. Medles, E. de Carvalho, and D.T.M. Slock. Linear Prediction Based Semi-Blind Estimation of MIMO FIR Channels. In *Proc. 3rd Workshop on Signal Processing Advances in Wireless Communications(SPAWC 2001)*, Taoyuan, Taiwan, March 2001. [141, 146, 196]

[91] A. Medles and D.T.M. Slock. Augmenting the Training Sequence Part in Semiblind Estimation for MIMO Channels. In *Proc. 37th Asilomar Conf. on Signals, Systems & Computers*, Pacific Grove, CA, Nov. 2003. [141]

[92] G.H. Golub and C.F. Van Loan. *Matrix Computations*. The Johns Hopkins University Press, third edition edition, 1996. [146]

[93] G. Harikumar and Y. Bresler. FIR perfect signal reconstruction from multiple convolutions: minimum deconvolver orders. *IEEE Trans. Signal Processing*, 46(1):215–218, Jan. 1998. [149, 151]

[94] D.T.M. Slock. Blind Joint Equalization of Multiple Synchronous Mobile Users Using Oversampling and/or Multiple Antennas. In *Proc. 28th Asilomar Conf. on Signals, Systems & Computers*, pages 1154–1158, Pacific Grove, CA, Oct-Nov 1994. [149]

[95] J. Götze and A. van der Veen. On-Line Subspace Estimation Using a Schur-Type Method. *IEEE Trans. Signal Processing*, 44(6):1585–1589, Jun. 1996. [150]

[96] R. Horn and C.R. Johnson. *Matrix Analysis*. Cambridge University Press, 1991. [160]

[97] S.A. Jafar, S. Vishwanath, and A. Goldsmith. Channel capacity and beamforming for multiple transmit and receive antennas with covariance feedback. In *Proc. ICC*, Helsinki, Finland, Jun. 2001. [160]